Dynamic analysis of vehicle-bridge interaction system with uncertain parameters

Author:
Liu, Nengguang

Publication Date:
2014

DOI:
https://doi.org/10.26190/unsworks/2595

License:
https://creativecommons.org/licenses/by-nc-nd/3.0/au/
Link to license to see what you are allowed to do with this resource.

Downloaded from http://hdl.handle.net/1959.4/53726 in https://unsworks.unsw.edu.au on 2024-04-30

Dynamic Analysis of Vehicle-Bridge Interaction System with Uncertain Parameters

Nengguang Liu

A thesis submitted in fulfilment of the requirements for the degree of

DOCTOR OF PHILOSOPHY

UNSW

School of Civil and Environmental Engineering

Faculty of Engineering

March 2014

Copyright Statement

'I hereby grant the University of New South Wales or its agents the right to archive and to make available my thesis or dissertation in whole or part in the University libraries in all forms of media, now or here after known, subject to the provisions of the Copyright Act 1968. I retain all proprietary rights, such as patent rights. I also retain the right to use in future works (such as articles or books) all or part of this thesis or dissertation.

I also authorise University Microfilms to use the 350 word abstract of my thesis in Dissertation Abstract International (this is applicable to doctoral theses only).

I have either used no substantial portions of copyright material in my thesis or I have obtained permission to use copyright material; where permission has not been granted I have applied/will apply for a partial restriction of the digital copy of my thesis or dissertation.'

Signed: …………………………………………….........................

Date: ……………………………………….....................................

Authenticity Statement

'I certify that the Library deposit digital copy is a direct equivalent of the final officially approved version of my thesis. No emendation of content has occurred and if there are any minor variations in formatting, they are the result of the conversion to digital format.'

Signed: ……………………………………………..........................

Date: …….…………………………..…………..........................

Originality Statement

‘I hereby declare that this submission is my own work and to the best of my knowledge it contains no materials previously published or written by another person, or substantial proportions of material which have been accepted for the award of any other degree or diploma at UNSW or any other educational institution, except where due acknowledgement is made in the thesis. Any contribution made to the research by others, with whom I have worked at UNSW or elsewhere, is explicitly acknowledged in the thesis. I also declare that the intellectual content of this thesis is the product of my own work, except to the extent that assistance from others in the project's design and conception or in style, presentation and linguistic expression is acknowledged.’

Signed: ………………………………………………..............

Date: ………..………………………….………….............

Acknowledgments

I would like to take this opportunity to express my sincere gratitude to my supervisor *Dr. Wei Gao* for his patient guidance, encouragements and valuable suggestions throughout the research program. Thank you for all the efforts you have put in to help me finish and thank you for your friendship throughout my time studying at UNSW. I am also thankful to my co-supervisor *Professor Chongmin Song* for his insightful comments. The success of the present research would not be possible without their initiation and supports.

I would like to show my thanks to the University of New South Wales and the School of Civil and Environmental Engineering for providing the opportunity to carry on my PhD program. I am also grateful to *Professor Nong Zhang, Professor Francis Tin-Loi* and *Dr. Sawekchai Tangaramvong* for their help and advice. In addition, I also thank *Dr. Ngai M. Kwok* for his help in the writing of this thesis.

I express my deepest gratitude to my loving, encouraging and patient wife, *Dr. Tianran Ren,* for her unconditional love, understanding and endless support during my PhD study.

Last, but not the least, I must acknowledge my parents and my lovely daughter *Isabella* and son *George*, for their deep love, continuing support and encouragement throughout my PhD study. This thesis is dedicated to them.

Abstract

Dynamic behaviour of vehicle-bridge interaction systems with uncertain properties is presented in this thesis. The motivation of the research is the growing need of engineers and researchers to understand the vehicle-bridge coupling dynamics accounting for the unavoidable variations in the system parameters. Anticipation of the dynamic responses of a bridge excited by moving vehicles is crucial to the bridge design as bridge vibration is a significant cause of its deterioration and reduction in long-term serviceability. It is vital to provide insight into the influences of existing uncertainties on the dynamic behaviour of vehicle-bridge coupling systems which are commonplace in structural engineering. The PhD study aims to develop a rational non-deterministic framework for dynamic analysis of a vehicle-bridge interaction system considering the uncertainties in all the system parameters.

Probabilistic analyses are firstly implemented to calculate the statistical moments of bridge responses considering all the system parameters as random variables. Moving spring-mass and quarte-car models are adopted to represent a moving vehicle. Euler-Bernoulli beam is employed to model the bridge. Random variable functional moment method, combined with modal analysis, is extended to develop the mathematical expressions for calculating the mean value and variance of bridge dynamic response. Investigations into the effects of the individual system parameters and the road surface roughness on the bridge response are carried out.

Non-probabilistic approaches are proposed to account for the uncertainties in the vehicle-bridge interaction systems when sufficient statistical data are unavailable. Half-car model is adopted to describe a moving vehicle. Interval operations, Taylor

expansions and perturbation theory are integrated to analyse the vehicle-bridge interaction dynamic problem with predefined small intervals of system parameters. Mathematical formulations are formed for the midpoint value, interval width, lower and upper bounds of interval bridge dynamic response. Furthermore, a heuristic optimization method, improved particle swarm optimization algorithm with low-discrepancy sequence initialized particles and high-order nonlinear time-varying inertia weight and constant acceleration coefficients (LHNPSO), is developed to capture the extreme values of bridge responses regardless of the interval width of system parameters.

Hybrid probabilistic and non-probabilistic analysis is introduced into the vehicle-bridge interaction dynamic system considering a mixture of random and interval uncertainties in the system. The random interval moment method is incorporated in the implementations to obtain the intervals of the first two statistical moments of bridge response. Random interval perturbation method is further developed while the bridge is represented by a finite element model.

The effectiveness and accuracy of the presented approaches are demonstrated by Monte-Carlo simulations and hybrid simulations combining direct simulations for interval variables and Monte-Carlo simulations for random variables. The research reported in this thesis will assist engineers to perform the cost effective design and assessment of non-deterministic dynamic response of vehicle-bridge interaction systems with uncertain properties.

Lists of Publications

Journal papers

J. Dai, W. Gao, N. Zhang, N. Liu, Seismic random vibration analysis of shear beams with random structural parameters, Journal of mechanical science and technology, 24 (2010) 497-504.

N. Liu, W. Gao, C. Song, N. Zhang, Probabilistic dynamic analysis of vehicle-bridge interaction system with uncertain parameters, Computer Modeling in Engineering & Sciences (CMES), 72 (2011) 79-102.

N. Liu, W. Gao, C. Song, N. Zhang, Y.L. Pi, Interval dynamic response analysis of vehicle-bridge interaction system with uncertainty, Journal of Sound and Vibration, 332 (2013) 3218-3231.

N. Liu, W. Gao, C. Song, N. Zhang, Hybrid probabilistic interval dynamic analysis of vehicle-bridge interaction system with uncertainties, International Journal of Structural Stability and Dynamics, 14 (2014), 1350069, 25 pages.

Refereed Conference papers

N. Liu, W. Gao, C. Song, N. Zhang, Hybrid probabilistic interval dynamic analysis of vehicle-bridge interaction system with uncertainties, Proceedings of the 5th Asia Pacific Congress on Computational Mechanics & 4th International Symposium on Computational Mechanics (APCOM2013), 11-14 December 2013, Singapore.

N. Liu, W. Gao, C. Song, N. Zhang, Hybrid probabilistic and non-probabilistic dynamic analysis of vehicle-bridge interaction system with uncertainties, Proceedings of the 1st

Australasian conference on Computational mechanics (ACCM2013), 3-4 October 2013, Sydney, Australia.

N. Liu, W. Gao, C. Song, N. Zhang, Optimization-based interval dynamic response analysis of a bridge under a moving vehicle with uncertain properties, Proceedings of the 22nd Australasian Conference on the Mechanics of Structures and Materials (ACMSM22), 11-14 December 2012, Sydney, Australia.

N. Liu, W. Gao, C. Song, N. Zhang, Interval response analysis of a bridge under a moving vehicle with bounded system parameters based on particle swarm optimization algorithm, Proceedings of European Congress on Computational Methods in Applied Sciences and Engineering (ECCOMAS 2012), 10-14 September 2012, Vienna, Austria.

W. Gao, C. Yang, N. Liu, C. Song, An improved particle swarm optimization algorithm with nonlinearly decreasing inertia weight, Proceedings of the 4th International Conference on Computational Methods (ICCM2012), 25-28 November 2012, Gold Coast, Australia.

N. Liu, W. Gao, C. Song, N. Zhang, Dynamic analysis of vehicle-bridge interaction system with uncertainty, Proceedings of the International Conference on Computational & Experimental Engineering and Sciences (ICCES11), 17-21 April 2011, Nanjing, China.

N. Liu, W. Gao, C. Song, N. Zhang, Dynamic response of a beam bridge under a moving vehicle with bounded system parameters, Proceedings of the 14th Asia Pacific Vibration Conference (APVC14), 5-8 December 2011, Hong Kong, China.

N. Liu, W. Gao, N. Zhang, Dynamic response of bridges under moving vehicles with uncertainty in system parameters, Proceedings of the 21st Australasian Conference on the Mechanics of Structures and Materials (ACMSM21), 7-10 December 2010, Melbourne, Australia.

Table of Contents

List of Figures

List of Tables

LIST OF SYMBOLS

a	Exponent of the power spectral density
a_1	Distance of between the centre of the car and the front wheel
a_2	Distance of between the centre of the car and the back wheel
A	Cross-sectional area
A_r	Roughness coefficient
c_a, c_b	Constants of damping
c_{s1}, c_{s2}	Sprung damping of the vehicle
c_{t1}, c_{t2}	Tire damping
C	Damping of the bridge
C_1	Social parameter
C_2	Cognitive parameter
$[C_b]$	Damping matrix of bridge
$\left[C\left(\vec{a}^R, \vec{b}^I, t\right)\right]$	Stochastic damping matrix of bridge
$\left[C(t)\right]$	Global damping matrix
ΔC	Uncertain component of system damping matrix
E	Young's modulus
$f(x,t)$	Contact force
F	Vehicle-bridge interaction force
I	Moment of inertia
k_{s1}, k_{s2}	Sprung stiffness of the vehicle
k_{t1}, k_{t2}	Tire stiffness
$[K]$	Global stiffness matrix
$[K_b]$	Stiffness matrix of bridge
$\left[K\left(\vec{a}^R, \vec{b}^I, t\right)\right]$	Stochastic stiffness matrix of bridge

$\left[K(t)\right]$	Coupled stiffness matrix
ΔK	Uncertain component of system stiffness matrix
L	Length of bridge
L_c	Twice length of the bridge
$\left[L_b(F(x,t))\right]\left\{F(x,t)\right\}$	Equivalent nodal load vector
m_1	Front sprung mass of vehicle
m_2	Back sprung mass of vehicle
m_s	Sprung mass
m_u	Unsprung mass
m_v	Suspension mass of the vehicle
$\left[M\left(\vec{a}^R,\vec{b}^I,t\right)\right]$	Stochastic mass matrix of bridge
$\left[M(t)\right]$	Coupled mass matrix
ΔM	Uncertain component of system mass matrix
n	Dimension of particles
$\left\{P\left(\vec{a}^R,\vec{b}^I,t\right)\right\}$	Stochastic mass vector of bridge
$\left\{P(t)\right\}$	Equivalent nodal load vector of interaction force
q	Modal coordinate of bridge
$r(x)$	Road roughness
S	Length of the car
$S_r(w_s)$	Displacement PSD of the road roughness
$U(\cdot)$	Uniform distribution
$\left\{U\right\}$	Displacement vector
v	Velocity of the vehicle
$V_{j,k}$	Previous velocity of particle
w_s	Spatial frequency
w_{so}	Reference spatial frequency
$W_{g,k}$	Position of the global best
$W_{j,k}$	Position of the j th particle at the k th iteration

$\overline{W_{j,k}}$	Record of the best solution of particle
$W^{R}(x,t)$	Random vertical displacement of the bridge
$W^{I}(x,t)$	Interval vertical displacement of the bridge
$W^{RI}(x,t)$	Random interval vertical displacement of the bridge
$x_v(t)$	Vertical displacement of vehicle
$x_b(t)$	Vertical displacement of bridge
$x_{bj}(t)$	Vertical displacement of bridge associated modal coordinate
$\dot{x}_{bj}(t)$	Vertical velocity of bridge associated modal coordinate
$\ddot{x}_{bj}(t)$	Vertical acceleration of bridge associated modal coordinate
$\underline{y}$	Lower bound of the interval variable
$\overline{y}$	Upper bound of the interval variable
y^c	Midpoint value of the interval variable
Δy	Interval width of the interval variable
Δy^I	Uncertain interval of the interval variable
Δy_F	Interval change ratio of the interval variable
$\{Y_b\}$	Displacement response vector of bridge
$\{\dot{Y}_b\}$	Velocity response vector of bridge
$\{\ddot{Y}_b\}$	Acceleration response vector of bridge
$\{Y_v\}$	Displacement response vector of vehicle
$\{Y(t)\}$	Nodal displacement vector of bridge
$\{\dot{Y}(t)\}$	Nodal velocity vector of bridge
$\{\ddot{Y}(t)\}$	Nodal acceleration vector of bridge
$\delta(x-vt)$	Dirac delta function
$\phi_i(x)$	Mode shape
φ_k	Random phase angle
$\mu(\cdot)$	Mean value of the displacement of the bridge

$\sigma(\cdot)$	Standard deviation of the displacement of the bridge
π	Pi
ρ	Mass density of bridge
ω	Inertia weight factor
ω_{bj}	Natural frequency of bridge
ω_i	Undamped circular frequency
ω_v	Frequency of vehicle
ζ_{bj}	Damping ratio of bridge
ξ_i	i th modal damping
$(\cdot)^R$	Random variable
$(\cdot)^I$	Interval variable

Chapter 1 Introduction

1.1 Background

The dynamic behaviour of a bridge under the effect of moving vehicle induced loadings has drawn considerable research and practical interests. The problem of a vehicle or multiple vehicles travelling over a bridge is commonly encountered in transportation infrastructures such as highway bridges, railroad bridges, aircraft/taxiway bridges in airports, and many others. When a vehicle passes over a bridge, certain impact or dynamic amplification effect will be imposed on the bridge, which needs to be taken into account in their design and construction considerations. Prediction of the dynamic responses of bridges resulted from moving vehicles is of significance in bridge design because moving vehicles usually produce more destructive loadings than static vehicles do. Although major bridge failures are not usually caused directly by moving vehicles, vehicle induced the dynamic loading has become one of the important causes of deterioration and reduction in long-term serviceability of bridges. Theoretic and experimental investigations had indicated that the vehicle impact on a bridge mainly depends on several factors including the type of bridge and its natural frequencies of vibration, vehicle characteristics and the speed of the vehicle [1].

In the conventional dynamic analysis of a vehicle-bridge interaction system, vehicle and bridge parameters are treated as deterministic ones [2-5]. Although some variations around those base line parameters are taken into account, designs and analyses are performed using deterministic model of which some parameters are varied with prespecified ranges for a set of combined analyses. However, generally speaking, vehicles moving on a bridge have nondeterministic characteristics because the parameters of different kinds of vehicles are different. For instance, mass and tire stiffness of a light passenger car are obviously different from those of a heavy vehicle. Parameters of a bridge, i.e. mass, Young’s modulus and moment of inertial, usually have uncertainties resulting from construction and manufacturing processes as well as due to aging. Therefore, their values are no more equal to the nominal values given in the design.

Uncertainty can be described by randomness, fuzziness and interval. The most common solution to problems of uncertainty is to model the system parameters as random variables. On the other hand, probabilistic approach is the most popular method to solve random problems, and the probabilistic analysis of structures is becoming a significant and hot research field in engineering [6]. Over the past 20 years, probabilistic methods based on the finite element analysis (FEA), such as Monte-Carlo simulation method (MCSM) [7], perturbation method (PM) [8] and stochastic finite element method [9], are widely used in the static and dynamic analysis of structures with random parameters. Probabilistic analysis of structures can provide not only the mean value but also the variance or standard deviation, thus, a better description of structural responses.

Uncertainty analysis is primarily based on probability theory, with the premise that a large number of experimental samples are available to construct the precise probability distributions of parameters. However, for some real engineering problems, it is challenging to obtain sufficient information from parameter sampling. The probabilistic method becomes difficult to use in this context. When objective information on the uncertainties is limited, results from the subjective probabilistic analysis prove to be of little value, and does not justify its high computational cost (see, e.g. [1] and [2]).

Consequently, alternative non-probabilistic concepts have been introduced into non-deterministic numerical modelling. Non-probabilistic approaches such as interval FEA and fuzzy FEA for non-deterministic analysis of structures with uncertain parameters are emerging. Static response, free vibration and forced vibration of structures with interval parameters have been investigated by using interval and/or fuzzy FEA. In the interval approach, uncertainties are considered to be confined within a predefined range. For each uncertain parameter, only its lower and upper bounds need to be provided. However, this approach may be too conservative due to the inherent dependency issues. The fuzzy approach extends this methodology by introducing a level of membership that represents to what extent that a certain value is in the range of possible input values. This concept provides the analyst with a tool to express a degree of possibility for a certain value.

In order to reduce the computational effort and simultaneously investigate the effect of the individual system parameters on the structural responses, Gao et al. [10-12] have proposed the random factor method, fuzzy factor method and interval factor method. These methods have been applied to the analysis of engineering structures with uncertainty.

A few researchers [13-15] have attempted to develop stochastic approaches for the dynamic analysis of vehicle-bridge system with uncertainty. The probabilistic analysis of a bridge under moving loads is usually performed by assuming the characteristic of the bridge as deterministic and the moving forces as stochastic. In general, this kind of analytical model is limited to bridge response assessment and the effect of the randomness of moving vehicles on responses of a bridge have not been investigated extensively. However, little concern has been engaged to identify which random variable has to be considered in the probabilistic analysis and what criteria should be selected to determine the probabilistic safety or serviceability. In particular, probabilistic modelling of a moving vehicle and probabilistic analysis of the interaction between vehicle and bridge systems have not been thoroughly and qualitatively investigated. In addition, sometimes, a complete probabilistic specification of the vehicle-bridge interaction systems uncertainty is impossible, and the capability for the development of reliable predictions, in terms of probability, is fundamentally limited. Consequently, non-probabilistic approaches should be developed to account for the uncertainties in the vehicle-bridge interaction systems when sufficient statistical data are unavailable. Based on the literature, non-probabilistic analysis has not been conducted for the dynamic response of the vehicle-bridge interaction system with uncertain properties. A rational framework for non-deterministic dynamic analysis of vehicle-bridge interaction systems, including the uncertainties in all the system parameters, should be developed. For real engineering applications and the quantitative analysis of vehicles and bridges, the uncertainties in all system parameters should be considered in the analytical model. In addition, it is very important to investigate the effect of the individual parameters on the bridge response and/or vehicle dynamic performance.

1.2 Literature Review

The aim of this section is to critically review the argumentation, and to study what extent to the non-probabilistic methods can be considered as useful alternatives to the existing probabilistic approach.

1.2.1 Uncertainty modelling

Uncertainty can enter mathematical models and experimental measurements in various contexts. A popular way of categorization is to classify uncertainty into two categories: aleatory uncertainty and epistemic uncertainty. They are distinguished respect to its sources [16].

Aleatory uncertainty, also known as statistical uncertainty, is typically irreducible as a property of the system associated with fluctuations/variability; examples include inherent variations in physical processes, such as weather conditions [17]. Therefore, aleatory uncertainties are something not controllable by an experimenter: they exist, and they cannot be suppressed by more accurate measurements. Consequently, aleatory uncertainty can be modelled and processed appropriately with the aid of pure probabilistic methods.

Epistemic uncertainty represents a lack of knowledge about the system due to limited data, measurement limitations, or simplified approximations in modelling system behaviour. This type of uncertainty can be typically reduced by gathering more information. Epistemic uncertainty can be viewed in two ways. It can be defined with reference to a stochastic but poorly known quantity or with reference to a fixed but poorly known physical quantity [18]. The term “stochastic but poorly known” refers to the uncertainty about the distribution type and parameters of a random variable. Epistemic uncertainty may be regarded as subjective uncertainty, the reason may be initiated against the probability of pure model range. These causes involve a lack of information, which hinders the probability model of a unique and potential power generation plan deviating from pure randomness qualitative observation specification.

In many engineering practical cases, however, not even subjective probabilistic information is available. Examples are uncertain quantities for which only bounds or linguistic expressions are known. A probabilistic modelling would then introduce unwarranted information in the form of a distribution function that is totally unjustified. Even the assumption of a uniform distribution ascribes a certain probabilistic regularity and, thus, much more information than that is given by just bounds for a quantity. In more frequent cases, the knowledge about the fluctuations of the structural parameters is very limited so that a clear probabilistic specification of their associated uncertainty is impossible, and the capability for the development of reliable predictions, in terms of probability, is fundamentally limited.

Epistemic uncertainty generally requires further specific models oriented to particular characteristics of the uncertainty associated with the available information. These uncertainty models are constituted on a non-probabilistic or on a mixed probabilistic/non-probabilistic mathematical basis.

This thesis focuses on handling aleatory uncertainty and the first definition of epistemic uncertainty, i.e., epistemic uncertainty with reference to a stochastic but poorly known quantity in a straightforward manner. Therefore, the uncertainty representation methods proposed in this thesis are purely probabilistic, non-probabilistic or a mixture.

1.2.2 Vehicle-bridge interaction system model

a) Bridge model

In dynamic analysis of bridge-vehicle interaction system, the bridge model is one of the three most important factors (the other two being the vehicle model and bridge deck roughness). In the literature, several bridge models have been developed to analyse the bridge response.

The first type of bridge model is Euler-Bernoulli beams. In the beam theories, the simplest model is the Euler-Bernoulli beam model in which cross sections are perpendicular to the neutral axis prior to bending remain plane and perpendicular to the neutral axis posterior to bending, i.e. the so-called Euler-Bernoulli hypothesis holds. For bridge decks modelled as Euler-Bernoulli beams in an early model developed by O'Connor and Chan [19], the bridge was modelled as an assembly of lumped masses interconnected by massless elastic beam elements. This model is usually referred to as the Beam-Element Model. Green and Cebon [20] gave the solution on the dynamic responses in the frequency domain under a quarter-car vehicle model using an iterative procedure. The algorithm was validated by extensive experiments on a typical highway bridge. The vibration behaviour of an elastic homogeneous isotropic beam with different boundary conditions due to a moving harmonic force was studied by Abu-Hilal and Mohsen [21]. Foda and Abduljabbar [22] used the Green function approach to determine the dynamic response of an Euler-Bernoulli beam subjected to a moving mass. Ichikawa et al. [23] investigated the dynamic behaviour of the multi-span continuous Euler-Bernoulli beam traversed by a moving mass at a constant velocity, and solution to this system is obtained by using both eigenfunction expansion and the direct integration method in combination. Michaltsos and Kounadis [24] performed the dynamic analysis of a simply-supported beam subjected to a moving mass including the effects of the centripetal and the Coriolis forces. Law and Zhu [25] investigated the influence of braking on a multi-span non-uniform bridge deck under moving vehicle axle forces. Results showed that vehicle braking generated an equivalent impulsive force covering a wide range of frequency spectrums. Mahmoud and Abou Zaid [26] developed an iterative modal analysis to determine the effect of transverse cracks on the dynamic response of a simply-supported Euler-Bernoulli beam under a moving mass. A large number of vibration modes are excited and they are required in the computation for a high accuracy in the dynamic response of the structure. Nikkhoo et al. [27] investigated the dynamic response of an Euler-Bernoulli beam subjected to a moving mass and used a linear classical optimal control algorithm with a time varying gain matrix with displacement-velocity feedback to control the response of the beam.

It is well known that the Euler-Bernoulli beam is more suitable for slender beams and lower modes of vibration. This theory is inadequate to characterize higher modes of vibration, in particular for short composite beams due to lower shear modulus or shear rigidity. By taking into account the effects of shear deformation, Timoshenko proposed a further improvement of the beam theory. Timoshenko beams are the second type of bridge model which have been widely used. The vibration of a continuous bridge deck modelled as a multi-span Timoshenko beam under a vehicle modelled by a mass-spring system with two DOFs was studied by Chatterjee et al. [28]. Lee [29] obtained the dynamic deflections of a Timoshenko beam under a moving mass by using the Lagrangian approach and the assumed mode method. Wang [30] proposed a method for modal analysis to investigate the vibration of a multi-span Timoshenko beam under a moving force. The ratio of the radius of gyration of the cross-section to the span length was defined as a parameter and the effect of this parameter on the first modal frequency of the beam was studied [31]. Wang and Chou [32] employed the large deflection theory to derive the equation of motion of the Timoshenko beam due to the coupling effect of an external force with the weight of the beam. Results showed that the fundamental natural frequency of the structure increases with the weight of the beam. Esmailzadeh and Ghorashi [33] dealt with the problem of a Timoshenko beam traversed by uniform partially distributed moving masses by using a finite difference based algorithm. Both the dynamic deflection and moment of the beam predicated by the theory, including the effect of weight of the beam, are less than those predicated either by the small deflection theory or by the large deflection theory without including the effect of weight of beam. It can be recognized that a beam model cannot truly represent the three dimensional behaviour of the bridge, particularly a moving vehicle has a path that does not follow the centreline of the bridge.

The third type of bridge models are plates. It is obvious that a simple beam model cannot precisely represent three dimensional behavior particularly in the case of a moving vehicle with paths that are not along the centreline of the bridge. For those reasons, the bridges will be modeled here with plates while the vehicles will be modelled with two or three dimensional models [34]. Marchesiello et al. [35] presented an analytical approach to the vehicle-bridge dynamic interaction problem with a seven DOFs vehicle system moving on a multi-span continuous bridge deck modelled as an isotropic plate. Both the flexural and torsional mode shapes were included in the study. An iterative method was adopted to calculate the responses of the bridge deck and vehicle separately, i.e., the equations of motion of the bridge and vehicle system respectively are not coupled. The theoretical modes, defined by means of the Rayleigh-Ritz approach, had been found to be in good agreement with that from finite element model. Zhu and Law [36] investigated the dynamic behaviour of orthotropic rectangular plates under moving loads. Results showed that the impact factor of the orthotropic plate increased with the ratio between the flexural and torsional rigidities of the plate, and an equivalent beam model of the bridge deck could give an estimate on the impact factor along the centreline of the deck with an under-estimation of the dynamic response at the edge of the structure. The dynamic behaviour of the bridge deck under single and several vehicles moving in different lanes was analysed using the orthotropic plate theory and modal superposition technique. The impact factor was found varying in an opposite trend with the dynamic responses in the different loading cases studied.

b) Dynamic vehicle load model

In studying bridge vibrations, the simplest model of vehicle is assumed as the moving load that can be conceived for a vehicle [37] and [38]. Yang et al. [4] investigated the dynamic response of the beam by using the moving load assumption. The moving loads can be simplified into a moving force for vibration analysis. From this model, the primary bridge dynamic features can be taken due to the vehicle motion. However, the ignorance of the interaction between the bridge and moving vehicle is the main drawback. Therefore, when the mass of the vehicle is small relative to that of the bridge, and only when the vehicle response is not desired, the moving load model is absolutely valid and can be used.

Compared to the moving load model, the moving mass model is an improvement of the moving load model when the effect of the vehicle needs to be taken into account [39]. Sadiku and Leipholz [40] compared the solutions for both the moving mass and moving force problem and the equivalent moving force problem and concluded that the approximate solution for the moving force problem was not always an upper bound solution in terms of the deflection. Whereas, the limitation of this model is that the bouncing action of the moving vehicle relative to the bridge cannot be considered. Such an effect is expected to be significant in the presence of pavement roughness or for vehicles moving at rather high speeds.

The sprung mass model, that a spring can be attached to the moving mass, is developed to investigate the suspension action of the moving vehicle. This is the simplest model that can be used to study the dynamic interaction between the moving vehicle and the supporting bridge. The vehicle is modelled as a single degree-of-freedom (DOF) or two DOFs sprung-mass system which is very useful for modelling multiple vehicles. They are modelled as a set of independent discrete units moving with the same velocity [41]. This eliminates the inertia effects due to roll, pitch and yaw motions of the vehicle. The masses of the vehicles are lumped on the suspension systems which are modelled as linear springs and dashpots. All movements of the suspensions, except the vertical motions, are constrained. Pesterev et al. [42] studied the dynamic response of a one-dimensional distributed parameter system carrying multiple moving oscillators.

It is true in the past two decades that researchers continue to develop vehicle models of various complexities to account for the dynamic properties of the vehicle, for instance, Yang and Wu [4] researched the dynamic interaction response by using a versatile element model. Li et al. [43] considered the influence of the surface profile on the dynamic amplification of a simply supported bridge when it subjects to a quarter-car vehicle model.

The half-car model is usually represented by a planar, two-axle or three-axle and sprung mass system with frictional device. This model was used to study the effects of vehicle braking on the bridge [44]. The effect of the bridge transverse flexibility is considered firstly by including an additional degree-of-freedom in the simple beam representation. The response studies are extended into the braking of vehicle on the bridge approach as well as on the span. The effect of the bridge transverse flexibility on the bridge response is studied by obtaining the response for symmetric as well as eccentric vehicular loading on the bridge. Bridge idealization as an orthotropic plate was used to simulate the transverse flexibility of the bridge deck. The three-axle half-truck model was also used to identify the effect of various parameters on the dynamic load [45].

In most works the bridge was modelled as a line beam (or one-dimensional beam). As a result, the vehicle model was usually limited to a single DOF system or two DOFs system. All the beam-model-based methodologies would become impractical if the entire bridge system is to be modelled for applications. Moreover, the over-simplified vehicle models may not be able to represent well the real vehicles travelling on bridges. Therefore, more sophisticated car models have been developed to analyse the vehicle-bridge interaction system. Deng and Cai [46] presented a method for identifying the parameters of vehicles moving on bridges, In their paper, a single-degree-of-freedom model and a full-scale vehicle model are used.

Tan et al. [47] developed three-dimensional (3D) vehicle model having seven DOFs and analysed the bridge-vehicle interaction problem. The influence of various parameters on the behaviour of the coupled system is studied in three numerical examples. Henchi et al. [31] presented a 3D vehicle model with seven DOFs for the solution of the dynamic interaction problem between the bridge and vehicles. Huang et al. [48] developed a procedure for obtaining the dynamic response of thin-walled curve box girder bridges due to truck loading. The truck simulated as a nonlinear vehicle model with 11 DOFs. Xia et al. [49] proposed a 15-DOF vehicle model and analysed the passage of the high speed train on a concrete box-girder bridge. Zhang et al. [50] developed the space model for dynamic analysis of bridge-train interaction and the train can have one carriage or any amount of carriages. Liu et al. [51] studied the impact behaviour of a multi-girder concrete bridge under single and multiple moving vehicles and presented a 3D nonlinear vehicle model with 11 DOFs. Zhu and Law [36] investigated the dynamic loading on a multi-lane continuous bridge due to vehicles moving on top of the bridge deck. The analytical vehicle is simulated as a two-axle 3D vehicle model with seven DOFs. Song et al. [52] proposed a high-speed train model with 38 DOFs for the 3D finite element analysis of high-speed train-bridge interactions. Kim et al. [53] proposed a three-dimensional means of analysis for the bridge-vehicle interaction to investigate the dynamic responses of a steel girder bridge and vehicles. The governing equations of motion for a three-dimensional bridge-vehicle interaction system taking the roadway surface into account are derived using the Lagrange equation of motion while the coupled bridge-vehicle interaction system is solved using Newmark-β method.

1.2.3 Dynamic analysis of vehicle–bridge interaction system

For dynamic analysis of vehicle-bridge interaction system, various methods have been developed to predict the dynamic response of bridges. In basic and simple cases, where the moving load or moving mass models are considered together with basic beam models, closed-form solutions are available. For more complex vehicle-bridge interaction models, the modal superposition method has been extensively used. The modal superposition methods are typically used to decompose the equation of motion of a bridge–vehicle system in which the response of structure is represented in terms of a set of modal shapes with different amplitudes. The equations of motion of the dynamic system, which are partial differential equations, are transformed into a set of ordinary differential equations which can be easily solved by numerical methods.

Yang and Lin [3] investigated the dynamic interaction between a moving vehicle and the supporting bridge using the modal superposition method with closed-form solution. Zheng et al. [54] studied a multi-span non-uniform beam subjected to a moving load by using model superposition methods. The modal superposition methods have been used by other researchers [55-57]. The modal superposition method can represent the equation of motion in modal coordinate space and therefore can further reduce the size of the problem.

In addition, some direct integration methods have been developed to investigate the dynamic response of vehicle-bridge interaction system such as Newmark-β method [58-60], Runge-Kutta method [61] and others. Moreover, the Fourier transformation method has also been used [62]. In the vehicle–bridge interaction analysis based on the time history, most of the methods are iterative incremental analyses where a convergence criterion is verified in each time increment.

In the modal superposition technique, mode shapes are required to decompose the system equation and they may be difficult to obtain for complex structures. As analytical methods are often limited to simple moving load problems, many researchers have resorted to various numerical methods, such as the finite element method. The finite element method is capable of handling more complex vehicle–bridge models with complex boundary conditions in the dynamic analysis. Research work conducted on simple finite element model of the bridge–vehicle system has already been summarized in the monograph by Fryba [63].

Researchers have often used numerical methods such as FEM to analyse the vibration of slab bridges under moving vehicles [64, 65]. In these studies, the continuous plate was first modeled as an assemblage of suitable plate elements and then direct integration methods were employed to find the dynamic response. Yang and Yau [66] also analysed the dynamic responses of the vehicle (train)-bridge system using finite element method and Newmark finite difference formula. Henchi et al. [67] proposed an algorithm for dynamic analysis of bridges under moving vehicles, using a coupled modal and physical components approach. In their study, a bridge was discretized by two- or three-dimensional finite elements. The vehicular axle loads acting on the bridge deck were represented as nodal forces using shape functions. Numerical simulation showed that the proposed coupled method was much more efficient than the uncoupled iterative method. It also emphasized that there is no limitation concerning the complexity (number of degrees-of-freedom) of the bridge structure in this method if the stability criterion was satisfied. Law and Zhu [68] investigated the dynamic response of long-span box-bridges subject to moving vehicles by using numerical simulations and the results also are verified by experiments. Ju and Lin [69] analysed the dynamic response of the vehicle-bridge interaction system with a finite element model while the effect of braking and acceleration of vehicle were considered. Numerical examples indicated that the bridge longitudinal response was more sensitive than the bridge vertical response when the vehicle braking or acceleration was active, especially for higher piers.

There are other methods based on a finite element model of the structure, especially for the interaction problems. Yang and Wu [4] firstly introduced a vehicle-bridge interaction element to solve the vehicle-bridge interaction problem. This element is versatile to represent vehicles of various complexities, ranging from the moving load, moving mass, sprung mass to the suspended rigid bar. Wu [70] examined the dynamic behaviour of inclined beams subjected to moving masses by using finite element method and by considering the effects of the centripetal and Coriolis forces. Pan and Li

[71] solved the transient response of a vehicle–structure interaction system in time domain. A car of the moving train was modelled as a three DOFs mass-spring-damper system. The rail was modelled as an infinite Euler-Bernoulli beam so that the element would never reach the end of the beam. Contrasting with the finite element method, the moving vehicle always acts at the same point in the numerical model, thereby eliminating the need for keeping track of the contact point with respect to individual elements. Mohebpour et al. [72] developed a beam finite element based on the first-order shear deformation theory to study the dynamic response of laminated composite beams subjected to moving oscillators.

1.2.4 Vehicle-Bridge interaction dynamics with uncertainties

In practice, uncertainty in the vehicle-bridge interaction problem is usually substantial and cannot be neglected. When performing deterministic dynamic analysis of the bridge-vehicle interaction system, different samples of response data are obtained in different computations for a full description of the response statistics of the bridge-vehicle system. Besides, the bridge structure often exhibits with inherent uncertainty. For example, the values of system parameters in the bridge model such as the Young's modulus, mass density, etc. are often varying at different locations. Moreover, concrete bridges in use often contain local damages. Uncertainties also exist in the modelling of the prestressing effect and in the constraints of bridge structures.

Generally speaking, vehicles moving on a bridge have nondeterministic characteristics, because the parameters of different types of vehicles are different. Parameters of a bridge, i.e. mass, Young's modulus, and moment of inertial and others, usually have uncertainty resulting from construction and manufacturing tolerances or caused by corrosion of steel and deterioration of concrete during its lifetime. The contact forces between the bridge and the vehicle are random due to the road surface roughness. The road pavement roughness also has significantly random characteristics in vehicle-bridge interaction system.

Road surface roughness is usually the key point source of dynamic excitation and affects the dynamic behaviour of a vehicle-bridge interaction system. This is also a critical point for vehicle–bridge dynamic analysis. It is generally accepted that road profiles can be represented with a zero-mean normal stationary ergodic random process described by their power spectral density (PSD) [73]. Chatterjee et al. [28] modelled the pavement surface irregularity as a stationary random process characterised by a power spectral density function and it was generated from Monte-Carlo simulations in their study of vehicle–bridge interaction.

Over the years different bridge-vehicle models have been proposed to study the dynamic interaction between bridges and vehicles, and a number of analysis methods have been proposed [74-76]. Among all the methods of identifying dynamic vehicle loads, existing research on the bridge–vehicle interaction problem can mainly be grouped into two categories. Although deterministic analyses of vehicle-bridge interaction problems have been extensively implemented, non-deterministic vehicle-bridge coupled problems need to be studied deeply.

a) Probabilistic Method

According to the conventional structural analysis procedures, external excitations and structural parameters should be modelled as random variables or processed with a probability distribution representing the distribution of the measured values. This modelling results in random response of structural systems in question. When the system uncertainties parameters are expressed as random variables with probability distributions, probabilistic methods are widely employed to analyse the uncertainty problems and can be developed by three main ways:

Firstly, Monte-Carlo simulation (MCS) method is one of the most popular methods used for the simulation of engineering models in past studies due to its effectiveness. Though this method requires a large amount of computation, it becomes more popular especially in structural dynamic analysis as it can be computed by some widespread and inexpensive computational systems [77]. Moreover, Lu et al. [78] presented that MCS is usually a reference method to check the correctness of the new simulation method as it can provide a certain range of the result. In vehicle-bridge interaction system, MCS may be adopted to obtain a group of structural uncertain parameters. For example, Soyoz et al. [79] used the MCS to generate random value of the bridge surface roughness based on mean and standard deviation. Currently the stochastic analysis of a structural system with uncertain system parameters is usually performed with the Monte-Carlo simulation method which is very versatile but comparatively time-consuming [80]. This technique often serves to validate other approximate analytical and numerical methods.

Secondly, perturbation based methods are the other alternative approaches widely used for evaluating the stochastic characteristics [81]. The principle of the perturbation method is to replace the equations which describe the random part of a dynamic system with an infinite series of deterministic equations. In order to evaluate this infinite series, it is often reduced into a Taylor series with only one or two terms [82]. A random parameter of the stochastic system is expressed as a sum of a deterministic component and a random component. The random component usually consists of one or two terms, depending on the order of the perturbation, which represents the randomness in the system. This method has the advantage of making use of existing deterministic modelling techniques such as finite element analysis. It is however restricted by the fact that the uncertainties must be small in order for the assumption in reducing the infinite series to that of a finite one to be accurate. An overview of the method applied to static and dynamic systems and specific examples have been presented by Benaroya and Rehak [83]. These include applications to a quadratic isoparametric triangular element and an axially loaded rod.

Thirdly, stochastic finite element method is another traditional probabilistic approach. This method usually is identified as the traditional finite element method coupled with the perturbation technique. Fryba et al. [84] evaluated the statistics of the dynamic response of a beam under a single moving force using the stochastic finite element analysis by means of the first order perturbation in which the stiffness and damping ware modelled as Gaussian random variables. Wang et al. [85] investigated the dynamic loading on girder bridges with different number of girders and span lengths due to several vehicles moving across rough bridge decks. The maximum impact factors from different bridge girders are obtained for different numbers of loading trucks, road surface roughness, transverse loading positions and the vehicle speeds. Law and Zhu [86] also investigated the random dynamic behaviour of bridges subject to moving vehicles with numerical simulation and experimental verification. The stochastic finite element method [89, 90] is powerful in solving the random eigenvalue problem, static analysis problem and structural stability problem, but the method is haunted by the notorious secular term in structural random dynamical response analysis.

b) Non-Probabilistic Methods

Elishakoff [91] revealed that unjustified assumptions in constructing a probabilistic model for input quantities may be dangerous, and even small Differences between the assumed distribution data and the real ones may yield misleading predictions in the probabilistic reliability analysis. Therefore, non-probabilistic uncertainty models have been considered as beneficial supplements to the traditional probabilistic models [92,93], in particular, when sufficient samples are not available and thus the probabilistic distribution data of the inputs cannot be readily extracted from the results of physical tests or measurements. Recently, a number of non-probabilistic approaches for non-deterministic analysis are emerging. Interval and fuzzy approaches are becoming increasingly popular for the analysis of numerical models that incorporate uncertainty in their description. However, based on the literature review, those non-probabilistic methods for non-deterministic analysis have not been applied to vehicle-bridge interaction systems. Non-probabilistic methods need be extended to analyse the dynamic response of vehicle-bridge interaction system, because of inherent uncertainties in vehicle-bridge interaction system which have been discussed previously.

Interval analysis was first developed by Moore [94] in 1960's. Moore [95] and Alefeld and Herzberger [96] discussed the application of interval properties to various systems. It is useful to describe a property in terms of its upper and lower bounds in engineering analysis and design, especially in the early stage. In the interval approach, uncertainties are considered to be contained within a predefined range, where this range is denoted by upper and lower limits. For each of structural system parameters, the lower and upper bounds need to be provided. The interval method only predicts the response within an interval and no information is given regarding the likely distribution of the response within that interval.

Gao [97] used interval method to investigate the uncertain response of truss structures with varying geometric and material properties. Chen et al. [98] applied interval approach with matrix perturbation technique to investigate the eigenvalues of frame-type structures with uncertain-but-bounded uncertainties. Qiu and Wang [99] also used interval methods based on perturbation theory to analyse structures with uncertain properties. To date, interval finite element analysis, integrating interval concepts and numerical methods for the description of non-deterministic properties in structures and mechanics, has been studied on academic level only. It is should be noted that the interval finite element method is incapable of solving large scale engineering problems due to the dependency issue.

The fuzzy approach extends this methodology by introducing a level of membership that represents the range of possible input values [100]. This concept provides the analyst with a tool to express a degree of possibility for a certain value. Current research activities on this subject mainly concentrate on the actual solution and implementation of interval analysis. The Fuzzy FEA is basically an extension of the interval finite element analysis, and has been studied in a number of specific research domains: static structural analysis [101], dynamic analysis [102, 103]. Recently, Rao et al. [104] used a procedure similar to Fuzzy FEM to derive a fuzzy boundary element method. The numerical procedures developed for the non-probabilistic approaches are all strongly influenced by the specific properties of the analysed physical phenomenon, and only academic examples with very limited size and complexity are considered. Also, the non-probabilistic concepts are almost exclusively applied for the representation of random variables.

The growing interest for non-probabilistic methods for non-deterministic numerical analysis mainly originates from criticism on the credibility of probabilistic analysis when it is based on limited information. Especially when extremely high reliabilities are analysed based on numerical models, design engineers often remain very sceptic regarding the trustworthiness of the numerical predictions. The recent development of the non-probabilistic approaches stems from the argumentation that this lack of credibility is always present in probabilistic analysis results. It is argued that the non-probabilistic concepts could be more appropriate to model certain types of non-deterministic information, resulting in a better representation of the simulated non-deterministic physical behaviour. Especially in early design stages when objective probabilistic information often is not available, non-probabilistic concepts are believed to be of great value.

1.3 Objectives

Non-deterministic analysis of vehicle-bridge interaction system with uncertainty and predictive techniques for the dynamic response of bridge are growing research fields. In the thesis, a vehicle-bridge system model is considered as nondeterministic due to the uncertainties existing in the vehicle and bridge parameters. The displacement responses of bridge are assessed quantitatively using the nondeterministic model and methods. The specific objectives of this thesis are:

1) Developing a theoretical base for the quantitative analysis of dynamic response

of a vehicle-bridge interaction system with uncertain parameters.

2) Developing a rational non-deterministic framework for dynamic analysis of vehicle-bridge interaction problem.
3) Deriving probabilistic, non-probabilistic and hybrid uncertain methods to predict the dynamic responses of the bridge considering different types of uncertainties in all the system parameters.
4) Investigating the effects of system uncertainties on bridge responses.

1.4 Contributions

The proposed quantitative analysis of dynamic response of vehicle-bridge system with uncertainties, to our knowledge, is the worldwide first of its kind and the key theoretical novelties include:

1) Developing rational non-deterministic methodologies for dynamic analysis of a vehicle-bridge interaction system considering the different types of uncertainties in all the system parameters. Considering the vehicle-bridge interaction system model as non-deterministic due to the uncertainties existing in the vehicles and bridge parameters.
2) Developing a probabilistic approach by extending the random variable functional moment method (RVFMM) to analyse the dynamic response of bridge when the system parameters are considered as random variables.
3) Integrating the interval arithmetic, Taylor expansions and perturbation theory to study the dynamic response of bridge when the system parameters are considered as interval variables.

4) Developing a heuristic optimization method, namely improved particle swarm optimization algorithm with low-discrepancy sequence initialized particles and high-order nonlinear time-varying inertia weight and constant acceleration coefficients (LHNPSO), to capture the extreme values of bridge displacement regardless of the interval width of system parameters.
5) Extending the hybrid probabilistic and non-probabilistic methods, random interval moment method (RIMM) and random interval perturbation method (RIPM), to predict the interval random dynamic response of bridge when the system parameters are considered as a mixture random and interval variables.
6) Investigating the effects on the bridge response produced by the individual system parameters and the road surface roughness.
7) Demonstrating the effectiveness and accuracy of the presented approaches by using Monte-Carlo simulation method and a hybrid simulation method combining direct simulation for interval variables and Monte-Carlo simulations for random variables.

1.5 Thesis Outline

The main objective of this dissertation is to develop methodologies for systematically studying the vibration response of bridge-vehicle coupled systems with uncertainties. A brief summary of the content in each chapter of this thesis is provided in the following.

Chapter 2 presents the random variable functional moment method (RVFMM) used in this thesis to investigate the dynamic response of vehicle-bridge interaction system with uncertainty. The vehicle is modelled as moving spring-mass and quarter-car subsystems, as well as the bridge is modelled as a simply supported beam. Two kinds of surface conditions are considered for the bridge deck: smooth and roughness. Monte-Carlo simulation method (MCSM) is adopted as the reference method to verify the results obtained by the RVFMM.

Chapter 3 studies the analytical and computational models used to obtain the dynamic responses of vehicle-bridge interaction system with uncertainties. A non-probabilistic approach called interval method is adopted to address the uncertain problem. The vehicle is represented by a half-car model and the bridge is assumed as a beam. All system parameters are considered as interval variables and the effect of individual system parameter is investigated. In addition, a stochastic optimization method, that is the particle swarm optimization (PSO) method, has been improved to obtain the sharp bounds of bridge displacement response. MCSM is also referred to verify the results obtained from interval method and PSO method.

Chapter 4 presents the analytical and computational results for the vehicle-bridge interaction system and with application of a new hybrid method. In this chapter, the vehicle-bridge interaction model is same as that presented in chapter 3. However, the system parameters are assumed as a mixture type of uncertainties. A non-probabilistic method called random interval moment method is adopted to analyse the dynamic response of the bridge.

In Chapter 5, another method, namely random interval perturbation method (RIPM), is used. The vehicle-bridge interaction system is modelled by the finite element model. Simulation results are also presented to validate the computational results produced by RIPM.

Chapter 6 provides a summary of and a discussion on the work presented in this thesis. The scope for further work is also anticipated.

Chapter 2 Probabilistic Dynamic Analysis of Vehicle-Bridge Interaction System

2.1 Introduction

Dynamic response analysis of vehicle-bridge system is one of the most crucial steps in bridge design as moving vehicles induced vibrations are significant causes of bridge fatigues. Over the past few decades, the interactive problem between vehicles and bridge structures has attracted much more attention due to the rapid increase in the proportion of vehicles and high-speed vehicles in highway and railway traffic [4, 105-107]. Fryba [63] presented the analytical solutions for simply supported and continuous beams with uniform cross-section under moving loads. Green and Cebon [20] gave the solution on the dynamic response of an Euler-Bernoulli beam under a "quarter-car" vehicle model in the frequency domain using an iterative procedure with experimental verification. Yang and Lin [3] investigated the dynamic interaction between a moving vehicle and the supporting bridge by means of the modal superposition technique with closed-form solution. The beam bridge model was extended by Law and Zhu [25] to an orthotropic rectangular plate simply supported on a pair of parallel edges under a stream of moving loads based on the Lagrange equation and modal superposition. Yang and Chang [108,109] studied the extraction of the bridge frequencies from the dynamic response of a passing vehicle using the beam and moving spring-mass model.

The traditional deterministic analysis provides only an "approximation" of the results due to uncertainties in the structural properties as well as in the loading processes. Generally speaking, vehicles moving on a bridge have nondeterministic characteristics because the parameters of different types of vehicles are different. Parameters of a bridge are also having uncertainties resulting from construction and manufacturing tolerances or caused by corrosion of steel and deterioration of concrete during its lifetime. The road pavement roughness also has significantly random characteristics in vehicle-bridge interaction system. Some studies have been carried out on the dynamic response of a bridge deck with the road surface roughness. Gupta [110] used a sine function to simulate the road surface roughness. In order to take into account its random characteristics, a stationary Gaussian random process with certain power spectral density function is used to describe the road roughness profile [15, 25, 111, 112]. Recently, some pioneering research on stochastic dynamic analysis of vehicle-bridge interaction systems have been conducted considering uncertainties in bridge parameters or in moving loadings [15, 25]. The uncertainties of the moving loadings are caused by the road surface roughness and/or vehicle speed. However, for practical engineering applications and the quantitative dynamic analysis response of bridges, the uncertainty of both vehicle and bridge parameters should be included in the analytical model at the same time, which has rarely been investigated in the vehicle-bridge interaction problem. In addition, it is very important to investigate the effect of an individual system parameter on the bridge response.

The most popular approaches to deal with the problems of uncertainty are the probabilistic methods. In the probabilistic approaches, the system parameters are modelled as random variables. Monte-Carlo simulation method [7] is the simplest method for uncertain analysis from a theoretical point of view and is applicable to many different types of systems. This method may suffer from high computational costs if a structural system has a large number of degrees of freedom and/or uncertain parameters. Monte Carlo simulation method is still considered as the most robust probabilistic method and is usually used as a reference method to test the accuracy of other probability approaches [113]. Perturbation method (PM) [8] is also a very popular method to handle the uncertain problems. Perturbation based methods involve first- and second-order Taylor expansions normally. Mean and variance of the response can be found in terms of mean and variance of the basic random variables, thus, distribution information is not required. To increase the accuracy of the statistical moments of the system response, higher order items of the Taylor expansions may be adopted, but more computational efforts are required. For stochastic finite element method [9,114] and spectral stochastic finite element method (SSFEM) [115, 116], the main advantage of this kind approaches is that the complete probability distributions of random variables can be provided. The limitation is that the computational burden increases sharply when the number of random variables increases. This is why the application of SSFEM has been limited to the stochastic systems with a small number of degrees of freedom in the past time. Furthermore, the application range of SSFEM is strongly depended on the approaches adopted to calculate the coefficients of expansion. To reduce the computational effort and simultaneously investigate the effect of the individual system parameters on the structural responses, the random variable functional moment Method

(RVFMM) has also been developed to analyse structures with uncertain parameters [10-12].

In this chapter, the random variable functional moment method is employed to study the dynamic response of vehicle-bridge interaction system by considering the effect of the road surface roughness and the uncertainties in bridge and vehicle parameters. A moving mass and a two-degree-of-freedom vehicle model are used to represent the moving vehicle and the bridge is treated as a simply supported Euler-Bernoulli beam. The expressions for the mean value and standard deviation of bridge response are developed. The effects produced by the road surface roughness, bridge and vehicle parameters on bridge response are also investigated.

The work presented in this chapter is mainly dependent on the research reported by Liu et al. in Computer Modeling in Engineering & Sciences (CMES), 72 (2011) 79-102.

2.2 Road Surface Roughness

In this study, the road surface roughness is regarded as a periodic modulated random process. In ISO-8608 [117] specifications, the road roughness is related to the vehicle velocity by a formula between the velocity power spectral density (PSD) and the displacement PSD. The common formulation of displacement PSD of the roughness is [118]

$$S_r(w_s) = A_r \cdot (\frac{w_s}{w_{so}})^{-a} \tag{2.1}$$

where $S_r(w_s)$ is the displacement PSD of the road surface roughness, A_r is the roughness coefficient in m^2 /cycle/m, w_{so} is the reference spatial frequency, a is an exponent of the PSD and w_s is the spatial frequency in cycle/m, respectively. In the time domain, the road surface roughness function $r(x)$ is given by

$$r(x) = \sum_{k=1}^{N} ([4A_r(\frac{(2\pi k)}{L_c w_{so}})^{-2}]^{1/2} \cdot \cos(w_{sk}x - \varphi_k)) \tag{2.2}$$

where

$$w_{sk} = k \cdot \Delta w_s, k = 1, 2, \cdots N, \Delta w_s = 2\pi / L_c$$

$$w_{so} = \frac{1}{2\pi}$$

L_c is twice of the length of the bridge, φ_k is generated between 0 and 2π by using the Monte Carlo simulations.

2.3 Bridge and Vehicle Models

2.3.1 Moving mass on bridge

The bridge is modelled as a simply supported beam and the vehicle is represented as a concentrated mass m_v supported by a spring of stiffness k_v with the effect of damping of the suspension system neglected as shown in Figure 2.1. The damping property or pavement irregularity of the bridge is not considered in this study. The beam is assumed to be of the Euler-Bernoulli type with constant cross sections. ρ, E, I, L and C are the mass per unit length, elastic modulus, moment of inertia, length and damping of the beam, respectively.

The equation of motion governing the transverse or vertical vibration of the bridge and moving vehicle can be written as

$$\rho \frac{\partial^2 W(x,t)}{\partial t^2} + C \frac{\partial W(x,t)}{\partial t} + EI \frac{\partial^4 W(x,t)}{\partial x^4} = f(t)\delta(x - vt) \tag{2.3}$$

$$f(t) = -m_v g + k_v (x_v(t) - W\big|_{x=vt}) \tag{2.4}$$

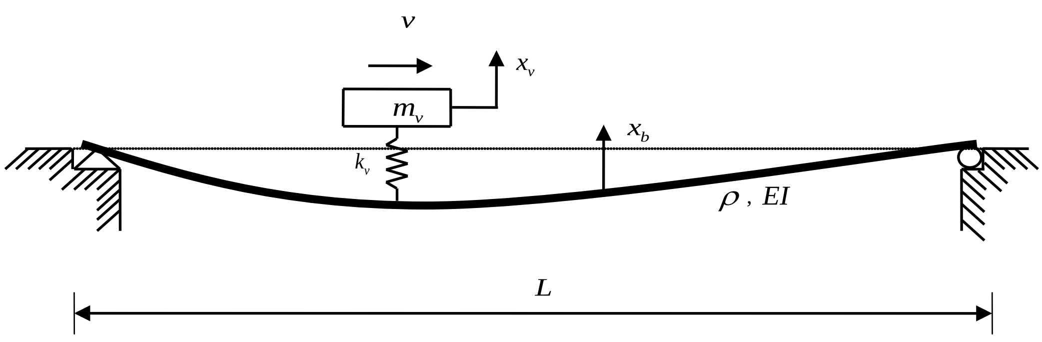

Figure 2.1 Vehicle moving on a simply supported bridge.

where $W(x,t)$ is the vertical displacement of the bridge, $x_v(t)$ is the vertical displacement of the moving vehicle, $f(t)$ is the contact force, $\delta(x - vt)$ is the Dirac delta function evaluated at the contact point at position $x = vt$, and v is the speed of the moving vehicle.

Using the modal superposition method, the solution to Eq. (2.3) can be expressed in terms of the mode shapes $\varphi_j(x)$ and associated modal coordinates $x_{bj}(t)$

$$W(x,t) = \sum_{j=1}^{\infty} \varphi_j(x) x_{bj}(t) \tag{2.5}$$

For simply supported beam, the mode shapes of the bridge are given by

$$\varphi_j(x) = \sin \frac{j\pi x}{L} \tag{2.6}$$

Substituting Eq. (2.6) into Eq. (2.5) yields

$$W(x,t)=\sum_{j=1}^{\infty}\sin\frac{j\pi x}{L}x_{bj}(t) \tag{2.7}$$

Substituting Eq. (2.7) into Eq. (2.3), multiplying both sides of the equation by $\varphi_j^T(x)$, and integrating with respect to x over the length L of the beam, obtains

$$\int_0^L \rho\varphi_j^T(x)\sum_{j=1}^{\infty}\varphi_j(x)\ddot{x}_{bj}(t)dx+\int_0^L C\varphi_j^T(x)\sum_{j=1}^{\infty}\varphi_j(x)\dot{x}_{bj}(t)dx+\int_0^L EI\varphi_j^T(x)\sum_{j=1}^{\infty}\frac{\partial^4\varphi_j(x)}{\partial x^4}x_{bj}(t)dx$$

$$=\int_0^L \varphi_j^T(x)\left[-m_v g+k_v(x_v(t)-W\big|_{x=vt})\right]\delta(x-vt)dx \tag{2.8}$$

where

$$\varphi_j^T(x)=\sin\frac{j\pi x}{L} \tag{2.9}$$

Eq.(2.8) can also be rewritten as

$$\rho\ddot{x}_{bj}(t)\int_0^L\sin^2\frac{j\pi x}{L}dx+C\dot{x}_{bj}(t)\int_0^L\sin^2\frac{j\pi x}{L}dx+EI\left(\frac{n\pi}{L}\right)^4 x_{bj}(t)\int_0^L\sin^2\frac{j\pi x}{L}dx$$

$$=-m_v g\int_0^L\sin\frac{j\pi x}{L}\delta(x-vt)dx+k_v x_v(t)\int_0^L\sin\frac{j\pi x}{L}\delta(x-vt)dx\text{-}$$

$$k_v W\big|_{x=vt}\int_0^L\sin\frac{j\pi x}{L}\delta(x-vt)dx \tag{2.10}$$

In this chapter, the Wilson’s damping hypothesis is adopted, that is

$$C=2\rho\zeta_{bj}\omega_{bj} \tag{2.11}$$

where ζ_{bj} is the damping ratio of the *jth* vibration mode, and ω_{bj} is the corresponding natural frequency of the bridge

$$\omega_{bj}=\frac{j^2\pi^2}{L^2}\sqrt{\frac{EI}{\rho}} \tag{2.12}$$

Using the orthogonality conditions for the mode shapes, Eq.(2.8) becomes

$$\ddot{x}_{bj}(t)+2\zeta_{bj}\omega_{bj}\dot{x}_{bj}(t)+\omega_{bj}^{2}x_{bj}(t)$$

$$=-\frac{2m_v g}{\rho L}\sin\frac{j\pi vt}{L}+\frac{2k_v}{\rho L}x_v(t)\sin\frac{j\pi vt}{L}-\frac{2k_v}{\rho L}\left[\sum_{j=1}^{\infty}\sin\frac{j\pi x}{L}x_{bj}(t)\right]\sin\frac{j\pi vt}{L} \tag{2.13}$$

The frequency of vibration of the vehicle is

$$\omega_v=\sqrt{\frac{k_v}{m_v}} \tag{2.14}$$

Substituting Eq.(2.14) into Eq.(2.13) yields

$$\ddot{x}_{bj}(t)+2\zeta_{bj}\omega_{bj}\dot{x}_{bj}(t)+\omega_{bj}^{2}x_{bj}(t)$$

$$=-\frac{2m_v g}{\rho L}\sin\frac{j\pi vt}{L}+\frac{2\omega_v^2 m_v}{\rho L}x_v(t)\sin\frac{j\pi vt}{L}-\frac{2\omega_v^2 m_v}{\rho L}\left[\sum_{j=1}^{\infty}\sin\frac{j\pi x}{L}x_{bj}(t)\right]\sin\frac{j\pi vt}{L} \tag{2.15}$$

If we assume that the vehicle mass m_v is much less than the bridge mass ρL, Eq.(2.15) can be approximated as

$$\ddot{x}_{bj}(t)+2\zeta_{bj}\omega_{bj}\dot{x}_{bj}(t)+\omega_{bj}^{2}x_{bj}(t)=-\frac{2m_v g}{\rho L}\sin\frac{j\pi vt}{L} \tag{2.16}$$

Assuming zero initial conditions, the solution to Eq.(2.16) is

$$x_{bj}(t)=-\frac{2m_v g}{\rho L\omega_{dbj}}\int_0^t e^{-\zeta_{bj}\omega_{bj}(t-\tau)}\sin\omega_{dbj}(t-\tau)\sin\frac{j\pi vt}{L}d\tau \tag{2.17}$$

where

$$\omega_{dbj}=\sqrt{1-\zeta_{bj}^{2}}\,\omega_{bj} \tag{2.18}$$

Substituting Eqs.(2.12) and (2.18) into Eq.(2.17) yields

$$x_{bj}(t)=\frac{2m_v g}{L\sqrt{1-\zeta_{bj}^2}\frac{j^2\pi^2}{L^2}\sqrt{\rho EI}}\int_0^t e^{-\zeta_{bj}\frac{j^2\pi^2}{L^2}\sqrt{\frac{EI}{\rho}}(t-\tau)}\sin\left(\sqrt{1-\zeta_{bj}^2}\frac{j^2\pi^2}{L^2}\sqrt{\frac{EI}{\rho}}(t-\tau)\right)\sin\frac{j\pi vt}{L}d\tau \tag{2.19}$$

Then, the vertical displacement of the bridge can be expressed as

$$W(x,t)=-\sum_{j=1}^{\infty}\sin\frac{j\pi x}{L}$$

$$\cdot\frac{2m_v g}{L\sqrt{1-\zeta_{bj}^2}\frac{j^2\pi^2}{L^2}\sqrt{\rho EI}}\int_0^t e^{-\zeta_{bj}\frac{j^2\pi^2}{L^2}\sqrt{\frac{EI}{\rho}}(t-\tau)}\sin\left(\sqrt{1-\zeta_{bj}^2}\frac{j^2\pi^2}{L^2}\sqrt{\frac{EI}{\rho}}(t-\tau)\right)\sin\frac{j\pi vt}{L}d\tau \tag{2.20}$$

2.3.2 Quarter-car moving on bridge

In the vehicle-bridge interaction system demonstrated in Figure 2.2, the bridge is modelled as an Euler-Bernoulli beam; the vehicle is represented by a quarter-car model. Over the years various types of bridge models have been used in studies on bride-vehicle dynamics. Continuum models of simply supported Euler-Bernoulli beams are the most popular ones, mainly due to its simplicity and ability to obtain closed-form solution. The two-degree-of-freedom quarter-car model is generally reputed to be sufficiently accurate for capturing the essential features of dynamic performance of a moving vehicle. Here, m_s and m_u denote the sprung mass and unsprung mass respectively; a linear spring of stiffness k_s and a linear damper with damping rate c_s is used to represent the unsprung system, the tire is also modelled by a linear spring of stiffness k_t, and a linear damper with damping rate c_t.

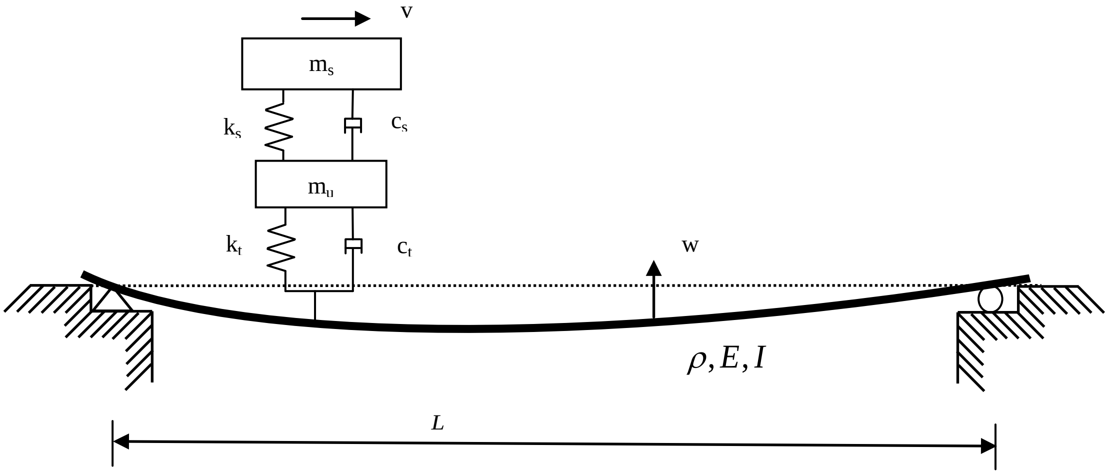

Figure 2.2 Quarter-car moving on a simply supported bridge.

The equation of motion for the bridge can be expressed same as Eq. (2.1). For vehicle moving on a smooth road surface, $f(x,t)$ can be expressed as

$$f(x,t) = k_t[x_u - w] + c_t[\dot{x}_u - \dot{w}] - (m_u + m_s)g \tag{2.21}$$

where k_t, c_t, m_u and m_s are the tire stiffness, tire damping, sprung mass and unsprung mass of the vehicle, respectively.

Considering the roughness of the road surface, $f(x,t)$ can be expressed as

$$f(x,t) = k_t[x_u - w - r(x)] + c_t[\dot{x}_u - \dot{w} - \dot{r}(x)] - (m_u + m_s)g \tag{2.22}$$

where $r(x)$ is the road surface roughness of the bridge.

Using the modal superposition method, the bridge response can be calculated with the following equation

$$\int_0^L \rho\phi_j^T(x)\sum_{j=1}^{\infty}\phi_j(x)\ddot{x}_{bj}(t)dx + \int_0^L C\phi_j^T(x)\sum_{j=1}^{\infty}\phi(x)\dot{x}_{bj}(t)dx + \int_0^L EI\phi_j^T(x)\cdot\sum_{j=1}^{\infty}\frac{\partial^4\phi_j(x)}{\partial x^4}x_{bj}(t)dx$$

$$= \int_0^L \rho\phi_j^T(x)[k_t[x_u - W|_{x=vt}] + c_t[\dot{x}_u - \dot{W}|_{x=vt} - (m_s + m_u)g]\delta(x - vt)dx \qquad (2.23)$$

and

$$\rho\ddot{x}_{bj}(t)\cdot\frac{L}{2} + C\dot{x}_{bj}(t)\cdot\frac{L}{2} + EI\cdot(\frac{j\pi}{L})^4\cdot\frac{L}{2}\cdot x_{bj}(t) = -(m_s + m_u)g\cdot\sin\frac{j\pi vt}{L}$$

$$+k_t(x_u - W|_{x=vt})\cdot\sin\frac{j\pi vt}{L} + c_t(\dot{x}_u - \dot{W}|_{x=vt})\cdot\sin\frac{j\pi vt}{L} \qquad (2.24)$$

Dividing the two sides of Eq.(2.24) by $\rho\cdot\frac{L}{2}$, we have

$$\ddot{x}_{bj}(t) + \frac{C}{\rho}\dot{x}_{bj}(t) + \frac{EI}{\rho}\cdot(\frac{j\pi}{L})^4\cdot x_{bj}(t) = -\frac{2(m_s + m_u)g}{\rho L}\cdot\sin\frac{j\pi vt}{L}$$

$$+\frac{2k_t(x_u - W|_{x=vt})}{\rho L}\cdot\sin\frac{j\pi vt}{L} + \frac{2c_t(\dot{x}_u - \dot{W}|_{x=vt})}{\rho L}\cdot\sin\frac{j\pi vt}{L} \qquad (2.25)$$

Assuming that the vehicle mass is much less than the bridge mass, Eq. (2.25) can be approximated as

$$\ddot{x}_{bj}(t) + 2\zeta_{bj}\omega_{bj}\cdot\dot{x}_{bj}(t) + \omega_{bj}^2\cdot\dot{x}_{bj}(t) = -\frac{2(m_s + m_u)g}{\rho L}\cdot\sin\frac{j\pi vt}{L} \qquad (2.26)$$

The solution of Eq.(2.26) can be obtained by using the Convolution Integral (Duhamel Integral)

$$x_{bj} = \frac{1}{\omega_{bj}}\int_0^t e^{-\zeta_{bj}\omega_{bj}(t-\tau)}\sin\omega_{dbj}(t-\tau)\cdot(-\frac{2(m_s + m_u)g}{\rho L}\cdot\sin\frac{j\pi v\tau}{L})d\tau$$

(2.27)

Eq.(2.27) can be rewritten as

$$x_{bj} = -\frac{2(m_s + m_u)g}{\rho L\omega_{dbj}}\int_0^t e^{-\zeta_{bj}\omega_{bj}(t-\tau)}\sin\omega_{dbj}(t-\tau)\cdot\sin\frac{j\pi v\tau}{L}d\tau \qquad (2.28)$$

Therefore, the bridge response can be calculated by

$$W(x,t) = -\frac{2(m_s + m_u)g}{\rho L\omega_{dbj}}\sum_{j=1}^{\infty}\sin\frac{n\pi x}{L}\int_0^t e^{-\zeta_{bj}\omega_{bj}(t-\tau)}\sin\omega_{dbj}(t-\tau)\cdot\sin\frac{j\pi v\tau}{L}d\tau \qquad (2.29)$$

2.3.3 Dynamic response of bridge considering road surface roughness

Accounting for the road surface roughness of the bridge, Eq. (2.23) becomes

$$\int_0^L \rho\phi_j^T(x)\sum_{j=1}^{\infty}\phi_j(x)\ddot{x}_{bj}(t)dx+\int_0^L C\phi_j^T(x)\sum_{j=1}^{\infty}\phi(x)\dot{x}_{bj}(t)dx+\int_0^L EI\phi_j^T(x)\cdot\sum_{j=1}^{\infty}\frac{\partial^4\phi_j(x)}{\partial x^4}x_{bj}(t)dx$$
$$=\int_0^L \rho\phi_j^T(x)[k_t[x_u-W|_{x=vt}-r(x)]+c_t[\dot{x}_u-\dot{W}|_{x=vt}-\dot{r}(x)-(m_s+m_u)g]\delta(x-vt)dx \quad (2.30)$$

Eq. (2.30) can be rewritten as

$$\rho\ddot{x}_{bj}(t)\int_0^L \sin^2\frac{j\pi x}{L}dx+C\dot{x}_{bj}(t)\int_0^L \sin^2\frac{j\pi x}{L}dx+EI(\frac{n\pi}{L})^4 x_{bj}(t)\int_0^L \sin^2\frac{j\pi x}{L}dx$$

$$=-(m_s+m_u)g\int_0^L \sin\frac{j\pi x}{L}\delta(x-vt)dx+k_t(x_u-W|_{x=vt}-r\left(x\right))\int_0^L \sin\frac{j\pi x}{L}\delta(x-vt)dx$$

$$+c_t(\dot{x}_u-\dot{W}|_{x=vt}-\dot{r}\left(x\right))\int_0^L \sin\frac{j\pi x}{L}\delta(x-vt)dx \quad (2.31)$$

Similarly as Eq.(2.25) is derived from Eq.(2.22), Eq. (2.31) can be further developed as

$$\ddot{x}_{bj}(t)+2\zeta_{bj}\omega_{bj}\cdot\dot{x}_{bj}(t)+\omega_{bj}^2\cdot\dot{x}_{bj}(t)=-\frac{2(m_s+m_u)g}{\rho L}\cdot\sin\frac{j\pi vt}{L}$$

$$-\frac{2[k_t r(x)+C_t\dot{r}(x)]}{\rho L}\cdot\sin\frac{j\pi vt}{L} \quad (2.32)$$

Then, the jth modal displacement can be obtained as

$$x_{bj}=-\frac{2}{\rho L\omega_{dbj}}\int_0^t((m_s+m_u)g-[k_t r(x)+c_t\dot{r}(x)])e^{-\zeta_{bj}\omega_{bj}(t-\tau)}\sin\omega_{dbj}(t-\tau)\cdot\sin\frac{j\pi v\tau}{L}d\tau \quad (2.33)$$

Therefore, the bridge response can be expressed as

$$W(x,t) = -\frac{2}{\rho L\omega_{dbj}}\sum_{j=1}^{\infty}\sin\frac{j\pi x}{L}\int_0^t((m_s+m_u)g-[k_t r(x)+c_t\dot{r}(x)])$$

$$\cdot e^{-\zeta_{bj}\omega_{bj}(t-\tau)}\sin\omega_{dbj}(t-\tau)\cdot\sin\frac{j\pi v\tau}{L}d\tau \quad (2.34)$$

2.4 Mean Value and Variance of Random Bridge Response

In this study, the vehicle and bridge parameters, such as m_s, m_u, ρ, E and I, are considered as random variables. The mean value (μ) and standard deviation (σ) of the each random variable are given respectively. The coefficient of variation (Cov) $\nu = \sigma / \mu$ is also used to describe the dispersal degree of a random variable. In the following, the expressions for the mean value and variance of bridge displacement response are developed by means of the random variable functional moment method (RVFMM). The uncertainty of bridge parameters will lead to the randomness of its natural frequencies. Consequently, the combination of uncertainties in bridge dynamic characteristics, system parameters and road surface will result in the randomness of bridge response.

2.4.1 Numerical characteristics of bridge response with smooth road surface under moving mass

Vehicle and bridge parameters, m_v, ρ, E and I, are considered as random variables. Uncertainty of bridge response introduced by random system parameters can also be described by randomness. The expressions for mean value and standard deviation of bridge displacement response can be derived by means of the random variable functional moment method [12]

$$\mu_{W(x,t)} = -\sum_{j=1}^{\infty} \sin\frac{j\pi x}{L} \frac{2\mu_{m_v} g}{S_1\sqrt{\mu_\rho \mu_E \mu_I}} \int_0^t S_2 \sin(S_3) \sin\frac{j\pi vt}{L} d\tau \tag{2.35}$$

$$\sigma_{W(x,t)} = \left\{ -\sum_{j=1}^{\infty} \sin\frac{j\pi x}{L} \right.$$

$$\{\frac{2g}{S_1\sqrt{\mu_\rho \mu_E \mu_I}} \int_0^t S_2 \sin(S_3) \sin\frac{j\pi vt}{L} d\tau\}^2 \sigma_{m_v}^2$$

$$+\{\frac{\mu_{m_v} g}{S_1\sqrt{\mu_\rho^3 \mu_E \mu_I}} \int_0^t S_2 \sin(S_3) \sin\frac{j\pi vt}{L} d\tau\}^2 \sigma_\rho^2$$

$$+\{\frac{2\mu_{m_v} g}{S_1\sqrt{\mu_\rho \mu_E \mu_I}} \int_0^t S_2 \frac{1}{2}\zeta_{bj} \frac{j^2\pi^2}{L^2} \sqrt{\frac{\mu_E \mu_I}{\mu_\rho^3}} (t-\tau) \sin(S_3) \sin\frac{j\pi vt}{L} d\tau\}^2 \sigma_\rho^2$$

$$+\{\frac{2\mu_{m_v} g}{S_1\sqrt{\mu_\rho \mu_E \mu_I}} \int_0^t S_2 \cos(S_3) \frac{1}{2}\sqrt{1-\zeta_{bj}^2}\, \frac{j^2\pi^2}{L^2} \sqrt{\frac{\mu_E \mu_I}{\mu_\rho^3}} (t-\tau) \sin\frac{j\pi vt}{L} d\tau\}^2 \sigma_\rho^2$$

$$+\{\frac{\mu_{m_v} g}{S_1\sqrt{\mu_\rho \mu_E^3 \mu_I}} \int_0^t S_2 \sin(S_3) \sin\frac{j\pi vt}{L} d\tau\}^2 \sigma_E^2$$

$$+\{\frac{2\mu_{m_v} g}{S_1\sqrt{\mu_\rho \mu_E \mu_I}} \int_0^t S_2 \frac{1}{2}\zeta_{bj} \frac{j^2\pi^2}{L^2} \sqrt{\frac{\mu_I}{\mu_E \mu_\rho}} (t-\tau) \sin(S_3) \sin\frac{j\pi vt}{L} d\tau\}^2 \sigma_E^2$$

$$+\{\frac{2\mu_{m_v} g}{S_1\sqrt{\mu_\rho \mu_E \mu_I}} \int_0^t S_2 \cos(S_3) \frac{1}{2}\sqrt{1-\zeta_{bj}^2}\, \frac{j^2\pi^2}{L^2} \sqrt{\frac{\mu_I}{\mu_E \mu_\rho}} (t-\tau) \sin\frac{j\pi vt}{L} d\tau\}^2 \sigma_E^2$$

$$+\{\frac{\mu_{m_v} g}{S_1\sqrt{\mu_\rho \mu_E \mu_I^3}} \int_0^t S_2 \sin(S_3) \sin\frac{j\pi vt}{L} d\tau\}^2 \sigma_I^2$$

$$+\{\frac{2\mu_{m_v}g}{S_1\sqrt{\mu_\rho\mu_E\mu_I}}\int_0^t S_2\frac{1}{2}\zeta_{bj}\frac{j^2\pi^2}{L^2}\sqrt{\frac{\mu_E}{\mu_I\mu_\rho}}(t-\tau)\sin(S_3)\sin\frac{j\pi vt}{L}d\tau\}^2\sigma_I^2$$

$$+\{\frac{2\mu_{m_v}g}{S_1\sqrt{\mu_\rho\mu_E\mu_I}}\int_0^t S_2\cos(S_3)\frac{1}{2}\sqrt{1-\zeta_{bj}^2}\frac{j^2\pi^2}{L^2}\sqrt{\frac{\mu_E}{\mu_I\mu_\rho}}(t-\tau)\sin\frac{j\pi vt}{L}d\tau\}^2\sigma_I^2\Bigg\}^{\frac{1}{2}} \tag{2.36}$$

where symbol $\mu_{(\bullet)}$ and $\sigma_{(\bullet)}$ denote the mean value and standard deviation of the random variable $(\bullet)$ respectively. The items S_1, S_2 and S_3 are given by

$$S_1 = L\sqrt{1-\zeta_{bj}^2}\frac{j^2\pi^2}{L^2}, S_2 = e^{-\zeta_{bj}\frac{j^2\pi^2}{L^2}\sqrt{\frac{\mu_E\mu_I}{\mu_\rho}}(t-\tau)}, S_3 = \sqrt{1-\zeta_{bj}^2}\frac{j^2\pi^2}{L^2}\sqrt{\frac{\mu_E\mu_I}{\mu_\rho}}(t-\tau) \tag{2.37}$$

2.4.2 Numerical characteristics of bridge response with smooth road surface under moving quarter-car model

From Eq. (2.29) and by using the RVFMM, the mean value of the bridge displacement can be expressed as

$$\mu_{W(x,t)} = -\frac{2(\mu_{m_s}+\mu_{m_u})g}{S_1\sqrt{\mu_\rho\mu_E\mu_I}}\sum_{j=1}^{\infty}\sin\frac{j\pi x}{\mu_L}\int_0^t S_2\sin(S_3)\cdot\sin\frac{j\pi v\tau}{\mu_L}d\tau \tag{2.38}$$

where

$$\mu_I = \frac{1}{12}\mu_b\mu_h^3$$
$$\mu_{\omega_{bj}} = \frac{j^2\pi^2}{\mu_L^2}\sqrt{\frac{\mu_E\mu_h^2}{12\mu_\rho}},$$

The variance of bridge displacement response can be calculated by

$$\sigma^2_{W(x,t)} = [\frac{\partial W_{(x,t)}}{\partial m_s}]^2 \cdot \sigma^2_{m_s} + [\frac{\partial W(x,t)}{\partial m_u}]^2 \cdot \sigma^2_{m_u} + [\frac{\partial W_{(x,t)}}{\partial \rho}]^2 \cdot \sigma^2_{\rho} + [\frac{\partial W_{(x,t)}}{\partial L}]^2 \cdot \sigma^2_L$$

$$+ [\frac{\partial W_{(x,t)}}{\partial E}]^2 \cdot \sigma^2_E + [\frac{\partial W_{(x,t)}}{\partial I}]^2 \cdot \sigma^2_I \tag{2.39}$$

where

$$\frac{\partial W(x,t)}{\partial m_s} = -\frac{2(1+\mu_{m_u})g}{S_1\sqrt{\mu_\rho \mu_E \mu_I}} \sum_{j=1}^{\infty} \sin\frac{j\pi \cdot x}{\mu_L} \int_0^t S_2 \sin(S_3) \sin\frac{j\pi v\tau}{\mu_L} d\tau \tag{2.40}$$

$$\frac{\partial W(x,t)}{\partial m_u} = -\frac{2(1+\mu_{m_s})g}{\mu_A \mu_\rho \mu_L \mu_{\omega_{dbj}}} \sum_{j=1}^{\infty} \sin\frac{j\pi \cdot x}{\mu_L} \int_0^t e^{-\mu_{\zeta_{bj}} \mu_{\omega_{bj}}(t-\tau)} \sin \mu_{\omega_{dbj}}(t-\tau) \sin\frac{j\pi v\tau}{\mu_L} d\tau \tag{2.41}$$

$$\frac{\partial W(x,t)}{\partial E} = \frac{4(\mu_{m_u}+\mu_{m_s})g}{\mu_A \mu_\rho \mu_L \mu_{\omega_{dbj}}} \sum_{j=1}^{\infty} \sin\frac{j\pi \cdot x}{\mu_L} \int_0^t e^{-\mu_{\zeta_{bj}} \mu_{\omega_{bj}}(t-\tau)} \sin \mu_{\omega_{dbj}}(t-\tau) \sin\frac{j\pi v\tau}{\mu_L} d\tau \tag{2.42}$$

$$\frac{\partial W(x,t)}{\partial I} = \frac{(\mu_{m_u}+\mu_{m_s})g}{S_1\sqrt{\mu_\rho \mu_E \mu_I^3}} \sum_{j=1}^{\infty} \sin\frac{j\pi \cdot x}{\mu_L} \int_0^t S_2 \sin(S_3) \sin\frac{j\pi v\tau}{\mu_L} d\tau$$

$$+\frac{(\mu_{m_u}+\mu_{m_s})g}{S_1\sqrt{\mu_\rho \mu_E \mu_I}} \int_0^t S_2 \zeta_{bj} \frac{j^2\pi^2}{\mu_L^2} \cdot \sqrt{\frac{\mu_E}{\mu_I \mu_\rho}} (t-\tau) \sin(S_3) \tag{2.43}$$

$$\frac{\partial W(x,t)}{\partial \rho} = \frac{(\mu_{m_u}+\mu_{m_s})g}{S_1\sqrt{\mu_\rho^3 \mu_E \mu_I}} \sum_{j=1}^{\infty} \sin\frac{j\pi \cdot x}{\mu_L} \int_0^t S_2 \sin(S_3) \sin\frac{j\pi v\tau}{\mu_L} d\tau$$

$$+\frac{(\mu_{m_u}+\mu_{m_s})g}{S_1\sqrt{\mu_\rho \mu_E \mu_I}} \int_0^t S_2 \zeta_{bj} \frac{j^2\pi^2}{\mu_L^2} \cdot \sqrt{\frac{\mu_E \mu_I}{\mu_\rho^3}} (t-\tau) \sin(S_3) \sin\frac{j\pi v\tau}{\mu_L} d\tau \sin\frac{j\pi v\tau}{\mu_L} d\tau \tag{2.44}$$

$$\frac{\partial W(x,t)}{\partial L} = \frac{(\mu_{m_u}+\mu_{m_s})g}{S_1\sqrt{\mu_\rho^3 \mu_E \mu_I}} \sum_{j=1}^{\infty} \sin\frac{j\pi \cdot x}{\mu_L} \int_0^t S_2 \sin(S_3) \sin\frac{j\pi v\tau}{\mu_L} d\tau$$

$$+\frac{(\mu_{m_u}+\mu_{m_s})g}{S_1\sqrt{\mu_\rho \mu_E \mu_I}} \int_0^t S_2 \zeta_{bj} \frac{j^2\pi^2}{\mu_L^2} \cdot \sqrt{\frac{\mu_E \mu_I}{\mu_\rho^3}} (t-\tau) \sin(S_3) \sin\frac{j\pi v\tau}{\mu_L} d\tau \tag{2.45}$$

2.4.3 Numerical characteristics of bridge response with road surface roughness under moving quarter-car model

Similarly, from Eq. (2.34) and by using the RVFMM, the mean value of the bridge displacement considering the road surface roughness can be expressed as

$$\mu_{W(x,t)} = -\frac{2}{S_1\sqrt{\mu_\rho \mu_E \mu_I}} \sum_{j=1}^{\infty} \sin\frac{j\pi x}{\mu_L} \int_0^t ((\mu_{m_s} + \mu_{m_u})g - [\mu_{k_t}\mu_{r(x)} + \mu_{c_t}\mu_{\dot{r}(x)}])$$

$$\cdot S_2 \sin(S_3) \cdot \sin\frac{j\pi v\tau}{\mu_L} d\tau \tag{2.46}$$

The variance of the bridge displacement can be computed by

$$\sigma^2_{W(x,t)} = [\frac{\partial W_{(x,t)}}{\partial m_s}]^2 \cdot \sigma^2_{m_s} + [\frac{\partial W(x,t)}{\partial m_u}]^2 \cdot \sigma^2_{m_u} + [\frac{\partial W_{(x,t)}}{\partial \rho}]^2 \cdot \sigma^2_\rho + [\frac{\partial W_{(x,t)}}{\partial L}]^2 \cdot \sigma^2_L + [\frac{\partial W_{(x,t)}}{\partial I}]^2 \cdot \sigma^2_I$$

$$+[\frac{\partial W_{(x,t)}}{\partial E}]^2 \cdot \sigma^2_E + [\frac{\partial W_{(x,t)}}{\partial k_t}]^2 \cdot \sigma^2_{k_t} + [\frac{\partial W_{(x,t)}}{\partial c_t}]^2 \cdot \sigma^2_{c_t} + [\frac{\partial W_{(x,t)}}{\partial \varphi}]^2 \cdot \sigma^2_\varphi \tag{2.47}$$

where

$$\frac{\partial W(x,t)}{\partial m_s} = -\frac{2((1+\mu_{m_u})g - [\mu_{k_t}\mu_{r(x)} + \mu_{c_t}\mu_{\dot{r}(x)}])}{S_1\sqrt{\mu_\rho \mu_E \mu_I}} \sum_{j=1}^{\infty} \sin\frac{j\pi \cdot x}{\mu_L} \cdot \int_0^t S_2 \sin(S_3) \sin\frac{j\pi v\tau}{\mu_L} d\tau \tag{2.48}$$

$$\frac{\partial W(x,t)}{\partial m_u} = -\frac{2((1+\mu_{m_s})g - [\mu_{k_t}\mu_{r(x)} + \mu_{c_t}\mu_{\dot{r}(x)}])}{S_1\sqrt{\mu_\rho \mu_E \mu_I}} \sum_{j=1}^{\infty} \sin\frac{j\pi \cdot x}{\mu_L} \cdot \int_0^t S_2 \sin(S_3) \sin\frac{j\pi v\tau}{\mu_L} d\tau \tag{2.49}$$

$$\frac{\partial W(x,t)}{\partial E} = \frac{4(\mu_{m_u} + \mu_{m_s})g}{\mu_A \mu_\rho \mu_L \mu_{\omega_{dbj}}} \sum_{j=1}^{\infty} \sin\frac{j\pi \cdot x}{\mu_L} \int_0^t e^{-\mu_{\zeta_{bj}}\mu_{\omega_{bj}}(t-\tau)} \sin\mu_{\omega_{dbj}}(t-\tau) \sin\frac{j\pi v\tau}{\mu_L} d\tau$$

$$+\frac{2}{\mu_A \mu_\rho \mu_L \mu_{\omega_{dbj}}} \cdot \int_0^t e^{-\mu_{\zeta_{bj}}\mu_{\omega_{bj}}(t-\tau)} \sin\mu_{\omega_{dbj}}(t-\tau) \cdot [\mu_{k_t}\mu_{r(x)} + \mu_{c_t}\mu_{\dot{r}(x)}] d\tau \tag{2.50}$$

$$\frac{\partial W(x,t)}{\partial I}=\frac{(\mu_{m_u}+\mu_{m_s})g}{S_1\sqrt{\mu_\rho\mu_E\mu_I^3}}\sum_{j=1}^{\infty}\sin\frac{j\pi\cdot x}{\mu_L}\int_0^t S_2\sin(S_3)\sin\frac{j\pi v\tau}{\mu_L}d\tau$$

$$+\frac{2}{S_1\sqrt{\mu_\rho\mu_E\mu_I^3}}\cdot\int_0^t S_2\sin(S_3)\cdot[\mu_{k_t}\mu_{r(x)}+\mu_{c_t}\mu_{\dot{r}(x)}]d\tau$$

$$+\frac{(\mu_{m_u}+\mu_{m_s})g}{S_1\sqrt{\mu_\rho\mu_E\mu_I}}\int_0^t S_2\zeta_{bj}\frac{j^2\pi^2}{\mu_L^2}\cdot\sqrt{\frac{\mu_E}{\mu_I\mu_\rho}}(t-\tau)\sin(S_3)\sin\frac{j\pi v\tau}{\mu_L}d\tau$$

$$+\frac{2}{S_1\sqrt{\mu_\rho\mu_E\mu_I}}\cdot\int_0^t\frac{1}{2}\zeta_{bj}\frac{j^2\pi^2}{\mu_L^2}\cdot\sqrt{\frac{\mu_E}{\mu_I\mu_\rho}}(t-\tau)\sin(S_3)\cdot[\mu_{k_t}\mu_{r(x)}+\mu_{c_t}\mu_{\dot{r}(x)}]d\tau$$

$$+\frac{(\mu_{m_u}+\mu_{m_s})g}{S_1\sqrt{\mu_\rho\mu_E\mu_I}}\int_0^t S_2\zeta_{bj}\frac{j^2\pi^2}{\mu_L^2}\cdot\sqrt{\frac{\mu_E}{\mu_I\mu_\rho}}(t-\tau)\cos(S_3)\sin\frac{j\pi v\tau}{\mu_L}d\tau$$

$$+\frac{2}{S_1\sqrt{\mu_\rho\mu_E\mu_I}}\cdot\int_0^t\frac{1}{2}\zeta_{bj}\frac{j^2\pi^2}{\mu_L^2}\cdot\sqrt{\frac{\mu_E}{\mu_I\mu_\rho}}(t-\tau)\cos(S_3)\cdot[\mu_{k_t}\mu_{r(x)}+\mu_{c_t}\mu_{\dot{r}(x)}]d\tau \qquad (2.51)$$

$$\frac{\partial W(x,t)}{\partial \rho}=\frac{(\mu_{m_u}+\mu_{m_s})g}{S_1\sqrt{\mu_\rho^3\mu_E\mu_I}}\sum_{j=1}^{\infty}\sin\frac{j\pi\cdot x}{\mu_L}\int_0^t S_2\sin(S_3)\sin\frac{j\pi v\tau}{\mu_L}d\tau$$

$$+\frac{2}{S_1\sqrt{\mu_\rho^3\mu_E\mu_I}}\cdot\int_0^t S_2\sin(S_3)\cdot[\mu_{k_t}\mu_{r(x)}+\mu_{c_t}\mu_{\dot{r}(x)}]d\tau$$

$$+\frac{(\mu_{m_u}+\mu_{m_s})g}{S_1\sqrt{\mu_\rho\mu_E\mu_I}}\int_0^t S_2\zeta_{bj}\frac{j^2\pi^2}{\mu_L^2}\cdot\sqrt{\frac{\mu_E\mu_I}{\mu_\rho^3}}(t-\tau)\sin(S_3)\sin\frac{j\pi v\tau}{\mu_L}d\tau$$

$$+\frac{(\mu_{m_u}+\mu_{m_s})g}{S_1\sqrt{\mu_\rho\mu_E\mu_I}}\int_0^t S_2\zeta_{bj}\frac{j^2\pi^2}{\mu_L^2}\cdot\sqrt{\frac{\mu_E\mu_I}{\mu_\rho^3}}(t-\tau)\cos(S_3)\sin\frac{j\pi v\tau}{\mu_L}d\tau$$

$$+\frac{2}{S_1\sqrt{\mu_\rho\mu_E\mu_I}}\cdot\int_0^t\frac{1}{2}\zeta_{bj}\frac{j^2\pi^2}{\mu_L^2}\cdot\sqrt{\frac{\mu_E\mu_I}{\mu_\rho^3}}(t-\tau)\cos(S_3)\cdot[\mu_{k_t}\mu_{r(x)}+\mu_{c_t}\mu_{\dot{r}(x)}]d\tau \qquad (2.52)$$

$$\frac{\partial W(x,t)}{\partial L}=\frac{(\mu_{m_u}+\mu_{m_s})g}{S_1\sqrt{\mu_\rho^3\mu_E\mu_I}}\sum_{j=1}^{\infty}\sin\frac{j\pi\cdot x}{\mu_L}\int_0^t S_2\sin(S_3)\sin\frac{j\pi v\tau}{\mu_L}d\tau$$

$$+\frac{2}{S_1\sqrt{\mu_\rho^3\mu_E\mu_I}}\cdot\int_0^t S_2\sin(S_3)\cdot[\mu_{k_t}\mu_{r(x)}+\mu_{c_t}\mu_{\dot{r}(x)}]d\tau$$

$$+\frac{(\mu_{m_u}+\mu_{m_s})g}{S_1\sqrt{\mu_\rho\mu_E\mu_I}}\int_0^t S_2\zeta_{bj}\frac{j^2\pi^2}{\mu_L^2}\cdot\sqrt{\frac{\mu_E\mu_I}{\mu_\rho^3}}(t-\tau)\sin(S_3)\sin\frac{j\pi v\tau}{\mu_L}d\tau$$

$$+\frac{2}{S_1\sqrt{\mu_\rho\mu_E\mu_I}}\cdot\int_0^t\frac{1}{2}\zeta_{bj}\frac{j^2\pi^2}{\mu_L^2}\cdot\sqrt{\frac{\mu_E\mu_I}{\mu_\rho^3}}(t-\tau)\sin(S_3)\cdot[\mu_{k_t}\mu_{r(x)}+\mu_{c_t}\mu_{\dot{r}(x)}]d\tau$$

$$+\frac{2}{S_1\sqrt{\mu_\rho\mu_E\mu_I}}\cdot\int_0^t\frac{1}{2}\zeta_{bj}\frac{j^2\pi^2}{\mu_L^2}\cdot\sqrt{\frac{\mu_E\mu_I}{\mu_\rho^3}}(t-\tau)\cos(S_3)\cdot[\mu_{k_t}\mu_{r(x)}+\mu_{c_t}\mu_{\dot{r}(x)}]d\tau$$

$$+\frac{(\mu_{m_u}+\mu_{m_s})g}{S_1\sqrt{\mu_\rho\mu_E\mu_I}}\int_0^t S_2\zeta_{bj}\frac{j^2\pi^2}{\mu_L^2}\cdot\sqrt{\frac{\mu_E\mu_I}{\mu_\rho^3}}(t-\tau)\cos(S_3)\sin\frac{j\pi v\tau}{\mu_L}d\tau \tag{2.53}$$

$$\frac{\partial W(x,t)}{\partial k_t}=-\frac{2((\mu_{m_s}+\mu_{m_u})g-[\mu_{r(x)}+\mu_{c_t}\mu_{\dot{r}(x)}])}{S_1\sqrt{\mu_\rho\mu_E\mu_I}}\sum_{j=1}^{\infty}\sin\frac{j\pi\cdot x}{\mu_L}\cdot\int_0^t S_2\sin(S_3)\sin\frac{j\pi v\tau}{\mu_L}d\tau \tag{2.54}$$

$$\frac{\partial W(x,t)}{\partial c_t}=-\frac{2((\mu_{m_s}+\mu_{m_u})g-[\mu_{k_t}\mu_{r(x)}+\mu_{\dot{r}(x)}])}{S_1\sqrt{\mu_\rho\mu_E\mu_I}}\sum_{j=1}^{\infty}\sin\frac{j\pi\cdot x}{\mu_L}\cdot\int_0^t S_2\sin(S_3)\sin\frac{j\pi v\tau}{\mu_L}d\tau \tag{2.55}$$

$$\frac{\partial W(x,t)}{\partial\varphi}=-\frac{2((\mu_{m_s}+\mu_{m_u})g-[\mu_{k_t}\mu_{\dot{r}(x)}+\mu_{c_t}\mu_{r(x)}])}{S_1\sqrt{\mu_\rho\mu_E\mu_I}}\sum_{j=1}^{\infty}\sin\frac{j\pi\cdot x}{\mu_L}\cdot\int_0^t S_2\sin(S_3)\sin\frac{j\pi v\tau}{\mu_L}d\tau \tag{2.56}$$

2.5 Numerical Simulations

2.5.1 Example 1: Moving mass on the bridge

The nominal values of vehicle and bridge parameters are listed in Table 2.1. To investigate the influence of vehicle speed on bridge response, two different moving speeds, $v = 5m/s$ and $v = 10m/s$, are taken into account. The corresponding vertical displacement responses of the bridge midpoint are plotted in Figures 2.3 and 2.4, respectively.

Table 2.1 Parameters of the vehicle-bridge interaction system

Description	Notation	Value
Length of the bridge	L	40m
Moment of inertia	I	0.16m^4
Young's modulus	E	$2.3 \times 10^{10} N/m^2$
Mass density	ρ	5000kg/m^3
Vehicle mass	m_v	1500kg
Stiffness	k_v	550kN/m

The amplitude of the bridge vertical displacement in Figure 2.4 is larger than that in Figure 2.3, which means the amplitude of the bridge response increases along the speed of moving vehicle. Meanwhile, the period of periodic displacement response of the bridge is longer for lower moving speed of the vehicle.

It can also be observed from Figures 2.3 and 2.4 that the maximum amplitudes of bridge response at its midpoint do not occur at the time when the vehicle pass this position. The similar phenomenon can also be found in research literature [4].

To investigate the effects of system parameters on the bridge response, the randomness of each of parameters is considered separately first and then simultaneously. The coefficient of variations (Cov, that is the ratio of the standard deviation to mean value of a random variable) of m_v, ρ, E and I is taken as 0.1. The vehicle speed is constant and $v = 10\,m/s$. The standard deviations (SD) of the vertical displacement response of bridge midpoint are given in Figures 2.5-2.9 to demonstrate the changes of bridge responses produced by the uncertainties of system parameters.

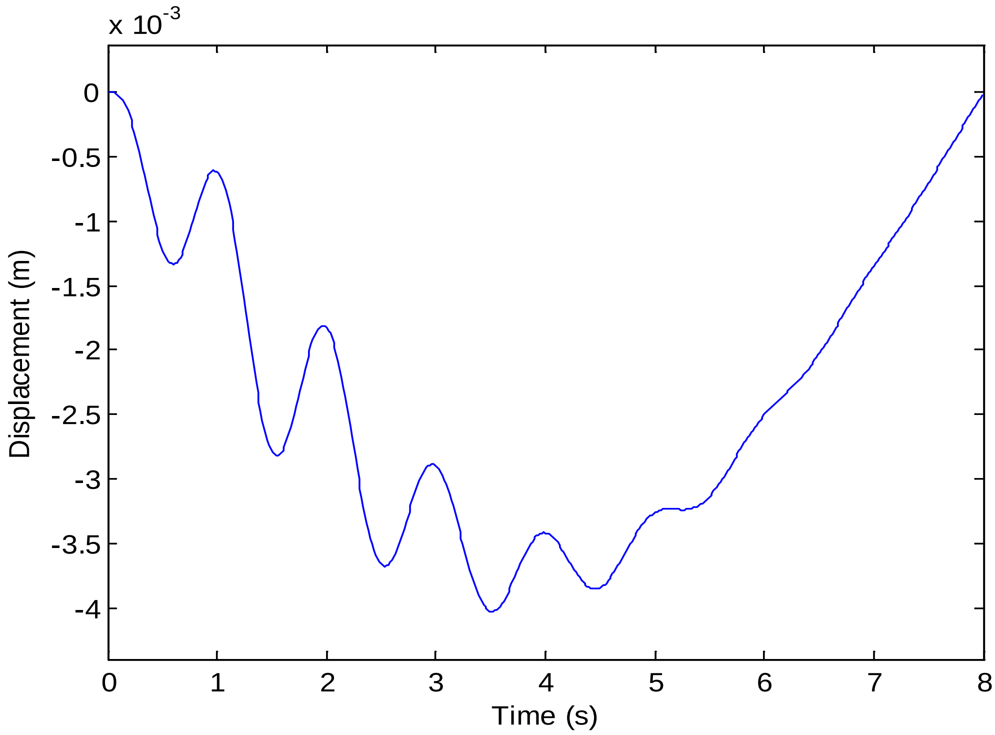

Figure 2.3 Vertical displacement response of bridge midpoint

($v = 5m/s$).

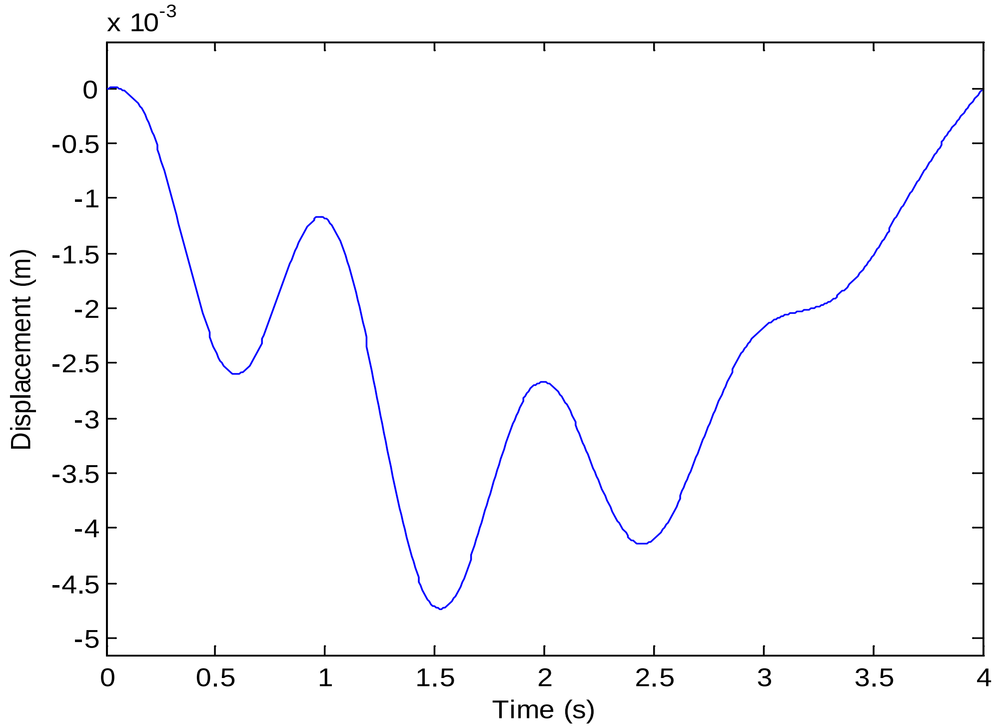

Figure 2.4 Vertical displacement response of bridge midpoint

($v = 10\, m/s$).

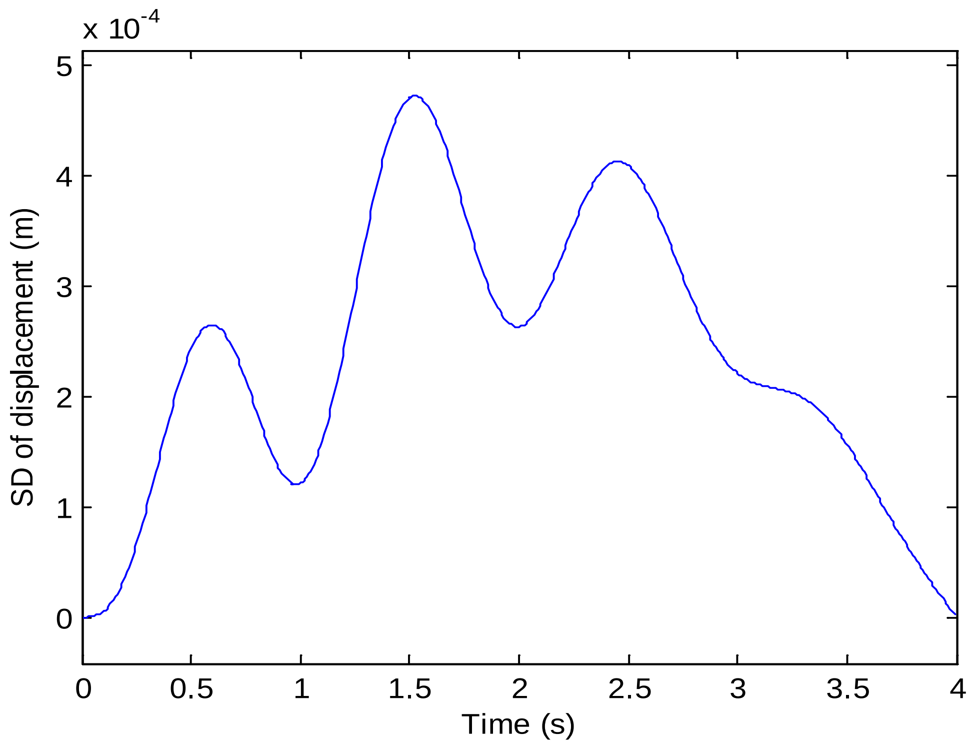

Figure 2.5 Standard deviation of displacement response of bridge midpoint

($Cov(m) = 0.1$).

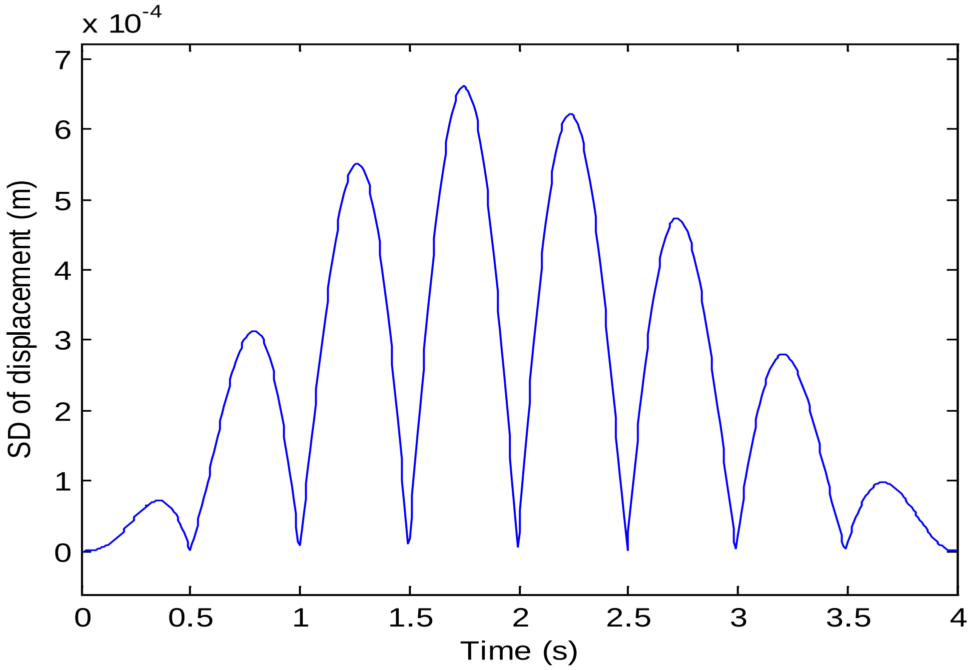

Figure 2.6 Standard deviation of displacement response of bridge midpoint ($Cov(\rho)=0.1$).

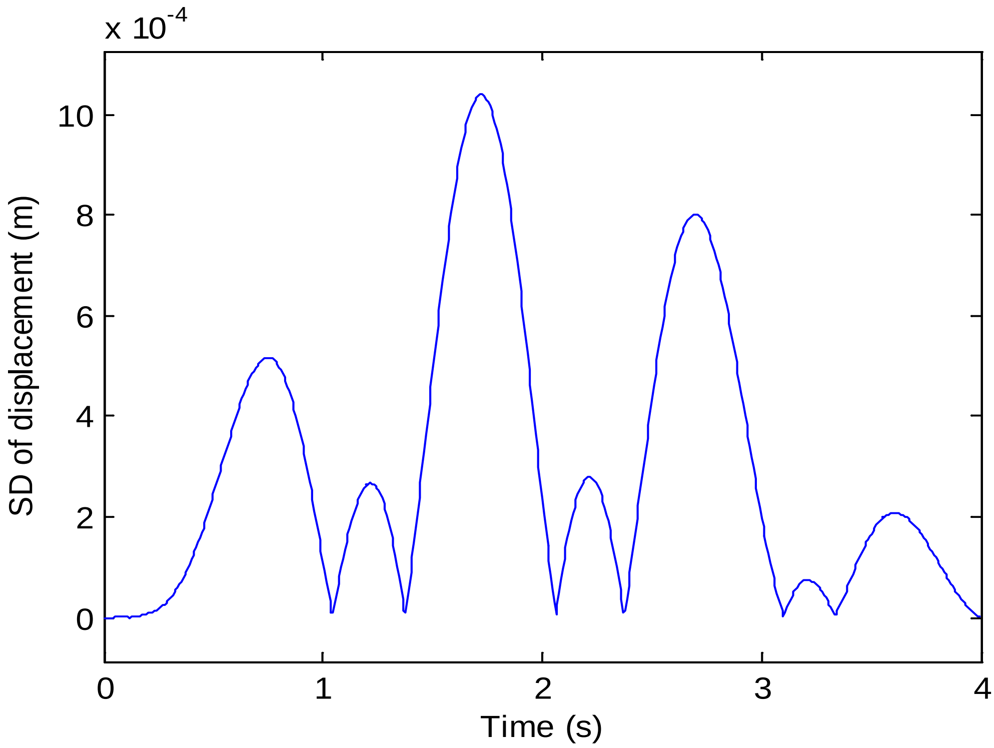

Figure 2.7 Standard deviation of displacement response of bridge midpoint ($Cov(E)=0.1$).

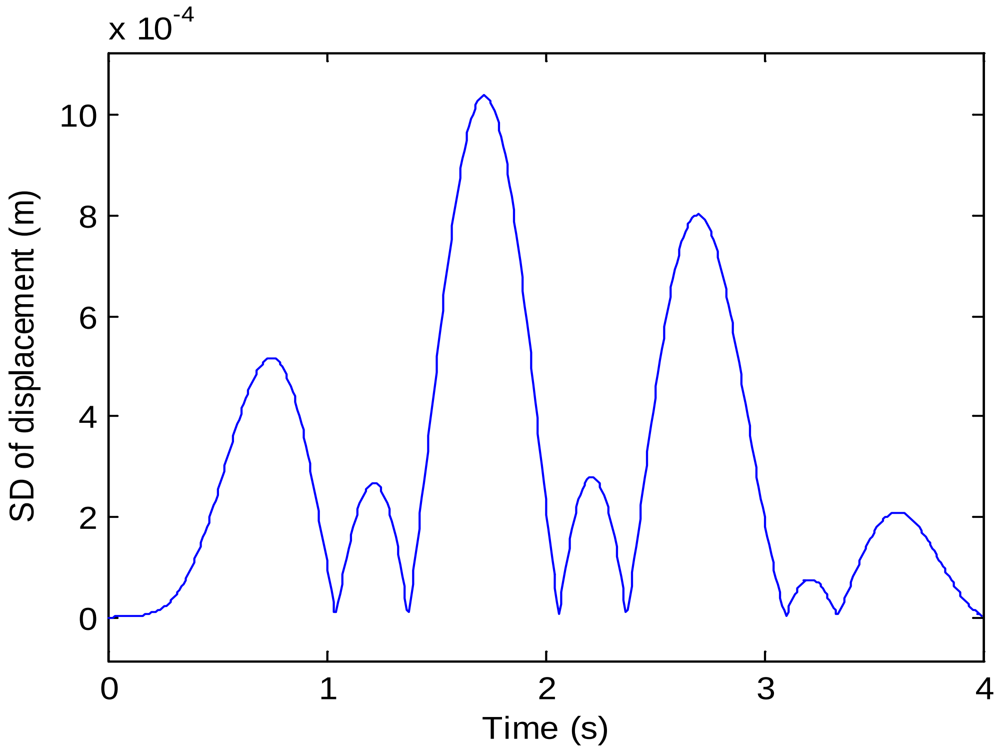

Figure 2.8 Standard deviation of displacement response of bridge midpoint

($Cov(I) = 0.1$)**.**

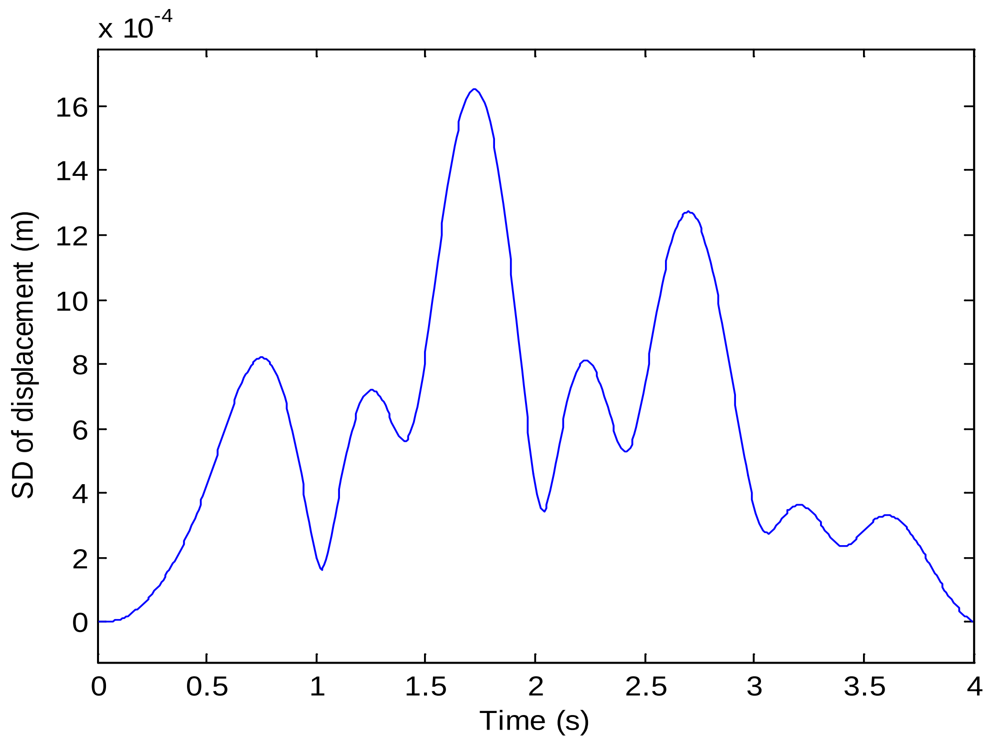

Figure 2.9 Standard deviation of displacement response of bridge midpoint

($Cov(all\ \ parameters) = 0.1$)**.**

Comparing Figure 2.5 with Figures 2.6-2.8, it can be found that the uncertainty of bridge parameters produces greater effects on bridge displacement response. In another word, bridge response is more sensitive to the changes of its own parameters. The elastic modulus and inertia moment of area of the bridge have quite similar influences on the bridge response, and the changes of the bridge response caused by their uncertainties are bigger than that caused by the mass per unit. The standard deviation of bridge response becomes significantly large if the randomness of all parameters is considered simultaneously.

The differences of periods between the standard deviations shown in Figures 2.5-2.9 and the mean value shown in Figure 2.5 of displacement response are mainly caused by the random variable functional moment method employed in this study.

2.5.2 Example 2: Quarter-car moving on the bridge

Vehicle and bridge parameters are considered as random variables in the following examples. The mean values of system parameters used in the numerical simulations are given in Tables 2.2 and 2.3. The vehicle parameters are typical for a lightly damped passenger car [118].

Table 2.2 Parameters of the bridge model

Description	Notation	Value
Length of the bridge	L	$40m$
Moment of inertia	I	$0.15m^4$
Damping ratio	ζ	0.05
Young's modulus	E	$3.2 \times 10^{10} N/m^2$
Mass density	ρ	$5200 kg/m^3$

Table 2.3 Parameters of the vehicle model

Description	Notation	Value
Sprung mass	m_s	1600*kg*
Unsprung mass	m_u	160*kg*
Suspension damping	c_s	960*Ns/m*
Tire damping	c_t	960*Ns/m*
Suspension stiffness	k_s	1.8×10^{7}*N/m*
Vehicle stiffness	k_t	7.2×10^{7}*N/m*

2.5.2.1 Random response analysis of vehicle-bridge system with smooth road surface (Quarter-car model)

Two different vehicle speeds, $v = 5m/s$ and $v = 20m/s$, are used to investigate the influence caused by vehicle speed on bridge response. The corresponding bridge displacement responses at mid-span are shown in Figures 2.10 and 2.11, respectively. Again, the amplitude of the bridge mid-span displacement in Figure 2.11 is bigger than that in Figure 2.10, which means the bridge displacement response increases along with the increase of the vehicle speed. Meanwhile, the period of periodic displacement response of the bridge is longer for lower moving speed of the vehicle. Again, it can also be observed from Figures 2.10 and 2.11 that the maximum amplitudes of bridge response at its mid-span do not occur at the time when the vehicle pass this position. The similar phenomenon can also be found in research literature [3].

To investigate the effects of system parameters on the bridge response, the randomness of each of parameters is considered separately first and then simultaneously. The coefficient of variation (COV) is assumed as 0.05 for random variables m_s, m_u, ρ, E, I . The velocity of vehicle is constant ($v = 5m/s$). The standard deviations (SD) of the bridge mid-span displacement response are given in Figures 2.12(a)-(f) to demonstrate the changes of bridge responses produced by the uncertainty of system parameters.

From Figures 2.12(a) and 2.12(b), it can be seen that the vehicle sprung and unsprung masses produce the similar effects on the bridge response. The elastic modulus and inertia moment of area of the bridge have quite similar influences on the bridge response, and the changes of the bridge response caused by their uncertainties are bigger than that caused by the mass per unit, which can be found from Figures 2.12(c)-(e). Comparing Figures 2.12(a)-(b) with 2.12(c)-(e), it can be observed that the standard deviations of bridge response caused by the randomness of its own parameters are greater than those caused by vehicle parameters. In other words, vehicle response is more sensitive to the uncertainty of bridge parameters. Figure 2.12(f) shows that the standard deviation of bridge response is much bigger if the randomness of all parameters is considered simultaneously.

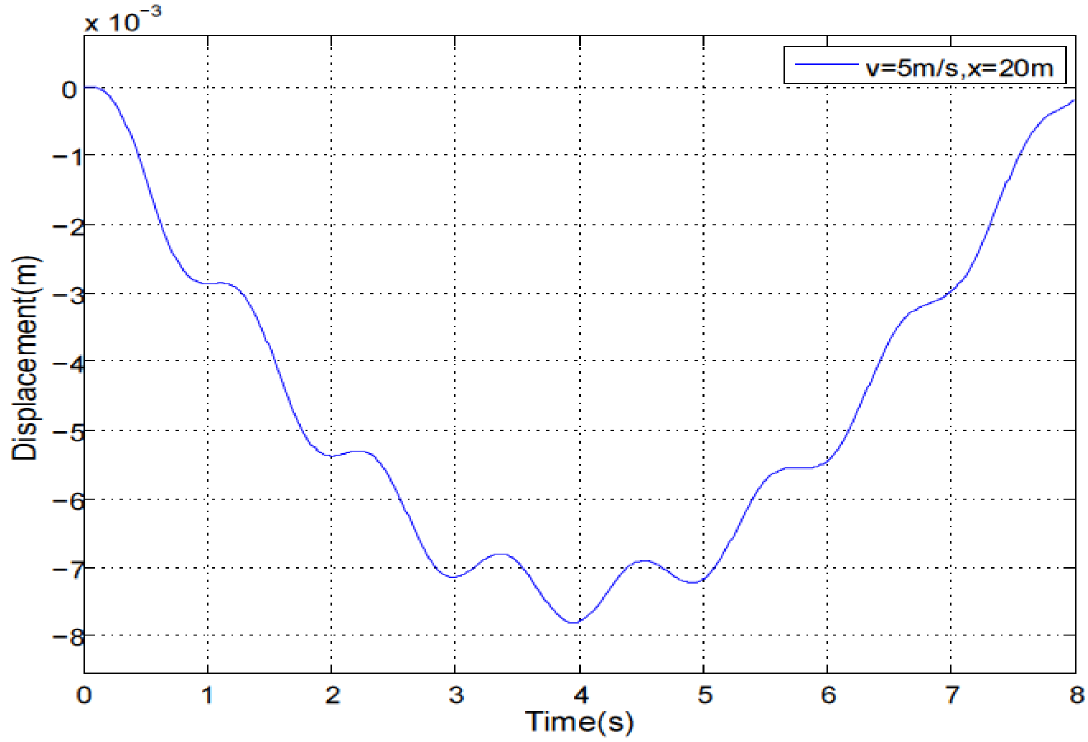

Figure 2.10 Displacement response of bridge mid-span (v=5m/s, x=20m)

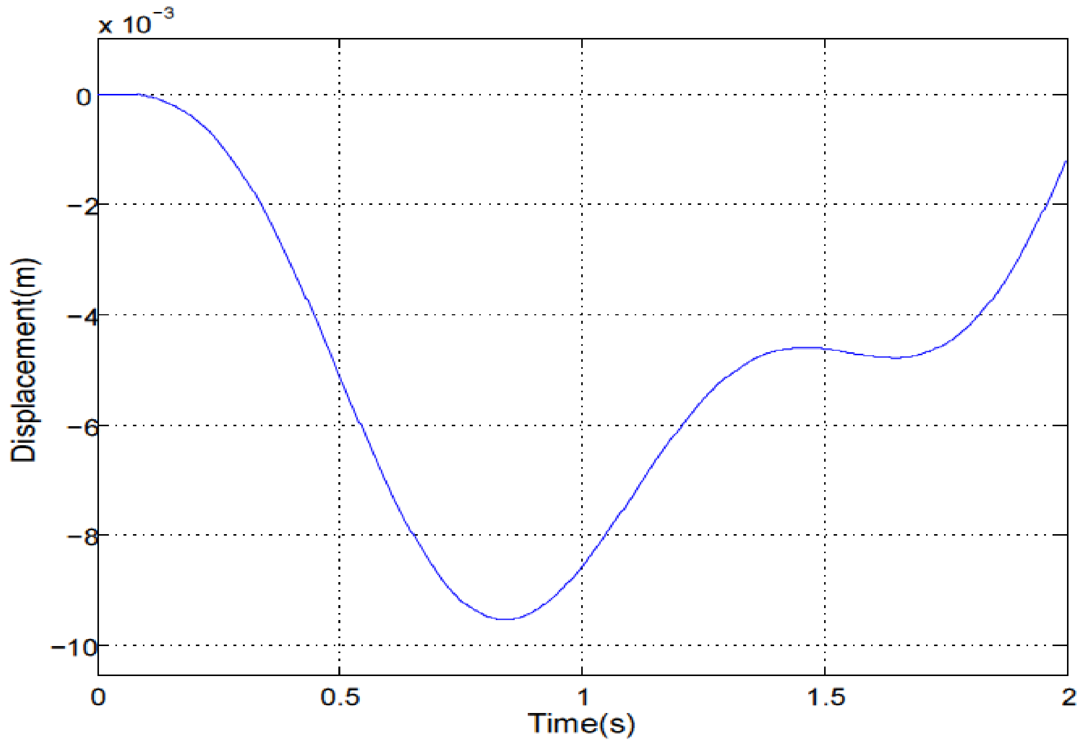

Figure 2.11 Displacement response of bridge mid-span (v=20m/s, x=20m)

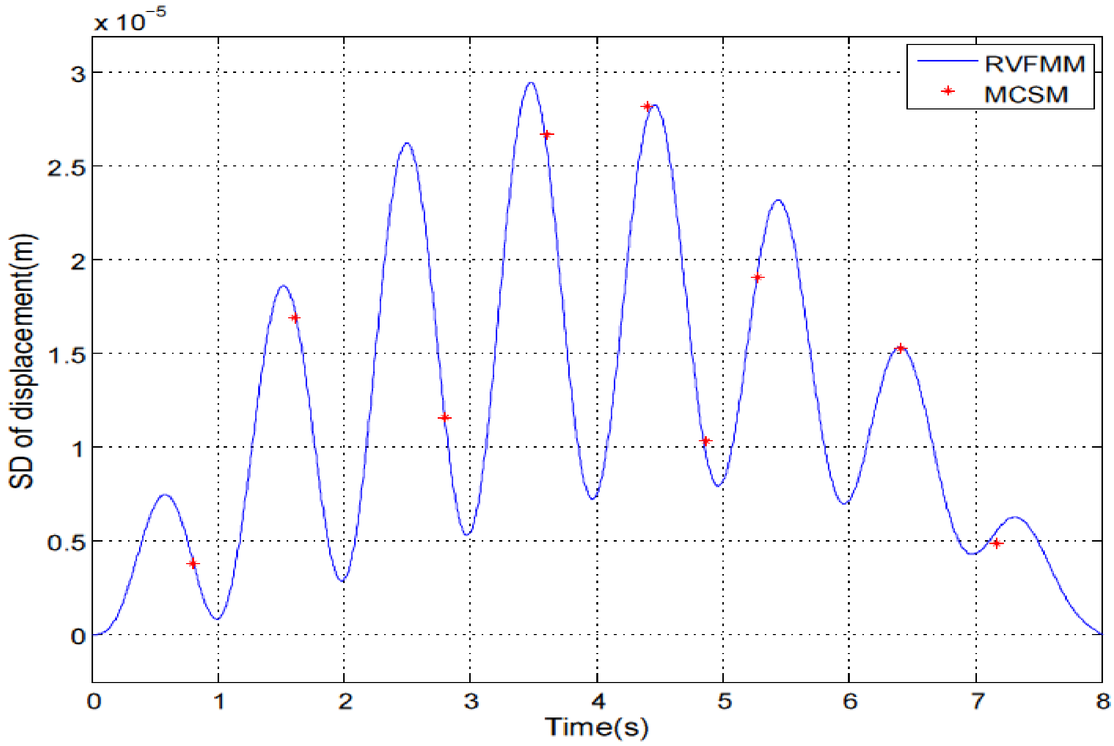

(a) COV of sprung mass =0.05

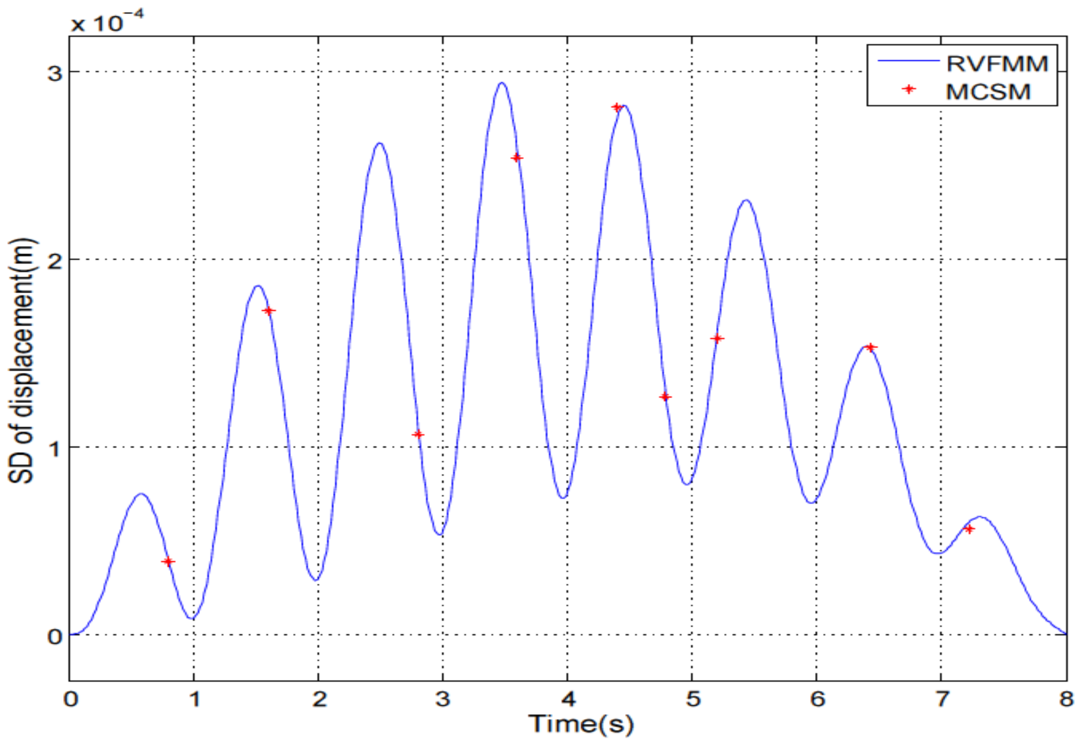

(b) COV of unsprung mass =0.05

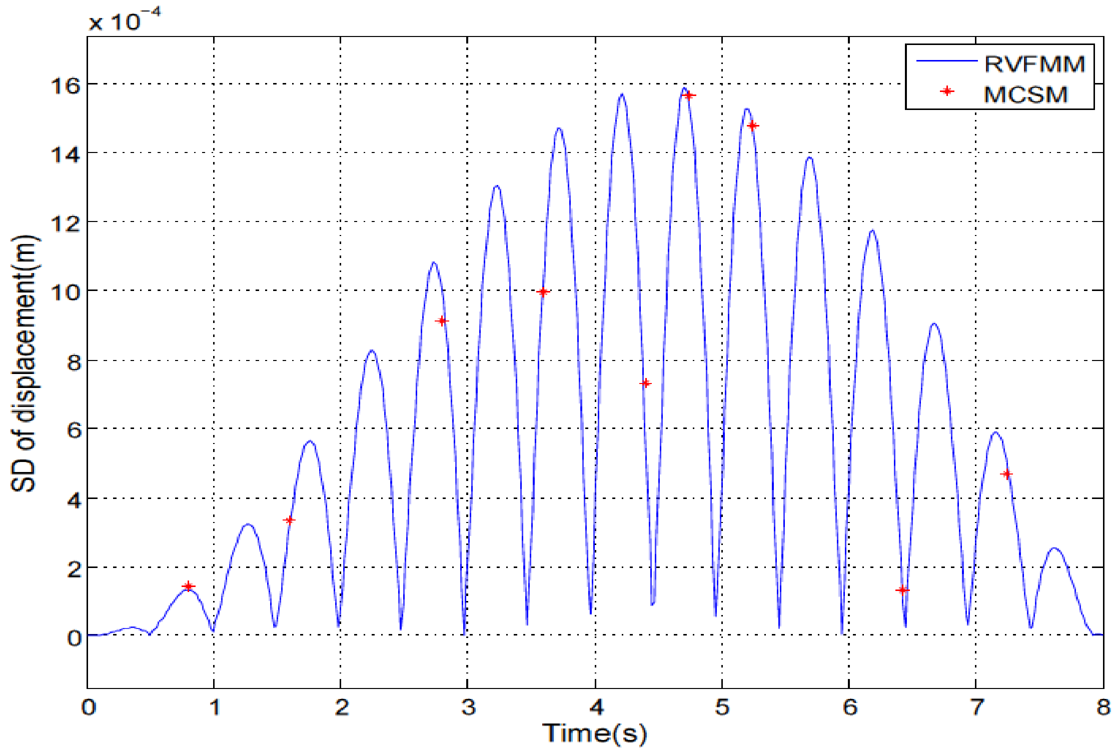

(c) COV of density =0.05

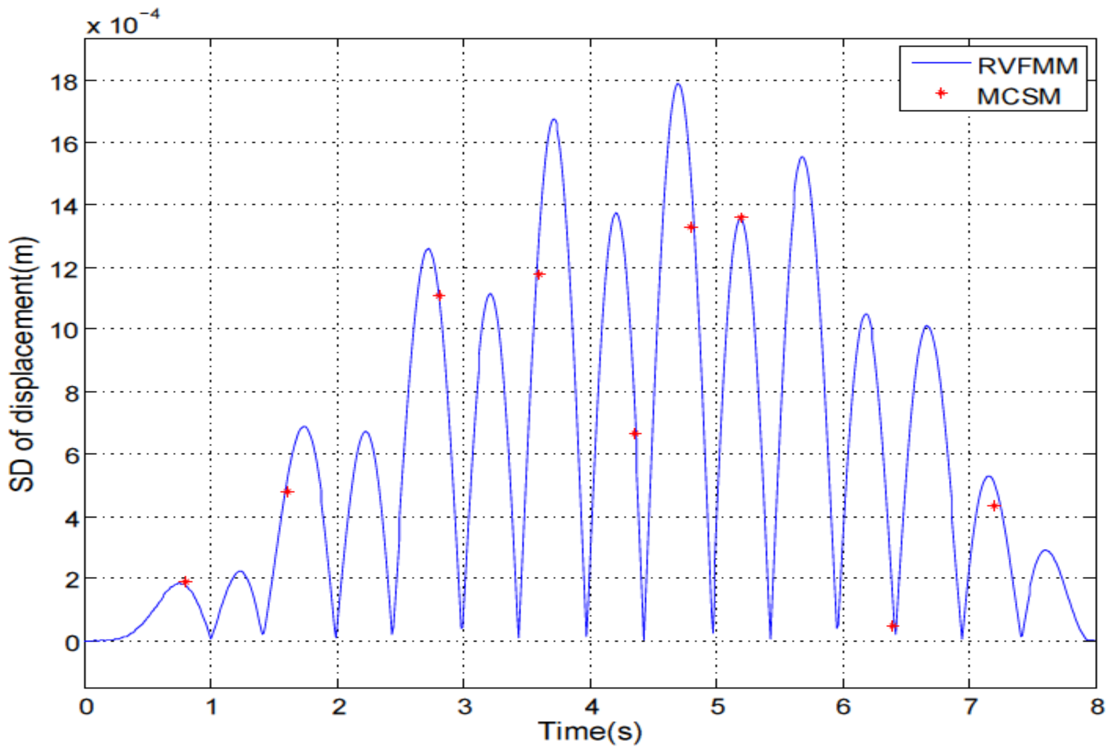

(d) COV of Young's Modulus =0.05

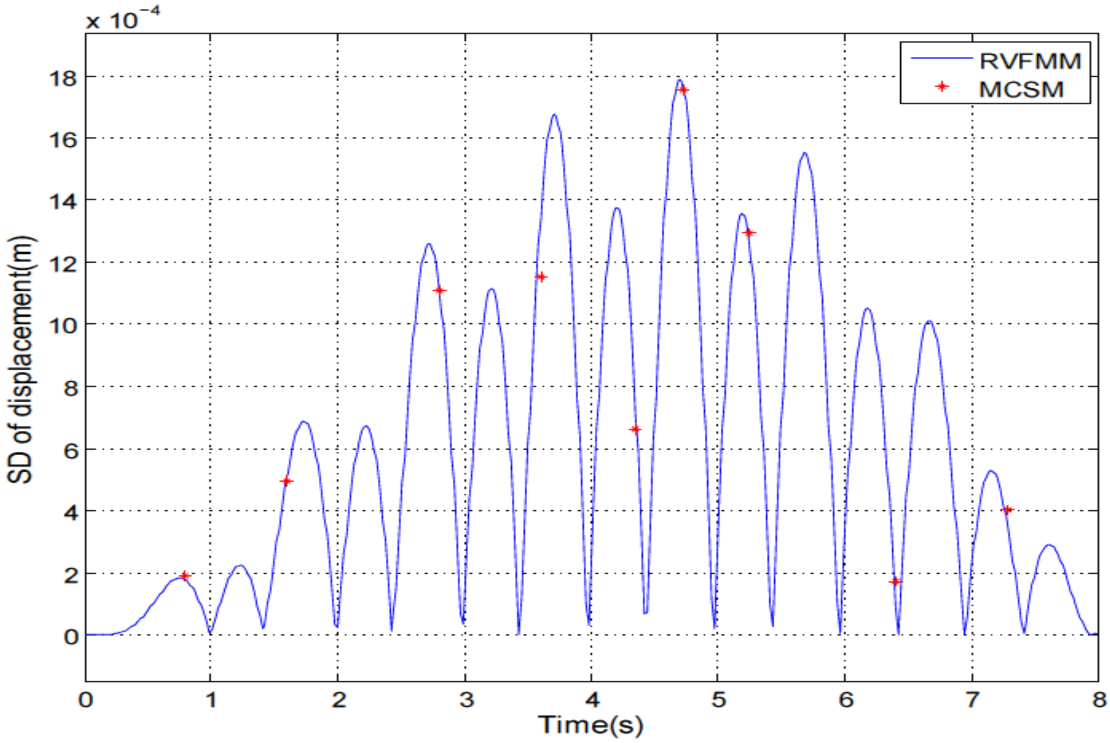

(e) COV of moment inertia =0.05

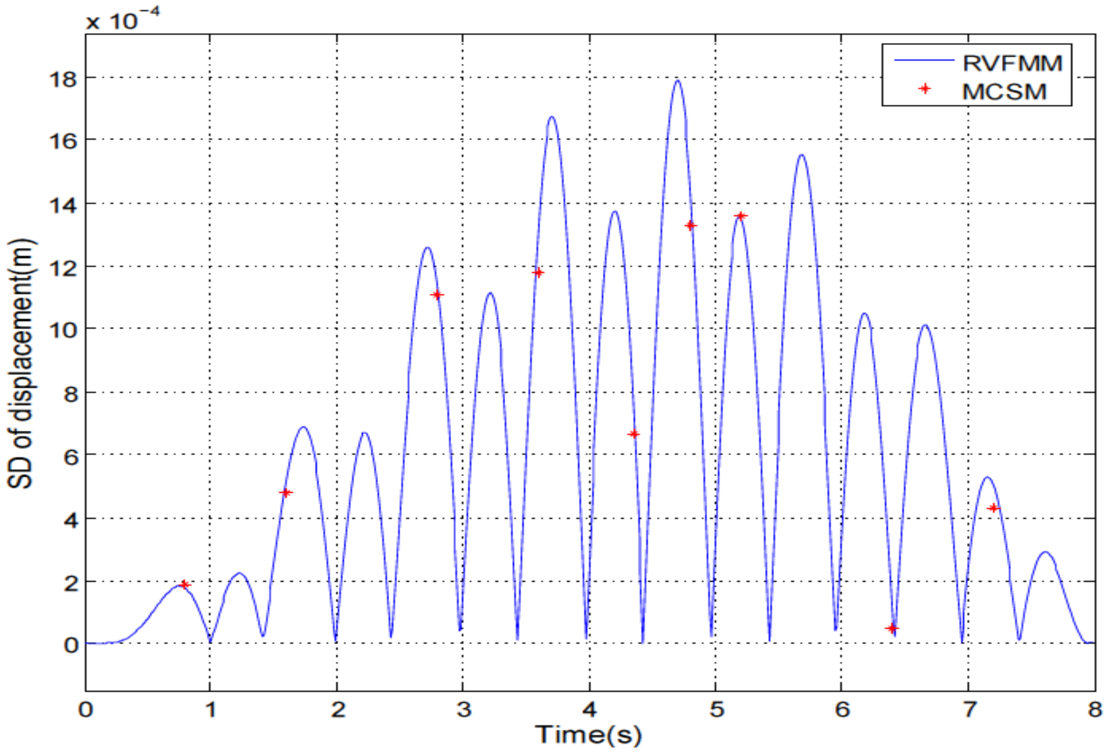

(f) COV of all parameters =0.05

Figure 2.12 Standard deviation of bridge mid-span displacement.

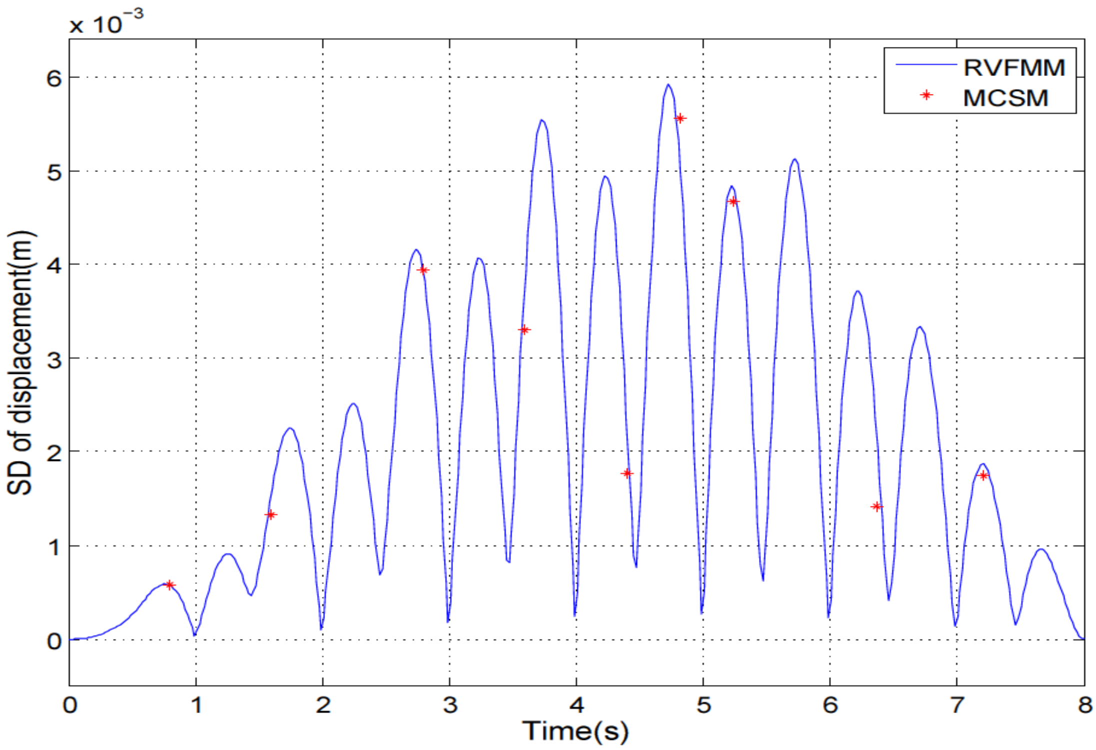

Figure 2.13 Standard deviation of bridge mid-span displacement

(COV of all parameters is 0.1)

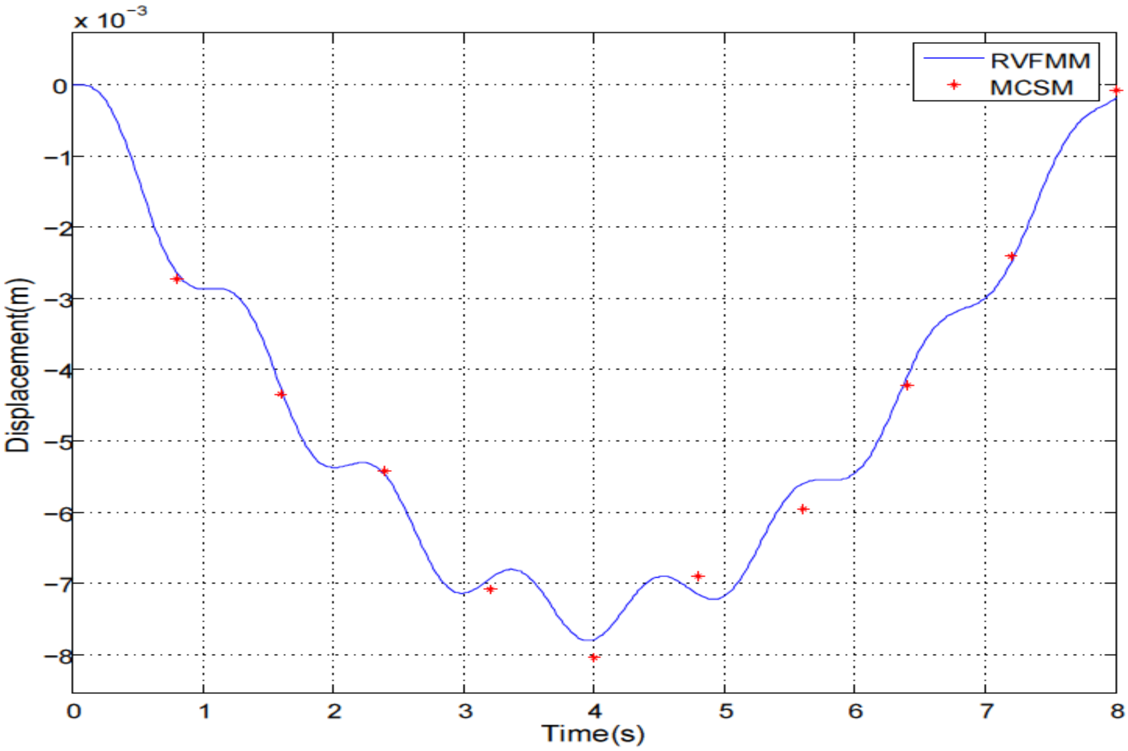

Figure 2.14 Mean value of bridge mid-span displacement

(COV of all parameters is 0.1)

In order to validate the method presented in this chapter, Monte Carlo simulation method is used as a reference approach. The standard deviations obtained by 10000 Monte Carlo simulations are also shown in Figures 2.12(a)-(f). In addition, the mean value and standard deviation of bridge mid-span response calculated by the proposed method and Monte Carlo simulations are given in Figures 2.13 and 2.14, respectively, when the coefficient of variation of all random parameters is taken as 0.1. The differences between the results obtained by the two methods and the consumed time are listed in Tables 2.4-2.10.

In general, computational results obtained by the proposed method (RVFMM) are in good agreement with those computed by the Monte-Carlo simulation method. The results obtained by the two methods agree with very well when the coefficient of variation of random system parameters is small as shown in Figure 2.12 and Tables 2.4-2.9. The difference is increased when the variations of random parameters become bigger as shown in Figure 2.13 and Table 2.10. In Table 2.10, the difference is still acceptable when the vehicle and bridge parameters are considered as random variables simultaneously and their coefficients of variation are equals to 0.1. The accuracy of the RVFMM can be improved if the second-order Taylor expansion is used. It can be expected that the differences will be smaller if more simulations are also used in the Monte Carlo method. From Tables 2.4-2.10, it can be also found that the time consumed by the Monte Carlo simulation is much greater than that used by the proposed method, the computer, which is used to simulate this example, is HP Compaq dc7800, CPU is Intel Core 2 Duo E8400.

Table 2.4 Comparison of results obtained from two different methods

COV (m_1) = 0.05

Time(s)		1.6	2.8	3.6	4.4	time
*COV (m*1*)* = 0.05	RVFMM	1.12e-05	1.71e-05	1.86e-05	1.79e-05	6.25s
	MCSM	1.13e-05	1.71e-05	1.86e-05	1.79e-05	7.53hrs
	Difference	0.17%	0.18%	0.22%	0.15%	

Table 2.5 Comparison of results obtained from two different methods

COV (m_2) = 0.05

Time(s)		1.6	2.8	3.6	4.4	time
*COV (m*2*)* = 0.05	RVFMM	1.72e-04	1.07e-04	2.54e-04	2.81e-04	6.38s
	MCSM	1.72e-05	1.07e-05	2.55e-05	2.82e-05	7.86hrs
	Difference	0.09%	0.08%	0.39%	0.35%	

Table 2.6 Comparison of results obtained from two different methods

COV *(E)* = 0.05

Time(s)		1.6	2.8	3.6	4.4	time
	RVFMM	4.96e-05	1.12e-03	1.15e-03	6.62e-04	5.486s

COV (E) = 0.05	MCSM	4.95e-04	1.11e-03	1.15e-03	6.64e-04	6.29hrs
	Difference	0.20%	0.90%	0.09%	0.30%	

Table 2.7 Comparison of results obtained from two different methods

COV (ρ) = 0.05

Time(s)		1.6	2.8	3.6	4.4	time
COV (ρ) = 0.05	RVFMM	3.33e-04	9.15e-04	9.98e-04	7.33e-04	4.256s
	MCSM	3.33e-04	9.12e-04	9.98e-04	7.35e-04	5.29hrs
	Difference	0.06%	0.33%	0.07%	0.27%	

Table 2.8 Comparison of results obtained from two different methods

COV (I) = 0.05

Time(s)		1.6	2.8	3.6	4.4	time
COV (I) = 0.05	RVFMM	4.96e-05	1.11e-03	1.16e-03	6.62e-04	4.569s
	MCSM	4.96e-04	1.11e-03	1.15e-03	6.63e-04	5.97hrs
	Difference	0.09%	0.13%	0.86%	0.15%	

Table 2.9 Comparison of results obtained from two different methods

COV *(all)* = 0.05

Time(s)		1.6	2.8	3.6	4.4	time
	RVFMM	7.70e-04	1.81e-03	2.15e-03	1.32e-03	12.138s

COV (all) = 0.05	MCSM	7.66e-04	1.81e-03	2.16e-03	1.32e-03	10.58hrs
	Difference	0.52%	0.08%	0.46%	0.12%	

Table 2.10 Comparison of results obtained from two different methods

COV *(all)* = 0.1

Time(s)		1.6	2.8	3.6	4.4	time
COV (all) = 0.1	RVFMM	1.35e-03	3.96e-03	3.33e-03	1.79e-03	13.486s
	MCSM	1.33e-03	3.94e-03	3.30e-03	1.77e-03	11.29hrs
	Difference	1.35%	0.53%	1.06%	1.18%	

2.5.2.2 Random response analysis of vehicle-bridge system with road surface roughness (Quarter-car model)

The road surface roughness of bridge can significantly change the force exerted on the bridge by the moving vehicle. According to ISO8068 and Honda et al. [117], the road surface is considered as a random process with a Gaussian probability distribution and the road roughness coefficient is assuming as $2 \times 10^6\ m^2/rad/m$. The interactive force caused by the road roughness and the moving vehicle is shown in Figure 2.15 when the velocity of vehicle is $5 m/s$. It should be noted that this force is a random process but the effects of the randomness of vehicle and bridge parameters are not included.

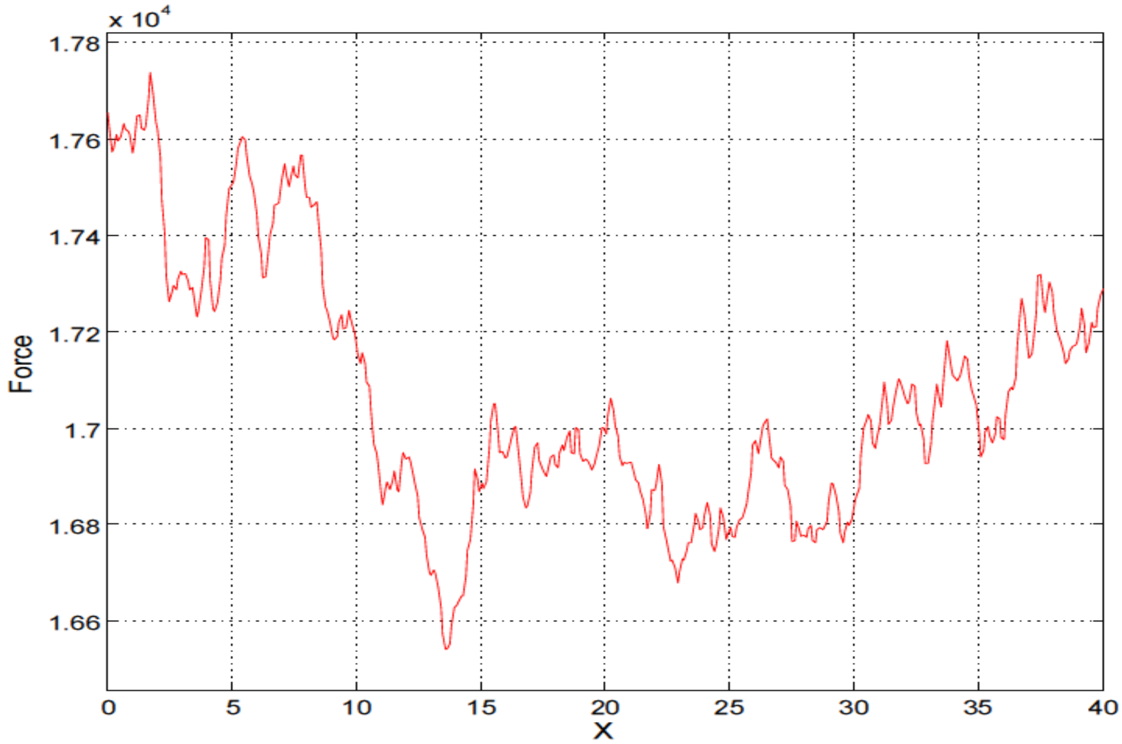

Figure 2.15 interactive forces with road surface roughness.

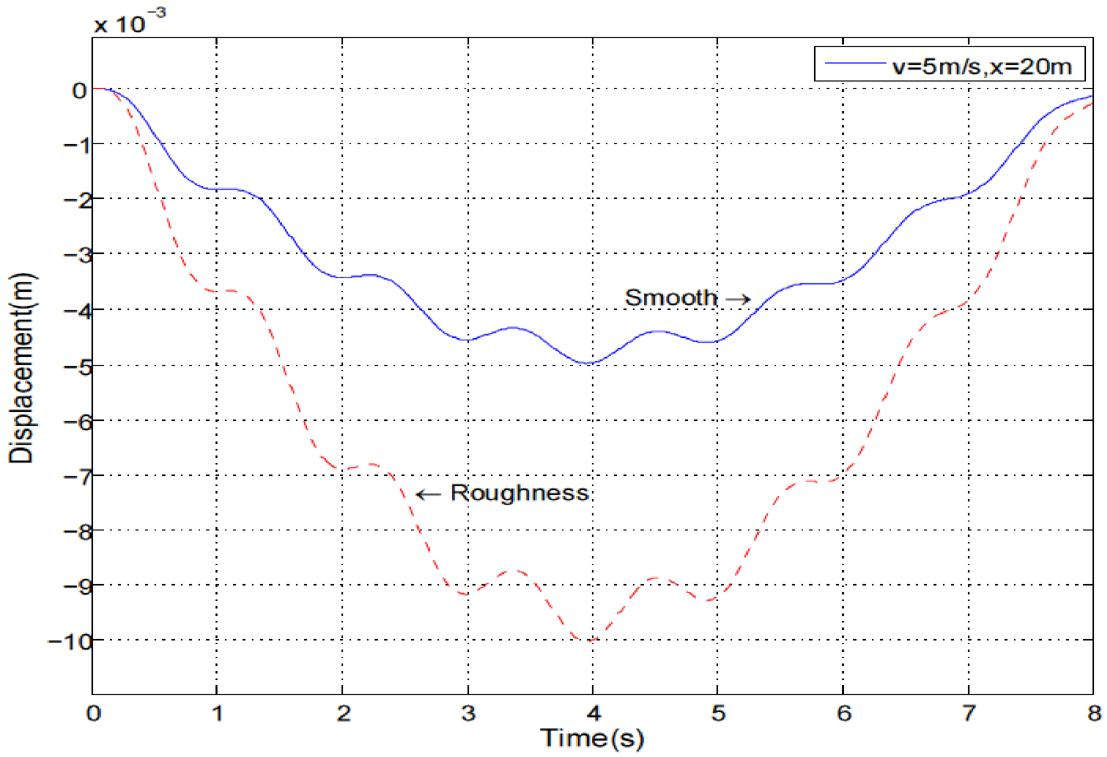

Figure 2.16 Mean value of bridge mid-span displacement with different road conditions

$$(v = 5m / s, x = 20m)$$

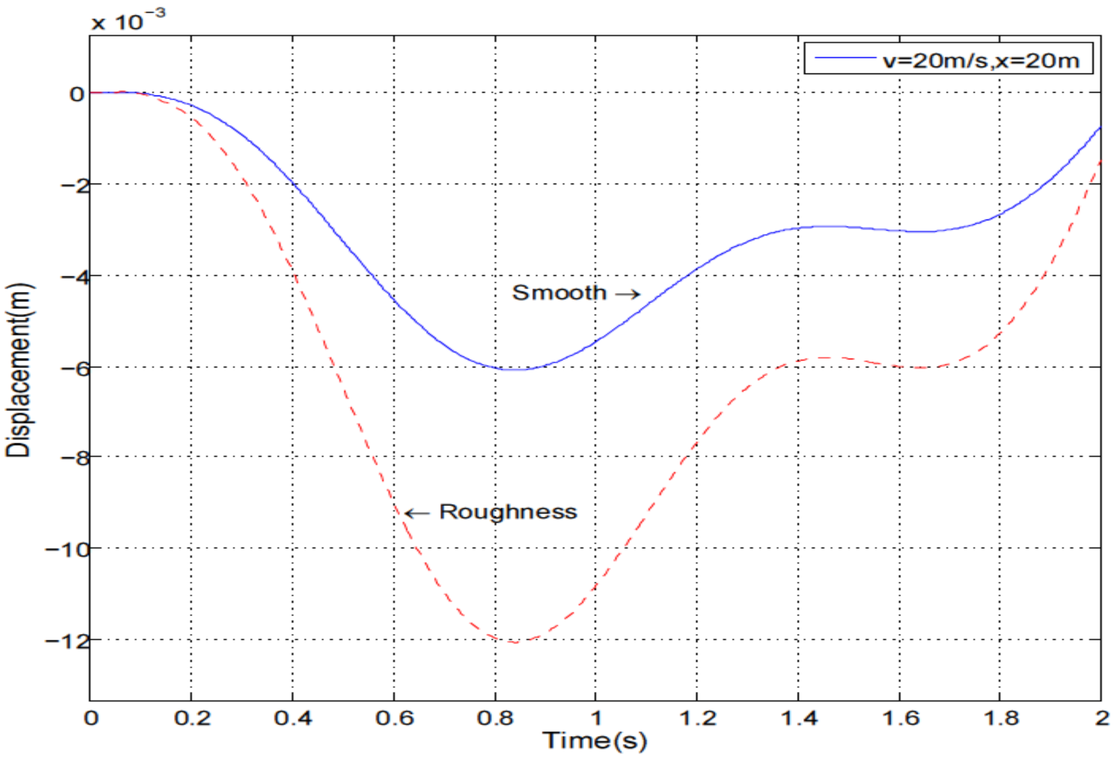

Figure 2.17 Mean value of bridge mid-span displacement with different road conditions

$(v = 20m / s, x = 20m)$

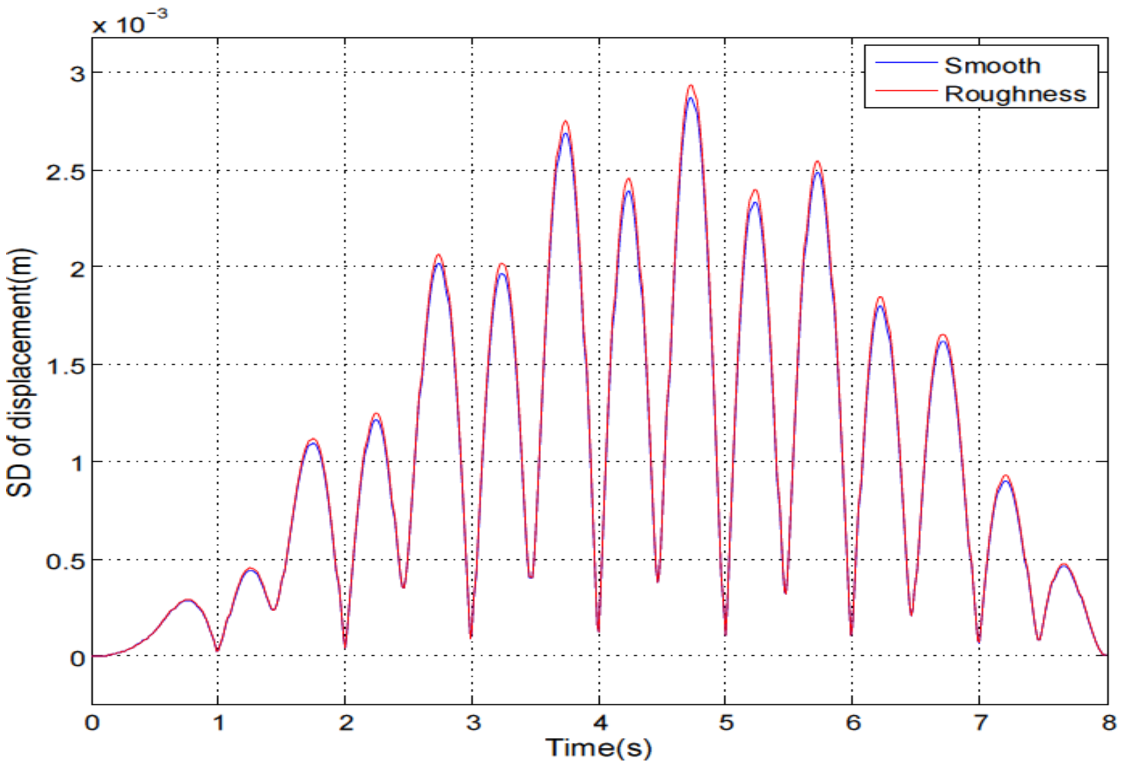

Figure 2.18 Standard deviation of bridge mid-span displacement

The bridge Young's modulus, mass density and moment of inertia as well as vehicle sprung mass, unsprung masses, tire stiffness and damping are considered as random variables in this part. The mean value and standard deviation of the displacement response of the bridge mid-span for smooth and rough road conditions are shown in Figures 2.16, 2.17 and 2.18, respectively. It can be easily observed that the bridge response is greatly increased when the road surface roughness is considered as shown in Figures 2.16 and 2.17. The standard deviation of the rough road condition is also bigger than that of the smooth road condition in Figure 2.18 as expected.

2.6 Conclusions

The dynamic response of bridge under moving vehicle is investigated in this chapter. The uncertainties in the vehicle-bridge interaction system are considered and vehicle and bridge parameters are modelled as random variables. Two different road conditions, smooth road surface and rough road surface, are also included in the model for the dynamic analysis of the vehicle-bridge coupled system. The modal superposition method and random variable functional moment method are employed to predict the first and second moments of the bridge response. The effects produced by the individual system parameters and road roughness on the bridge response are demonstrated by numerical examples. The effectiveness of the presented method is validated by the Monte Carlo simulation method.

The accuracy of the presented method can be improved if the second-order Taylor expansion is adopted in the RVFMM but it requires more computational efforts. The method can be further developed for dynamic analysis of vehicle-bridge interaction system using complex models such as bridge and full car-bridge and multi vehicle as well as vehicle and multi-span bridge models. The RVFMM could be combined with other methods rather than superposition method for the dynamic analysis of train-bridge system if it is modelled as a time-dependent system.

Chapter 3 Interval Dynamic Analysis of Vehicle-bridge Interaction System With uncertainty

3.1 Introduction

Probabilistic approaches have been widely used to account for uncertainties, under the premise that the statistical characteristics of uncertain quantities are presumed to be known [13]. The key point to justify the probability densities of the random variables is to obtain appropriate measurement data and sufficient statistical information. However, the major obstacle is lack of available data of such measurements and statistical information is scarce to permit a probabilistic analysis. Meanwhile, loads of many scenarios can hardly be modelled as random variables due to large changes in their magnitudes. Alternatively, a discipline, called interval analysis [10, 95-97], has been developed for structural analyses and for applied mechanics problems to account for the uncertainties. In interval analysis, the uncertain input variables are defined in closed bounded intervals. The bounds on system response are sought through various interval analytical and numerical approaches. It should be noted that, for complex systems, it is very hard to use interval methods to determine the tight bounds of system response due to their inherent drawbacks, i.e. dependency issue.

Actually, in interval analysis, lower and upper bounds are the minimum and maximum of system outputs respectively. Then, interval analysis problems can be converted to optimization problems. In the recent two decades, a bio-inspired optimization algorithm called particle swarm optimization (PSO) has been proposed and developed to solve optimization problems and find the global optimum [120-122]. PSO is a population-based heuristic optimization technique motivated by animal social behaviours such as bird flocking and fish schooling. Although PSO has attracted comprehensive attention and has been applied in many areas, very little research has been conducted for solving structural optimization problems [123-125].

In this chapter, the dynamic response of a bridge under a moving vehicle with uncertain but bounded system parameters is studied. The vehicle is represented by a half-car model [13] and the bridge is modelled as an Euler-Bernoulli beam [3] same as the previous chapter. The vehicle masses and the bridge parameters corresponding to Young's modulus, mass and moment of inertia, are all considered as interval variables. The computational expressions for the midpoint, interval width, lower and upper bounds of the vertical responses of the bridge are developed by using the modal superposition method and interval operations. Meanwhile, an improved PSO algorithm called LHNPSO is developed to determine the lower and upper bounds of bridge displacement response. The LHNPSO algorithm, with low-discrepancy sequence initialized particles and high-order nonlinear time-varying inertia weight and constant acceleration coefficients, can converge fast and generate accurate solutions. Through the comparisons between the results computed by interval analysis method and LHNPSO, the effectiveness of them is demonstrated. Monte-Carlo simulations are also implemented to validate the presented methods. In addition, the effects of the vehicle and bridge parameters on bridge response are investigated.

This chapter is organized as follows. Section 3.2 provides a brief introduction of the interval analysis method. Section 3.3 presents the model of a vehicle-bridge interaction system. In Section 3.4, the dynamic response analysis of the bridge based on the interval analysis method is presented. The improved LHNPSO algorithm is implemented to determine the intervals of bridge response in Section 3.5. Numerical examples and calculated results are given in section 3.6. Conclusions are stated in the last section.

The work presented in this chapter is mainly dependent on the research reported by Liu et al. in Journal of Sound and Vibration, 332 (2013) 3218-3231.

3.2 Interval Analysis Method

Let $I(R)$, $I(R^n)$ and $I(R^{n\times n})$ denote the sets of all closed real interval numbers, n dimensional real interval vectors and $n\times n$ real interval matrices, respectively. R is the set of all real numbers. $x^I=[\underline{x},\overline{x}]=\left\{ l, \underline{x}\le l\le \overline{x} \middle| \underline{x},\overline{x}\in R \right\}$ is an interval variable of $I(R)$. $\underline{x}$ and $\overline{x}$ are the lower and upper bounds of x^I, respectively. Interval variable x^I can also be expressed as

$$x^I=[\underline{x},\overline{x}]=x^c+\Delta x^I \tag{3.1a}$$

$$\Delta x^I=[-\Delta x,+\Delta x] \tag{3.1b}$$

$$x^c = \frac{\underline{x} + \overline{x}}{2} \tag{3.1c}$$

$$\Delta x_F = \frac{\Delta x}{x^c} \tag{3.1d}$$

where x^c, Δx, Δx^I and Δx_F represent the midpoint value, maximum width (interval width), uncertain interval and interval change ratio of the interval variable x^I, respectively.

The core of interval arithmetic consists of a generalization of operations [94-96]

$$X^I + Y^I = [\underline{x}, \overline{x}] + [\underline{y}, \overline{y}] = [\underline{x} + \underline{y}, \overline{x} + \overline{y}] \tag{3.2a}$$

$$X^I - Y^I = [\underline{x}, \overline{x}] - [\underline{y}, \overline{y}] = [\underline{x} - \overline{y}, \overline{x} - \underline{y}] \tag{3.2b}$$

$$X^I \times Y^I = [\underline{x}, \overline{x}] \times [\underline{y}, \overline{y}] = [\min(\underline{x} \cdot \underline{y}, \underline{x} \cdot \overline{y}, \overline{x} \cdot \underline{y}, \overline{x} \cdot \overline{y}), \max(\underline{x} \cdot \underline{y}, \underline{x} \cdot \overline{y}, \overline{x} \cdot \underline{y}, \overline{x} \cdot \overline{y})] \tag{3.2c}$$

$$\frac{X^I}{Y^I} = \frac{[\underline{x}, \overline{x}]}{[\underline{y}, \overline{y}]} = [\underline{x}, \overline{x}] \left[\frac{1}{\overline{y}} \quad \frac{1}{\underline{y}} \right] \tag{3.2d}$$

The general form of equation of a vehicle-bridge interaction system with interval variables can be taken as

$$y = f(x^I, t) \tag{3.3}$$

Based on the first-order Taylor series expansion, from Eq. (3.3), we have

$$y = f(x^I, t) = f(x^c, t) + \frac{\partial f(x^c, t)}{\partial x} \cdot (x^I - x^c) \tag{3.4}$$

From Eq. (3.4), the midpoint and interval width of $f(x^I, t)$ can be obtained as

$$f^c(x^I, t) = f(x^c, t) \tag{3.5}$$

$$\Delta f(x^I, t) = \frac{\partial f(x^c, t)}{\partial x} \cdot \Delta x \tag{3.6}$$

Then, the lower and upper bounds of $f(x^I, t)$ can be calculated by

$$\underline{f(x^I, t)} = f(x^c, t) - \Delta f(x^I, t) = f(x^c, t) - \frac{\partial f(x^c, t)}{\partial x} \cdot \Delta x \tag{3.7}$$

$$\overline{f(x^I, t)} = f(x^c, t) + \Delta f(x^I, t) = f(x^c, t) + \frac{\partial f(x^c, t)}{\partial x} \cdot \Delta x \tag{3.8}$$

3.3 Vehicle-Bridge Interaction Model

In the vehicle-bridge interaction system, the bridge is modelled as a simply supported beam and the vehicle is represented by a half-car model as shown in Figure 3.1. Here, a1 and a2 are the position parameters; S is the axle spacing ; m_v, m_1 and m_2 denote the sprung mass and suspension masses respectively; the suspension system is represented by two linear springs of stiffness k_{s1}, k_{s2} and two linear dampers with damping rates c_{s1}, c_{s2} ; the tires are also modelled by two linear springs of stiffness k_{t1}, k_{t2} and two linear dampers with damping rates c_{t1}, c_{t2} ; ρ, E, I and L are the mass per unit length, elastic modulus, moment of inertia and length of the beam respectively.

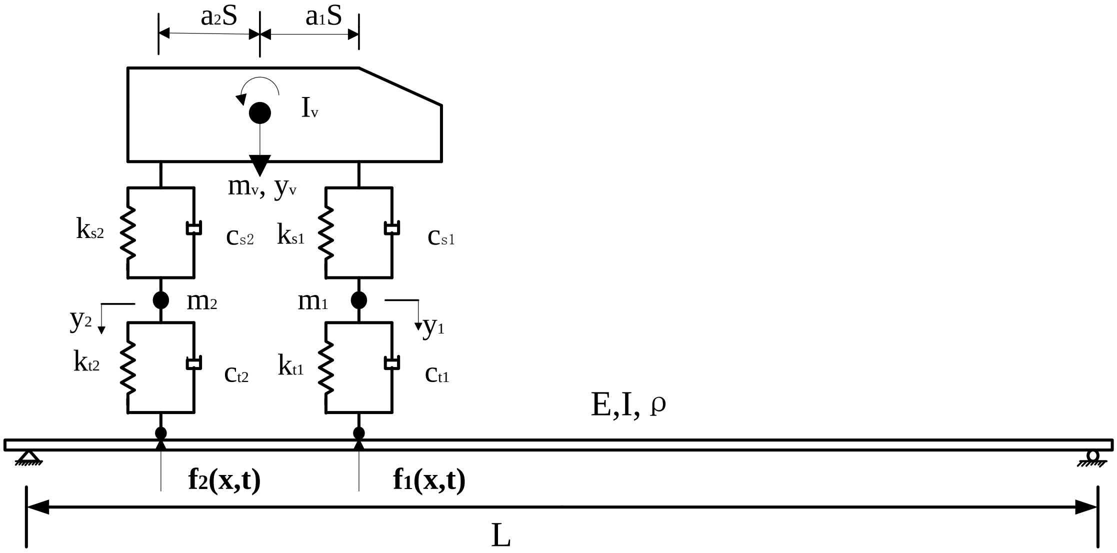

Figure 3.1 Model of vehicle-bridge interaction system (half-car model)

The equation of motion governing the transverse or vertical vibration of the bridge under the moving vehicle can be written as

$$\rho\frac{\partial^2 W(x,t)}{\partial t^2}+C\frac{\partial W(x,t)}{\partial t}+EI\frac{\partial^4 W(x,t)}{\partial x^4}=(f_1(x,t)+f_2(x,t))\delta(x-vt) \tag{3.9}$$

$$\begin{cases} f_1(x,t)=-(m_1+a_2m_v)g-k_{t1}(y_1-W|_{x=vt})-c_{t1}(\dot{y}_1-\dot{W}|_{x=vt}) \\ f_2(x,t)=-(m_2+a_1m_v)g-k_{t2}(y_2-W|_{x=vt})-c_{t2}(\dot{y}_2-\dot{W}|_{x=vt}) \end{cases} \tag{3.10}$$

where $W(x,t)$ is the vertical displacement of the bridge, y_1 and y_2 are the vertical displacement of the suspension system of the vehicle, $f_1(x,t)$ and $f_2(x,t)$ are the contact forces, $\delta(x-vt)$ is the Dirac delta function evaluated at the contact point at position $x=vt$, and v is the speed of the moving vehicle.

Using the modal superposition method [3], the solution to Eq. (3.9) can be expressed as in terms of the mode shapes $\varphi_j(x)$ and associated modal coordinates $x_{bj}(t)$ of the bridge

$$W(x,t)=\sum_{j=1}^{\infty}\varphi_j(x)x_{bj}(t) \tag{3.11}$$

For simply supported beam, the mode shapes of the bridge are same as Eq. (2.9). From Eqs. (2.9), (3.9) and (3.11), it obtains

$$\int_0^L \rho\varphi_j^T(x)\sum_{j=1}^{\infty}\varphi_j(x)\ddot{x}_{bj}(t)dx+\int_0^L C\varphi_j^T(x)\sum_{j=1}^{\infty}\varphi_j(x)\dot{x}_{bj}(t)dx+\int_0^L EI\varphi_j^T(x)\sum_{j=1}^{\infty}\frac{\partial^4\varphi_j(x)}{\partial x^4}x_{bj}(t)dx$$

$$=\int_0^L \varphi_j^T(x)(f_1(x,t)+f_2(x,t))\cdot\delta(x-vt)dx$$

$$=-\int_0^L \varphi_j^T(x)((m_1+a_2m_v)g+k_{t1}(x_v(t)-W\big|_{x=vt})+c_{t1}(\dot{x}_v(t)-\dot{W}\big|_{x=vt})$$

$$+(m_2+a_1m_v)g+k_{t2}(x_v(t)-W\big|_{x=vt})+c_{t2}(\dot{x}_v(t)-\dot{W}\big|_{x=vt}))\cdot\delta(x-vt)dx \tag{3.12}$$

As vehicle mass is much less than the bridge mass and the tires' damping is quite small, Eq. (3.12) can be approximated as [3]

$$\ddot{x}_{bj}(t)+2\zeta_{bj}\omega_{bj}\dot{x}_{bj}(t)+\omega_{bj}^2x_{bj}(t)=-\frac{2(m_1+m_2+(a_1+a_2)m_v)g}{\rho L}\sin\frac{j\pi vt}{L} \tag{3.13}$$

where

$$a_1+a_2=1$$

Assuming zero initial conditions, the solution to Eq. (3.13) is

$$x_{bj}(t)=-\frac{2(m_1+m_2+(a_1+a_2)m_v)g}{\rho L\omega_{dbj}}\int_0^t e^{-\zeta_{bj}\omega_{bj}(t-\tau)}\cdot\sin\omega_{dbj}(t-\tau)\sin\frac{j\pi v t}{L}d\tau \tag{3.14}$$

where

$$\omega_{dbj} = \sqrt{1-\zeta_{bj}^2}\,\omega_{bj} \tag{3.15}$$

Then, the displacement response of the bridge can be calculated by

$$\begin{aligned} W(x,t) = &-\sum_{j=1}^{\infty} \sin\frac{j\pi x}{L} x_{bj}(t) \frac{2(m_1+m_2+m_v)g}{L\sqrt{1-\zeta_{bj}^2}\frac{j^2\pi^2}{L^2}\sqrt{\rho EI}} \\ &\cdot \int_0^t e^{-\zeta_{bj}\frac{j^2\pi^2}{L^2}\sqrt{\frac{EI}{\rho}}(t-\tau)} \sin\left(\sqrt{1-\zeta_{bj}^2}\frac{j^2\pi^2}{L^2}\sqrt{\frac{EI}{\rho}}(t-\tau)\right)\sin\frac{j\pi vt}{L}\,d\tau \end{aligned} \tag{3.16}$$

The contribution of tires' stiffness to bridge vertical displacement response is omitted due to the assumption that the bridge mass is much greater than that of the vehicle. Actually, it is not difficult to include the vehicle stiffness in the bridge response using the Duhamel integral solution.

3.4 Interval Dynamic Responses Analysis of the Bridge Using the Interval Analysis Method

Vehicle and bridge parameters, m_1, m_2, m_v, ρ, E and I, are considered as interval variables. By means of the interval operations, the interval dynamic response of structures with uncertain-but-bounded parameters can be determined by using the interval analysis method. The midpoint value and interval width of the interval bridge response can be computed by

$$W^c(x,t) = -\sum_{j=1}^{\infty} \sin\frac{j\pi x}{L} x_{bj}(t) \frac{2(m_1^c + m_2^c + m_v^c)g}{S_1\sqrt{\rho^c E^c I^c}} \int_0^t S_2 \sin\left(S_3\right) \sin\frac{j\pi vt}{L} d\tau \tag{3.17}$$

$$\begin{aligned}
\Delta W(x,t) = &-\sum_{j=1}^{\infty} \sin\frac{j\pi x}{L} x_{bj}(t) \\
&\{\frac{2g}{S_1\sqrt{\rho^c E^c I^c}} \int_0^t S_2 \sin\left(S_3\right) \sin\frac{j\pi vt}{L} d\tau\} \cdot \Delta m_1 - \{\frac{2g}{S_1\sqrt{\rho^c E^c I^c}} \int_0^t S_2 \sin\left(S_3\right) \sin\frac{j\pi vt}{L} d\tau\} \cdot \Delta m_2 \\
&-\{\frac{2g}{S_1\sqrt{\rho^c E^c I^c}} \int_0^t S_2 \sin\left(S_3\right) \sin\frac{j\pi vt}{L} d\tau\} \cdot \Delta m_v - \{\frac{(m_1^c + m_2^c + m_v^c)g}{S_1\sqrt{\left(\rho^c\right)^3 E^c I^c}} \int_0^t S_2 \sin\left(S_3\right) \sin\frac{j\pi vt}{L} d\tau\} \cdot \Delta\rho \\
&+\{\frac{2(m_1^c + m_2^c + m_v^c)g}{S_1\sqrt{\rho^c E^c I^c}} \int_0^t S_2 \frac{1}{2}\zeta_{bj} \frac{j^2\pi^2}{L^2} \sqrt{\frac{E^c I^c}{\left(\rho^c\right)^3}} (t-\tau) \sin\left(S_3\right) \sin\frac{j\pi vt}{L} d\tau\} \cdot \Delta\rho \\
&-\{\frac{2(m_1^c + m_2^c + m_v^c)g}{S_1\sqrt{\rho^c E^c I^c}} \int_0^t S_2 \cos\left(S_3\right) \frac{1}{2}\sqrt{1-\zeta_{bj}^2} \frac{j^2\pi^2}{L^2} \sqrt{\frac{E^c I^c}{\left(\rho^c\right)^3}} (t-\tau) \sin\frac{j\pi vt}{L} d\tau\} \cdot \Delta\rho \\
&-\{\frac{(m_1^c + m_2^c + m_v^c)g}{S_1\sqrt{\rho^c \left(E^c\right)^3 I^c}} \int_0^t S_2 \sin\left(S_3\right) \sin\frac{j\pi vt}{L} d\tau\} \cdot \Delta E \\
&-\{\frac{2(m_1^c + m_2^c + m_v^c)g}{S_1\sqrt{\rho^c E^c I^c}} \int_0^t S_2 \frac{1}{2}\zeta_{bj} \frac{j^2\pi^2}{L^2} \sqrt{\frac{I^c}{E^c \rho^c}} (t-\tau) \sin\left(S_3\right) \sin\frac{j\pi vt}{L} d\tau\} \cdot \Delta E \\
&+\{\frac{2(m_1^c + m_2^c + m_v^c)g}{S_1\sqrt{\rho^c E^c I^c}} \int_0^t S_2 \cos\left(S_3\right) \frac{1}{2}\sqrt{1-\zeta_{bj}^2} \frac{j^2\pi^2}{L^2} \sqrt{\frac{I^c}{E^c \rho^c}} (t-\tau) \sin\frac{j\pi vt}{L} d\tau\} \cdot \Delta E \\
&-\{\frac{(m_1^c + m_2^c + m_v^c)g}{S_1\sqrt{\rho^c E^c \left(I^c\right)^3}} \int_0^t S_2 \sin\left(S_3\right) \sin\frac{j\pi vt}{L} d\tau\} \cdot \Delta I \\
&-\{\frac{2(m_1^c + m_2^c + m_v^c)g}{S_1\sqrt{\rho^c E^c I^c}} \int_0^t S_2 \frac{1}{2}\zeta_{bj} \frac{j^2\pi^2}{L^2} \sqrt{\frac{E^c}{I^c \rho^c}} (t-\tau) \sin\left(S_3\right) \sin\frac{j\pi vt}{L} d\tau\} \cdot \Delta I \\
&+\{\frac{2(m_1^c + m_2^c + m_v^c)g}{S_1\sqrt{\rho^c E^c I^c}} \int_0^t S_2 \cos\left(S_3\right) \frac{1}{2}\sqrt{1-\zeta_{bj}^2} \frac{j^2\pi^2}{L^2} \sqrt{\frac{E^c}{I^c \rho^c}} (t-\tau) \sin\frac{j\pi vt}{L} d\tau\} \cdot \Delta I
\end{aligned} \tag{3.18}$$

where $W^c(x,t)$ and $\Delta W(x,t)$ denote the midpoint value and interval width of the interval bridge response $W^I(x,t)$, respectively. The items S_1 , S_2 and S_3 have been given in Chapter 2.

The lower and upper bounds of the interval bridge response can be calculated by

$$\underline{W(x,t)} = W^c(x,t) - \Delta W(x,t) \tag{3.19a}$$

$$\overline{W(x,t)} = W^c(x,t) + \Delta W(x,t) \tag{3.19b}$$

3.5 Optimization Algorithm

3.5.1 Particle swarm optimization algorithm

Particle swarm optimization (PSO) algorithm is a simple and robust strategy based on the social and cooperative behaviour shown by various species like flock of bird, school of fish and so on. The concept of PSO was proposed by Kennedy and Eberhart in 1995 [96]. It has become one of the most promising techniques for solving global optimization problems. The PSO system consists of a population (swarm) of potential solutions called particles. These particles move through the search space with a specified velocity in search of optimal solution. Each particle maintains a memory which helps it in keeping the track of its previous best position. The positions of the particles are distinguished as personal best and global best. In the recent years, PSO has been successfully applied in many areas. It has been demonstrated that PSO can get better results in a faster and cheaper way in comparison with other heuristic methods like genetic algorithm (GA) and simulated annealing (SA) [130].

Mathematically, the PSO algorithm is described by the following expressions

$$V_{j,k+1} = \omega V_{j,k} + C_1(W_{g,k} - W_{j,k}) + C_2(\overline{W}_{j,k} - W_{j,k}) \tag{3.20}$$

$$W_{j,k+1} = (W_{j,k} + V_{j,k+1}) \tag{3.21}$$

where $V_{j,k}$ represents the previous velocity of particle j, which serves as a memory of the previous flight velocity and direction. ω is the weighting factor employed to control the impact of previous velocity on the current velocity [104-106]. C_1 and C_2 are acceleration coefficients indicating the weighting of the stochastic acceleration terms that pull each particle towards personal best and global best positions. They are random numbers in $U(0, C_{1,\max})$ and $U(0, C_{2,\max})$. $U(\cdot)$ stands for a uniform distribution, $C_{1,\max}$ is the maximum value of C_1 and $C_{2,\max}$ is the maximum value of C_2 . Position $W_{g,k}$ is the global best one in the group of all particles while $\overline{W}_{j,k}$ is a record of the best solution of particle j over the past iterations. $C_1(W_{g,k} - W_{j,k})$ is named as the social component because it represents the cooperation among particles. The effect of this term is that each particle is to be drawn towards the best position which is found by its neighbour particles. $C_2(\overline{W}_{j,k} - W_{j,k})$ represents the personal experience of particle j and is called cognitive parameters. The effect of this term is to draw individual particles back to their own best positions that were most satisfying in the past. $W_{j,k}$ represents the position of the *jth* particle at the *kth* iteration. The main parameters of the PSO algorithm are given in Table 3.1. Figure 3.2 shows the pseudo code of the general PSO algorithm.

Table 3.1 Main PSO parameters

Symbol	Description	Details
n	Dimension of particles	Determined by the problem to be optimized
ω	Inertia weight factor	Usually less than 1
C_1	Social parameters	Usually $C_1 = C_2 = 2$, other values can also be used
C_2	Cognitive parameters	$0 < C_1 + C_2 \leq 4$ (Perez and Behdinan [130])

The PSO algorithm

For each particle **do**

  Initialize the particle position and its velocity randomly

End for

Set a finite number of iterations

Set iteration count to 0

While not terminate **do**

  For each particle **do**

   Evaluate fitness value

   If the fitness value is better than the local best fitness value in history **then**

    Update the local bests and their fitness

   End if

  End for

  Choose the particle with the best fitness value of all the particle as the global best

  For each particle **do**

Calculate particle velocity

Update particle position

End for

End while

Terminate if generation count expires

Figure 3.2 The pseudo code of the general PSO algorithm

3.5.2 LHNPSO

Although numerous variants of PSO algorithms have been developed, solving optimization problems with high accuracy and fast convergence speed is still an important task. A novel PSO method, called low-discrepancy sequence initialized particle swarm optimization algorithm with high-order nonlinear time-varying inertia weight (LHNPSO), has been proposed recently [131]. In the LHNPSO, particles are initialized by using low-discrepancy sequences rather than pseudo random numbers which are widely used in other PSO algorithms. These deterministic sequences can fill the sample area efficiently and uniformly [132], and have been successfully used to solve globally optimal problems [132,133]. The LHNPSO uses the constant acceleration coefficients $C_1 = C_2 = 2$, and the nonlinearly decreasing inertial weight is varied according to the following formulation

$$\omega(k+1) = \omega_{\max} - (\omega_{\max} - \omega_{\min})\left(\frac{k}{k_{\max}}\right)^{\frac{1}{\pi^2}} \tag{3.22}$$

where $\omega_{\max} = 0.9$ and $\omega_{\min} = 0.4$.

It has been verified that the easily implemented LHNPSO can converge faster and give a much more accurate final solution for a set of benchmark optimization problems, in comparison with the classical and a couple of improved PSO algorithms.

In this chapter, LHNPSO is adopted to determine the change range of bridge response. The interval bridge response $W(x,t)$ is used as the fitness function and the lower and upper bounds of this fitness function are respectively the maximum and minimum values of the objective function

$$\begin{cases} F_{\min}(x,t) = \min W(x,t) \\ F_{\max}(x,t) = \max W(x,t) \end{cases} \tag{3.23}$$

3.6 Numerical Examples

The vehicle and bridge parameters are considered as interval variables, and their nominal values (midpoints) taken in the numerical simulation are listed in Table 3.2. The moving velocity of vehicle is $v = 10m/s$. The unit of the bridge displacement response used in this chapter is meter.

Table 3.2 Data of the bridge and vehicle models

Data of the bridge	Data of the vehicle	
$L = 40m$	$m_1 = 1000kg$	$m_2 = 1500kg$
E=33 GN/m^2	$m_v = 17800kg$	$I_v = 1.5 \times 10^5 kg.m^2$
$I = 0.16m^4$	$k_{s1} = 2.5 \times 10^6 N/m$	$k_{s2} = 4.2 \times 10^6 N/m$
$\rho = 7800kg / m$	$k_{t1} = 5.2 \times 10^6 N / m$	$k_{t2} = 7.2 \times 10^6 N / m$
	$a_1 = 0.52$	$a_2 = 0.48$
	$c_{s1} = 9000N/m$	$c_{s2} = 9600N/m$
	$c_{t1} = 920N/m$	$c_{t2} = 960N/m$
	$S = 4.27m$	

3.6.1 Interval analysis method

To investigate the influences of system parameters on the bridge response, the interval change ratio (ICR) of them changes from 0 to 0.1. The midpoint value and interval width of the bridge displacement response at its mid-span are given in Figures 3.3 and 3.4, respectively. Figure 3.4(a) shows that the changes of vehicle masses m_1 and m_2 produce the similar effect on the interval width of the bridge response as expected from Eq. (3.17). The effects caused by suspension (unsprung) masses m_1 and m_2 are smaller than that produced by the sprung mass m_v as their interval width is smaller when the interval change ratios of these three masses are same. Figure 3.4(b) shows that bridge Young's modulus and moment of inertia produce the same effects on the bridge response too, which is greater than that caused by the density. From Figures 3.4(a) and (b), it can be easily observed that the bridge response is more sensitive to the change of its own parameters. Figure 3.4 also shows that when the dispersal degree of system parameters increases, the interval width of bridge displacement increases too.

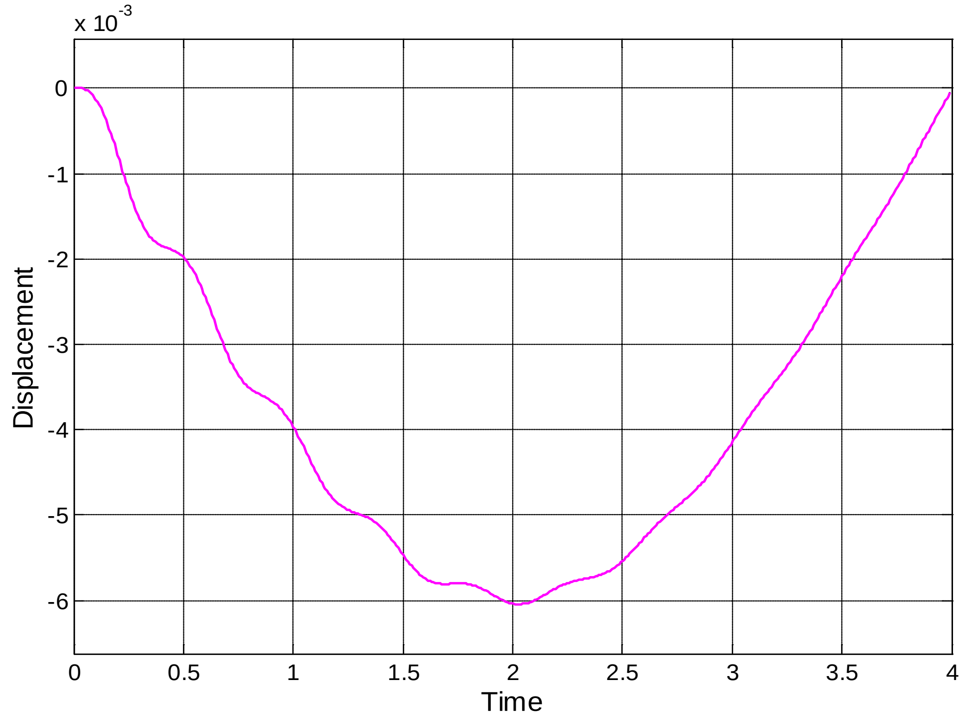

Figure 3.3 Midpoint of bridge displacement at mid-span.

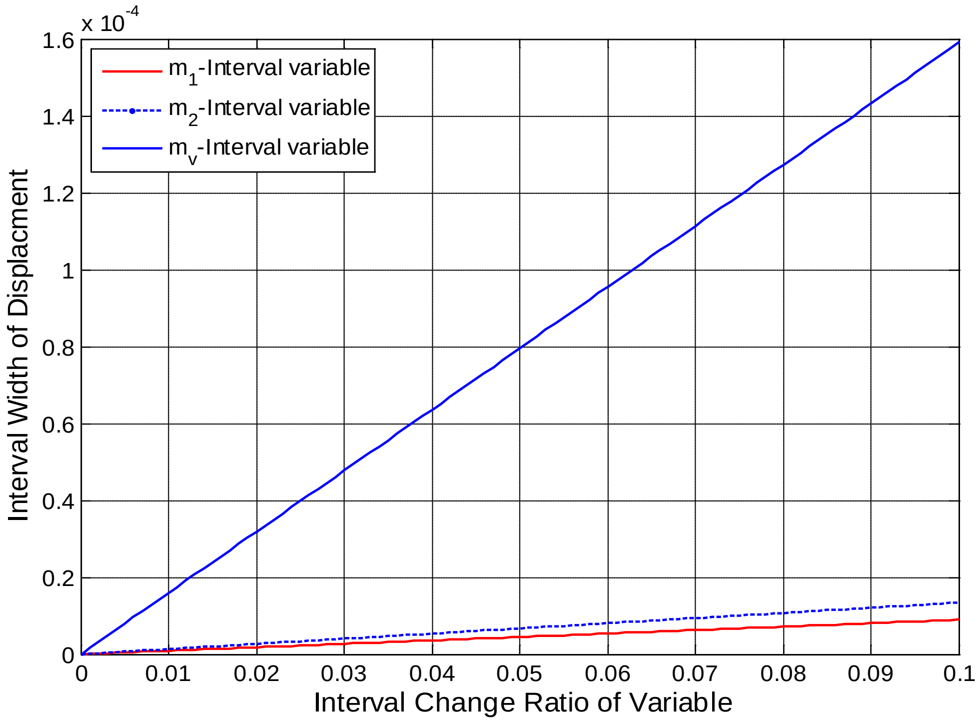

(a) Vehicle parameters are interval variables

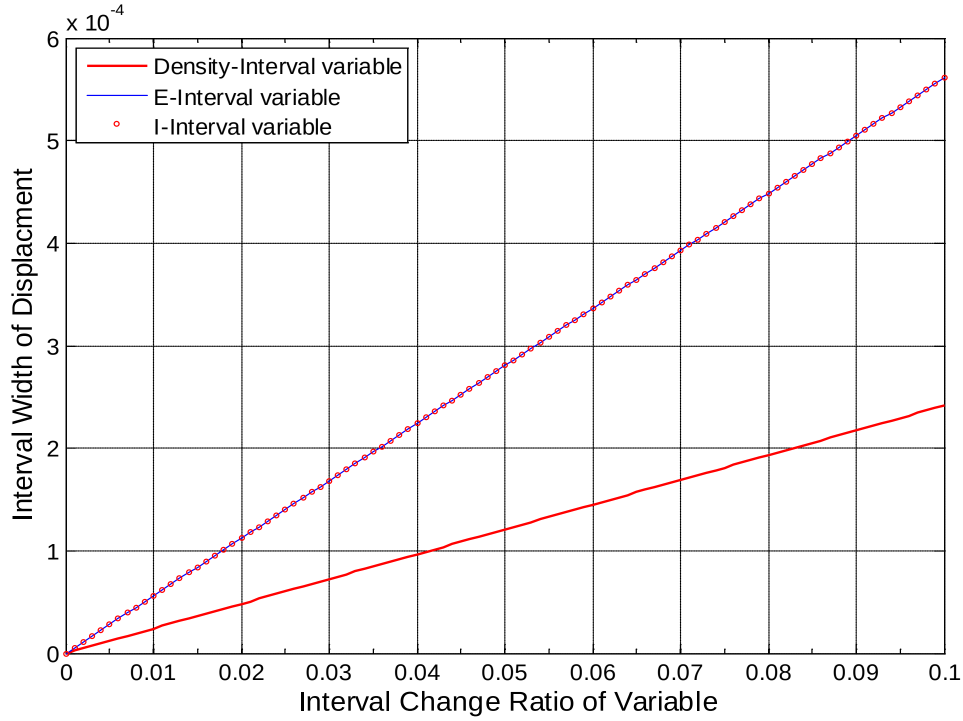

(b) Bridge parameters are interval variables

Figure 3.4 Interval width of bridge displacement at mid-span (x=20m,t=2s)

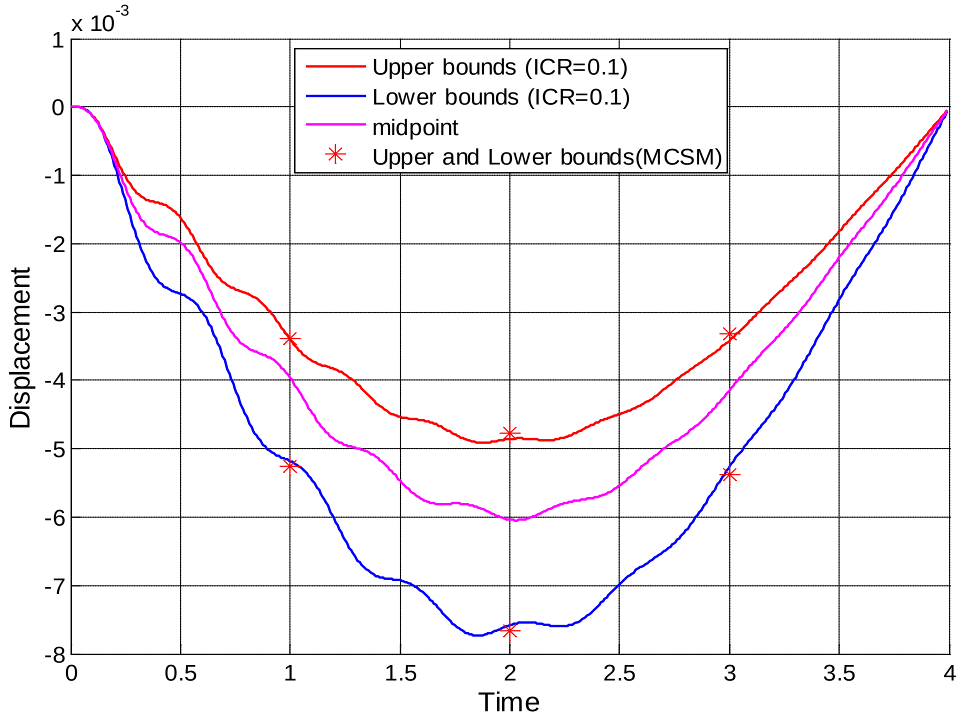

Figure 3.5 Verification by Monte-Carlo simulation method

To verify the results obtained by the presented method IAM, 10,000 Monte-Carlo simulations are also implemented when the interval change ratios of all parameters are 0.1. Figure 3.5 shows that the results calculated by the interval analysis method (IAM) agree very well with those are obtained by the Monte-Carlo simulation method (MCSM), however, the later one requires much more computational efforts.

3.6.2 LHNPSO

In this section, LHNPSO algorithm is used to solve the interval problem. The particle size is 50 and the iteration times are 200. Young's modulus is considered as an interval variable. The lower and upper bounds of bridge displacement at mid-span found by the LHNPSO are listed in Table 3.3. Results computed by 10,000 Monte-Carlo simulations are also given in this table for comparison. To further illustrate the effectiveness of LHNPSO, the lower and upper bounds of bridge displacement at mid-span versus the iteration times are given in Figures 3.6-3.12 while individual parameters are considered as interval variables in turn and then all system parameters are treated as interval variables.

From Table 3.3, it can be easily observed that the results obtained by LHNPSO are in good agreement with those calculated by MCSM as the differences are not big. The lower bounds determined by LHNPSO are less than what are generated by MCSM, whereas, the upper bounds found by LHNPSO are greater than those searched by MCSM. The intervals obtained by LHNPSO contain the change ranges by MCSM, hence, LHNPSO can give more accurate results. The main reason is that 10,000 Monte-Carlo simulations cannot give reliable results and are not able to capture the minimum and maximum values. Theoretically, MCSM will provide exact intervals of bridge response if infinite simulations are implemented. Therefore, the differences will be decreased, and the intervals obtained by MCSM will become bigger and tends to reach those determined by LHNPSO, if more simulations are performed.

Figures 3.6-3.12 show that convergence speed of LHNPSO is quite fast. Generally, the lower and upper bounds can converge at 200 iterations. In some cases, it can even converge at 100 iterations. For 50 particles and 200 iterations, the total calculation times for determining the minimum and maximum of bridge response are equal to $200 \times 50 = 10000$. Certainly, the results produced by the same number of Monte-Carlo simulations are not accurate enough. The computational effort requested by LHNPSO is much less than MCSM.

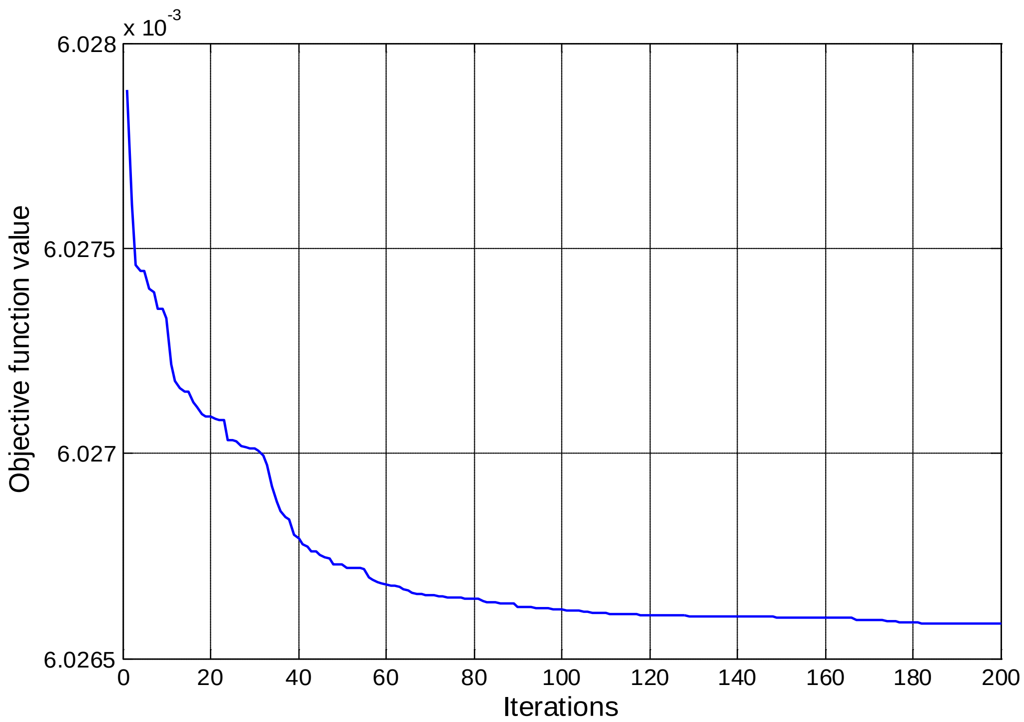

(a) Lower bound

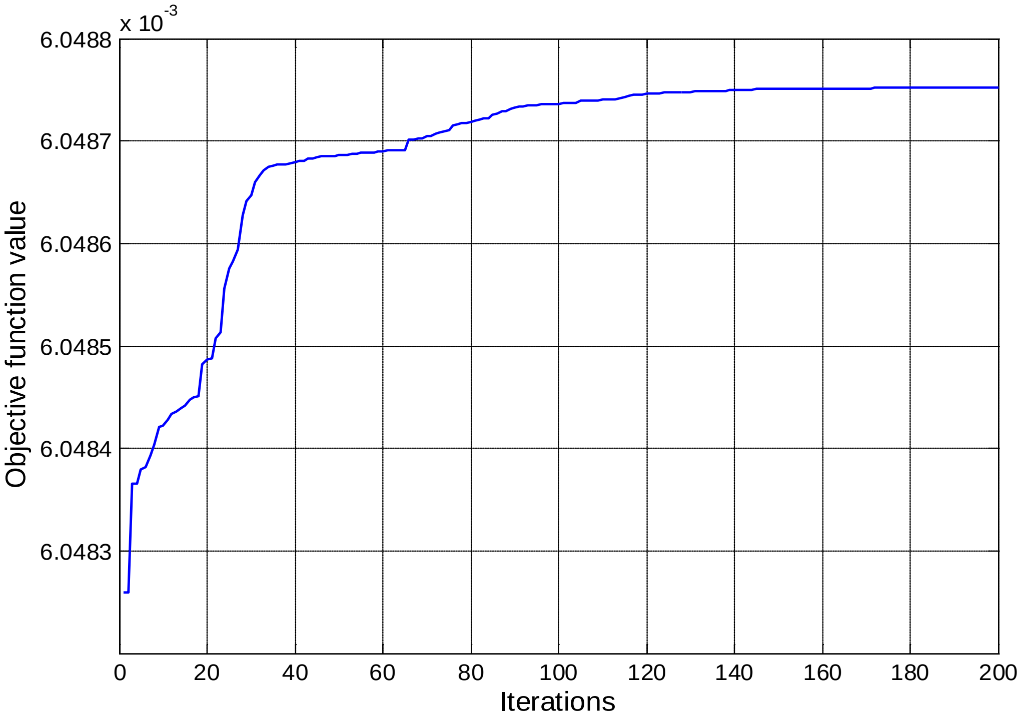

(b) Upper bound

Figure 3.6 Interval bridge displacement at mid-span ($\Delta m_{1F} = 0.1$)

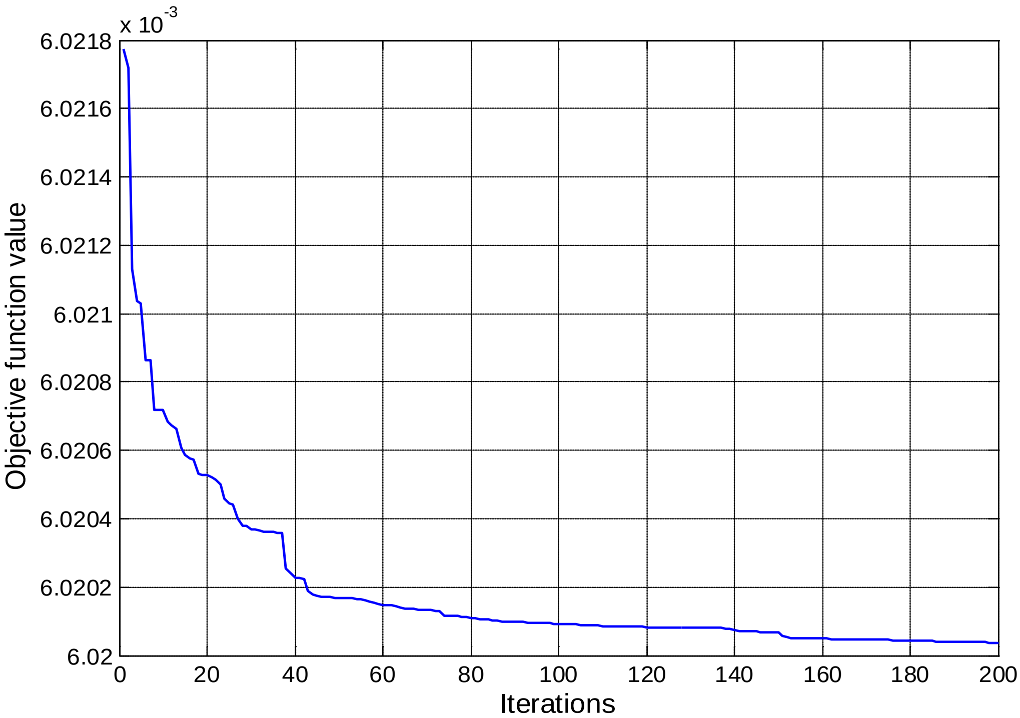

(a) Lower bound

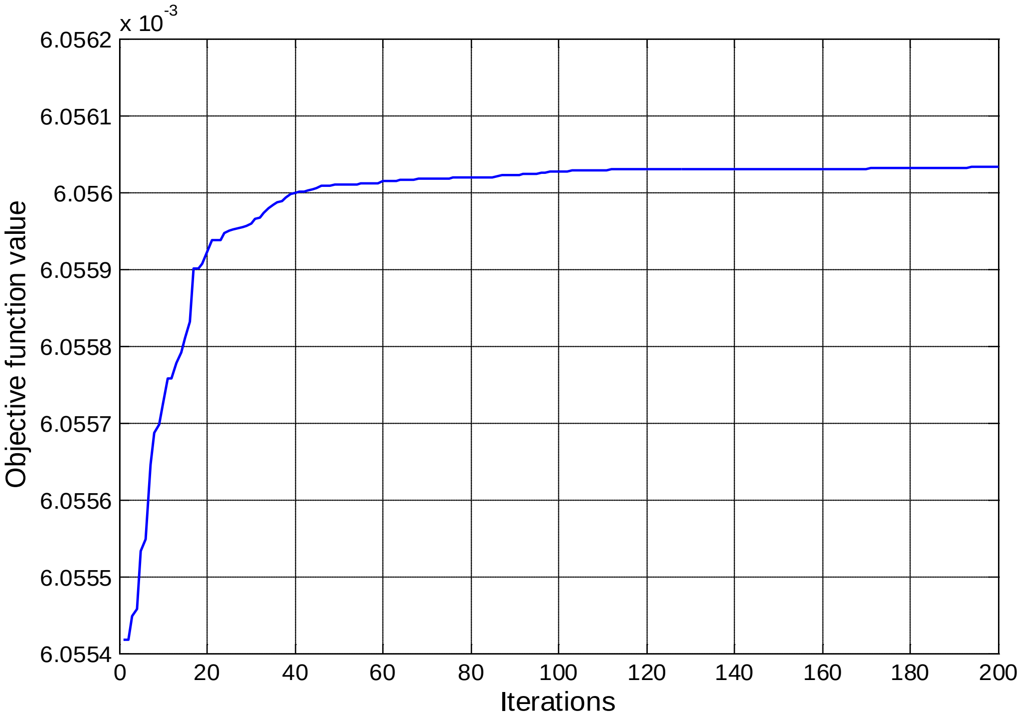

(b) Upper bound

Figure 3.7 Interval bridge displacement at mid-span ($\Delta m_{2F} = 0.1$)

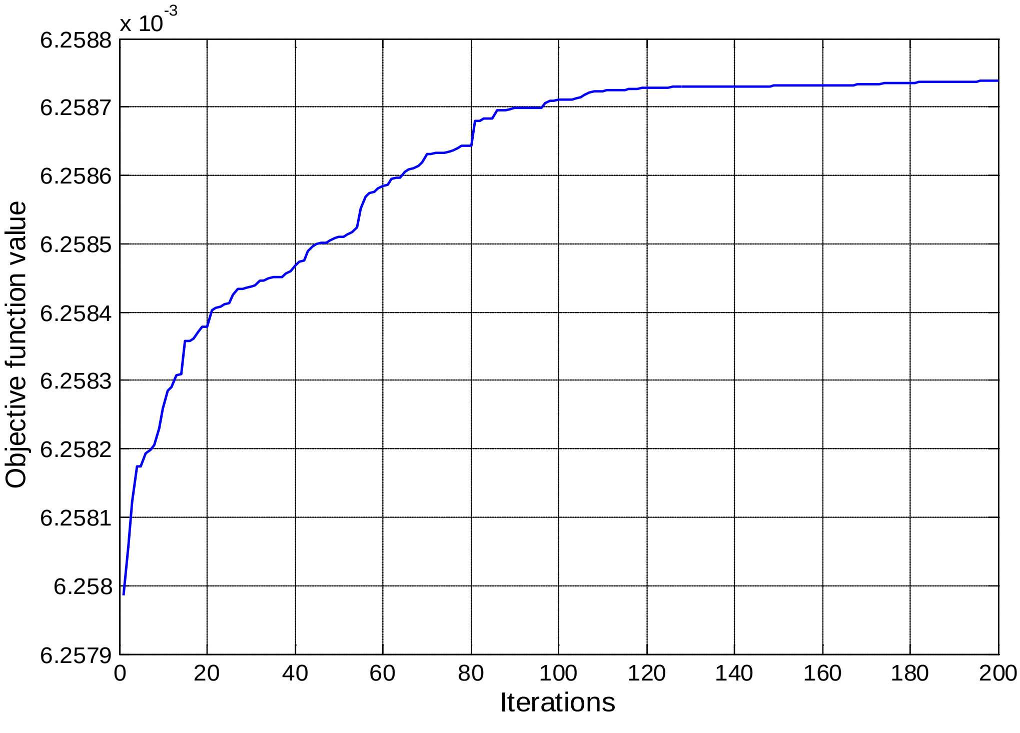

(a) Upper bound

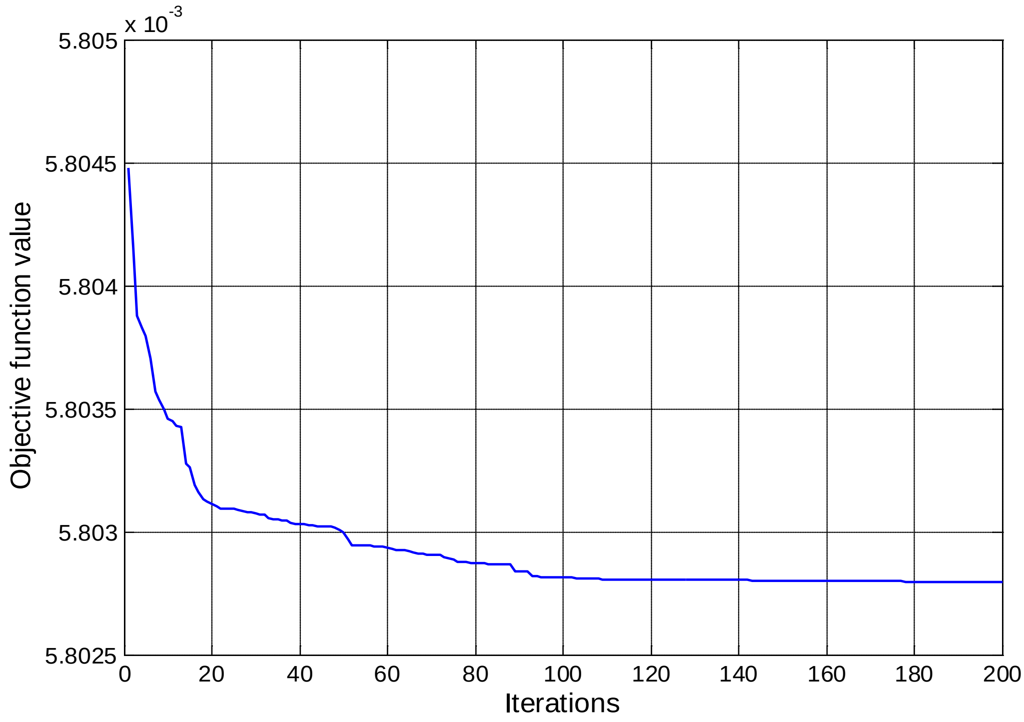

(b) Lower bound

Figure 3.8 Interval bridge displacement at mid-span ($\Delta m_{vF} = 0.1$)

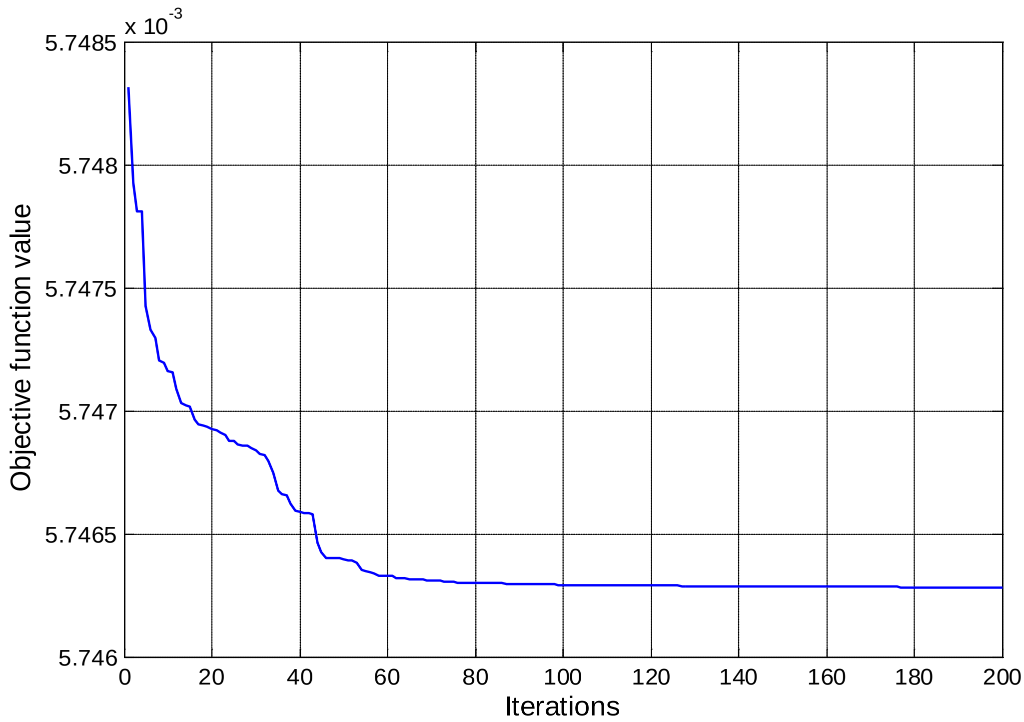

(a) Lower bound

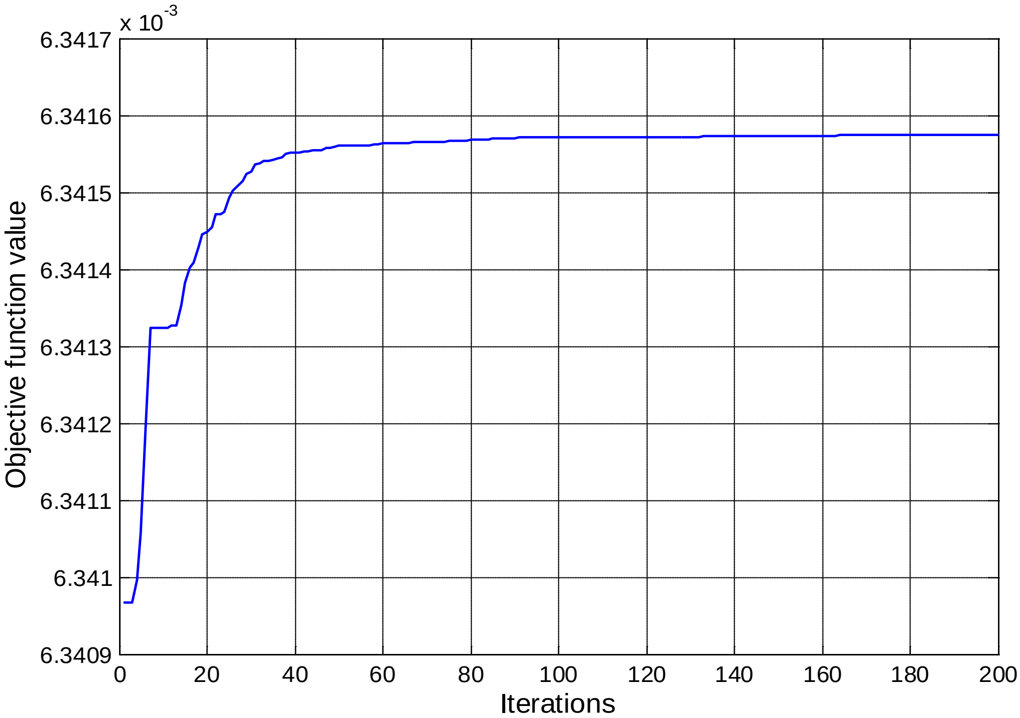

(b) Upper bound

Figure 3.9 Interval bridge displacement at mid-span ($\Delta\rho_F = 0.1$)

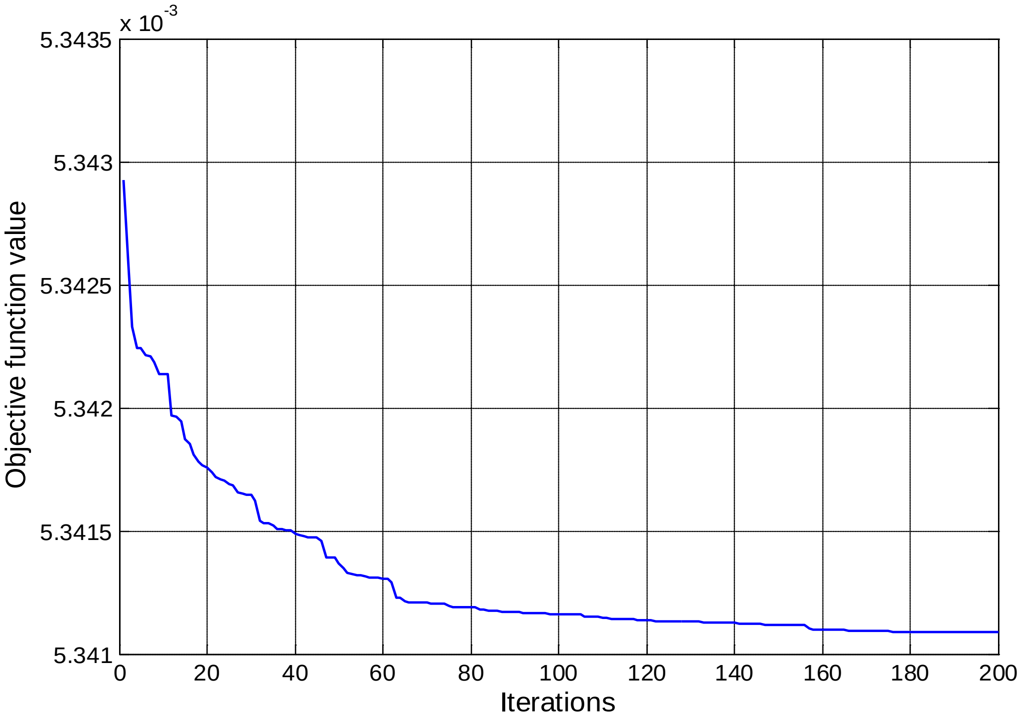

(a) Lower bound

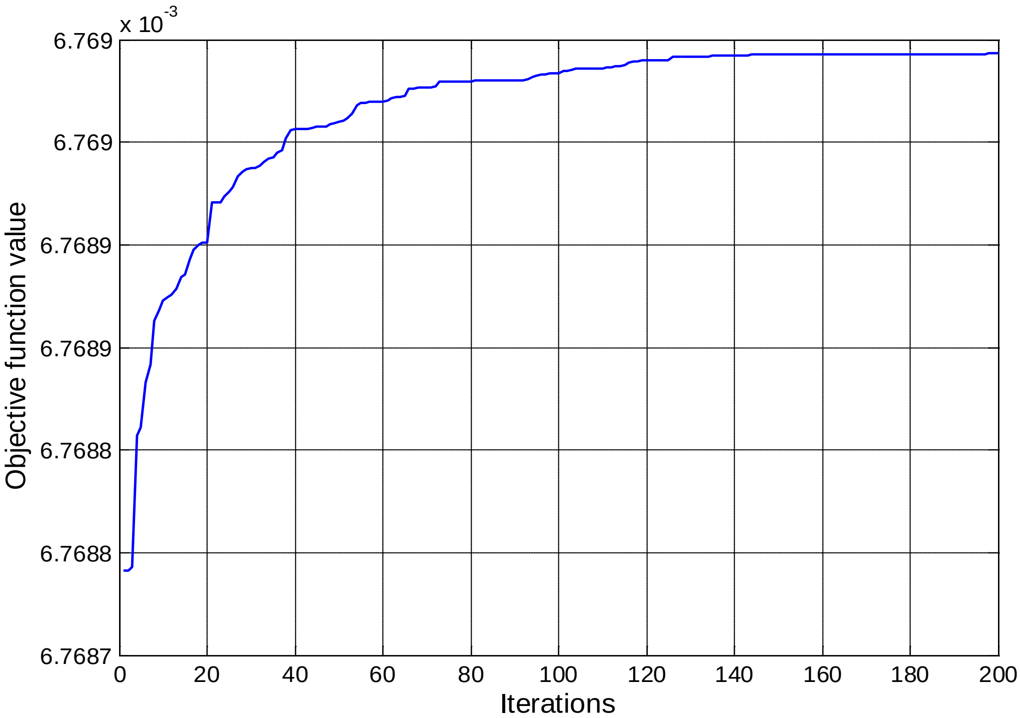

(b) Upper bound

Figure 3.10 Interval bridge displacement at mid-span ($\Delta E_F = 0.1$)

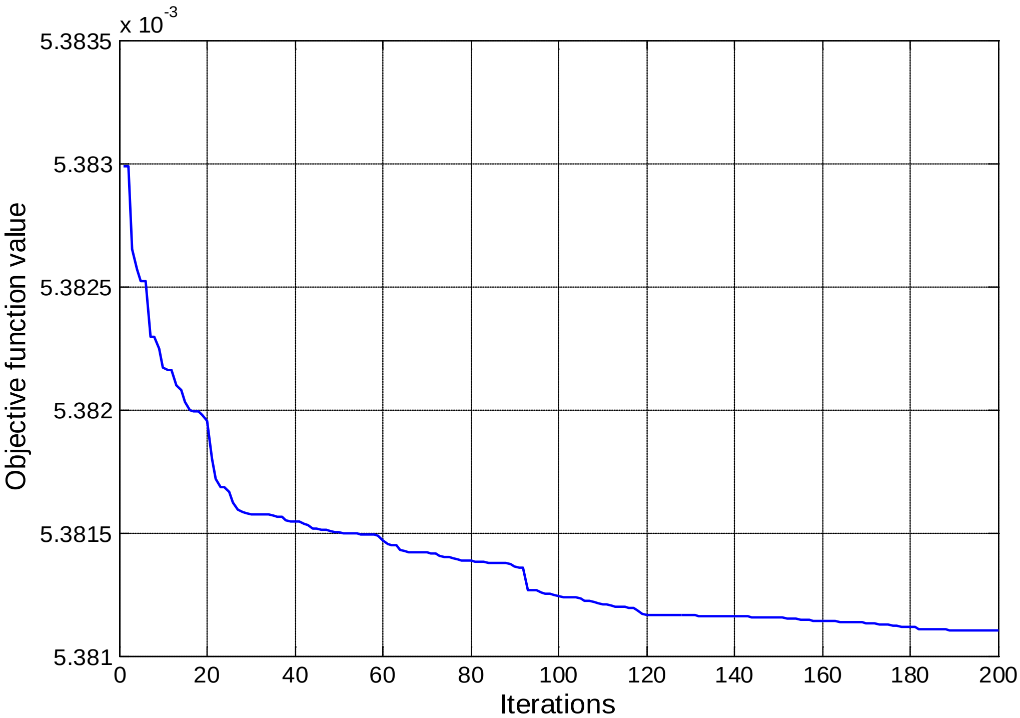

(a) Lower bound

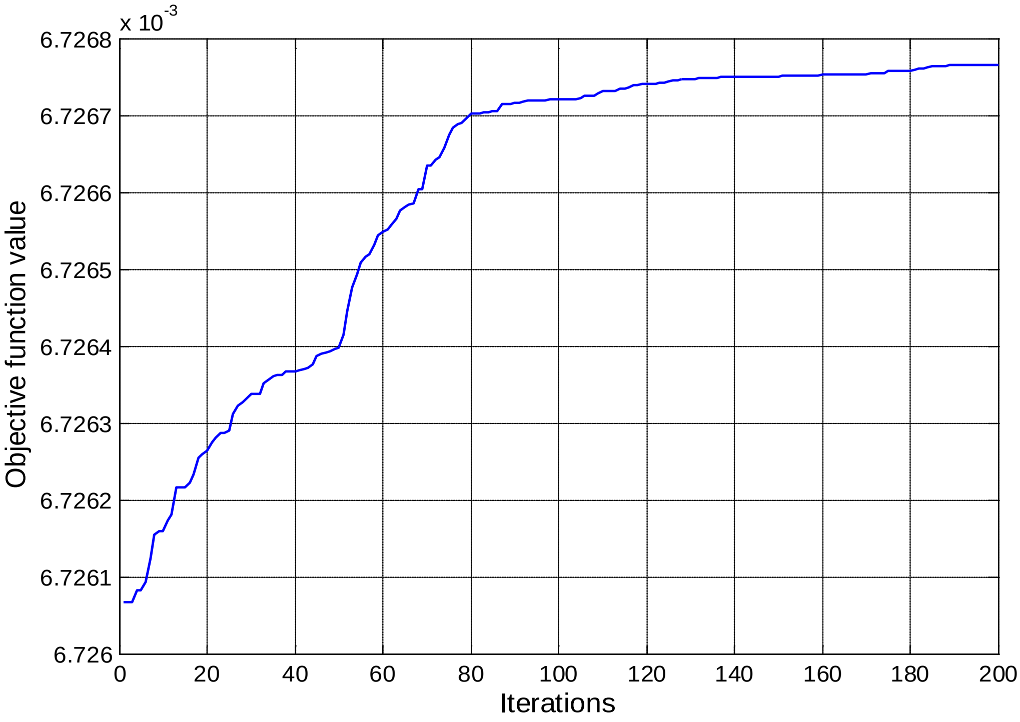

(b) Upper bound

Figure 3.11 Interval bridge displacement at mid-span ($\Delta I_F = 0.1$)

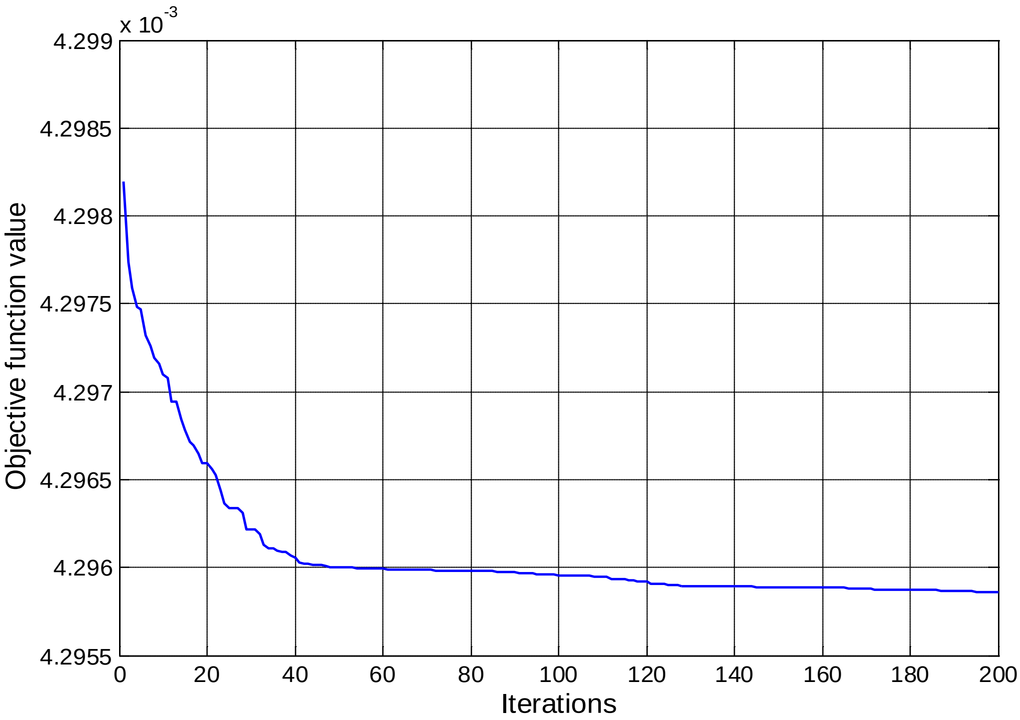

(a) Lower bound

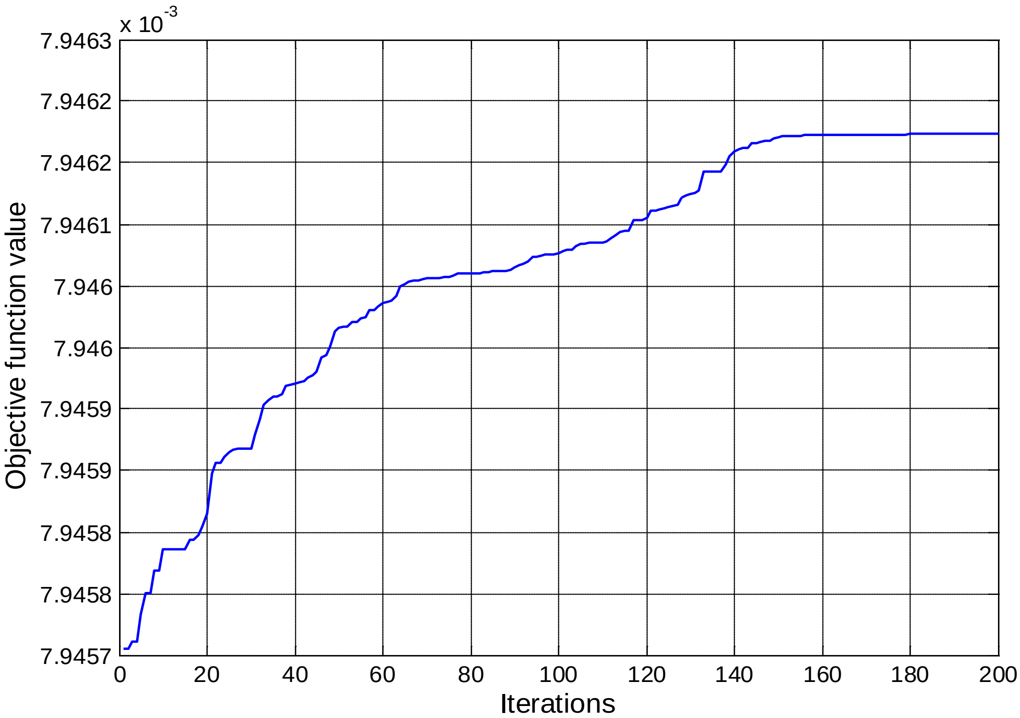

(b) Upper bound

Figure 3.12 Interval bridge displacement at mid-span

($\Delta m_{1F} = \Delta m_{2F} = \Delta m_{vF} = \Delta \rho_F = \Delta E_F = \Delta I_F = 0.1$)

Table 3.3 Comparison of results by LHNPSO and MCSM

ΔE_F	Lower bounds		Difference	Upper bounds		Difference
	LHNPSO	MCSM		PSO	MCSM	
0.05	5.67591E-03	5.69459E-03	0.32918%	6.39404E-03	6.36210E-03	0.49949%
0.08	5.50036E-03	5.57430E-03	1.34439%	6.59301E-03	6.52330E-03	1.05725%
0.1	5.34117E-03	5.44117E-03	1.87225%	6.76946E-03	6.70936E-03	0.88781%

3.6.3 Comparison of results obtained by IAM and LHNPSO

To further evaluate the performances of IAM and LHNPSO, the lower and upper bounds of bridge displacement at mid-span are given in Figures 3.13(a)-(g) when the interval change ratios of system parameters are changing. The differences are listed in Tables 3.4-3.10.

From Figures 3.13(a)-(g), it can be easily seen that the ranges of changes in bridge response computed by IAM are smaller than those determined by LHNPSO. As the first order Taylor expansion is used in IAM to calculate the interval width, IAM cannot give a conservative result. However, IAM requires only one time calculation to get the result.

From Tables 3.4-3.10, it can be also easily observed that the results obtained by the two methods agree well as the differences are not big. The difference becomes bigger and bigger along with the increase of change ranges of system parameters. When the interval change ratio is 0.1, the biggest difference is 4.7947% when all system parameters are considered as interval variables, but it is much smaller if the uncertainty of only one system parameter is under consideration.

In summary, when the ranges of change in system parameters become bigger, the differences between the results obtained by the two methods become more obvious. LHNPSO can give more accurate results but requires more computational effort. For important structures, it is better to use LHNPSO to predict the change ranges of structural response. Interval analysis method (IAM) is also available for many structures as it is much time-saving and its accuracy is acceptable especially when the intervals of system inputs are not too big.

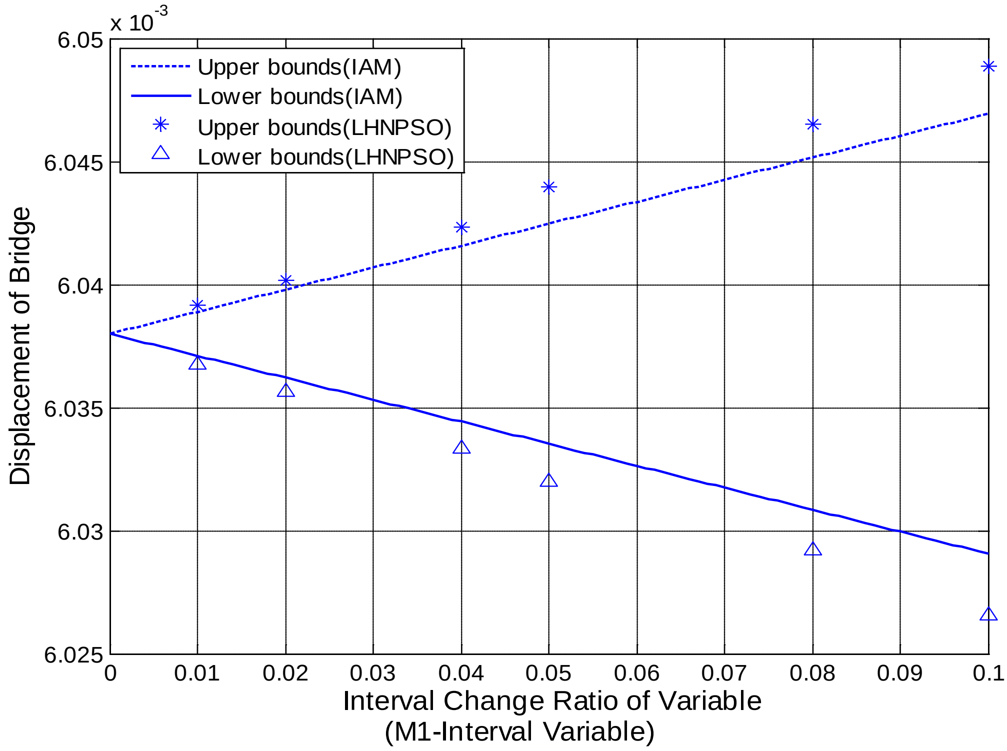
x 10^-3
6.05
6.045
6.04
6.035
6.03
6.025
Upper bounds(IAM)
Lower bounds(IAM)
Upper bounds(LHNPSO)
Lower bounds(LHNPSO)
Displacement of Bridge
0
0.01
0.02
0.03
0.04
0.05
0.06
0.07
0.08
0.09
0.1
Interval Change Ratio of Variable
(M1-Interval Variable)

(a)

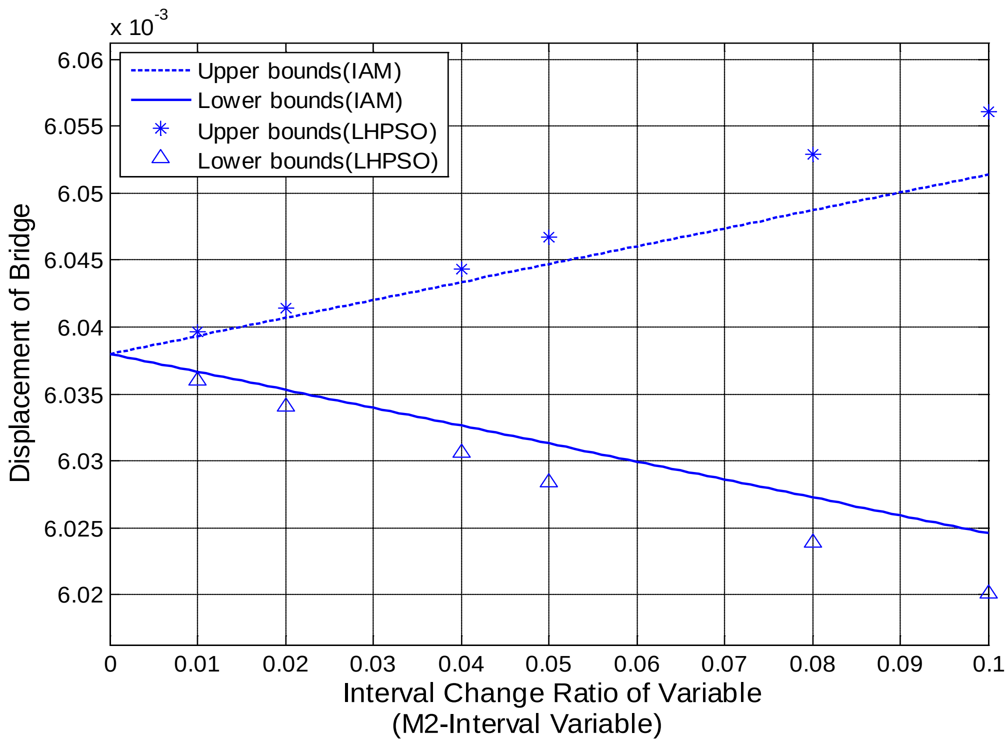
x 10^-3
6.06
6.055
6.05
6.045
6.04
6.035
6.03
6.025
6.02
Upper bounds(IAM)
Lower bounds(IAM)
Upper bounds(LHPSO)
Lower bounds(LHPSO)
Displacement of Bridge
0
0.01
0.02
0.03
0.04
0.05
0.06
0.07
0.08
0.09
0.1
Interval Change Ratio of Variable
(M2-Interval Variable)

(b)

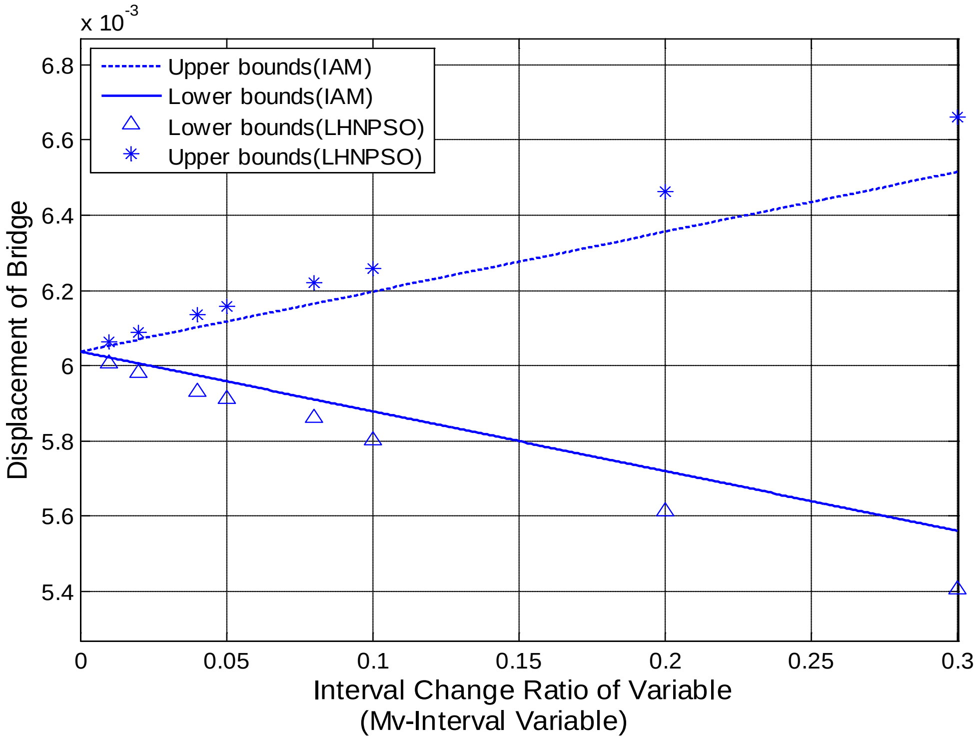
x 10^-3
6.8
6.6
6.4
6.2
6
5.8
5.6
5.4
Upper bounds(IAM)
Lower bounds(IAM)
Lower bounds(LHNPSO)
Upper bounds(LHNPSO)
Displacement of Bridge
0
0.05
0.1
0.15
0.2
0.25
0.3
Interval Change Ratio of Variable
(Mv-Interval Variable)

(c)

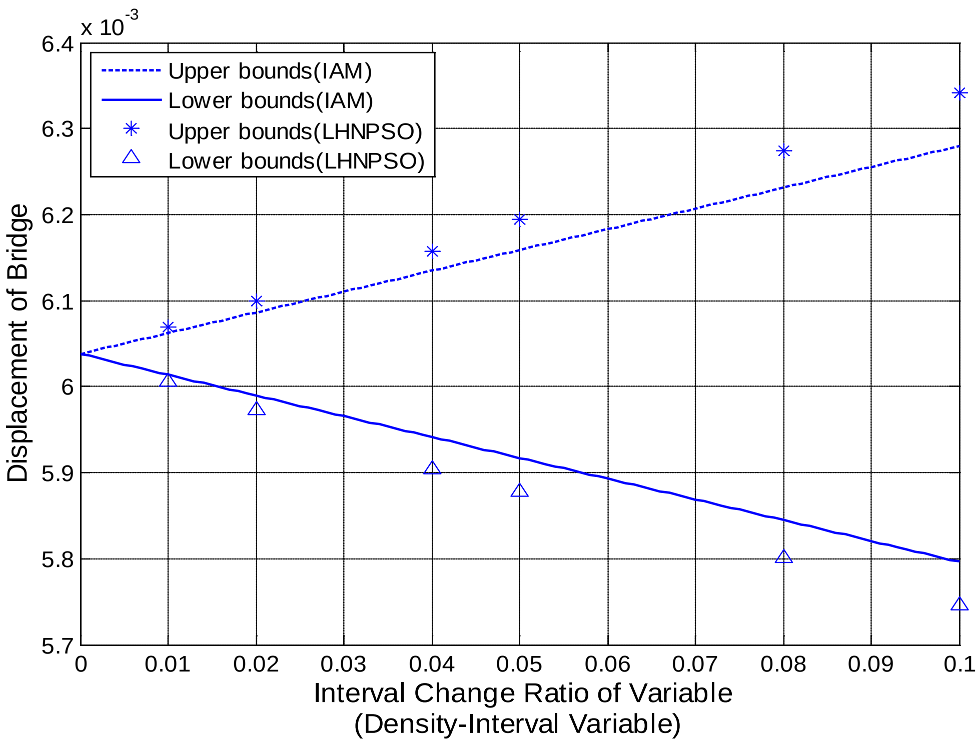
x 10^-3
6.4
6.3
6.2
6.1
6
5.9
5.8
5.7
Upper bounds(IAM)
Lower bounds(IAM)
Upper bounds(LHNPSO)
Lower bounds(LHNPSO)
Displacement of Bridge
0
0.01
0.02
0.03
0.04
0.05
0.06
0.07
0.08
0.09
0.1
Interval Change Ratio of Variable
(Density-Interval Variable)

(d)

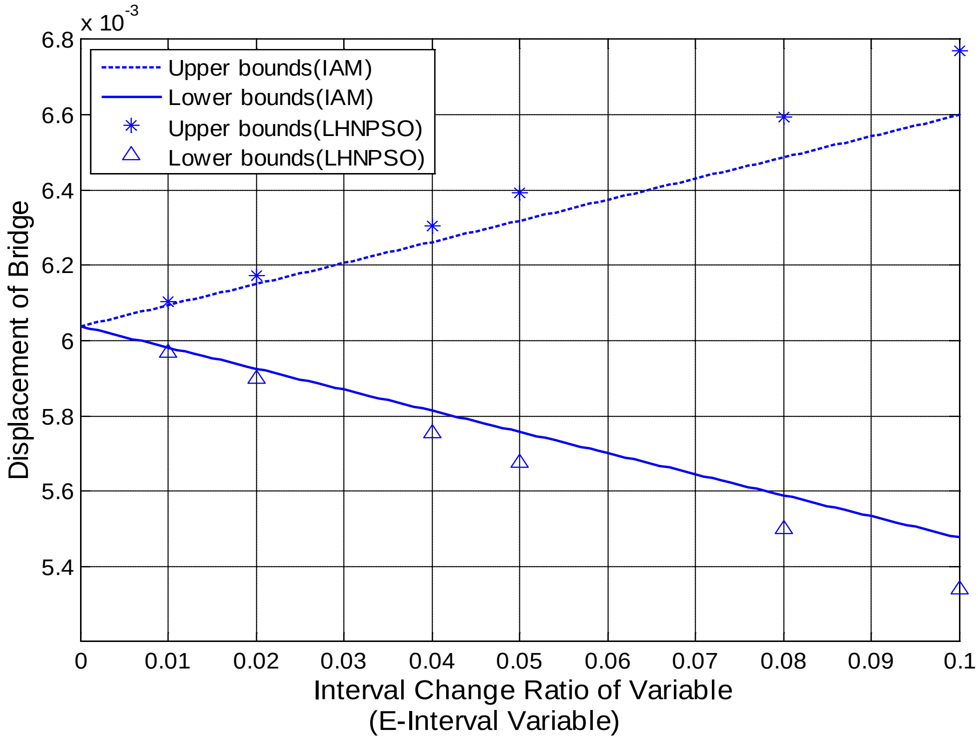
x 10^-3
Upper bounds(IAM)
Lower bounds(IAM)
Upper bounds(LHNPSO)
Lower bounds(LHNPSO)
Displacement of Bridge
6.8
6.6
6.4
6.2
6
5.8
5.6
5.4
0
0.01
0.02
0.03
0.04
0.05
0.06
0.07
0.08
0.09
0.1
Interval Change Ratio of Variable
(E-Interval Variable)

(e)

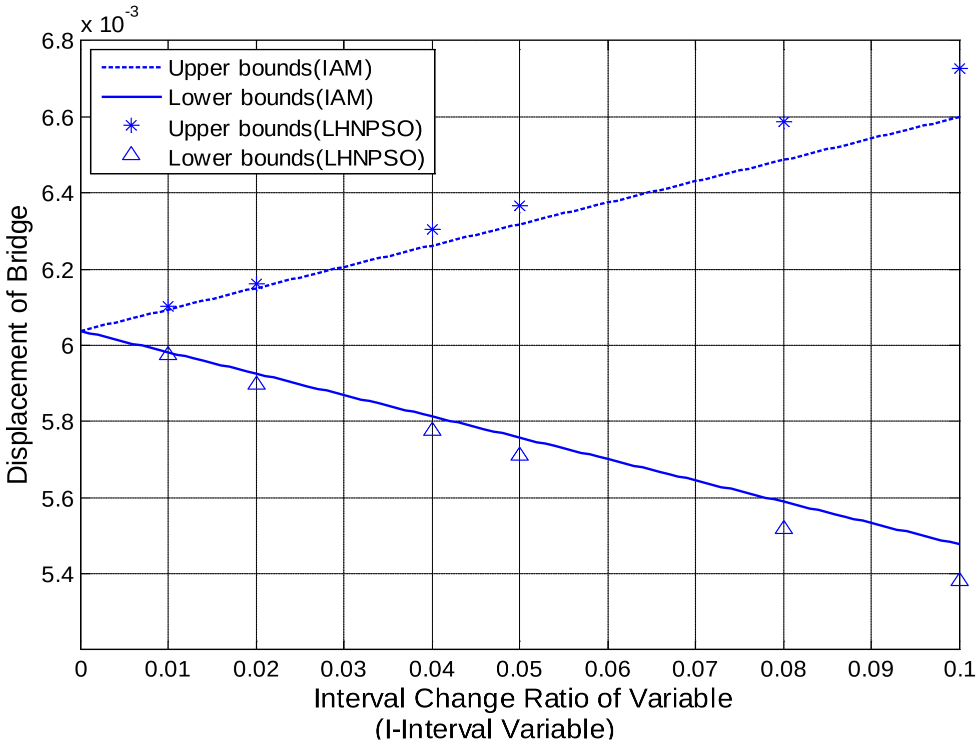
x 10^-3
Upper bounds(IAM)
Lower bounds(IAM)
Upper bounds(LHNPSO)
Lower bounds(LHNPSO)
Displacement of Bridge
6.8
6.6
6.4
6.2
6
5.8
5.6
5.4
0
0.01
0.02
0.03
0.04
0.05
0.06
0.07
0.08
0.09
0.1
Interval Change Ratio of Variable
(I-Interval Variable)

(f)

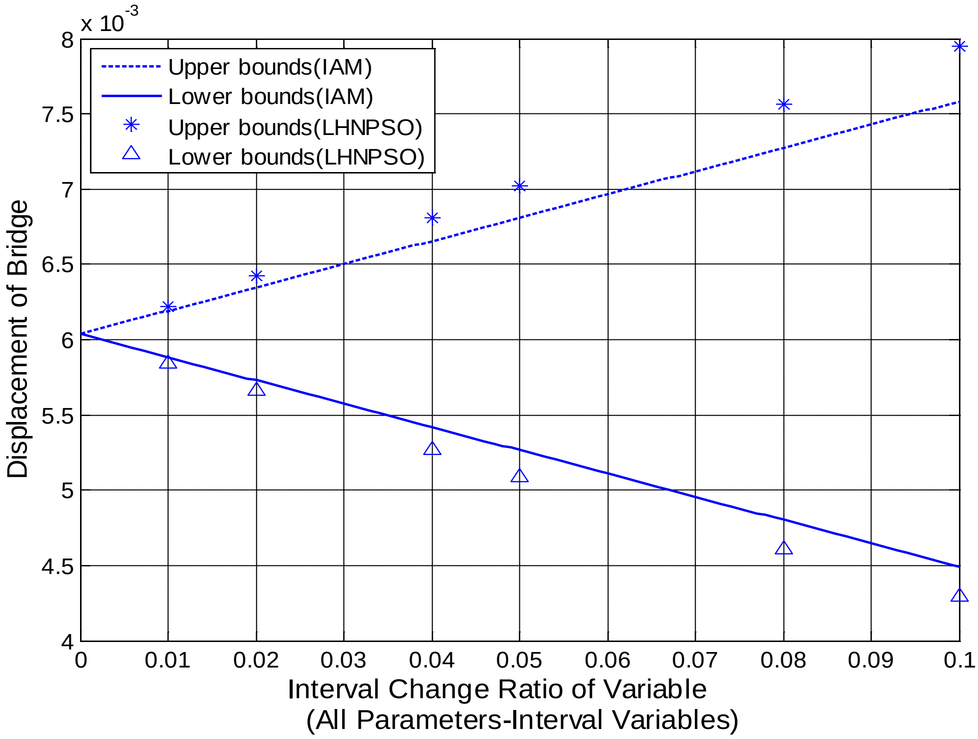

(g)

Figure 3.13 Lower and upper bounds obtained by IAM and LHNPSO

Table 3.4 Comparison of the results by IAM and LHNPSO

Δm_{1F}	Lower bounds		Difference	Upper bounds		Difference
	IAM	PSO		IAM	PSO	
0.01	6.03889E-03	6.03917E-03	0.0046%	6.03711E-03	6.03677E-03	0.0056%
0.02	6.03979E-03	6.04017E-03	0.0063%	6.03621E-03	6.03564E-03	0.0095%
0.04	6.04158E-03	6.04234E-03	0.0126%	6.03442E-03	6.03334E-03	0.0179%
0.05	6.04247E-03	6.04396E-03	0.0247%	6.03353E-03	6.03198E-03	0.0257%
0.08	6.04515E-03	6.04652E-03	0.0226%	6.03085E-03	6.02919E-03	0.0275%
0.1	6.04694E-03	6.04876E-03	0.0301%	6.02906E-03	6.02654E-03	0.0418%

Table 3.5 Comparison of the results by IAM and LHNPSO

Δm_{2F}	Lower bounds		Difference	Upper bounds		Difference
	IAM	PSO		IAM	PSO	
0.01	6.03934E-03	6.03961E-03	0.00442%	6.03666E-03	6.03603E-03	0.01050%
0.02	6.04068E-03	6.04144E-03	0.01260%	6.03532E-03	6.03410E-03	0.02013%
0.04	6.04336E-03	6.04432E-03	0.01594%	6.03264E-03	6.03061E-03	0.03363%
0.05	6.04470E-03	6.04668E-03	0.03278%	6.03130E-03	6.02843E-03	0.04762%
0.08	6.04872E-03	6.05287E-03	0.06867%	6.02728E-03	6.02389E-03	0.05630%
0.1	6.05140E-03	6.05603E-03	0.07659%	6.02460E-03	6.02013E-03	0.07418%

Table 3.6 Comparison of the results by IAM and LHNPSO

Δm_{vF}	Lower bounds		Difference	Upper bounds		Difference
	IAM	PSO		IAM	PSO	
0.01	6.05390E-03	6.06495E-03	0.18250%	6.02210E-03	6.00722E-03	0.24715%
0.02	6.06980E-03	6.08969E-03	0.32770%	6.00620E-03	5.98247E-03	0.39502%
0.04	6.10160E-03	6.13505E-03	0.54824%	5.97440E-03	5.93299E-03	0.69313%
0.05	6.11750E-03	6.15773E-03	0.65765%	5.95850E-03	5.91237E-03	0.77417%
0.08	6.16520E-03	6.21959E-03	0.88217%	5.91080E-03	5.86196E-03	0.82631%
0.1	6.19700E-03	6.25874E-03	0.99634%	5.87900E-03	5.80278E-03	1.29642%

Table 3.7 Comparison of the results by IAM and LHNPSO

$\Delta\rho_F$	Upper bounds		Difference	Lower bounds		Difference
	IAM	PSO		IAM	PSO	
0.01	6.06215E-03	6.06957E-03	0.1224%	6.01385E-03	6.00584E-03	0.1332%
0.02	6.08630E-03	6.09988E-03	0.2232%	5.98970E-03	5.97242E-03	0.2885%
0.04	6.13460E-03	6.15739E-03	0.3716%	5.94140E-03	5.90480E-03	0.6159%
0.05	6.15875E-03	6.19392E-03	0.5711%	5.91725E-03	5.87760E-03	0.6700%
0.08	6.23120E-03	6.27475E-03	0.6989%	5.84480E-03	5.80133E-03	0.7437%
0.1	6.27950E-03	6.34158E-03	0.9887%	5.79651E-03	5.74625E-03	0.8670%

Table 3.8 Comparison of the results by IAM and LHNPSO

ΔE_F	Upper bounds		Differen ce	Lower bounds		Difference
	IAM	PSO		IAM	PSO	
0.01	6.09409E-03	6.10337E-03	0.1522%	5.98191E-03	5.96969E-03	0.2043%
0.02	6.15018E-03	6.17176E-03	0.3509%	5.92582E-03	5.89819E-03	0.4663%
0.04	6.26235E-03	6.30389E-03	0.6633%	5.81365E-03	5.75518E-03	1.0057%
0.05	6.31844E-03	6.39404E-03	1.1965%	5.75756E-03	5.67591E-03	1.4182%
0.08	6.48670E-03	6.59301E-03	1.6388%	5.58930E-03	5.50036E-03	1.5913%
0.1	6.59888E-03	6.76948E-03	2.5852%	5.47712E-03	5.34117E-03	2.4822%

Table 3.9 Comparison of the results by IAM and LHNPSO

ΔI_F	Upper bounds		Difference	Lower bounds		Difference
	IAM	PSO		IAM	PSO	
0.01	6.09409E-03	6.10257E-03	0.1391%	5.98191E-03	5.97569E-03	0.1040%
0.02	6.15018E-03	6.16266E-03	0.2029%	5.92582E-03	5.89672E-03	0.4911%
0.04	6.26235E-03	6.30379E-03	0.6617%	5.81365E-03	5.77518E-03	0.6617%
0.05	6.31844E-03	6.36540E-03	0.7433%	5.75756E-03	5.70991E-03	0.8277%
0.08	6.48670E-03	6.58623E-03	1.5344%	5.58930E-03	5.51854E-03	1.2661%
0.1	6.59888E-03	6.72677E-03	1.9381%	5.47712E-03	5.38120E-03	1.7513%

Table 3.10 Comparison of the results by IAM and LHNPSO

ICR of all	Upper bounds		Difference	Lower bounds		Difference
	IAM	PSO		IAM	PSO	
0.01	6.19247E-03	6.21901E-03	0.4286%	5.88353E-03	5.84539E-03	0.6483%
0.02	6.34693E-03	6.42562E-03	1.2398%	5.72907E-03	5.66405E-03	1.1349%
0.04	6.65587E-03	6.80579E-03	2.2524%	5.42013E-03	5.26994E-03	2.7709%
0.05	6.81033E-03	7.02066E-03	3.0884%	5.26567E-03	5.08843E-03	3.3660%
0.08	7.27373E-03	7.56612E-03	4.0197%	4.80227E-03	4.61136E-03	3.9755%
0.1	7.58266E-03	7.94623E-03	4.7947%	4.49334E-03	4.29587E-03	4.3948%

3.7 Conclusions

In this chapter, dynamic response of vehicle-bridge interaction system with uncertain but bounded parameters is investigated by using the interval analysis method and LHNPSO. The expressions for calculating the lower and upper bounds of bridge response have been derived by using the interval analysis method. Using these formulations, the intervals can be very easily obtained by one time calculation. LHNPSO requires more computational effort but it can provide more accurate results. The results obtained by these two methods are in very good agreement with those determined by Monte-Carlo simulation method. The differences of IAM and LHNPSO are quite small when the change ranges of system parameters are not big. In the future, the IAM and LHNPSO will be further developed to investigate the non-deterministic behaviour of a bridge under dynamic loadings induced by multi-vehicles.

Chapter 4 Hybrid probabilistic interval dynamic analysis of vehicle-bridge interaction system with uncertainties

4.1 Introduction

Powerful probabilistic approaches have been widely used to predict responses and to implement reliability assessment of structural systems with uncertainties [7-11]. In probabilistic methods, uncertain parameters are modelled as random variables/fields and uncertainties of loads are described by random processes/variables. The most important factor for correctly using probabilistic methods is to justify the probability densities of the random variables and is to obtain appropriate measurement data and sufficient statistical information. Probabilistic methods are the first choice when information about an uncertain parameter in the form of a preference probability function is available. Over the lifetime of a structure, the progressive deterioration of concrete and corrosion of steel will lead to significant variations of structural parameters. Sometimes it is hard to get the enough probabilistic information for structural parameters as their values are affected by a lot of non-deterministic factors such as time, temperature, humidity, cracks and so on. Meanwhile, loads of many scenarios can hardly be modelled as random variables due to large changes in their magnitudes. Therefore, interval analysis has been developed to handle this kind of uncertainties. Interval methods can be used when the probability function is unavailable but the range of the uncertain parameter can be defined.

It is desirable to model structural parameters/loads as random variables if sufficient information can be obtained to form the probability density functions. Meanwhile, some structural parameters/loads might be best considered as interval variables if the information/data are not enough to model uncertain structural parameters and loadings as random variables, especially in the early design stages. Consequently, hybrid probabilistic interval analysis and reliability assessment of structures with a mixture of random and interval properties has been conducted [134-136]. The random interval moment method has been developed to determine the mean value and standard deviation of random interval responses of structures under static forces [10].

Efforts have been made on dynamic response of a bridge under a moving vehicle/force considering the uncertainties in the system [13, 15,137,138]. Stochastic approaches have been developed for the dynamic analysis of vehicle-bridge interaction system with random parameters in the past decade. As aforementioned, some parameters of vehicle-bridge interaction system could be considered as random variables and some of them might be assumed as interval variables. Therefore, a hybrid probabilistic interval analysis model for vehicle-bridge coupled systems needs to be developed.

In this chapter, dynamic response of a bridge under a moving vehicle with uncertain parameters is studied. The vehicle is represented by a half-car model and the bridge is modelled as an Euler-Bernoulli beam as Chapter 3. The vehicle parameters are assumed as interval variables, and the bridge parameters corresponding to Young's modulus, mass and moment of inertia, are considered as random variables. Random interval moment method proposed for static probabilistic interval analysis is extended to derive the computational expressions for the lower and upper bounds of expectation and variance of the random interval dynamic responses of the bridge. Monte-Carlo simulations are also implemented to validate the presented method. In addition, the effects of the vehicle and bridge parameters on the bridge response are investigated.

This chapter is organized as follows. Section 4.2 introduces the random interval moment method briefly. Section 4.3 presents the random interval model of a vehicle-bridge interaction system. In Section 4.4, the dynamic response analysis of the bridge based on the random interval moment method is presented. Numerical examples and computational results are given in section 4.5. Conclusions are stated in the last section.

This work presented in this chapter is mainly dependent on the research reported in by Liu et al. in International Journal of Structural Stability and Dynamics, 14 (2014), 1350069, 25 pages.

4.2 Random Interval Moment Method

Let $X(R)$ be the set of all real random variables on a probability space (Ω, A, P), x^R is a random variable of $\mathrm{X}(R)$. R denotes the set of all real numbers. μ_x (or $\bar{x}$) and σ_x are the mean (deterministic) value and standard deviation of x^R, respectively. $y^I = [\underline{y}, \overline{y}] = \left\{ t, \underline{y} \le t \le \overline{y} \middle| \underline{y}, \overline{y} \in R \right\}$ is an interval variable of $I(R)$ which denotes the set of all the closed real intervals. $\underline{y}$ and $\overline{y}$ are the lower and upper bounds of interval variable y^I, respectively. For the purpose of completeness, the basic information of interval variable y^I is repeated here

$$y^I = y^c + \Delta y^I \,;\ \Delta y^I = [-\Delta y, +\Delta y]\,;\ y^c = \frac{\underline{y} + \overline{y}}{2}\,;\ \Delta y = \frac{\overline{y} - \underline{y}}{2}\quad \Delta y_F = \frac{\Delta y}{y^c} \tag{4.1}$$

where y^c, Δy, Δy^I and Δy_F represent the midpoint value, maximum width (interval width), uncertain interval and interval change ratio of the interval variable y^{I}.

Without loss of generality, random interval variable Z^{RI} is the function of multiple random and interval variables, which are respectively represented by random vector $\vec{X}^R = (x_1^R, x_2^R, \cdots, x_n^R)$ and interval vector $\vec{Y}^I = (y_1^I, y_2^I, \cdots, y_m^I)$. The deterministic values of $\vec{X}^R$ and $\vec{Y}^I$ are $\bar{\vec{X}} = (\bar{x}_1, \bar{x}_2, \cdots, \bar{x}_n)$ and $\vec{Y}^c = (y_1^c, y_2^c, \cdots, y_m^c)$, respectively.

The Taylor series to the first-order of the random interval variable $Z^{RI} = f(\vec{X}^R, \vec{Y}^I)$ about ($\vec{X}^R, \vec{Y}^I$) is expressed as

$$Z^{RI} = f(\vec{X}^R, \vec{Y}^I) = f(\bar{\vec{X}}, \vec{Y}^I) + \sum_{i=1}^{n} \left\{ \left. \frac{\partial f}{\partial x_i^R} \right|_{\bar{\vec{X}}, \vec{Y}^I} \right\} \cdot (x_i^R - \bar{x}_i) + R$$

$$= f(\bar{\vec{X}}, \vec{Y}^c) + \sum_{j=1}^{m} \left\{ \left. \frac{\partial f}{\partial y_j^I} \right|_{\bar{\vec{X}}, \vec{Y}^c} \right\} \cdot \Delta y_j^I$$

$$+\sum_{i=1}^{n}\left\{\left.\frac{\partial f}{\partial x_i^R}\right|_{\bar{\vec{X}},\vec{Y}^c}+\sum_{j=1}^{m}\left\{\left.\frac{\partial^2 f}{\partial x_i^R \partial y_j^I}\right|_{\bar{\vec{X}},\vec{Y}^c}\right\}\cdot \Delta y_j^I\right\}\cdot(x_i^R-\bar{x}_i)+R \qquad (4.2)$$

where R is the remainder term.

From this equation, ignoring the higher order terms represented by R, the expectation and variance of random interval variables $Z^{RI}=f(\vec{X}^R,\vec{Y}^I)$ can be calculated as [33]

$$\mu_{Z^{RI}}=E(Z^{RI})=f(\bar{\vec{X}},\vec{Y}^c)+\sum_{j=1}^{m}\{\left.\frac{\partial f}{\partial y_j^I}\right|_{\bar{\vec{X}},\vec{Y}^c}\}\Delta y_j^I \qquad (4.3)$$

$$\sigma_{Z^{RI}}^2=E\left(Z^{RI}-E(Z^{RI})\right)^2=\sum_{i=1}^{n}\sum_{k=1}^{n}\left\{\left.\frac{\partial f}{\partial x_i^R}\right|_{\bar{\vec{X}},\vec{Y}^c}+\sum_{j=1}^{m}\left\{\left.\frac{\partial^2 f}{\partial x_i^R \partial y_j^I}\right|_{\bar{\vec{X}},\vec{Y}^c}\right\}\Delta y_j^I\right\}$$

$$\cdot\left\{\left.\frac{\partial f}{\partial x_k^R}\right|_{\bar{\vec{X}},\vec{Y}^c}+\sum_{j=1}^{m}\left\{\left.\frac{\partial^2 f}{\partial x_k^R \partial y_j^I}\right|_{\bar{\vec{X}},\vec{Y}^c}\right\}\Delta y_j^I\right\}Cov(x_i^R,x_k^R)$$

$$=\sum_{i=1}^{n}\left\{\left.\frac{\partial f}{\partial x_i^R}\right|_{\bar{\vec{X}},\vec{Y}^c}+\sum_{j=1}^{m}\left\{\left.\frac{\partial^2 f}{\partial x_i^R \partial y_j^I}\right|_{\bar{\vec{X}},\vec{Y}^c}\right\}\Delta y_j^I\right\}^2\cdot Var\left(x_i^R\right)$$

$$+\sum_{i(\neq k)=1}^{n}\sum_{k=1}^{n}\left\{\left.\frac{\partial f}{\partial x_i^R}\right|_{\bar{\vec{X}},\vec{Y}^c}+\sum_{j=1}^{m}\left\{\left.\frac{\partial^2 f}{\partial x_i^R \partial y_j^I}\right|_{\bar{\vec{X}},\vec{Y}^c}\right\}\Delta y_j^I\right\}$$
$$\cdot\left\{\left.\frac{\partial f}{\partial x_i^R}\right|_{\bar{\vec{X}},\vec{Y}^c}+\sum_{j=1}^{m}\left\{\left.\frac{\partial^2 f}{\partial x_i^R \partial y_j^I}\right|_{\bar{\vec{X}},\vec{Y}^c}\right\}\Delta y_j^I\right\}\cdot Cov\left(x_i^R,x_k^R\right) \qquad (4.4)$$

4.3 Vehicle-Bridge Interaction Model

In the vehicle-bridge interaction system, the bridge is modelled as a simply supported beam and the vehicle is represented by a half-car model as shown in Figure 3.1. In this chapter, parameters of the vehicle m_1^I, m_2^I, and m_v^I, are considered as interval variables, meanwhile, bridge parameters, ρ^R, E^R and I^R, are treated as random variables. The equation of motion governing the transverse vibration of the bridge under the moving vehicle with uncertain parameters can be written as

$$\rho^R \frac{\partial^2 W^{RI}(x,t)}{\partial t^2} + C\frac{\partial W^{RI}(x,t)}{\partial t} + E^R I^R \frac{\partial^4 W^{RI}(x,t)}{\partial x^4} = (f_1^{RI}(x,t) + f_2^{RI}(x,t))\delta(x-vt) \tag{4.5}$$

$$\begin{cases} f_1^{RI}(x,t) = -(m_1^I + a_2 m_v^I)g - k_{t1}^R(x_v(t)^{RI} - W^{RI}(x,t)\big|_{x=vt}) - C_{t1}^R(\dot{x}_v(t) - \dot{W}^{RI}(x,t)\big|_{x=vt}) \\ f_2^{RI}(x,t) = -(m_2^I + a_1 m_v^I)g - k_{t2}^R(x_v(t)^{RI} - W^{RI}(x,t)\big|_{x=vt}) - C_{t2}^R(\dot{x}_v(t) - \dot{W}^{RI}(x,t)\big|_{x=vt}) \end{cases} \tag{4.6}$$

where $W^{IR}(x,t)$ is the random interval vertical displacement of the bridge, $x_v(t)^{RI}$ is the random interval vertical displacement of the moving vehicle, $f_1^{RI}(x,t)$ and $f_2^{RI}(x,t)$ are the random interval contact forces, $\delta(x-vt)$ is the Dirac delta function evaluated at the contact point at position $x = vt$, and v is the speed of the moving vehicle.

Using the modal superposition method, the solution to Eq. (4.5) can be expressed as in terms of the mode shapes $\varphi_j(x)$ and associated modal coordinates $x_{bj}^{RI}(t)$ of the bridge

$$W^{RI}(x,t)=\sum_{j=1}^{\infty}\varphi_j(x)x_{bj}^{RI}(t) \tag{4.7}$$

For the simply supported beam (Euler-Bernoulli beam), the mode shapes of the bridge are given by

$$\varphi_j(x)=\sin\frac{j\pi x}{L} \tag{4.8}$$

Substituting Eq. (4.8) into Eq. (4.7) yields

$$W^{RI}(x,t)=\sum_{j=1}^{\infty}\sin\frac{j\pi x}{L}x_{bj}^{IR}(t) \tag{4.9}$$

Substituting Eq. (4.9) into Eq. (4.5), multiplying both sides of the equation by $\varphi_j^T(x)$, and integrating with respect to x over the length L of the beam, obtains

$$\int_0^L \rho^R\varphi_j^T(x)\sum_{j=1}^{\infty}\varphi_j(x)\ddot{x}_{bj}^{RI}(t)dx+\int_0^L C\varphi_j^T(x)\sum_{j=1}^{\infty}\varphi_j(x)\dot{x}_{bj}^{RI}(t)dx+$$

$$\int_0^L E^RI^R\varphi_j^T(x)\sum_{j=1}^{\infty}\frac{\partial^4\varphi_j(x)}{\partial x^4}x_{bj}^{RI}(t)dx$$

$$=\int_0^L\varphi_j^T(x)(f_1^{RI}(x,t)+f_2^{RI}(x,t))\cdot\delta(x-vt)dx$$

$$=-\int_0^L\varphi_j^T(x)((m_1{}^I+a_2m_v{}^I)g+k_{t1}^R(x_v(t)^{RI}-W^{RI}(x,t)\big|_{x=vt})+C_{t1}^R(\dot{x}_v(t)^{RI}-\dot{W}^{RI}(x,t)\big|_{x=vt})$$

$$+(m_2{}^I+a_1m_v{}^I)g+k_{t2}^R(x_v(t)^{RI}-W^{RI}(x,t)\big|_{x=vt})+C_{t2}^R(\dot{x}_v(t)^{RI}-\dot{W}^{RI}(x,t)\big|_{x=vt}))$$

$$\cdot\delta(x-vt)dx \tag{4.10}$$

In this chapter, the Wilson's damping hypothesis is adopted. As vehicle mass is much less than the bridge mass and the tires' damping is quite small, Eq.(4.10) can be approximated as

$$\ddot{x}_{bj}^{RI}(t)+2\zeta_{bj}\omega_{bj}^{R}\dot{x}_{bj}^{RI}(t)+\left(\omega_{bj}^{R}\right)^{2}x_{bj}^{RI}(t)=-\frac{2(m_{1}^{I}+m_{2}^{I}+(a_{1}+a_{2})m_{v}^{I})g}{\rho^{R}L}\sin\frac{j\pi vt}{L} \tag{4.11}$$

where

$$\omega_{bj}{}^{R}=\frac{j^{2}\pi^{2}}{L^{2}}\sqrt{\frac{E^{R}I^{R}}{\rho^{R}}} \tag{4.12}$$

Assuming zero initial conditions, the solution to Eq. (4.11) is

$$x_{bj}^{RI}(t)=-\frac{2(m_{1}^{I}+m_{2}^{I}+(a_{1}+a_{2})m_{v}^{I})g}{\rho^{R}L\omega_{dbj}^{R}}\int_{0}^{t}e^{-\zeta_{bj}\omega_{bj}^{R}(t-\tau)}\cdot\sin\omega_{dbj}^{R}(t-\tau)\sin\frac{j\pi vt}{L}d\tau \tag{4.13}$$

where

$$\omega_{dbj}^{R}=\sqrt{1-\zeta_{bj}^{2}}\,\omega_{bj}^{R} \tag{4.14}$$

where ζ_{bj} is damping ratio of the jth vibration mode.

Substituting Eqs. (4.12) and (4.14) into Eq.(4.13) yields

$$\begin{aligned}x_{bj}^{RI}(t)=&\frac{2(m_{1}^{I}+m_{2}^{I}+(a_{1}+a_{2})m_{v}^{I})g}{L\sqrt{1-\zeta_{bj}^{2}}\frac{j^{2}\pi^{2}}{L^{2}}\sqrt{\rho^{R}E^{R}I^{R}}}\cdot\int_{0}^{t}e^{-\zeta_{bj}\frac{j^{2}\pi^{2}}{L^{2}}\sqrt{\frac{E^{R}I^{R}}{\rho^{R}}}(t-\tau)}\\&\cdot\sin\left(\sqrt{1-\zeta_{bj}^{2}}\frac{j^{2}\pi^{2}}{L^{2}}\sqrt{\frac{E^{R}I^{R}}{\rho^{R}}}(t-\tau)\right)\sin\frac{j\pi vt}{L}d\tau\end{aligned} \tag{4.15}$$

where $a_1 + a_2 = 1$.

Then, the displacement response of the bridge can be calculated by

$$W^{RI}(x,t) = -\sum_{j=1}^{\infty} \sin\frac{j\pi x}{L} \cdot \frac{2(m_1^I + m_2^I + m_v^I)g}{L\sqrt{1-\zeta_{bj}^2}\,\frac{j^2\pi^2}{L^2}\sqrt{\rho^R E^R I^R}} \cdot \int_0^t e^{-\zeta_{bj}\frac{j^2\pi^2}{L^2}\sqrt{\frac{E^R I^R}{\rho^R}}(t-\tau)} \sin\left(\sqrt{1-\zeta_{bj}^2}\,\frac{j^2\pi^2}{L^2}\sqrt{\frac{E^R I^R}{\rho^R}}(t-\tau)\right)\sin\frac{j\pi v t}{L}\,d\tau \tag{4.16}$$

In this chapter, the contribution of tires' stiffness to bridge vertical displacement response is omitted due to the assumption that the bridge mass is much greater than that of the vehicle [2]. Actually, it is not difficult to include the vehicle stiffness in the bridge response using the Duhamel integral solution. Additionally, bridge damping is treated as deterministic because the existing research outcomes show that the mechanism of structural damping is still not clear enough.

4.4 Interval Statistical Moments of Random Interval Bridge Dynamic Response

For the sake of simplicity, the random interval displacement response of the bridge given in Eq.(4.16) can be rewritten as

$$W^{RI}(x,t)=\frac{-2}{S_1\sqrt{\rho^R E^R\ I^R}}\sum_{j=1}^{\infty}\sin\frac{j\pi x}{L}\cdot\int_0^t\left((m_1^I+m_2^I+m_v^I)g\right)S_2^R\sin\left(S_3^R\right)\sin\frac{j\pi v\tau}{L}d\tau \quad (4.17)$$

The items S_1, S_2^R and S_3^R are given by

$$S_1=L\sqrt{1-\zeta_{bj}^2}\,\frac{j^2\pi^2}{L^2},\ S_2^R=e^{-\zeta_{bj}\frac{j^2\pi^2}{L^2}\sqrt{\frac{E^R I^R}{\rho^R}}(t-\tau)},\ S_3=\sqrt{1-\zeta_{bj}^2}\,\frac{j^2\pi^2}{L^2}\sqrt{\frac{E^R I^R}{\rho^R}}(t-\tau) \quad (4.18)$$

By means of the random interval moment method, the mean value of the random interval bridge response can be computed by

$$\mu\left(W^{RI}(x,t)\right)=\frac{-2}{S_1\sqrt{\bar{\rho}^R\bar{E}^R\bar{I}^R}}\sum_{j=1}^{\infty}\sin\frac{j\pi x}{L}\cdot\int_0^t\left((m_1^c+m_2^c+m_v^c)g\right)\cdot\bar{S}_2\sin\left(\bar{S}_3\right)\sin\frac{j\pi v\tau}{L}d\tau$$

$$+\frac{-2g}{S_1\sqrt{\bar{\rho}^R\bar{E}^R\bar{I}^R}}\sum_{j=1}^{\infty}\sin\frac{j\pi x}{L}\cdot\int_0^t\ \bar{S}_2\sin\left(\bar{S}_3\right)\sin\frac{j\pi v\tau}{L}d\tau\cdot\left(\Delta m_1+\Delta m_2+\Delta m_v\right) \quad (4.19)$$

The variance of the random interval bridge response can be calculated by

$$\sigma^2\left(W^{RI}(x,t)\right)=\sum_{i=1}^{n}\ \sum_{k=1}^{n}\ \left\{\left.\frac{\partial W}{\partial x_i^R}\right|_{\bar{\bar{X}},\vec{Y}^c}+\sum_{j=1}^{m}\ \left\{\left.\frac{\partial^2 W}{\partial x_i^R\partial y_j^I}\right|_{\bar{\bar{X}},\vec{Y}^c}\right\}\Delta y_j^I\right\}$$

$$\cdot\left\{\left.\frac{\partial f}{\partial x_k^R}\right|_{\bar{\bar{X}},\vec{Y}^c}+\sum_{j=1}^{m}\ \left\{\left.\frac{\partial^2 f}{\partial x_k^R\partial y_j^I}\right|_{\bar{\bar{X}},\vec{Y}^c}\right\}\Delta y_j^I\right\}Cov(x_i^R,x_k^R)$$

$$=\sum_{i=1}^{n}\ \left\{\left.\frac{\partial W}{\partial x_i^R}\right|_{\bar{\bar{X}},\vec{Y}^c}+\sum_{j=1}^{m}\ \left\{\left.\frac{\partial^2 W}{\partial x_i^R\partial y_j^I}\right|_{\bar{\bar{X}},\vec{Y}^c}\right\}\Delta y_j^I\right\}^2\cdot Var\left(x_i^R\right)$$

$$+\sum_{i(\neq k)=1}^{n}\sum_{k=1}^{n}\left\{\left.\frac{\partial W}{\partial x_i^R}\right|_{\bar{\bar{X}},\vec{Y}^c}+\sum_{j=1}^{m}\left\{\left.\frac{\partial^2 W}{\partial x_i^R \partial y_j^I}\right|_{\bar{\bar{X}},\vec{Y}^c}\right\}\Delta y_j^I\right\}$$

$$\cdot\left\{\left.\frac{\partial W}{\partial x_i^R}\right|_{\bar{\bar{X}},\vec{Y}^c}+\sum_{j=1}^{m}\left\{\left.\frac{\partial^2 W}{\partial x_i^R \partial y_j^I}\right|_{\bar{\bar{X}},\vec{Y}^c}\right\}\Delta y_j^I\right\}\cdot Cov\left(x_i^R, x_k^R\right) \tag{4.20}$$

where

$$\left.\frac{\partial W}{\partial x_i^R}\right|_{\bar{X},\vec{Y}^c}=\frac{\partial W(x,t)}{\partial E^R}+\frac{\partial W(x,t)}{\partial \rho^R}+\frac{\partial W(x,t)}{\partial I^R} \tag{4.21}$$

$$\begin{aligned}
&\left.\frac{\partial W(x,t)}{\partial E}\right|_{\bar{X}^R,Y^c}=\frac{1}{S_1\sqrt{\bar{\rho}^R\left(\bar{E}^R\right)^3\bar{I}^R}}\\
&\cdot\sum_{j=1}^{\infty}\sin\frac{j\pi x}{L}\cdot\int_0^t\left(\left(m_1^c+m_2^c+m_v^c\right)g\right)S_2\sin(S_3)\sin\frac{j\pi vt}{L}d\tau\\
&+\frac{1}{S_1\sqrt{\bar{\rho}^R\bar{E}^R\bar{I}^R}}\cdot\sum_{j=1}^{\infty}\sin\frac{j\pi x}{L}\\
&\cdot\left(\int_0^t\left(\left(m_1^c+m_2^c+m_v^c\right)g\right)\cdot S_2\cdot\zeta_{bj}\left(\frac{j\pi}{L}\right)^2\cdot\sqrt{\frac{\bar{I}^R}{\bar{\rho}^R\bar{E}^R}}(t-\tau)\cdot\sin(S_3)\sin\frac{j\pi vt}{L}d\tau\right.\\
&\left.+\int_0^t\left(\left(m_1^c+m_2^c+m_v^c\right)g\right)S_2\cdot\zeta_{bj}\left(\frac{j\pi}{L}\right)^2\cdot\sqrt{\frac{\bar{I}^R}{\bar{\rho}^R\bar{E}^R}}(t-\tau)\cdot\cos(S_3)\sin\frac{j\pi vt}{L}d\tau\right)
\end{aligned} \tag{4.22}$$

$$\frac{\partial W(x,t)}{\partial I}=\frac{1}{S_1\sqrt{\bar{\rho}^R\bar{E}^R(\bar{I}^R)^3}}\cdot$$

$$\sum_{j=1}^{\infty}\sin\frac{j\pi x}{L}\cdot\int_0^t\left(\left(m_1^c+m_2^c+m_v^c\right)g\right)S_2\sin(S_3)\sin\frac{j\pi vt}{L}d\tau$$

$$+\frac{1}{S_1\sqrt{\bar{\rho}^R\bar{E}^R\bar{I}^R}}\cdot\sum_{j=1}^{\infty}\sin\frac{j\pi x}{L} \tag{4.23}$$

$$\cdot\left(\int_0^t\left(\left(m_1^c+m_2^c+m_v^c\right)g\right)\cdot S_2\cdot\zeta_{bj}(\frac{j\pi}{L})^2\cdot\sqrt{\frac{\bar{E}^R}{\bar{\rho}^R\bar{I}^R}}(t-\tau)\cdot\sin(S_3)\sin\frac{j\pi vt}{L}d\tau\right.$$

$$\left.+\int_0^t\left(\left(m_1^c+m_2^c+m_v^c\right)g\right)S_2\cdot\zeta_{bj}(\frac{j\pi}{L})^2\cdot\sqrt{\frac{\bar{E}^R}{\bar{\rho}^R\bar{I}^R}}(t-\tau)\cdot\cos(S_3)\sin\frac{j\pi vt}{L}d\tau\right)$$

$$\frac{\partial W(x,t)}{\partial \rho}=\frac{1}{S_1\sqrt{\left(\bar{\rho}^R\right)^3\bar{E}^R\bar{I}^R}}$$

$$\cdot\sum_{j=1}^{\infty}\sin\frac{j\pi x}{L}\cdot\int_0^t\left(\left(m_1^c+m_2^c+m_v^c\right)g\right)S_2\sin(S_3)\sin\frac{j\pi vt}{L}d\tau$$

$$+\frac{1}{S_1\sqrt{\bar{\rho}^R\bar{E}^R\bar{I}^R}}\cdot\sum_{j=1}^{\infty}\sin\frac{j\pi x}{L} \tag{4.24}$$

$$\cdot\left(\int_0^t\left(\left(m_1^c+m_2^c+m_v^c\right)g\right)\cdot S_2\cdot\zeta_{bj}(\frac{j\pi}{L})^2\cdot\sqrt{\frac{\bar{E}^R\bar{I}^R}{\left(\bar{\rho}^R\right)^3}}(t-\tau)\cdot\sin(S_3)\sin\frac{j\pi vt}{L}d\tau\right.$$

$$\left.+\int_0^t\left(\left(m_1^c+m_2^c+m_v^c\right)g\right)S_2\cdot\zeta_{bj}(\frac{j\pi}{L})^2\cdot\sqrt{\frac{\bar{E}^R\bar{I}^R}{\left(\bar{\rho}^R\right)^3}}(t-\tau)\cdot\cos(S_3)\sin\frac{j\pi vt}{L}d\tau\right)$$

$$\left.\frac{\partial^2 W^{RI}}{\partial x_i^R\partial y_j^I}\right|_{\bar{\bar{X}},\bar{Y}^c}=\frac{\partial^2 W^{RI}\left(x,t\right)}{\partial x^R\partial m_1^I}+\frac{\partial^2 W^{RI}\left(x,t\right)}{\partial x^R\partial m_2^I}+\frac{\partial^2 W^{RI}\left(x,t\right)}{\partial x^R\partial m_v^I}$$

$$=\frac{\partial^2 W^{RI}\left(x,t\right)}{\partial E^R\partial m_1^I}+\frac{\partial^2 W^{RI}\left(x,t\right)}{\partial E^R\partial m_2^I}+\frac{\partial^2 W^{RI}\left(x,t\right)}{\partial E^R\partial m_v^I}+\frac{\partial^2 W^{RI}\left(x,t\right)}{\partial I^R\partial m_1^I}+\frac{\partial^2 W^{RI}\left(x,t\right)}{\partial I^R\partial m_2^I} \tag{4.25}$$

$$+\frac{\partial^2 W^{RI}\left(x,t\right)}{\partial I^R\partial m_v^I}+\frac{\partial^2 W^{RI}\left(x,t\right)}{\partial \rho^R\partial m_1^I}+\frac{\partial^2 W^{RI}\left(x,t\right)}{\partial \rho^R\partial m_2^I}+\frac{\partial^2 W^{RI}\left(x,t\right)}{\partial \rho^R\partial m_v^I}$$

$$\left.\frac{\partial^2 W^{RI}(x,t)}{\partial E^R \partial m_1^I}\right|_{\bar{X}^R, Y^c} = \frac{g}{S_1\sqrt{\bar{\rho}^R\left(\bar{E}^R\right)^3 \bar{I}^R}} \cdot \sum_{j=1}^{\infty} \sin\frac{j\pi x}{L} \cdot \int_0^t S_2^R \sin(S_3^R) \sin\frac{j\pi v t}{L} d\tau$$

$$+\frac{g}{S_1\sqrt{\bar{\rho}^R \bar{E}^R \bar{I}^R}} \cdot \sum_{j=1}^{\infty} \sin\frac{j\pi x}{L} \cdot \int_0^t S_2^R \cdot \zeta_{bj}(\frac{j\pi}{L})^2 \cdot \sqrt{\frac{\bar{I}^R}{\bar{\rho}^R \bar{E}^R}} (t-\tau) \cdot \sin(S_3^R) \sin\frac{j\pi v t}{L} d\tau \qquad (4.26)$$

$$+\frac{g}{S_1\sqrt{\bar{\rho}^R \bar{E}^R \bar{I}^R}} \cdot \sum_{j=1}^{\infty} \sin\frac{j\pi x}{L} \cdot \int_0^t S_2^R \cdot \zeta_{bj}(\frac{j\pi}{L})^2 \cdot \sqrt{\frac{\bar{I}^R}{\bar{\rho}^R \bar{E}^R}} (t-\tau) \cdot \cos(S_3^R) \sin\frac{j\pi v t}{L} d\tau$$

$$\left.\frac{\partial^2 W(x,t)}{\partial E^R \partial m_2^I}\right|_{\bar{X}^R, Y^c} = \frac{g}{S_1\sqrt{\bar{\rho}^R\left(\bar{E}^R\right)^3 \bar{I}^R}} \cdot \sum_{j=1}^{\infty} \sin\frac{j\pi x}{L} \cdot \int_0^t S_2 \sin(S_3) \sin\frac{j\pi v t}{L} d\tau$$

$$+\frac{g}{S_1\sqrt{\bar{\rho}^R \bar{E}^R \bar{I}^R}} \cdot \sum_{j=1}^{\infty} \sin\frac{j\pi x}{L} \cdot \int_0^t S_2 \cdot \zeta_{bj}(\frac{j\pi}{L})^2 \cdot \sqrt{\frac{\bar{I}^R}{\bar{\rho}^R \bar{E}^R}} (t-\tau) \cdot \sin(S_3) \sin\frac{j\pi v t}{L} d\tau \qquad (4.27)$$

$$+\frac{g}{S_1\sqrt{\bar{\rho}^R \bar{E}^R \bar{I}^R}} \cdot \sum_{j=1}^{\infty} \sin\frac{j\pi x}{L} \cdot \int_0^t S_2 \cdot \zeta_{bj}(\frac{j\pi}{L})^2 \cdot \sqrt{\frac{\bar{I}^R}{\bar{\rho}^R \bar{E}^R}} (t-\tau) \cdot \cos(S_3) \sin\frac{j\pi v t}{L} d\tau$$

$$\left.\frac{\partial^2 W(x,t)}{\partial E^R \partial m_v^I}\right|_{\bar{X}^R, Y^c} = \frac{g}{S_1\sqrt{\bar{\rho}^R\left(\bar{E}^R\right)^3 \bar{I}^R}} \cdot \sum_{j=1}^{\infty} \sin\frac{j\pi x}{L} \cdot \int_0^t S_2 \sin(S_3) \sin\frac{j\pi v t}{L} d\tau$$

$$+\frac{g}{S_1\sqrt{\bar{\rho}^R \bar{E}^R \bar{I}^R}} \cdot \sum_{j=1}^{\infty} \sin\frac{j\pi x}{L} \cdot \int_0^t S_2 \cdot \zeta_{bj}(\frac{j\pi}{L})^2 \cdot \sqrt{\frac{\bar{I}^R}{\bar{\rho}^R \bar{E}^R}} (t-\tau) \cdot \sin(S_3) \sin\frac{j\pi v t}{L} d\tau \qquad (4.28)$$

$$+\frac{g}{S_1\sqrt{\bar{\rho}^R \bar{E}^R \bar{I}^R}} \cdot \sum_{j=1}^{\infty} \sin\frac{j\pi x}{L} \cdot \int_0^t S_2 \cdot \zeta_{bj}(\frac{j\pi}{L})^2 \cdot \sqrt{\frac{\bar{I}^R}{\bar{\rho}^R \bar{E}^R}} (t-\tau) \cdot \cos(S_3) \sin\frac{j\pi v t}{L} d\tau$$

$$\frac{\partial^2 W^{RI}(x,t)}{\partial I^R \partial m_1^I} = \frac{g}{S_1\sqrt{\bar{\rho}^R \bar{E}^R (\bar{I}^R)^3}} \cdot \sum_{j=1}^{\infty} \sin\frac{j\pi x}{L} \cdot \int_0^t S_2 \sin(S_3) \sin\frac{j\pi v t}{L} d\tau$$

$$+\frac{g}{S_1\sqrt{\bar{\rho}^R \bar{E}^R \bar{I}^R}} \cdot \sum_{j=1}^{\infty} \sin\frac{j\pi x}{L} \cdot \int_0^t S_2 \cdot \zeta_{bj}(\frac{j\pi}{L})^2 \cdot \sqrt{\frac{\bar{E}^R}{\bar{\rho}^R \bar{I}^R}} (t-\tau) \cdot \sin(S_3) \sin\frac{j\pi v t}{L} d\tau \qquad (4.29)$$

$$+\frac{g}{S_1\sqrt{\bar{\rho}^R \bar{E}^R \bar{I}^R}} \cdot \sum_{j=1}^{\infty} \sin\frac{j\pi x}{L} \cdot \int_0^t S_2 \cdot \zeta_{bj}(\frac{j\pi}{L})^2 \cdot \sqrt{\frac{\bar{E}^R}{\bar{\rho}^R \bar{I}^R}} (t-\tau) \cdot \cos(S_3) \sin\frac{j\pi v t}{L} d\tau$$

$$\frac{\partial^2 W^{RI}(x,t)}{\partial I^R \partial m_2^I} = \frac{g}{S_1\sqrt{\bar{\rho}^R \bar{E}^R (\bar{I}^R)^3}} \cdot \sum_{j=1}^{\infty} \sin\frac{j\pi x}{L} \cdot \int_0^t S_2 \sin(S_3) \sin\frac{j\pi v t}{L} d\tau$$
$$+ \frac{g}{S_1\sqrt{\bar{\rho}^R \bar{E}^R \bar{I}^R}} \cdot \sum_{j=1}^{\infty} \sin\frac{j\pi x}{L} \cdot \int_0^t S_2 \cdot \zeta_{bj} (\frac{j\pi}{L})^2 \cdot \sqrt{\frac{\bar{E}^R}{\bar{\rho}^R \bar{I}^R}} (t-\tau) \cdot \sin(S_3) \sin\frac{j\pi v t}{L} d\tau \qquad (4.30)$$
$$+ \frac{g}{S_1\sqrt{\bar{\rho}^R \bar{E}^R \bar{I}^R}} \cdot \sum_{j=1}^{\infty} \sin\frac{j\pi x}{L} \cdot \int_0^t S_2 \cdot \zeta_{bj} (\frac{j\pi}{L})^2 \cdot \sqrt{\frac{\bar{E}^R}{\bar{\rho}^R \bar{I}^R}} (t-\tau) \cdot \cos(S_3) \sin\frac{j\pi v t}{L} d\tau$$

$$\frac{\partial^2 W^{RI}(x,t)}{\partial I^R \partial m_v^I} = \frac{g}{S_1\sqrt{\bar{\rho}^R \bar{E}^R (\bar{I}^R)^3}} \cdot \sum_{j=1}^{\infty} \sin\frac{j\pi x}{L} \cdot \int_0^t S_2 \sin(S_3) \sin\frac{j\pi v t}{L} d\tau$$
$$+ \frac{g}{S_1\sqrt{\bar{\rho}^R \bar{E}^R \bar{I}^R}} \cdot \sum_{j=1}^{\infty} \sin\frac{j\pi x}{L} \cdot \int_0^t S_2 \cdot \zeta_{bj} (\frac{j\pi}{L})^2 \cdot \sqrt{\frac{\bar{E}^R}{\bar{\rho}^R \bar{I}^R}} (t-\tau) \cdot \sin(S_3) \sin\frac{j\pi v t}{L} d\tau \qquad (4.31)$$
$$+ \frac{g}{S_1\sqrt{\bar{\rho}^R \bar{E}^R \bar{I}^R}} \cdot \sum_{j=1}^{\infty} \sin\frac{j\pi x}{L} \cdot \int_0^t S_2 \cdot \zeta_{bj} (\frac{j\pi}{L})^2 \cdot \sqrt{\frac{\bar{E}^R}{\bar{\rho}^R \bar{I}^R}} (t-\tau) \cdot \cos(S_3) \sin\frac{j\pi v t}{L} d\tau$$

$$\frac{\partial^2 W^{RI}(x,t)}{\partial \rho^R \partial m_2^I} = \frac{g}{S_1\sqrt{\left(\bar{\rho}^R\right)^3 \bar{E}^R \bar{I}^R}} \cdot \sum_{j=1}^{\infty} \sin\frac{j\pi x}{L} \cdot \int_0^t S_2 \sin(S_3) \sin\frac{j\pi v t}{L} d\tau$$
$$+ \frac{g}{S_1\sqrt{\bar{\rho}^R \bar{E}^R \bar{I}^R}} \cdot \sum_{j=1}^{\infty} \sin\frac{j\pi x}{L} \cdot \int_0^t S_2 \cdot \zeta_{bj} (\frac{j\pi}{L})^2 \cdot \sqrt{\frac{\bar{E}^R \bar{I}^R}{\left(\bar{\rho}^R\right)^3}} (t-\tau) \cdot \sin(S_3) \sin\frac{j\pi v t}{L} d\tau \qquad (4.32)$$
$$+ \frac{g}{S_1\sqrt{\bar{\rho}^R \bar{E}^R \bar{I}^R}} \cdot \sum_{j=1}^{\infty} \sin\frac{j\pi x}{L} \cdot \int_0^t S_2 \cdot \zeta_{bj} (\frac{j\pi}{L})^2 \cdot \sqrt{\frac{\bar{E}^R \bar{I}^R}{\left(\bar{\rho}^R\right)^3}} (t-\tau) \cdot \cos(S_3) \sin\frac{j\pi v t}{L} d\tau$$

$$\frac{\partial^2 W^{RI}(x,t)}{\partial \rho^R \partial m_v^I} = \frac{g}{S_1\sqrt{\left(\bar{\rho}^R\right)^3 \bar{E}^R \bar{I}^R}} \cdot \sum_{j=1}^{\infty} \sin\frac{j\pi x}{L} \cdot \int_0^t S_2 \sin(S_3) \sin\frac{j\pi v t}{L} d\tau$$
$$+ \frac{g}{S_1\sqrt{\bar{\rho}^R \bar{E}^R \bar{I}^R}} \cdot \sum_{j=1}^{\infty} \sin\frac{j\pi x}{L} \cdot \int_0^t S_2 \cdot \zeta_{bj} (\frac{j\pi}{L})^2 \cdot \sqrt{\frac{\bar{E}^R \bar{I}^R}{\left(\bar{\rho}^R\right)^3}} (t-\tau) \cdot \sin(S_3) \sin\frac{j\pi v t}{L} d\tau \qquad (4.33)$$
$$+ \frac{g}{S_1\sqrt{\bar{\rho}^R \bar{E}^R \bar{I}^R}} \cdot \sum_{j=1}^{\infty} \sin\frac{j\pi x}{L} \cdot \int_0^t S_2 \cdot \zeta_{bj} (\frac{j\pi}{L})^2 \cdot \sqrt{\frac{\bar{E}^R \bar{I}^R}{\left(\bar{\rho}^R\right)^3}} (t-\tau) \cdot \cos(S_3) \sin\frac{j\pi v t}{L} d\tau$$

$$\frac{\partial^2 W^{RI}(x,t)}{\partial \rho^R \partial m_1^I} = \frac{g}{S_1\sqrt{\left(\bar{\rho}^R\right)^3 \bar{E}^R \bar{I}^R}} \cdot \sum_{j=1}^{\infty} \sin\frac{j\pi x}{L} \cdot \int_0^t S_2 \sin(S_3) \sin\frac{j\pi v t}{L} d\tau$$

$$+\frac{g}{S_1\sqrt{\bar{\rho}^R \bar{E}^R \bar{I}^R}} \cdot \sum_{j=1}^{\infty} \sin\frac{j\pi x}{L} \cdot \int_0^t S_2 \cdot \zeta_{bj} (\frac{j\pi}{L})^2 \cdot \sqrt{\frac{\bar{E}^R \bar{I}^R}{\left(\bar{\rho}^R\right)^3}} (t-\tau) \cdot \sin(S_3) \sin\frac{j\pi v t}{L} d\tau \tag{4.34}$$

$$+\frac{g}{S_1\sqrt{\bar{\rho}^R \bar{E}^R \bar{I}^R}} \cdot \sum_{j=1}^{\infty} \sin\frac{j\pi x}{L} \cdot \int_0^t S_2 \cdot \zeta_{bj} (\frac{j\pi}{L})^2 \cdot \sqrt{\frac{\bar{E}^R \bar{I}^R}{\left(\bar{\rho}^R\right)^3}} (t-\tau) \cdot \cos(S_3) \sin\frac{j\pi v t}{L} d\tau$$

Furthermore, the lower and upper bounds of the mean value of the bridge displacement $\mu(W^{RI})$ are given by

$$\underline{\mu\left(W^{RI}(x,t)\right)} = \frac{-2}{S_1\sqrt{\bar{\rho}\overline{EI}}} \sum_{j=1}^{\infty} \sin\frac{j\pi x}{L} \cdot \int_0^t \left((m_1^c + m_2^c + m_v^c) g\right) \cdot \bar{S}_2 \sin\left(\bar{S}_3\right) \sin\frac{j\pi v\tau}{L} d\tau$$
$$-\left|\frac{-2g}{S_1\sqrt{\bar{\rho}\overline{EI}}} \sum_{j=1}^{\infty} \sin\frac{j\pi x}{L} \cdot \int_0^t \bar{S}_2 \sin\left(\bar{S}_3\right) \sin\frac{j\pi v\tau}{L} d\tau \cdot \left(\Delta m_1 + \Delta m_2 + \Delta m_v\right)\right| \tag{4.35}$$

$$\overline{\mu\left(W^{RI}(x,t)\right)} = \frac{-2}{S_1\sqrt{\bar{\rho}\overline{EI}}} \sum_{j=1}^{\infty} \sin\frac{j\pi x}{L} \cdot \int_0^t \left((m_1^c + m_2^c + m_v^c) g\right) \cdot \bar{S}_2 \sin\left(\bar{S}_3\right) \sin\frac{j\pi v\tau}{L} d\tau$$
$$+\left|\frac{-2g}{S_1\sqrt{\bar{\rho}\overline{EI}}} \sum_{j=1}^{\infty} \sin\frac{j\pi x}{L} \cdot \int_0^t \bar{S}_2 \sin\left(\bar{S}_3\right) \sin\frac{j\pi v\tau}{L} d\tau \cdot \left(\Delta m_1 + \Delta m_2 + \Delta m_v\right)\right| \tag{4.36}$$

The lower and upper bounds of the variance of the bridge displacements $\sigma^2\left(W^{RI}(x,t)\right)$ are

$$\underline{\sigma^2\left(W^{RI}(x,t)\right)} =$$

$$\left\{\frac{\partial W^{RI}(x,t)}{\partial E^R} - \left(\frac{\partial^2 W^{RI}(x,t)}{\partial E^R \partial m_1^I}\cdot\Delta m_1 + \frac{\partial^2 W^{RI}(x,t)}{\partial E^R \partial m_2^I}\cdot\Delta m_2 + \frac{\partial^2 W^{RI}(x,t)}{\partial E^R \partial m_v^I}\cdot\Delta m_v\right)\right\}^2\cdot\sigma_E^2$$

$$+\left\{\frac{\partial W^{RI}(x,t)}{\partial I^R} - \left(\frac{\partial^2 W^{RI}(x,t)}{\partial I^R \partial m_1^I}\cdot\Delta m_1 + \frac{\partial^2 W^{RI}(x,t)}{\partial I^R \partial m_2^I}\cdot\Delta m_2 + \frac{\partial^2 W^{RI}(x,t)}{\partial I^R \partial m_v^I}\cdot\Delta m_v\right)\right\}^2\cdot\sigma_I^2$$

$$+\left\{\frac{\partial W^{RI}(x,t)}{\partial \rho^R} - \left(\frac{\partial^2 W^{RI}(x,t)}{\partial \rho^R \partial m_1^I}\cdot\Delta m_1 + \frac{\partial^2 W^{RI}(x,t)}{\partial \rho^R \partial m_2^I}\cdot\Delta m_2 + \frac{\partial^2 W^{RI}(x,t)}{\partial \rho^R \partial m_v^I}\cdot\Delta m_v\right)\right\}^2\cdot\sigma_\rho^2$$

(4.37)

$$\overline{\sigma^2\left(W^{RI}(x,t)\right)} =$$

$$\left\{\frac{\partial W^{RI}(x,t)}{\partial E^R} + \left(\frac{\partial^2 W^{RI}(x,t)}{\partial E^R \partial m_1^I}\cdot\Delta m_1 + \frac{\partial^2 W^{RI}(x,t)}{\partial E^R \partial m_2^I}\cdot\Delta m_2 + \frac{\partial^2 W^{RI}(x,t)}{\partial E^R \partial m_v^I}\cdot\Delta m_v\right)\right\}^2\cdot\sigma_E^2$$

$$+\left\{\frac{\partial W^{RI}(x,t)}{\partial I^R} + \left(\frac{\partial^2 W^{RI}(x,t)}{\partial I^R \partial m_1^I}\cdot\Delta m_1 + \frac{\partial^2 W^{RI}(x,t)}{\partial I^R \partial m_2^I}\cdot\Delta m_2 + \frac{\partial^2 W^{RI}(x,t)}{\partial I^R \partial m_v^I}\cdot\Delta m_v\right)\right\}^2\cdot\sigma_I^2$$

$$+\left\{\frac{\partial W^{RI}(x,t)}{\partial \rho^R} + \left(\frac{\partial^2 W^{RI}(x,t)}{\partial \rho^R \partial m_1^I}\cdot\Delta m_1 + \frac{\partial^2 W^{RI}(x,t)}{\partial \rho^R \partial m_2^I}\cdot\Delta m_2 + \frac{\partial^2 W^{RI}(x,t)}{\partial \rho^R \partial m_v^I}\cdot\Delta m_v\right)\right\}^2\cdot\sigma_\rho^2$$

(4.38)

4.5 Numerical Simulations

In this chapter, the bridge parameters are considered as Gaussian random variables and the parameters of vehicle are treated as interval variables. The nominal values (mean/midpoint values) of system parameters taken in the numerical simulation are listed in Table 4.1. The unit of the bridge displacement response is meter.

In this study, the bridge damping ratios ζ_{bj} for all modes are taken as 0.05. For the sake of simplicity, the coefficient of variation (COV, that is the ratio of the standard deviation to mean value of a random variable) of ρ^R, E^R and I^R is also adopted to represent the dispersal degree of random variables. Meanwhile, the interval change ratio (ICR, that is the ratio of interval width to midpoint value of an interval variable) of m_1^I, m_2^I, and m_v^I is used to describe the scatter level of interval variables. Two different vehicle speeds, $v = 5m/s$ and $v = 10m/s$ are taken into account to investigate the influence of vehicle velocity on the bridge response.

Table 4.1 Data of the vehicle-bridge model

Data of the bridge (mean value)	Data of the vehicle (midpoint)	
$L = 40m$	$m_1{}^c = 1000kg$	$m_2{}^c = 1500kg$
E=33 GN/m^2	$m_v{}^c = 17800kg$	$I_v = 1.5 \times 10^5 kg.m^2$
$I = 0.16m^4$	$k_{s1} = 2.5 \times 10^6 N/m$	$k_{s2} = 4.2 \times 10^6 N/m$
$\rho = 7800kg/m$	$k_{t1} = 5.2 \times 10^6 N/m$	$k_{t2} = 7.2 \times 10^6 N/m$
	$a_1 = 0.52$	$a_2 = 0.48$
	$C_{s1} = 9000N/m$	$C_{s2} = 9600N/m$
	$C_{t1} = 920N/m$	$C_{t2} = 960N/m$
	$S = 4.27m$	

The mean value of the random interval bridge displacement response at its mid-span is given in Figures 4.2(a)-(f) when different combinations of uncertain parameters are taken. Figure 4.2(a) shows the mean bridge displacement response when the randomness of all random parameters is considered and all interval parameters are taken as their midpoint values. The bridge response is a pure random process and is a special case of the hybrid random interval problem. However, the mean value of the bridge response is an interval if the system has interval parameters as shown in Figures 4.2(b)-(h). From Figures 4.2(e) and 4.2(h), it can be easily observed that the interval with of the mean value of the bridge response is same when the coefficients of variation of random variables are different, that is, the random variables do not affect the mean value of the random interval structural response.

Figures 4.2(b) and 4.2(c) show that the interval widths of the bridge displacement are slightly different when the uncertainties of interval variables m_1^I and m_2^I are accounted for. The effects caused by the changes of these two interval parameters on the bridge response are similar. Compared with Figures 4.2(b) and 4.2(c), it can be seen that the interval width produced by m_v^I is significantly larger as shown in Figure 4.2(d), which means bridge response is more sensitive to the change of sprung mass m_v^I. The change range of the bridge response is much larger when the uncertainties of all interval variables are included as shown in Figure 4.2(e). From Figures 4.2(e) and 4.2(f), it can be observed that the interval width of bridge response increases when the interval changes of interval variables become larger. Similarly the interval width of the mean bridge response is larger when the vehicle moves faster as shown in Figure 4.2(g).

In summary, the mean value of the random interval bridge response is independent of the dispersal degrees of random system parameters as expected from Eq.(4.19). The interval width of the mean value of bridge response is directly proportional to the uncertainties of interval variables and vehicle speed.

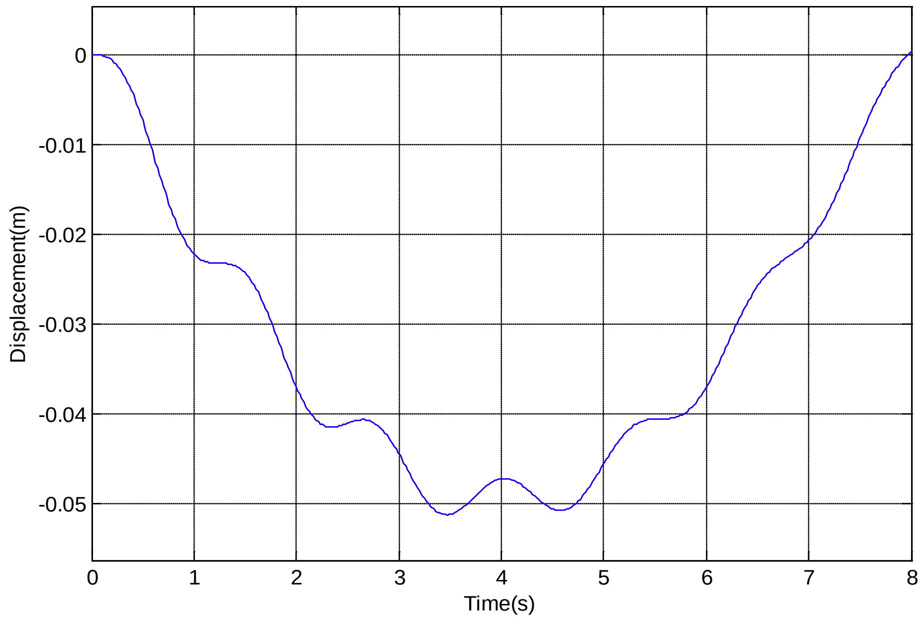

(a) COV(ρ^R, E^R, I^R)=0.05, ICR(m_1^I, m_2^I, m_v^I)=0, $v = 5m/s$

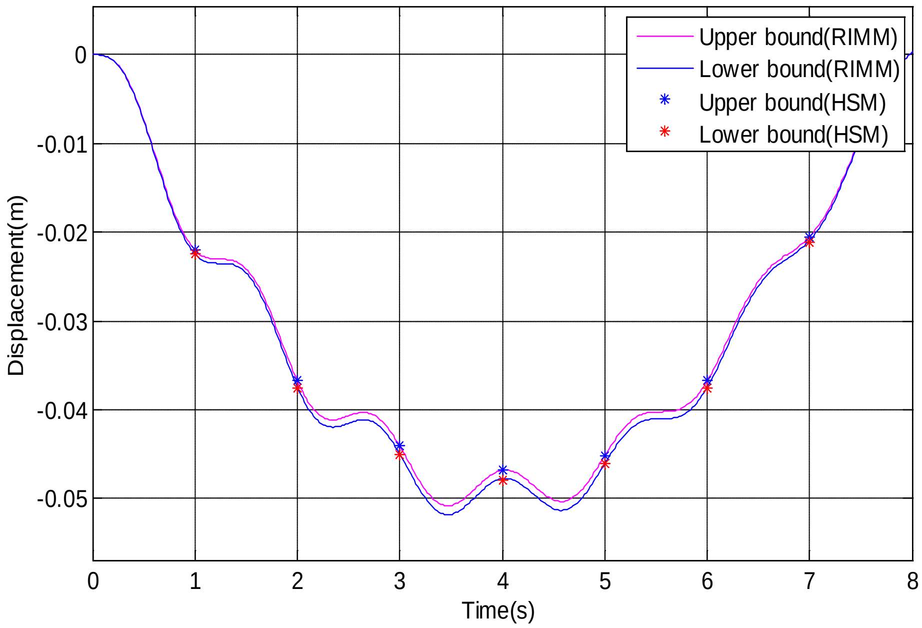

(b) ICR(m_1^I)=0.2, COV(ρ^R, E^R, I^R)=0.05, ICR(m_2^I, m_v^I)=0, $v = 5m/s$

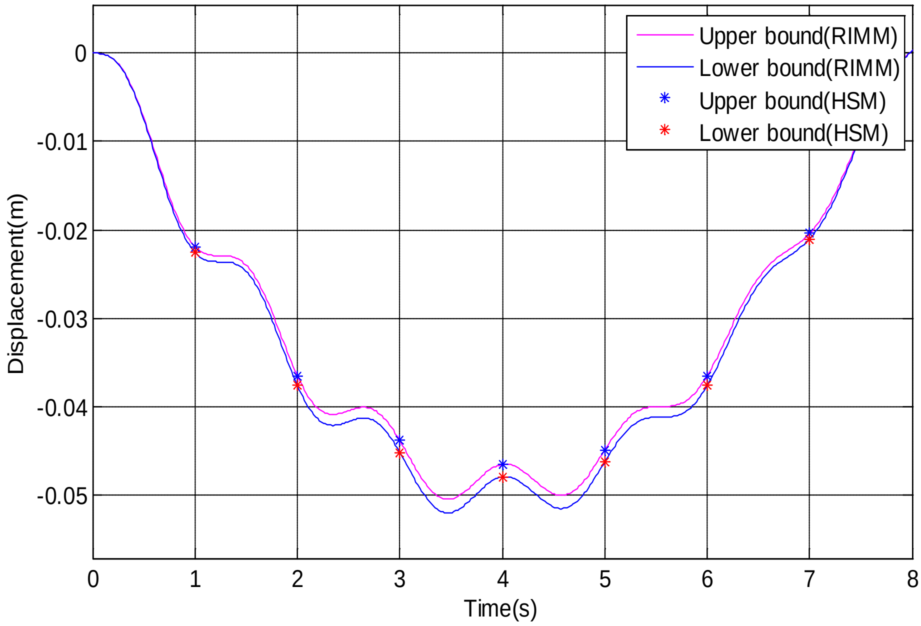

(c) ICR(m_2^I)=0.2, COV(ρ^R, E^R, I^R)=0.05, ICR(m_1^I, m_v^I)=0, $v = 5m/s$

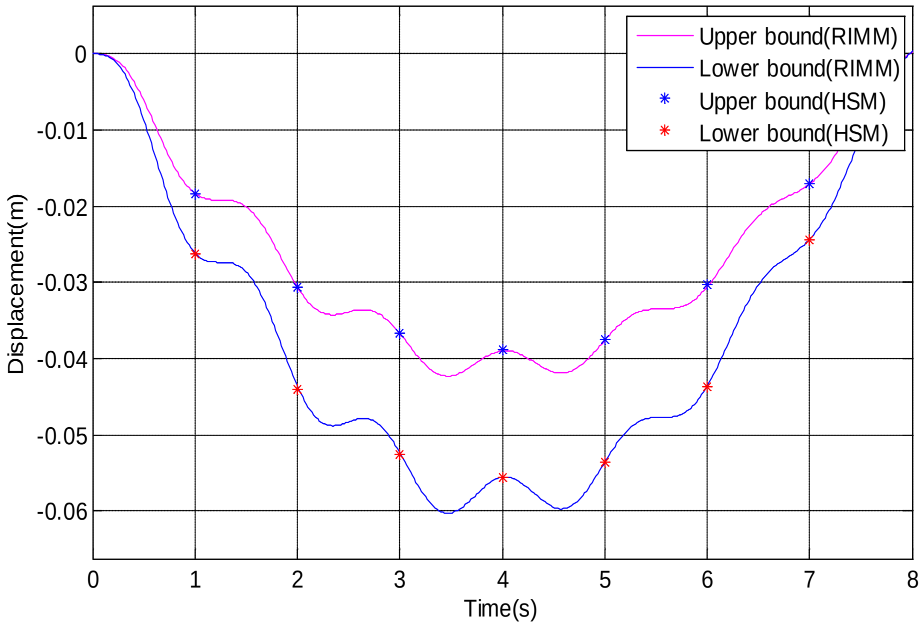

(d) ICR(m_v^I)=0.2, COV(ρ^R, E^R, I^R)=0.05, ICR(m_1^I, m_2^I)=0, $v = 5m/s$

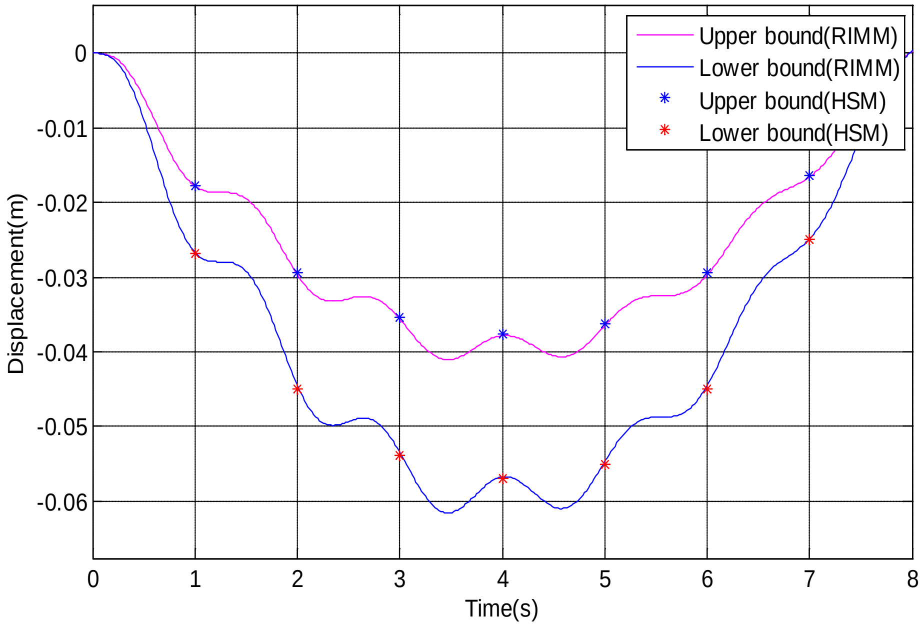

(e) COV(ρ^R, E^R, I^R)=0.05, ICR(m_1^I, m_2^I, m_v^I)=0.2, $v = 5m/s$

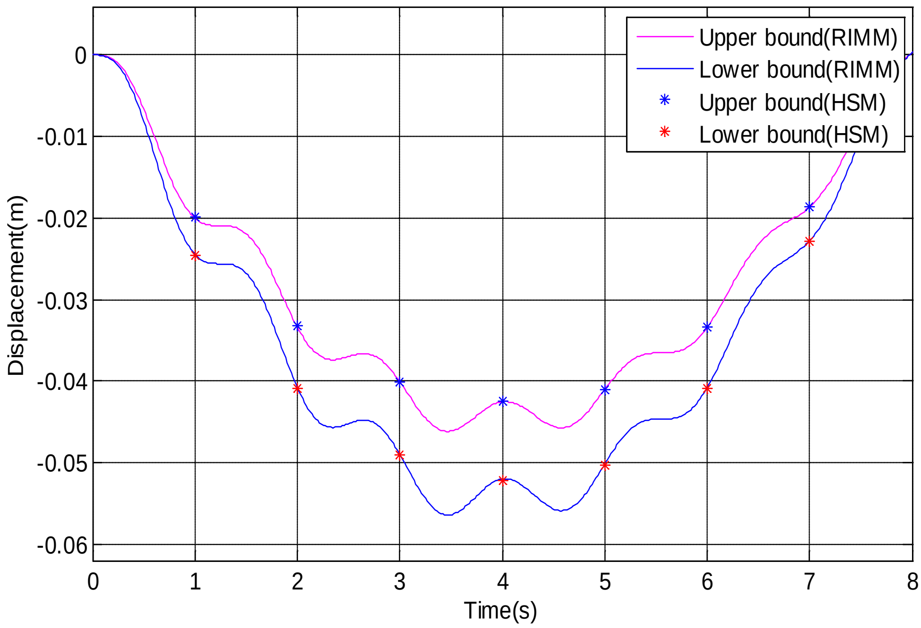

(f) COV(ρ^R, E^R, I^R)=0.05, ICR(m_1^I, m_2^I, m_v^I)=0.1, $v = 5m/s$

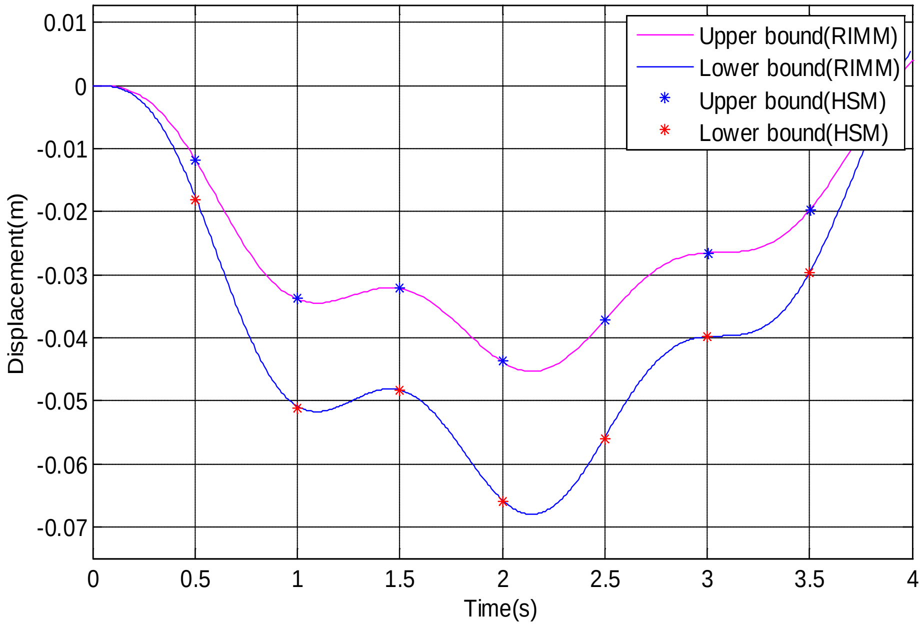

(g) COV(ρ^R, E^R, I^R)=0.05, ICR(m_1^I, m_2^I, m_v^I)=0.2, $v = 10m/s$

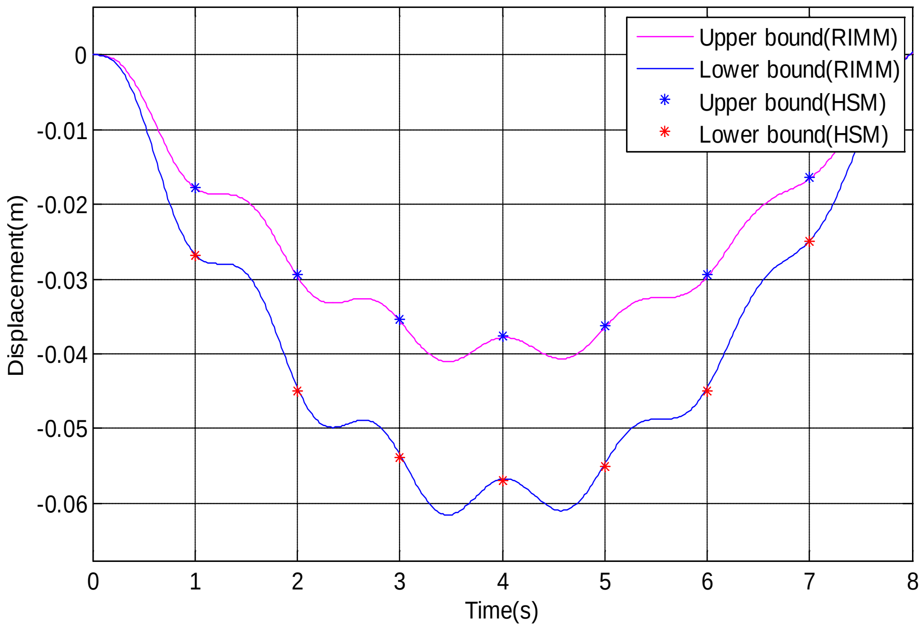

(h) COV(ρ^R, E^R, I^R)=0.02, ICR(m_1^I, m_2^I, m_v^I)=0.2, $v = 5m/s$

Figure 4.2 Mean value of random interval bridge displacement response at mid-span

The standard deviation (SD) of the random interval bridge displacement response at its mid-span is shown in Figures 4.3(a)-(f) when different conditions of uncertain parameters are under consideration. Figure 4.3(a) shows that the standard deviation of the bridge response is zero when only the uncertainties of interval parameters are taken into account, which is a pure interval problem and is also a special case of random interval problems. The Young’s modulus and moment of inertia produce the same effects on the bridge response as shown in Figures 4.3(b) and 4.3(c), which is greater than that caused by the density shown in Figure 4.3(d). In bridge design, changing moment of inertia of its cross-section will significantly affect the bridge behaviour. It can be easily seen from Figure 4.3(e) that the interval of the standard deviation of bridge response becomes much larger when the randomness of all bridge random parameters is included.

From Figures 4.3(e)-(h), it can be also observed that the interval width of the standard deviation of the random interval bridge response is directly proportional to the uncertainties of random and interval variables and vehicle speed.

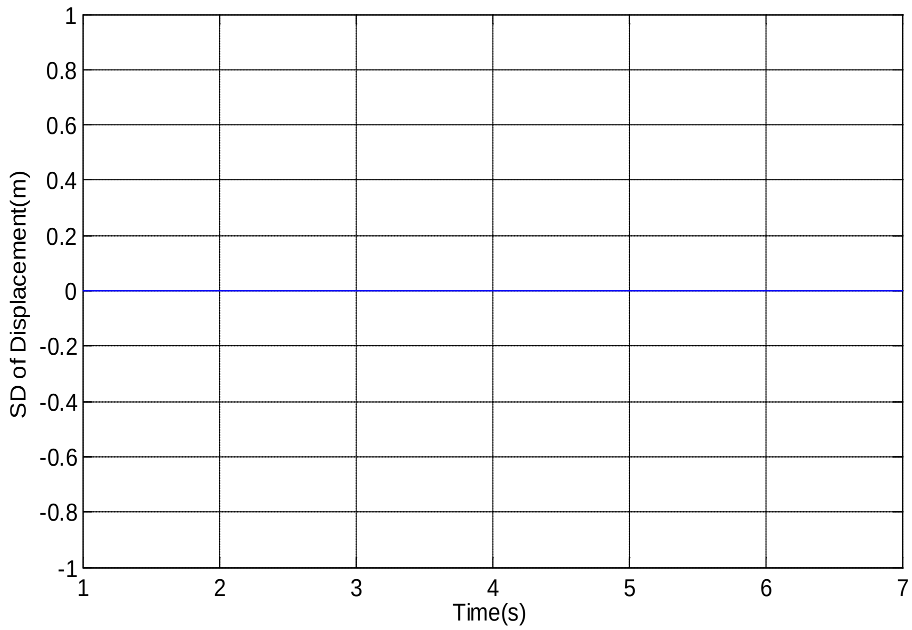

(a) COV(ρ^R, E^R, I^R)=0, ICR(m_1^I, m_2^I, m_v^I)=0.2, $v = 5m/s$

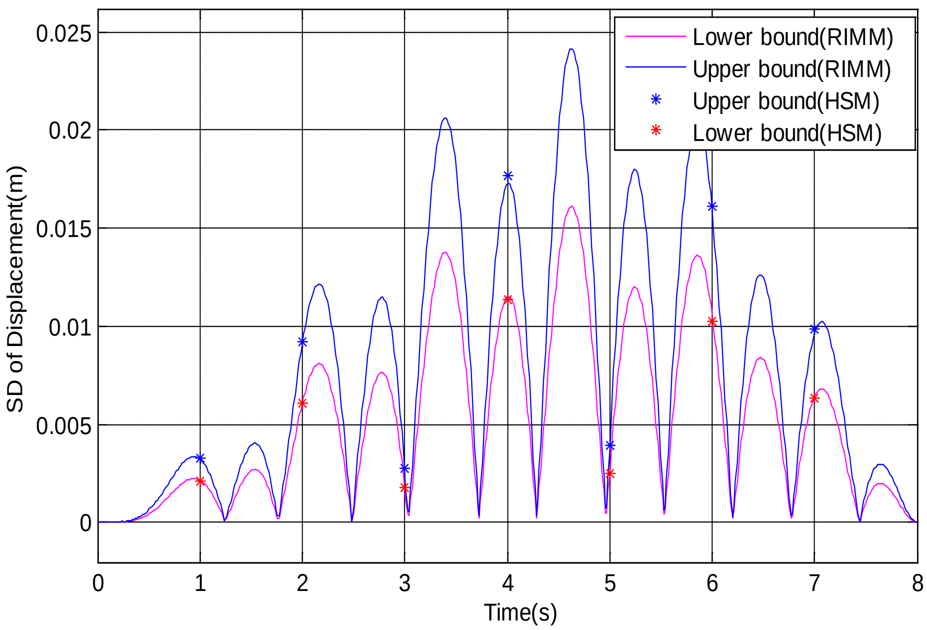

(b) COV(E^R)=0.05, COV(ρ^R, I^R)=0, ICR(m_1^I, m_2^I, m_v^I)=0.2, $v = 5m/s$

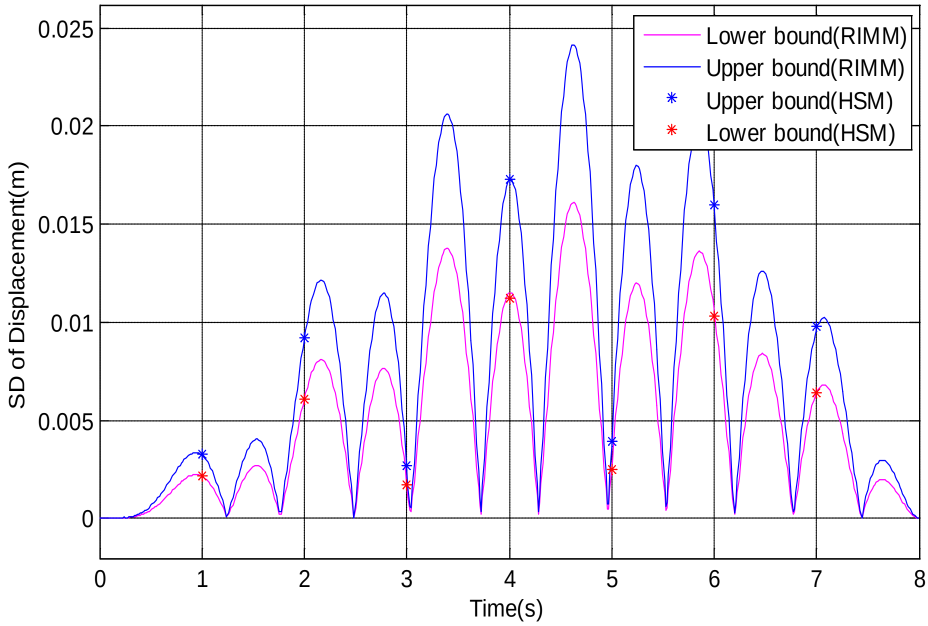

(c) COV(I^R)=0.05, COV(ρ^R, E^R)=0, ICR(m_1^I, m_2^I, m_v^I)=0.2, $v = 5m/s$

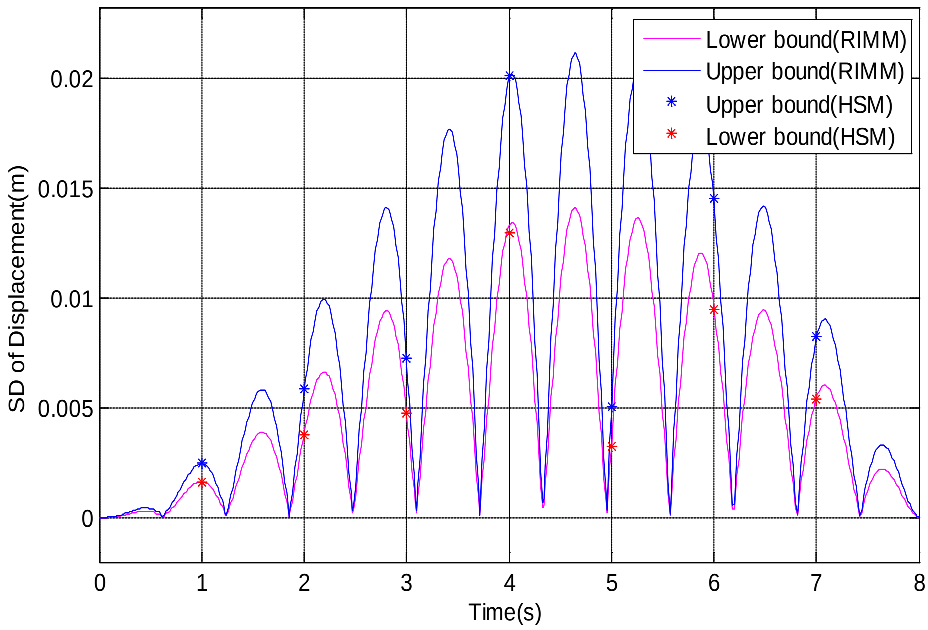

(d) COV(ρ^R)=0.05, COV(E^R, I^R)=0, ICR(m_1^I, m_2^I, m_v^I)=0.2, $v = 5m/s$

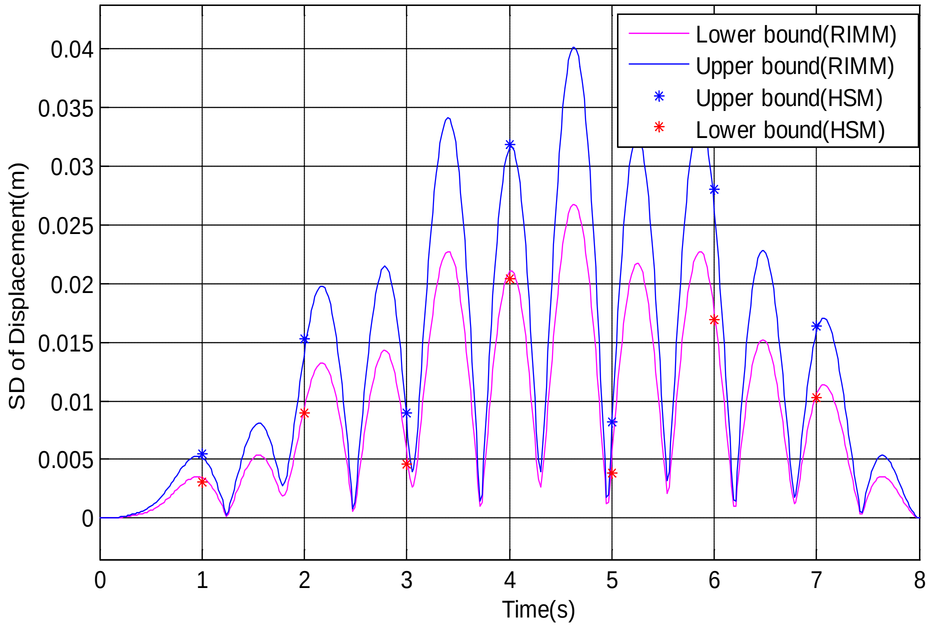

(e) COV(ρ^R, E^R, I^R)=0.05, ICR(m_1^I, m_2^I, m_v^I)=0.2, $v = 5m/s$

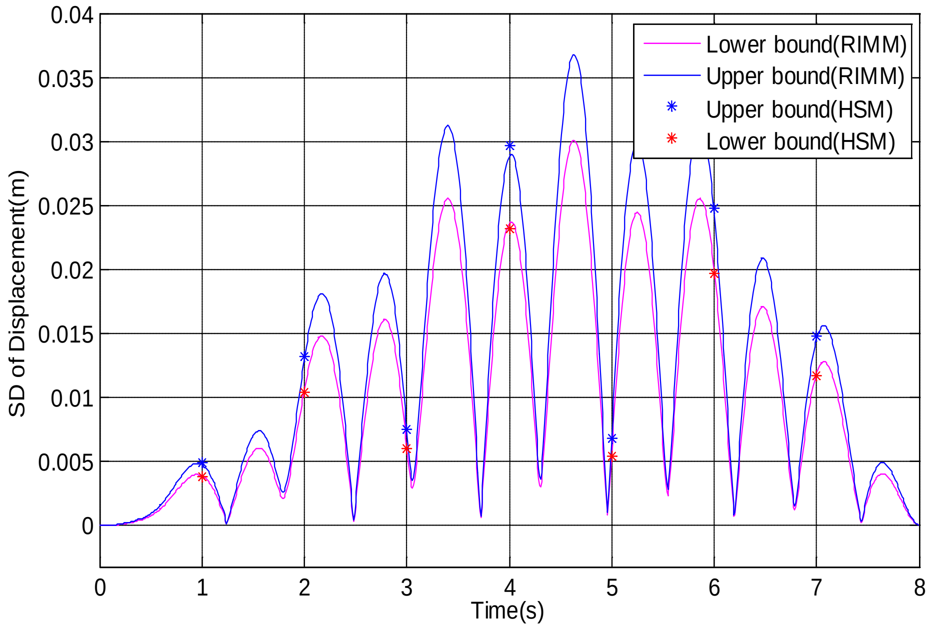

(f) COV(ρ^R, E^R, I^R)=0.05, ICR(m_1^I, m_2^I, m_v^I)=0.1, $v = 5m/s$

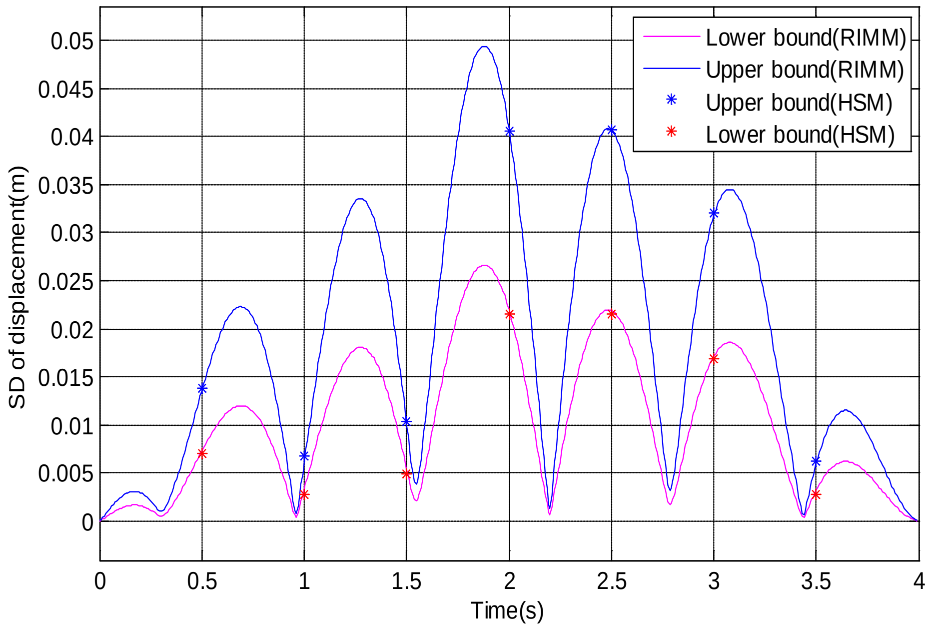

(g) COV(ρ^R, E^R, I^R)=0.05, ICR($.m_1^I, m_2^I, m_v^I$)=0.2, $v = 10m/s$

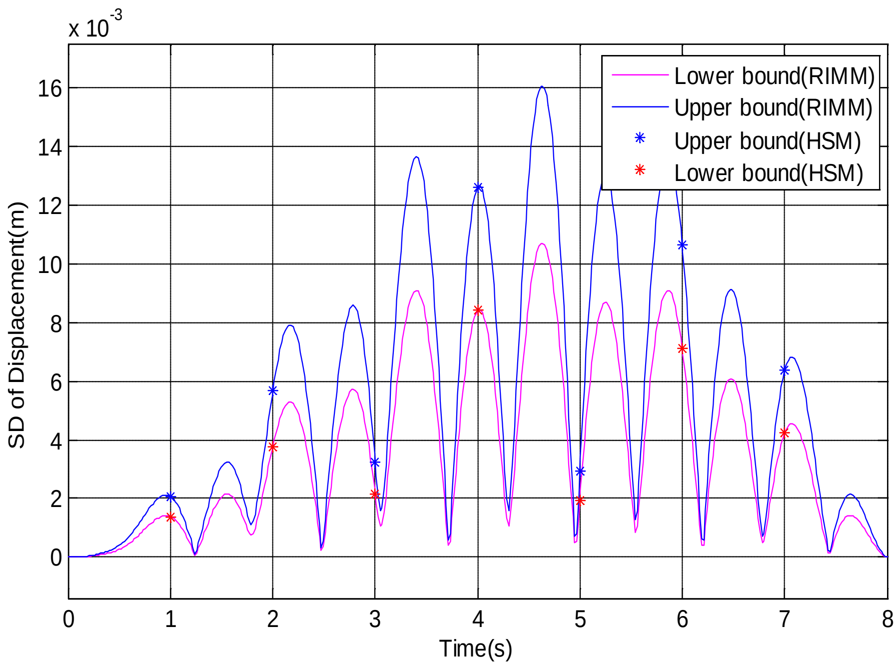

(h) COV(ρ^R, E^R, I^R)=0.02, ICR(m_1^I, m_2^I, m_v^I)=0.2, $v = 5m/s$

Figure 4.3 Standard deviation of random interval bridge displacement at mid-span

To validate the accuracy of the random interval moment method (RIMM) presented in this chapter, a hybrid simulation method (HSM) is employed. This hybrid simulation method (HSM) combines direct simulation for interval variables and Monte-Carlo simulations for random variables. In every hybrid simulation, the first step is to arbitrarily generate values within the given intervals for all interval variables, and the second step is using 10,000 times Monte-Carlo simulations to determine the mean value and standard deviation of structural response. After repeat the whole procedure 10,000 times, 10,000 mean values and 10,000 standard deviations can be obtained. Then the lower and upper bounds of them can be determined, respectively. More simulation times can be used for the two steps to improve the accuracy of the results. Hybrid simulations are implemented by using the MATLAB platform. The results obtained by the HSM are also given in Figures 4.2 and 4.3. It can be concluded that the results produced by the presented method are in very good agreement with those calculated by the HSM.

To show the differences between the results generated by the RIMM and HSM in detail, the differences of mean value and standard deviation of bridge displacement are listed in Tables 4.2 to 4.3. Given the maximum difference is 1.10%, while the coefficients of variation for all random parameters are 0.05 and the interval change ratios of all interval parameters are 0.2, the mean values calculated by the two methods are very closed to each other. For the standard deviation, the maximum difference is 6.45%, which can be accepted because the hybrid simulation times used in this study are not enough to provide convergent results. 10,000 simulations used in the two rounds of HSM cannot yield convergent and reliable results although the total simulations are 10^6. The accuracy of the results obtained by the HSM can be improved if more simulations are implemented.

Table 4.2 Comparison of mean values

(COV(ρ^R, E^R, I^R)=0.05, ICR(m_1^I, m_2^I, m_v^I)=0.2, $v = 5m/s$)

Time (s)	Upper bound			Lower bound		
	RIMM	HSM	Difference	RIMM	HSM	Difference
1	0.02663	0.02671	0.29%	0.01793	0.01790	0.17%
2	0.04437	0.04461	0.55%	0.02958	0.02947	0.36%
3	0.05327	0.05353	0.49%	0.03550	0.03549	0.02%
4	0.05671	0.05680	0.16%	0.03781	0.03768	0.35%
5	0.05459	0.05467	0.14%	0.03639	0.03610	0.81%
6	0.04420	0.04436	0.37%	0.02961	0.02929	1.10%
7	0.02482	0.02506	0.97%	0.01636	0.01625	0.68%

Table 4.3 Comparison of standard deviations

(COV(ρ^R, E^R, I^R)=0.05, ICR(m_1^I, m_2^I, m_v^I)=0.2, $v = 5m/s$)

Time	Upper bound			Lower bound		
	RIMM	HSM	Difference	RIMM	HSM	Difference
1	0.00521	0.00547	4.72%	0.00347	0.00339	2.33%
2	0.01394	0.01415	1.50%	0.00923	0.00894	3.22%
3	0.00886	0.00894	0.91%	0.00589	0.00577	2.14%
4	0.03162	0.03182	0.62%	0.02108	0.02095	0.63%
5	0.00852	0.00854	0.19%	0.00568	0.00549	3.54%
6	0.02617	0.02797	6.45%	0.01744	0.01713	1.83%
7	0.01596	0.01638	2.57%	0.01064	0.01024	3.87%

Generally, the accuracy of these results is satisfactory in practice. The presented random interval moment method has much less computational work than the simulation method. It should be noted that the accuracy of the results of random interval moment method can be further improved if second or higher order Taylor expansions are used.

4.6 Conclusions

In this chapter, non-deterministic dynamic response of vehicle-bridge interaction system with uncertain parameters is investigated by extending the random interval moment method to the dynamic coupling system. The uncertainties of system are modelled as random and interval variables. The expressions for calculating the bounds of expectation and variance of the random interval bridge response are derived. Using these formulations, the upper and lower bounds of mean value and standard deviation of bridge response can be very easily obtained.

The results obtained by the presented random interval moment method are in very good agreement with those determined by Monte-Carlo simulation method. The differences of these two methods are quite small when the change ranges of system parameters are not large. The random interval moment method will be further developed to investigate the non-deterministic dynamic behaviour of a bridge under multiple moving vehicles. In addition, optimization methods can be embedded to obtain more accurate bounds of statistical moments of the random interval structural response.

Chapter 5 Dynamic Analysis of Vehicle-Bridge Interaction System with Uncertainties Based on Finite Element Model

5.1 Introduction

As mentioned in previous chapters, for dynamic analysis of vehicle-bridge interaction system, two kinds of methods are developed to analyse dynamic response of bridge structure subjects to moving vehicles. Analytical methods are suitable to solve the interaction dynamic problems derived from simplified vehicle-bridge models. Governing equations are not large number of partial differential equations which can be solved easily. Although assumptions and simplifications may be made, analytical methods have good capability to predict the system response based on the simple models [2-6]. Numerical methods have been widely used to treat more realistic models. Among these numerical methods, finite element method is one of the most versatile one used by lots of researchers [64, 66, 69, 72, 75]. Finite element method enables handling more complex vehicle-bridge models for the dynamic interaction analysis. Henchi et al. [7] proposed an efficient algorithm for the dynamic analysis of a bridge discretized into three-dimensional finite elements with a stream of vehicles running on top at a prescribed speed. The vehicular axle loads acting on the bridge deck are represented as nodal forces using shape functions of the finite element. The coupled equations of motion of the vehicle bridge system are solved directly without the use of an iterative method.

In this chapter, a finite element model is developed to calculate the dynamic response of a bridge under a moving vehicle with inherent uncertain parameters in the vehicle-bridge interaction system. The algorithm, called random interval perturbation method, based on the proposed finite element model can handle a mixture random and interval uncertainties in the system parameters. A half-car model is used to represent the vehicle and beam elements are used to model the bridge. The vehicle parameters are assumed as interval variables, and the bridge parameters corresponding to Young's modulus, mass and moment of inertia, are considered as random variables. The computational expressions for the lower and upper bounds of the first two statistical moments of the vertical responses of the bridge are developed by using the random interval perturbation method. Hybrid simulations are also implemented to validate the accuracy of the results produce by the presented method.

5.2 Random Interval Perturbation Method

In this chapter, an approach called random interval perturbation method [10] is extended to calculate the mean value and variance of the random interval bridge response based on the finite element analysis framework. The finite element equilibrium equations of a structural system in displacement format is

$$[K]\{U\}=\{f\} \tag{5.1}$$

where $[K]$ is the global stiffness matrix, $\{U\}$ is the unknown displacement vector and $\{f\}$ is the load vector.

Let random vector $\vec{a}^R=(a_1^R,a_2^R,\cdots,a_n^R)$ represent all random variables of the structural system, whereas, $\vec{b}^I=(b_1^I,b_2^I,\cdots,b_m^I)$ represent all interval variables. The structural stiffness matrix $[K]$ and load vector $\{f\}$ are functions of $\vec{a}^R$ and $\vec{b}^I$. Obviously structural displacement vector $\{U\}$ is also the function of $\vec{a}^R$ and $\vec{b}^I$. Thus, the static equilibrium Eq.(5.1) can be written as

$$\left[K(\vec{a}^R,\vec{b}^I)\right]\left\{U(\vec{a}^R,\vec{b}^I)\right\}=\left\{f(\vec{a}^R,\vec{b}^I)\right\} \tag{5.2}$$

Using the Taylor expansion, the structural stiffness matrix and load vector can be expressed as

$$\left[K(\vec{a}^R,\vec{b}^I)\right]=\left[K(\bar{a},\vec{b}^c)\right]+\sum_{j=1}^{m}\frac{\partial\left[K(\bar{a},\vec{b}^c)\right]}{\partial b_j^I}\Delta b_j^I$$

$$+\sum_{i=1}^{n}\left\{\frac{\partial\left[K(\bar{a},\vec{b}^c)\right]}{\partial a_i^R}+\sum_{j=1}^{m}\frac{\partial^2\left[K(\bar{a},\vec{b}^c)\right]}{\partial a_i^R\partial b_j^I}\Delta b_j^I\right\}\left(a_i^R-\bar{a}_i\right)$$

$$+\frac{1}{2}\sum_{i=1}^{n}\sum_{l=1}^{n}\left\{\frac{\partial^2\left[K(\bar{a},\vec{b}^c)\right]}{\partial a_i^R\partial a_l^R}+\sum_{j=1}^{m}\frac{\partial^3\left[K(\bar{a},\vec{b}^c)\right]}{\partial a_i^R\partial a_l^R\partial b_j^I}\Delta b_j^I\right\}(a_i^R-\bar{a}_i)(a_l^R-\bar{a}_l)+R \tag{5.3}$$

$$\left\{f(\vec{a}^R,\vec{b}^I)\right\}=\left\{f(\bar{a},\vec{b}^c)\right\}+\sum_{j=1}^{m}\frac{\partial\left\{f(\bar{a},\vec{b}^c)\right\}}{\partial b_j^I}\Delta b_j^I$$

$$+\sum_{i=1}^{n}\left\{\frac{\partial\left\{f(\bar{a},\vec{b}^c)\right\}}{\partial a_i^R}+\sum_{j=1}^{m}\frac{\partial^2\left\{f(\bar{a},\vec{b}^c)\right\}}{\partial a_i^R\partial b_j^I}\Delta b_j^I\right\}\left(a_i^R-\bar{a}_i\right)$$

$$+\frac{1}{2}\sum_{i=1}^{n}\sum_{l=1}^{n}\left\{\frac{\partial^2\left\{f(\bar{a},\vec{b}^c)\right\}}{\partial a_i^R\partial a_l^R}+\sum_{j=1}^{m}\frac{\partial^3\left\{f(\bar{a},\vec{b}^c)\right\}}{\partial a_i^R\partial a_l^R\partial b_j^I}\Delta b_j^I\right\}(a_i^R-\bar{a}_i)(a_l^R-\bar{a}_l)+R \tag{5.4}$$

where $\bar{\bar{a}}=(\bar{a}_1,\bar{a}_2,\cdots,\bar{a}_n)$ and $\vec{b}^c=(b_1^c,b_2^c,\cdots,b_m^c)$.

Neglecting the remainder term, the random interval matrix can be rewritten as

$$\left[K(\vec{a}^R,\vec{b}^I)\right]=\left[K(\bar{a},\vec{b}^c)\right]+\Delta_1\left[K(\vec{a}^R,\vec{b}^I)\right]+\Delta_2\left[K(\vec{a}^R,\vec{b}^I)\right]$$

$$=K_d+\Delta_1 K+\Delta_2 K \tag{5.5}$$

where

$$\Delta_1 K=\sum_{j=1}^{m}\frac{\partial\left[K(\bar{a},\vec{b}^c)\right]}{\partial b_j^I}\Delta b_j^I+\sum_{i=1}^{n}\left\{\frac{\partial\left[K(\bar{a},\vec{b}^c)\right]}{\partial a_i^R}+\sum_{j=1}^{m}\frac{\partial^2\left[K(\bar{a},\vec{b}^c)\right]}{\partial a_i^R\partial b_j^I}\Delta b_j^I\right\}\left(a_i^R-\bar{a}_i\right)$$

$$=\sum_{j=1}^{m}K'_{b_j^I}\Delta b_j^I+\sum_{i=1}^{n}\left\{K'_{a_i^R}+\sum_{j=1}^{m}K''_{a_i^R b_j^I}\Delta b_j^I\right\}\left(a_i^R-\bar{a}_i\right) \tag{5.6}$$

$$\Delta_2 K = \frac{1}{2}\sum_{i=1}^{n}\sum_{l=1}^{n}\left\{\frac{\partial^2\left[K(\bar{\vec{a}},\vec{b}^c)\right]}{\partial a_i^R \partial a_l^R} + \sum_{j=1}^{m}\frac{\partial^3\left[K(\bar{\vec{a}},\vec{b}^c)\right]}{\partial a_i^R \partial a_l^R \partial b_j^I}\Delta b_j^I\right\}(a_i^R - \bar{a}_i)(a_l^R - \bar{a}_l)$$

$$= \frac{1}{2}\sum_{i=1}^{n}\sum_{l=1}^{n}\left\{K''_{a_i^R a_l^R} + \sum_{j=1}^{m} K'''_{a_i^R a_l^R b_j^I}\Delta b_j^I\right\}(a_i^R - \bar{a}_i)(a_l^R - \bar{a}_l) \quad (5.7)$$

Similarly the load vector can also be expressed as

$$\left\{f(\vec{a}^R,\vec{b}^I)\right\} = \left\{f(\bar{\vec{a}},\vec{b}^c)\right\} + \Delta_1\left\{f(\vec{a}^R,\vec{b}^I)\right\} + \Delta_2\left\{f(\vec{a}^R,\vec{b}^I)\right\}$$

$$= f_d + \Delta_1 f + \Delta_2 f \quad (5.8)$$

where

$$\Delta_1\left\{f(\vec{a}^R,\vec{b}^I)\right\} = \sum_{j=1}^{m}\frac{\partial\left\{f(\bar{\vec{a}},\vec{b}^c)\right\}}{\partial b_j^I}\Delta b_j^I + \sum_{i=1}^{n}\left\{\frac{\partial\left\{f(\bar{\vec{a}},\vec{b}^c)\right\}}{\partial a_i^R} + \sum_{j=1}^{m}\frac{\partial^2\left\{f(\bar{\vec{a}},\vec{b}^c)\right\}}{\partial a_i^R \partial b_j^I}\Delta b_j^I\right\}\left(a_i^R - \bar{a}_i\right)$$

$$= \sum_{j=1}^{m} f'_{b_j^I}\Delta b_j^I + \sum_{i=1}^{n}\left\{f'_{a_i^R} + \sum_{j=1}^{m} f''_{a_i^R b_j^I}\Delta b_j^I\right\}\left(a_i^R - \bar{a}_i\right) \quad (5.9)$$

$$\Delta_2 f = \frac{1}{2}\sum_{i=1}^{n}\sum_{l=1}^{n}\left\{\frac{\partial^2\left\{f(\bar{\vec{a}},\vec{b}^c)\right\}}{\partial a_i^R \partial a_l^R} + \sum_{j=1}^{m}\frac{\partial^3\left\{f(\bar{\vec{a}},\vec{b}^c)\right\}}{\partial a_i^R \partial a_l^R \partial b_j^I}\Delta b_j^I\right\}(a_i^R - \bar{a}_i)(a_l^R - \bar{a}_l)$$

$$= \frac{1}{2}\sum_{i=1}^{n}\sum_{l=1}^{n}\left\{f''_{a_i^R a_l^R} + \sum_{j=1}^{m} f'''_{a_i^R a_l^R b_j^I}\Delta b_j^I\right\}(a_i^R - \bar{a}_i)(a_l^R - \bar{a}_l) \quad (5.10)$$

Using the perturbation theory, we can get the following governing equation for static displacement response of the structure

$$\left(K_d + \Delta_1 K + \Delta_2 K\right)\left(U_d + \Delta_1 U + \Delta_2 U\right) = f_d + \Delta_1 f + \Delta_2 f \quad (5.11)$$

where

$$U_d = K_d^{-1} f_d \tag{5.12}$$

$$\Delta_1 U = K_d^{-1}\left(\Delta_1 f - \Delta_1 K U_d\right)$$

$$= K_d^{-1}\left(\Delta_1 f - \Delta_1 K K_d^{-1} f_d\right) \tag{5.13}$$

$$\Delta_2 U = K_d^{-1}\left(\Delta_2 f - \Delta_1 K \Delta_1 U - \Delta_2 K U_d\right)$$

$$= K_d^{-1}\left(\Delta_2 f - \Delta_1 K K_d^{-1}\left(\Delta_1 f - \Delta_1 K K_d^{-1} f_d\right) - \Delta_2 K K_d^{-1} f_d\right) \tag{5.14}$$

The random interval structural displacement based on the first-order perturbation can be obtained as

$$U^{RI1} = U_d + \Delta_1 U \tag{5.15}$$

The structural displacement based on the second-order perturbation is given by

$$U^{RI2} = U_d + \Delta_1 U + \Delta_2 U \tag{5.16}$$

Substituting Eqs.(5.6), (5.9), (5.12) and (5.13) into Eq.(5.15) yields

$$U^{RI1} = K_d^{-1} f_d + K_d^{-1}\left\{\sum_{j=1}^{m} f'_{b_j^I}\Delta b_j^I + \sum_{i=1}^{n}\left\{ f'_{a_i^R} + \sum_{j=1}^{m} f''_{a_i^R b_j^I}\Delta b_j^I\right\}\left(a_i^R - \overline{a}_i\right)\right.$$

$$\left. - \left\{\sum_{j=1}^{m} K'_{b_j^I}\Delta b_j^I + \sum_{i=1}^{n}\left\{K'_{a_i^R} + \sum_{j=1}^{m} K''_{a_i^R b_j^I}\Delta b_j^I\right\}\left(a_i^R - \overline{a}_i\right)\right\} K_d^{-1} f_d \right\}$$

$$= K_d^{-1} f_d + K_d^{-1}\left(\sum_{j=1}^{m} f'_{b_j^I} \Delta b_j^I - \sum_{j=1}^{m} K'_{b_j^I} \Delta b_j^I K_d^{-1} f_d \right)$$

$$+\sum_{i=1}^{n}\left\{ K_d^{-1}\left\{ f'_{a_i^R} + \sum_{j=1}^{m} f''_{a_i^R b_j^I} \Delta b_j^I \right\} - K_d^{-1}\left\{ K'_{a_i^R} + \sum_{j=1}^{m} K''_{a_i^R b_j^I} \Delta b_j^I \right\} K_d^{-1} f_d \right\}\left(a_i^R - \overline{a}_i \right) \quad (5.17)$$

Substituting Eqs.(5.6), (5.7), (5.9), (5.10), (5.12), (5.13) and (5.14) into Eq.(5.16) gives

$$U^{RI2} = K_d^{-1} f_d$$

$$+K_d^{-1}\left(\sum_{j=1}^{m} f'_{b_j^I} \Delta b_j^I - \sum_{j=1}^{m} K'_{b_j^I} \Delta b_j^I K_d^{-1} f_d \right)$$

$$-K_d^{-1} \sum_{j=1}^{m} K'_{b_j^I} \Delta b_j^I K_d^{-1} \sum_{j=1}^{m} f'_{b_j^I} \Delta b_j^I + K_d^{-1} \sum_{j=1}^{m} K'_{b_j^I} \Delta b_j^I K_d^{-1} \sum_{j=1}^{m} K'_{b_j^I} \Delta b_j^I K_d^{-1} f_d$$

$$+\sum_{i=1}^{n}\left\{ K_d^{-1}\left\{ f'_{a_i^R} + \sum_{j=1}^{m} f''_{a_i^R b_j^I} \Delta b_j^I \right\} - K_d^{-1}\left\{ K'_{a_i^R} + \sum_{j=1}^{m} K''_{a_i^R b_j^I} \Delta b_j^I \right\} K_d^{-1} f_d \right.$$

$$-K_d^{-1} \sum_{j=1}^{m} K'_{b_j^I} \Delta b_j^I K_d^{-1}\left\{ f'_{a_i^R} + \sum_{j=1}^{m} f''_{a_i^R b_j^I} \Delta b_j^I \right\} + K_d^{-1} \sum_{j=1}^{m} K'_{b_j^I} \Delta b_j^I K_d^{-1}\left\{ K'_{a_i^R} + \sum_{j=1}^{m} K''_{a_i^R b_j^I} \Delta b_j^I \right\} K_d^{-1} f_d$$

$$-K_d^{-1}\left\{ K'_{a_i^R} + \sum_{j=1}^{m} K''_{a_i^R b_j^I} \Delta b_j^I \right\} K_d^{-1} \sum_{j=1}^{m} f'_{b_j^I} \Delta b_j^I$$

$$\left. +K_d^{-1}\left\{ K'_{a_i^R} + \sum_{j=1}^{m} K''_{a_i^R b_j^I} \Delta b_j^I \right\} K_d^{-1} \sum_{j=1}^{m} K'_{b_j^I} \Delta b_j^I K_d^{-1} f_d \right\}\left(a_i^R - \overline{a}_i \right)$$

$$+\sum_{i=1}^{n} \sum_{l=1}^{n} \left\{ -K_d^{-1}\left\{ K'_{a_i^R} + \sum_{j=1}^{m} K''_{a_i^R b_j^I} \Delta b_j^I \right\} K_d^{-1}\left\{ f'_{a_l^R} + \sum_{j=1}^{m} f''_{a_l^R b_j^I} \Delta b_j^I \right\} \right.$$

$$+K_d^{-1}\left\{ K'_{a_i^R} + \sum_{j=1}^{m} K''_{a_i^R b_j^I} \Delta b_j^I \right\} K_d^{-1}\left\{ K'_{a_l^R} + \sum_{j=1}^{m} K''_{a_l^R b_j^I} \Delta b_j^I \right\} K_d^{-1} f_d$$

$$\left. +\frac{1}{2} K_d^{-1}\left\{ f''_{a_i^R a_l^R} + \sum_{j=1}^{m} f'''_{a_i^R a_l^R b_j^I} \Delta b_j^I \right\} - \frac{1}{2} K_d^{-1}\left\{ K''_{a_i^R a_l^R} + \sum_{j=1}^{m} K'''_{a_i^R a_l^R b_j^I} \Delta b_j^I \right\} K_d^{-1} f_d \right\}(a_i^R - \overline{a}_i)(a_l^R - \overline{a}_l)$$

(5.18)

Using the random interval moment method, the mean value and variance of the random interval structural displacements based on the first-order perturbation can be obtained as

$$\mu_{U^{RI1}} = K_d^{-1} f_d + K_d^{-1}\left(\sum_{j=1}^{m} f'_{b_j^I} \Delta b_j^I - \sum_{j=1}^{m} K'_{b_j^I} \Delta b_j^I K_d^{-1} f_d \right) \tag{5.19}$$

$$\sigma^2_{U^{RI1}} = \sum_{i=1}^{n} \left\{ K_d^{-1} \left\{ f'_{a_i^R} + \sum_{j=1}^{m} f''_{a_i^R b_j^I} \Delta b_j^I \right\} - K_d^{-1} \left\{ K'_{a_i^R} + \sum_{j=1}^{m} K''_{a_i^R b_j^I} \Delta b_j^I \right\} K_d^{-1} f_d \right\}^2 \sigma^2_{a_i^R}$$

$$+ \sum_{i(\neq k)=1}^{n} \sum_{k(\neq i)=1}^{n} \left\{ K_d^{-1} \left\{ f'_{a_i^R} + \sum_{j=1}^{m} f''_{a_i^R b_j^I} \Delta b_j^I \right\} - K_d^{-1} \left\{ K'_{a_i^R} + \sum_{j=1}^{m} K''_{a_i^R b_j^I} \Delta b_j^I \right\} K_d^{-1} f_d \right\}$$

$$\cdot \left\{ K_d^{-1} \left\{ f'_{a_k^R} + \sum_{j=1}^{m} f''_{a_k^R b_j^I} \Delta b_j^I \right\} - K_d^{-1} \left\{ K'_{a_k^R} + \sum_{j=1}^{m} K''_{a_k^R b_j^I} \Delta b_j^I \right\} K_d^{-1} f_d \right\} Cov(a_i^R, a_k^R) \tag{5.20}$$

U^{RI2} in Eq.(5.18) can be simply expressed as

$$U^{RI2} = K_d^{-1} f_d + K_d^{-1}\left(\sum_{j=1}^{m} f'_{b_j^I} \Delta b_j^I - \sum_{j=1}^{m} K'_{b_j^I} \Delta b_j^I K_d^{-1} f_d \right)$$

$$- K_d^{-1} \sum_{j=1}^{m} K'_{b_j^I} \Delta b_j^I K_d^{-1} \sum_{j=1}^{m} f'_{b_j^I} \Delta b_j^I + K_d^{-1} \sum_{j=1}^{m} K'_{b_j^I} \Delta b_j^I K_d^{-1} \sum_{j=1}^{m} K'_{b_j^I} \Delta b_j^I K_d^{-1} f_d$$

$$+ \sum_{i=1}^{n} A(a_i^R, \vec{b}^I)\left(a_i^R - \bar{a}_i\right) + \sum_{i=1}^{n} \sum_{l=1}^{n} B(a_i^R, a_l^R, \vec{b}^I)\left(a_i^R - \bar{a}_i\right)\left(a_i^R - \bar{a}_i\right) \tag{5.21}$$

where

$$A(a_i^R, \vec{b}^I) = K_d^{-1} \left\{ f'_{a_i^R} + \sum_{j=1}^{m} f''_{a_i^R b_j^I} \Delta b_j^I \right\} - K_d^{-1} \left\{ K'_{a_i^R} + \sum_{j=1}^{m} K''_{a_i^R b_j^I} \Delta b_j^I \right\} K_d^{-1} f_d$$

$$-K_d^{-1}\sum_{j=1}^{m} K'_{b_j^I}\Delta b_j^I K_d^{-1}\left\{f'_{a_i^R}+\sum_{j=1}^{m} f''_{a_i^R b_j^I}\Delta b_j^I\right\}$$

$$+K_d^{-1}\sum_{j=1}^{m} K'_{b_j^I}\Delta b_j^I K_d^{-1}\left\{K'_{a_i^R}+\sum_{j=1}^{m} K''_{a_i^R b_j^I}\Delta b_j^I\right\}K_d^{-1} f_d$$

$$-K_d^{-1}\left\{K'_{a_i^R}+\sum_{j=1}^{m} K''_{a_i^R b_j^I}\Delta b_j^I\right\}K_d^{-1}\sum_{j=1}^{m} f'_{b_j^I}\Delta b_j^I +K_d^{-1}\left\{K'_{a_i^R}+\sum_{j=1}^{m} K''_{a_i^R b_j^I}\Delta b_j^I\right\}K_d^{-1}\sum_{j=1}^{m} K'_{b_j^I}\Delta b_j^I K_d^{-1} f_d \tag{5.22}$$

$$B(a_i^R, a_l^R, \vec{b}^I) = -K_d^{-1}\left\{K'_{a_i^R}+\sum_{j=1}^{m} K''_{a_i^R b_j^I}\Delta b_j^I\right\}K_d^{-1}\left\{f'_{a_l^R}+\sum_{j=1}^{m} f''_{a_l^R b_j^I}\Delta b_j^I\right\}$$

$$+K_d^{-1}\left\{K'_{a_i^R}+\sum_{j=1}^{m} K''_{a_i^R b_j^I}\Delta b_j^I\right\}K_d^{-1}\left\{K'_{a_i^R}+\sum_{j=1}^{m} K''_{a_i^R b_j^I}\Delta b_j^I\right\}K_d^{-1} f_d$$

$$+\frac{1}{2}K_d^{-1}\left\{f''_{a_i^R a_l^R}+\sum_{j=1}^{m} f'''_{a_i^R a_l^R b_j^I}\Delta b_j^I\right\}-\frac{1}{2}K_d^{-1}\left\{K''_{a_i^R a_l^R}+\sum_{j=1}^{m} K'''_{a_i^R a_l^R b_j^I}\Delta b_j^I\right\}K_d^{-1} f_d \tag{5.23}$$

Similarly, the mean the mean value and variance of the random interval structural displacements based on the second-order perturbation can be developed.

5.3 Formulation of the Vehicle-Bridge Model

In the vehicle-bridge interaction system, the bridge is also modelled as an Euler-Bernoulli beam consisting of a number of elements and the vehicle is represented by a half-car model as shown in Figure 5.1. Again, m_v, m_1 and m_2 denote the sprung mass and unsprung masses respectively; a1 and a2 are the position parameters; S is the axle spacing; the suspension system is represented by two linear springs of stiffness k_{s1}, k_{s2} and two linear dampers with damping rates c_{s1}, c_{s2}; the tires are also modeled by two linear springs of stiffness k_{t1}, k_{t2} and two linear dampers with damping rates c_{t1}, c_{t2}; ρ, E, I and L are the mass per unit length, elastic modulus, moment of inertia and length of the beam respectively.

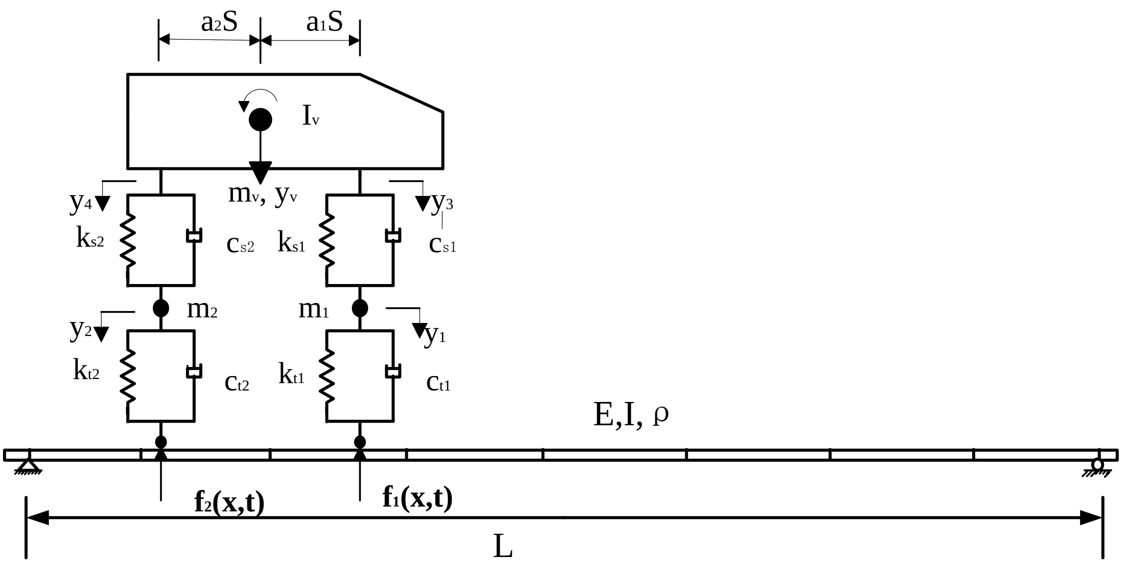

Figure 5.1 Model of vehicle-bridge interaction system

5.3.1 Equation of motion of the vehicle system

The equation of motion of the vehicle are derived as follows

$$m_v\ddot{y}_v + c_{s1}(\dot{y}_1 - \dot{y}_3) + c_{s2}(\dot{y}_2 - \dot{y}_4) + k_{s1}(y_1 - y_3) + k_{s2}(y_2 - y_4) = 0 \tag{5.24}$$

$$I_v\ddot{\theta}_v - a_1Sc_{s1}(\dot{y}_1 - \dot{y}_3) + a_2Sc_{s2}(\dot{y}_2 - \dot{y}_4) - a_1Sk_{s1}(y_1 - y_3) + a_2Sk_{s2}(y_2 - y_4) = 0 \tag{5.25}$$

$$m_1\ddot{y}_3 - c_{s1}(\dot{y}_1 - \dot{y}_3) - k_{s1}(y_1 - y_3)$$

$$= -k_{t1}(y_1 - W(x_1,t) - r(x_1,t)) - c_{t1}(\dot{y}_1 - \dot{W}(x_1,t) - \dot{r}(x_1,t)) \tag{5.26}$$

$$m_2\ddot{y}_4 - c_{s2}(\dot{y}_2 - \dot{y}_4) - k_{s2}(y_2 - y_4)$$

$$= -k_{t2}(y_2 - W(x_2,t) - r(x_2,t)) - c_{t2}(\dot{y}_2 - \dot{W}(x_2,t) - \dot{r}(x_2,t)) \tag{5.27}$$

$$y_1 = y_v - a_1 S\theta_v \ , \quad y_2 = y_v + a_2 S\theta_v \tag{5.28}$$

$$y_v = a_2 y_1 + a_1 y_2 \ , \quad \theta_v = \frac{(y_2 - y_1)}{S} \tag{5.29}$$

$$m_v(a_2\ddot{y}_1 + a_1\ddot{y}_2) + c_{s1}(\dot{y}_1 - \dot{y}_3) + c_{s2}(\dot{y}_2 - \dot{y}_4) + k_{s1}(y_1 - y_3) + k_{s2}(y_2 - y_4) = 0 \tag{5.30}$$

$$I_v \frac{(-\ddot{y}_1 + \ddot{y}_2)}{S^2} - a_1 c_{s1}(\dot{y}_1 - \dot{y}_3) + a_2 c_{s2}(\dot{y}_2 - \dot{y}_4) - a_1 k_{s1}(y_1 - y_3) + a_2 k_{s2}(y_2 - y_4) = 0 \tag{5.31}$$

$$\begin{aligned} & m_1\ddot{y}_3 - c_{s1}(\dot{y}_1 - \dot{y}_3) - k_{s1}(y_1 - y_3) = -k_{t1}(y_1 - W(x_1,t) - r(x_1,t)) \\ & -c_{t1}(\dot{y}_1 - \dot{W}(x_1,t) - \dot{r}(x_1,t)) \end{aligned} \tag{5.32}$$

$$\begin{aligned} & m_2\ddot{y}_4 - c_{s2}(\dot{y}_2 - \dot{y}_4) - k_{s2}(y_2 - y_4) = -k_{t2}(y_2 - W(x_2,t) - r(x_2,t)) \\ & -c_{t2}(\dot{y}_2 - \dot{W}(x_2,t) - \dot{r}(x_2,t)) \end{aligned} \tag{5.33}$$

The equation of motion for the vehicle can also be written in terms of matrices as

$$[M_v]\{\ddot{Y}_v\} + [C_v]\{\dot{Y}_v\} + [K_v]\{Y_v\} = \{F(x,t)\} \tag{5.34}$$

$$\{F(x,t)\} = \begin{Bmatrix} 0 \\ 0 \\ -f_1(x,t) \\ -f_2(x,t) \end{Bmatrix} \tag{5.35}$$

where $[M_v],[C_v],[K_v]$ are, respectively, the mass, damping and stiffness matrices of the vehicle system; $\{Y_v\}$ is the response vector of the vehicle. The details of the matrices in Eq. (5.34) are

$$
[M_v] = \begin{bmatrix} m_v a_2^2 + \frac{I_v}{S^2} & m_v a_1 a_2 - \frac{I_v}{S^2} & 0 & 0 \\ m_v a_1 a_2 - \frac{I_v}{S^2} & m_v a_1^2 + \frac{I_v}{S^2} & 0 & 0 \\ 0 & 0 & m_1 & 0 \\ 0 & 0 & 0 & m_2 \end{bmatrix};
$$

$$
[C_v] = \begin{bmatrix} c_{s1} & 0 & -c_{s1} & 0 \\ 0 & c_{s2} & 0 & -c_{s2} \\ -c_{s1} & 0 & c_{s1} & 0 \\ 0 & -c_{s2} & 0 & c_{s2} \end{bmatrix}
$$

$$
[K_v] = \begin{bmatrix} k_{s1} & 0 & -k_{s1} & 0 \\ 0 & k_{s2} & 0 & -k_{s2} \\ -k_{s1} & 0 & k_{s1} & 0 \\ 0 & -k_{s2} & 0 & k_{s2} \end{bmatrix};
$$

$$
\{Y_v\} = \begin{Bmatrix} y_1 \\ y_2 \\ y_3 \\ y_4 \end{Bmatrix}; \tag{5.36}
$$

The contact forces $f_1^{RI}(x,t)$ and $f_2^{RI}(x,t)$ are

$$
f_1(x,t) = k_{t1}(y_1 - W(x_1,t) - r(x_1,t)) + c_{t1}(\dot{y}_1 - \dot{W}(x_1,t) - \dot{r}(x_1,t)) \tag{5.37}
$$

$$
f_2(x,t) = k_{t2}(y_2 - W(x_2,t) - r(x_2,t)) + c_{t2}(\dot{y}_2 - \dot{W}(x_2,t) - \dot{r}(x_2,t)) \tag{5.38}
$$

5.3.2 Equation of motion of the bridge

In this study, the bridge is modelled as a simply supported beam consisting of a number of elements. The equation of motion of the bridge is given by

$$
[M_b]\{\ddot{Y}_b\} + [C_b]\{\dot{Y}_b\} + [K_b]\{Y_b\} = [L_b(F(x,t))]\{F(x,t)\} \tag{5.39}
$$

The equations of motion for a bridge in the modal space can be written as

$$\ddot{q} + \chi\dot{q} + \Omega q = \Phi F \tag{5.40}$$

where

$$\chi = diag\left\{2\xi_i\omega_i\right\}; \qquad q = \begin{Bmatrix} q_1(t) \\ q_2(t) \\ \vdots \\ q_N(t) \end{Bmatrix}; \ \Omega = diag\left\{\omega_i^2\right\};$$

$$\Phi = \begin{bmatrix} \phi_1(x_1(t)) & \phi_1(x_2(t)) & \cdots & \phi_1(x_N(t)) \\ \phi_2(x_1(t)) & \phi_2(x_2(t)) & & \phi_2(x_N(t)) \\ \vdots & & \ddots & \\ \phi_N(x_1(t)) & \phi_N(x_2(t)) & & \phi_N(x_N(t)) \end{bmatrix};$$

$$F = \begin{Bmatrix} (m_v a_2 + m_1) g + k_{t1}(y_3 - W(x_1,t) - r(x_1,t)) + c_{t1}(\dot{y}_3 - \dot{W}(x_1,t) - \dot{r}(x_1,t)) \\ (m_v a_1 + m_2) g + k_{t2}(y_3 - W(x_1,t) - r(x_1,t)) + c_{t2}(\dot{y}_3 - \dot{W}(x_1,t) - \dot{r}(x_1,t)) \end{Bmatrix} \tag{5.41}$$

where $[M_b],[C_b],[K_b]$ are, respectively, the mass, damping and stiffness matrices of the bridge; $\{Y_b\}$ is the response vector of the bridge. $q_i(t)$ is the ith modal coordinate of the bridge; N is the number of the modes; ξ_i is the ith modal damping; $\phi_i(x_j(t))$ is the ith modal shape function at $x_j(t)$, which is determined from the eigenvalue and eigenfunction analysis; ω_i is the undamped circular frequency. $[L_b(F(x,t))]\{F(x,t)\}$ is the equivalent nodal load vector of the vehicle-bridge interaction forces.

5.3.3 Equation of motion of the vehicle-bridge interaction system

From Eqs.(5.34) and (5.39), the equation of motion of the vehicle-bridge interaction system can be developed as

$$[M(t)]\{\ddot{Y}(t)\}+[C(t)]\{\dot{Y}(t)\}+[K(t)]\{Y(t)\}=\{P(t)\} \tag{5.42}$$

where

$$M(t)=\begin{bmatrix} I & \\ & M_v \end{bmatrix};\ C_t=\begin{bmatrix} c_{t1} & 0 \\ 0 & c_{t2} \end{bmatrix};\ K_t=\begin{bmatrix} k_{t1} & 0 \\ 0 & k_{t2} \end{bmatrix};$$

$$K(t)=\begin{bmatrix} \Omega+M_n\Phi K_t\Phi^T+M_n v\Phi' C_t\Phi^T & 0 & -M_n\Phi K_t \\ 0 & K_s & -K_s \\ -K_t\Phi^T-vC_t(\Phi')^T & -K_s & K_s+K_t \end{bmatrix};$$

$$C(t)=\begin{bmatrix} \chi+M_n\Phi C_t\Phi^T & 0 & -M_n\Phi C_t \\ 0 & C_s & -C_s \\ -C_t\Phi^T & -C_s & C_s+C_t \end{bmatrix};\ \{P(t)\}=\begin{Bmatrix} M_n\Phi \\ 0 \\ 0 \end{Bmatrix}\cdot\{P_g(t)\}$$

$$Y(t)=\begin{bmatrix} q_1 & q_2 & \cdots & q_N & y_1 & y_2 & y_3 & y_4 \end{bmatrix} \tag{5.43}$$

where $M(t), C(t), K(t)$ represent the coupled mass, stiffness and damping matrices respectively. $\{\ddot{Y}(t)\}, \{\dot{Y}(t)\}, \{Y(t)\}$ are the nodal acceleration, velocity and displacement vectors of the bridge deck respectively, and $\{P(t)\}$ is the equivalent nodal load vector from the bridge–vehicle interaction force .

In order to account for uncertainties uncertainty in the bridge, the equation of motion governing the transverse or vertical vibration of the bridge under the moving vehicle with uncertainties in the system parameters can be written as

$$\left[M(\vec{a}^R,\vec{b}^I,t)\right]\left\{\ddot{Y}^{RI}(\vec{a}^R,\vec{b}^I,t)\right\}+\left[C(\vec{a}^R,\vec{b}^I,t)\right]\left\{\dot{Y}^{RI}(\vec{a}^R,\vec{b}^I,t)\right\}$$

$$+\left[K(\vec{a}^R,\vec{b}^I,t)\right]\left\{Y^{RI}(\vec{a}^R,\vec{b}^I,t)\right\}=\left\{P(\vec{a}^R,\vec{b}^I,t)\right\} \tag{5.44}$$

$M(\vec{a}^R,\vec{b}^I,t)$, $C(\vec{a}^R,\vec{b}^I,t)$, $K(\vec{a}^R,\vec{b}^I,t)$ are the stochastic mass, damping and stiffness matrices of the bridge and they can be further expressed as

$$M(\vec{a}^R,\vec{b}^I,t)=\left[M(\bar{a},\vec{b}^c)\right]+\sum_{j=1}^{m}\frac{\partial\left[\mathrm{M}(\bar{a},\vec{b}^c)\right]}{\partial b_j^I}\Delta b_j^I$$
$$+\sum_{i=1}^{n}\left\{\frac{\partial\left[M(\bar{a},\vec{b}^c)\right]}{\partial a_i^R}+\sum_{j=1}^{m}\frac{\partial^2\left[M(\bar{a},\vec{b}^c)\right]}{\partial a_i^R\partial b_j^I}\Delta b_j^I\right\}\left(a_i^R-\bar{a}_i\right)$$

$$=M_b+\Delta M \tag{5.45}$$

$$C(\vec{a}^R,\vec{b}^I,t)=\left[C(\bar{a},\vec{b}^c)\right]+\sum_{j=1}^{m}\frac{\partial\left[C(\bar{a},\vec{b}^c)\right]}{\partial b_j^I}\Delta b_j^I$$
$$+\sum_{i=1}^{n}\left\{\frac{\partial\left[C(\bar{a},\vec{b}^c)\right]}{\partial a_i^R}+\sum_{j=1}^{m}\frac{\partial^2\left[C(\bar{a},\vec{b}^c)\right]}{\partial a_i^R\partial b_j^I}\Delta b_j^I\right\}\left(a_i^R-\bar{a}_i\right)$$

$$=C_b+\Delta C \tag{5.46}$$

$$K(\vec{a}^R,\vec{b}^I,t)=\left[K(\bar{a},\vec{b}^c)\right]+\sum_{j=1}^{m}\frac{\partial\left[K(\bar{a},\vec{b}^c)\right]}{\partial b_j^I}\Delta b_j^I$$
$$+\sum_{i=1}^{n}\left\{\frac{\partial\left[K(\bar{a},\vec{b}^c)\right]}{\partial a_i^R}+\sum_{j=1}^{m}\frac{\partial^2\left[K(\bar{a},\vec{b}^c)\right]}{\partial a_i^R\partial b_j^I}\Delta b_j^I\right\}\left(a_i^R-\bar{a}_i\right)$$

$$=K_b+\Delta K \tag{5.47}$$

$\Delta M,\Delta C,\Delta K$ are the uncertain components of the system mass, damping and stiffness matrices.

In addition, the Rayleigh damping is assumed as

$$C = c_a M + c_b K \tag{5.48}$$

where c_a and c_b are constants.

Using the strategy of random interval perturbation method, mean value and variance of the bridge dynamic response can be obtained as

$$\mu\left(Y(\vec{a}^R,\vec{b}^I,t)\right) = E\left(Y\left(\vec{a}^R,\vec{b}^I,t\right)\right) = \left[Y(\bar{\vec{a}},\vec{b}^c)\right] + \sum_{j=1}^{m}\frac{\partial\left[Y(\bar{\vec{a}},\vec{b}^c)\right]}{\partial b_j^I}\Delta b_j^I \tag{5.49}$$

$$Var\left(Y\left(\vec{a}^R,\vec{b}^I,t\right)\right) = E\left[\left(Y\left(\vec{a}^R,\vec{b}^I,t\right) - \mu\left(Y\left(\vec{a}^R,\vec{b}^I,t\right)\right)\right)^2\right]$$

$$\sum_{i=1}^{n}\sum_{k=1}^{n}\left\{\left.\frac{\partial Y\left(\vec{a}^R,\vec{b}^I,t\right)}{\partial \vec{a}_i^{\,R}}\right|_{\bar{\vec{a}},\vec{b}^c} + \sum_{j=1}^{m}\left\{\left.\frac{\partial^2\left[Y(\bar{\vec{a}},\vec{b}^c)\right]}{\partial a_i^R\partial b_j^I}\right|_{\bar{\vec{a}},\vec{b}^c}\right\}\Delta b_j^I\right\}$$

$$\left\{\left.\frac{\partial Y\left(\vec{a}^R,\vec{b}^I,t\right)}{\partial \vec{a}_k^{\,R}}\right|_{\bar{\vec{a}},\vec{b}^c} + \sum_{j=1}^{m}\left\{\left.\frac{\partial^2\left[Y(\bar{\vec{a}},\vec{b}^c)\right]}{\partial a_k^R\partial b_j^I}\right|_{\bar{\vec{a}},\vec{b}^c}\right\}\Delta b_j^I\right\}Cov\left(\vec{a}_i^{\,R},\vec{a}_k^{\,R}\right) \tag{5.48}$$

From above equations, mean value and variance of stochastic interval dynamic response can be evaluated by the first and second derivatives of dynamic response with respect to random and interval variables.

5.4 The Procedure of Implementation

The dynamic response of a bridge subjects to moving a vehicle can be calculated by the following procedure:

Step 1. Calculate the random/interval mass, stiffness and damping matrices of the vehicle and bridge.

Step 2. Calculate the random frequencies (ω_i) and mode shapes ($\phi(\mathrm{x}_j(\mathrm{t}))$) of the bridge.

Step 3. Calculate the random interval displacement response of bridge using the Newmark-β method.

Step 4. Calculate the interval mean value and standard deviation of the random interval displacement response of bridge.

5.5 Numerical Simulations

In this chapter, bridge parameters are considered as Gaussian random variables and vehicle parameters are treated as interval variables. Their nominal values (mean values or midpoints) taken in the numerical simulation are listed in Tables 5.1 and 5.2. The unit of the bridge displacement response is meter. The beam elements are used and the bridge is divided into 50 equal segments/elements. The vehicle parameters are typical for a lightly damped passenger car [119].

Table 5.1 Parameters of the vehicle model

Description	Notation	Value
Sprung mass	${m_1}^c$	$1000kg$
	${m_2}^c$	$1500kg$
Unsprung mass	${m_v}^c$	$17800kg$
Suspension stiffness	k_{s1}	$2.5 \times 10^6 N/m$
	k_{s2}	$4.2 \times 10^6 N/m$
Tyre stiffness	k_{t1}	$5.2 \times 10^6 N/m$
	k_{t2}	$7.2 \times 10^6 N/m$
Suspension damping	c_{s1}	$9000N/m$
	c_{s2}	$9600N/m$
Tyre damping	c_{t1}	$920N/m$
	c_{t2}	$960N/m$

Table 5.2 Parameters of the bridge model

Description	Notation	Value
Length of the bridge	L	40m
Moment of inertia	I	$0.16m^4$
Damping ratio	ζ	0.05
Young's modulus	E	3.3 × 1010N/m2
Mass density	ρ	7800 kg/m3

Similar as last chapter, the effect of each parameter (masses of the vehicle, elastic modulus and inertial moment of the area as well as the mass per unit of te bridge and so on) on the dynamic response of vehicle-bridge interaction system are analysed. In addition, uncertainties of the parameters in the vehicle-bridge interaction system are considered simultaneously. In the current example, the road surface roughness is not considered. The following properties of the bridge are use in the simulation: damping ratio ζ = 0.05 for all modes; Gaussian random variables are employed to model all bridge parameters (elastic modulus E, mass density ρ and second moment of inertia$I$). The coefficients of variation of E, I , ρ are all assumed as 0.05 or 0.02, respectively. All parameters of vehicle are assumed as interval variables and the interval change ratios (ICR) are considered as 0.1 or 0.2, respectively. The vehicle is assumed to move on the bridge with two different velocities, $v = 5m/s$ and $v = 10m/s$, which are taken into account to investigate the influence of vehicle velocity on the bridge response.

The mean values of the bridge displacement response under moving vehicle with $5m/s$ at its mid-span are given in Figures 5.2-5.8, respectively. A special case of random interval perturbation method is shown in Figure 5.2 when all system parameters are assumed as random variables. From Figure 5.2, it can be obviously observed that the random variables of system parameters do not affect the mean value of the random interval structural response. In other words, the mean value of structural response is not an interval but a deterministic value if system structural parameters and loads are random variables. However, the mean value of bridge response is an interval if the structural has interval parameters or loads. The interval width of structural response depends on the dispersal degree of the interval parameters.

The mean values of bridge displacement shown in Figures 5.3-5.7 consider the individual system parameter as a random variable in turn. From these figures, it can be easily obtained that the changes of vehicle masses m_1 and m_2 produce the similar effect on the bridge response. The effects caused by suspension (unsprung) masses m_1 and m_2 are smaller than that produced by the sprung mass m_v as their upper bounds and lower bounds are smaller when the interval change ratios of these three masses are same. Figures 5.7 and 5.8 denote the displacement response of bridge when uncertainties of all parameters of system are included. It is obvious that the interval width of bridge response is much larger than those when only one uncertain parameter is addressed.

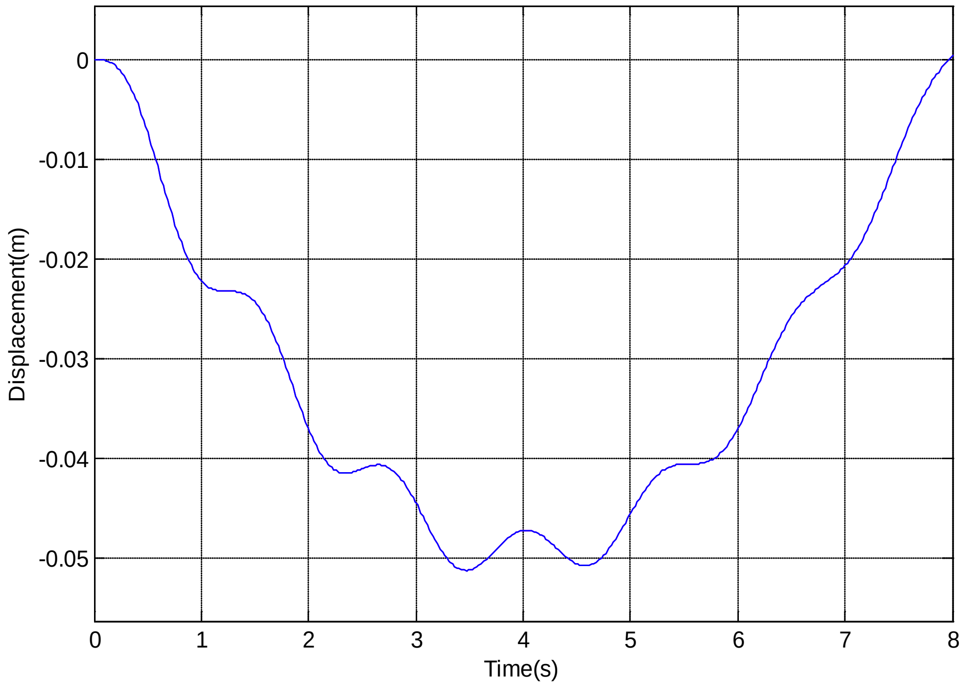

Figure 5.2 Mean value of displacement response of bridge at mid-span

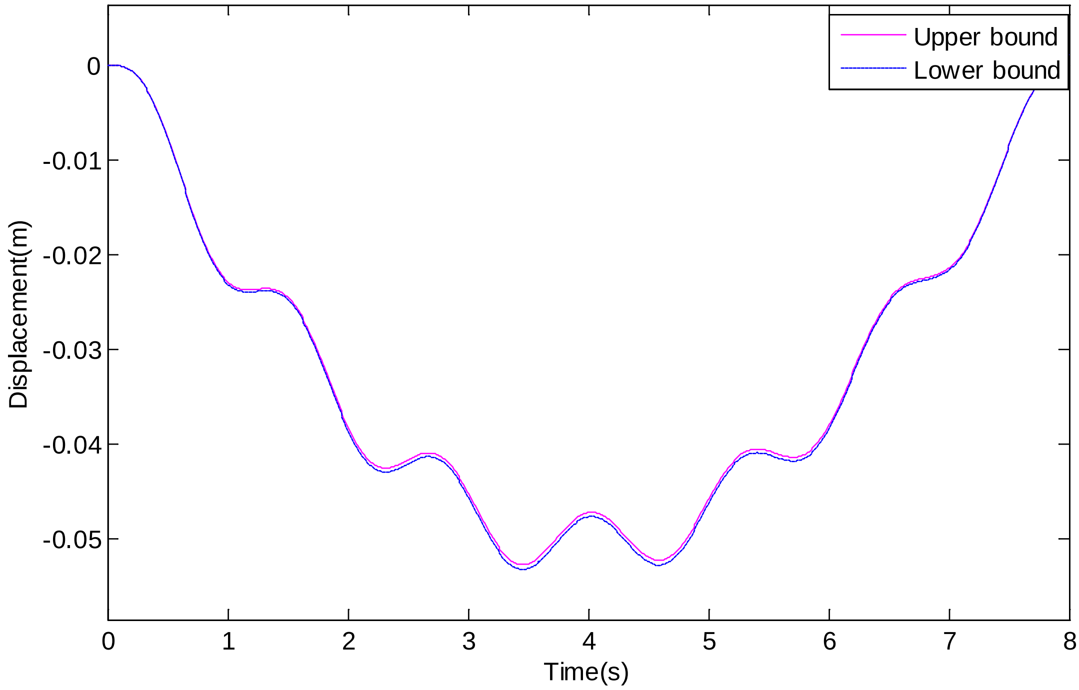

Figure 5.3 Displacement response of bridge at mid-span

(COV(ρ^R, E^R, I^R)=0.05, ICR(m_1^I)=0.1, $v = 5m/s$)

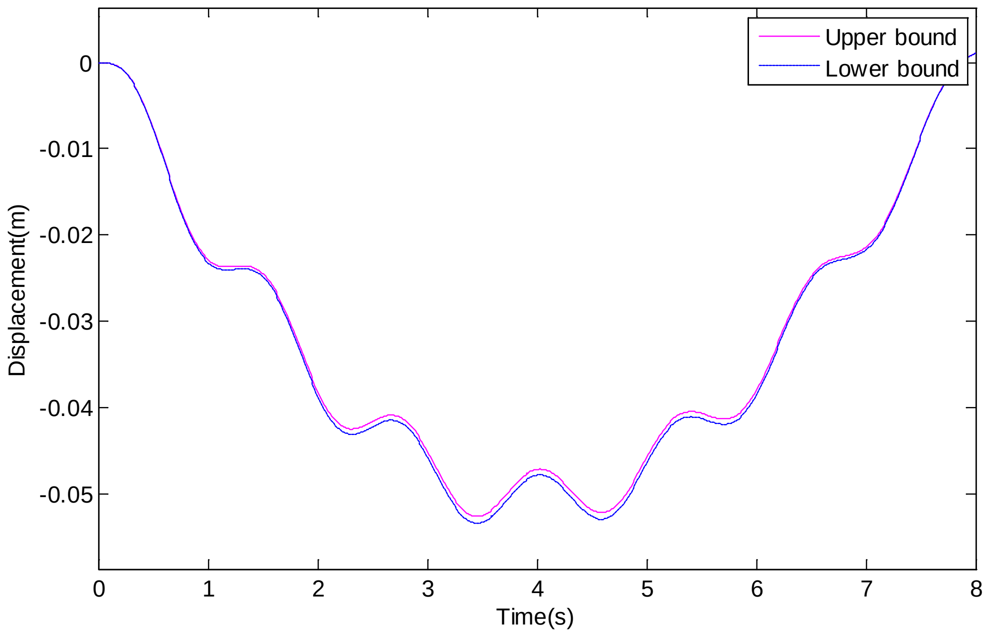

Figure 5.4 Displacement response of bridge at mid-span

(COV(ρ^R, E^R, I^R)=0.05, ICR(m_2^I)=0.1, $v = 5m/s$)

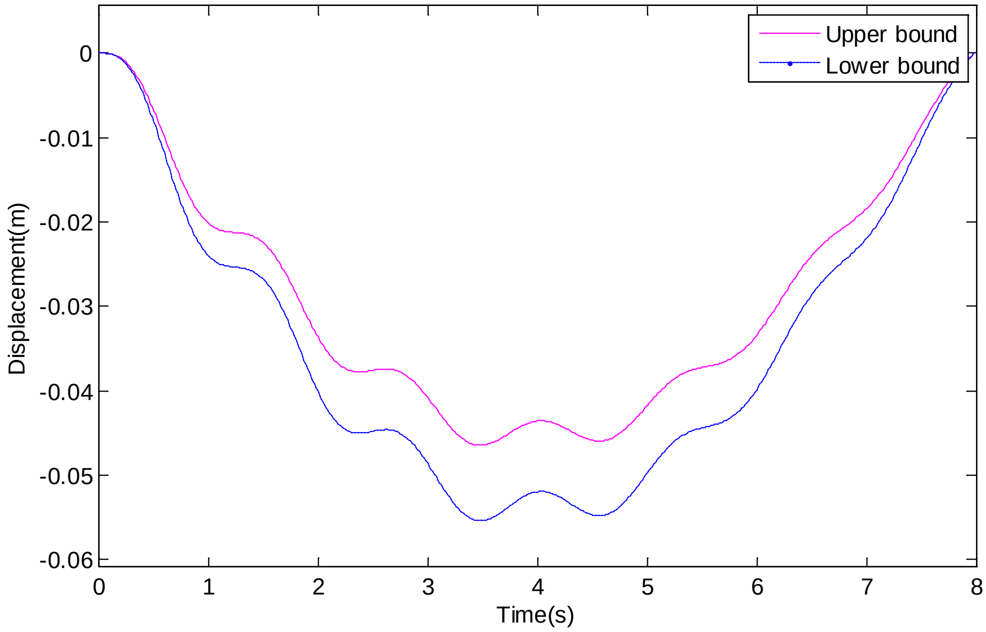

Figure 5.5 Displacement response of bridge at mid-span

(COV(ρ^R, E^R, I^R)=0.05, ICR(m_v^I)=0.1, $v = 5m/s$)

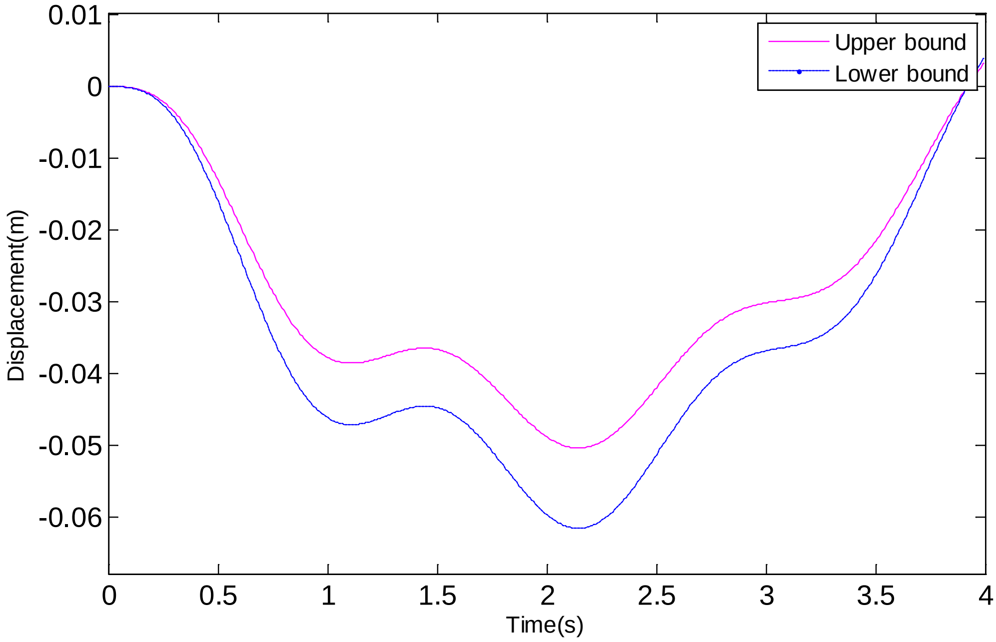

Figure 5.6 Displacement response of bridge at mid-span

(COV(ρ^R, E^R, I^R)=0.05, ICR(m_1^I, m_2^I, m_v^I)=0.1, $v = 10m/s$)

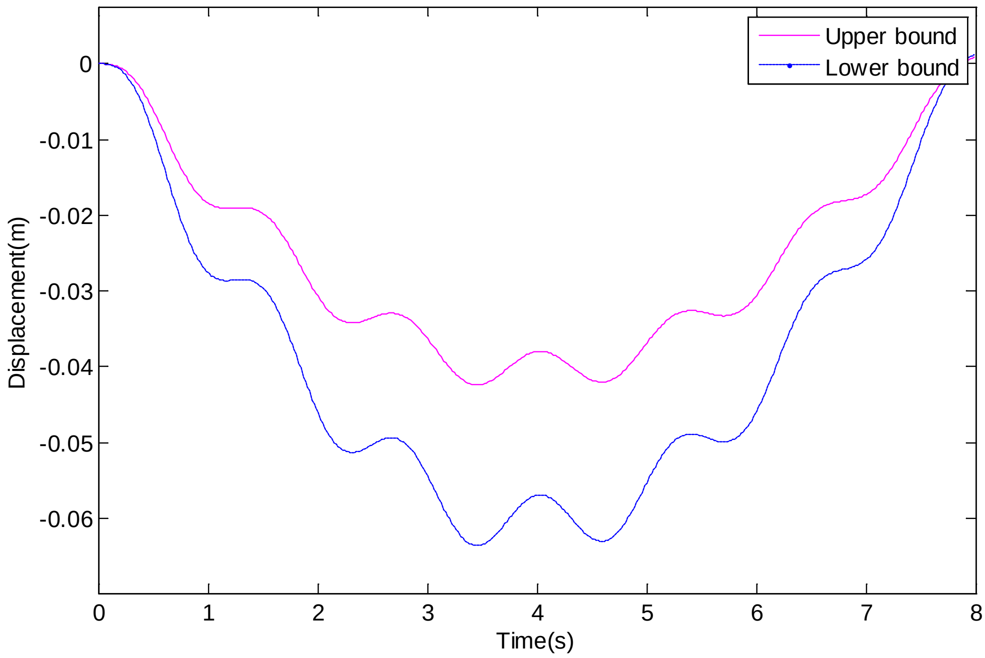

Figure 5.7 Displacement response of bridge at mid-span

(COV(ρ^R, E^R, I^R)=0.05, ICR(m_1^I, m_2^I, m_v^I)=0.2, $v = 5m/s$)

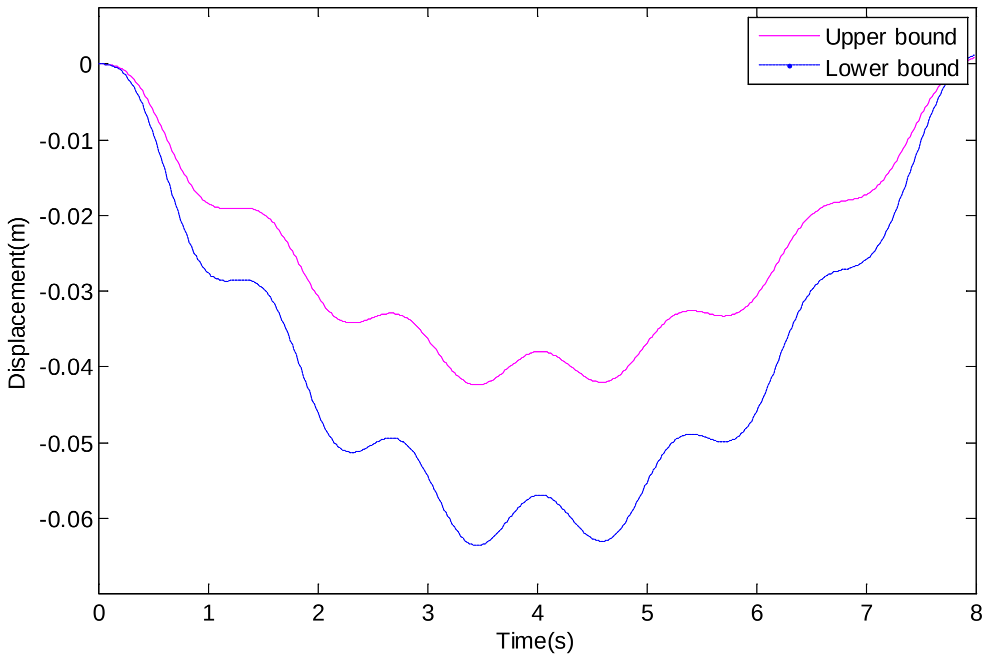

Figure 5.8 Displacement response of bridge at mid-span

(COV(ρ^R, E^R, I^R)=0.02, ICR(m_1^I, m_2^I, m_v^I)=0.2, $v = 5m/s$)

The standard deviation (SD) of the vertical displacement response of bridge at midpoint are shown in Figures 5.9-5.19 to demonstrate the variations and intervals of the bridge response which are produced by the uncertainties of system parameters. Figures 5.9-5.13 show the standard deviation of bridge response when vehicle parameters are considered as interval variables and the individual bridge parameter is assumed as a random variable.

From Figures 5.9 and 5.10, it can be observed that the interval width of the standard deviation of the random interval bridge response becomes larger when the change ranges of interval parameters. From Figure 5.10 and Figure 5.11, it can be easily obtained that Young’s modulus and moment of inertia of the bridge produce the same upper bounds on the bridge response, which is greater than that caused by the density shown in Figure 5.12. Figures 5.13-5.16 show the standard deviation of bridge displacement when all system parameters are treated as uncertain variables and the velocity of the vehicle is 5m/s. In order to investigate the effect of vehicle velocity to bridge response, the velocity of vehicle is increased from 5m/s to 10m/s and the results are shown in Figure 5.17.

From Figures 5.13-5.17, it can be obtained that the interval width of the standard deviation of the random interval bridge response is directly proportional to the dispersal degree of interval and random variables and vehicle velocity. In summary, it can be easily observed that the bridge response is more sensitive to the change of its own parameters. In addition, the upper bound and interval width of the standard deviation of the random interval bridge displacement will increase when the vehicle velocity increases.

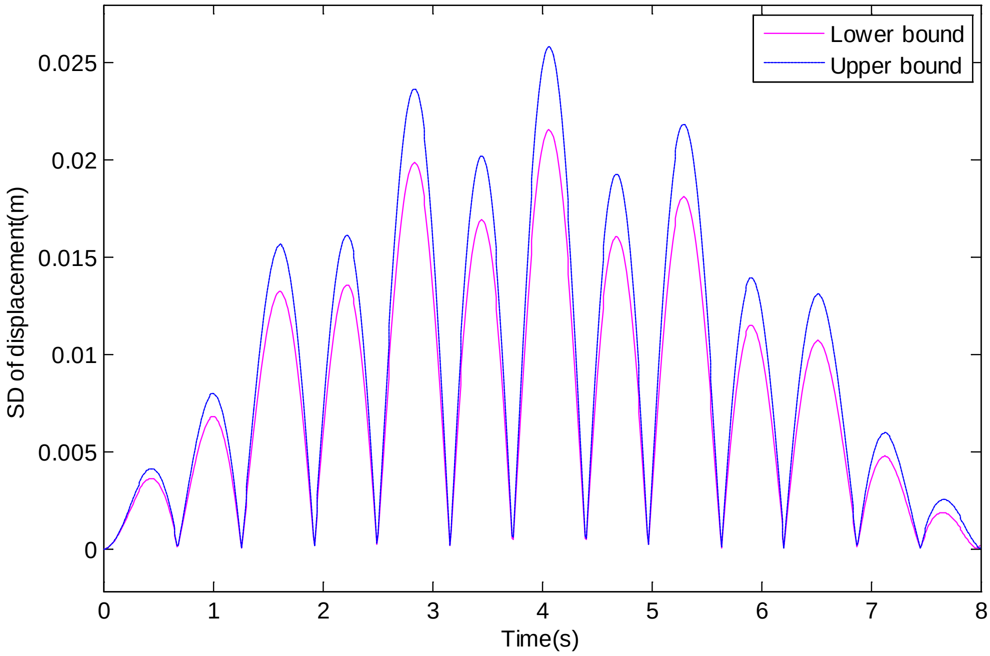

Figure 5.9 Standard deviation of bridge displacement at mid-span

(COV(E^R)=0.05, ICR(m_1^I, m_2^I, m_v^I)=0.1, $v = 5m/s$)

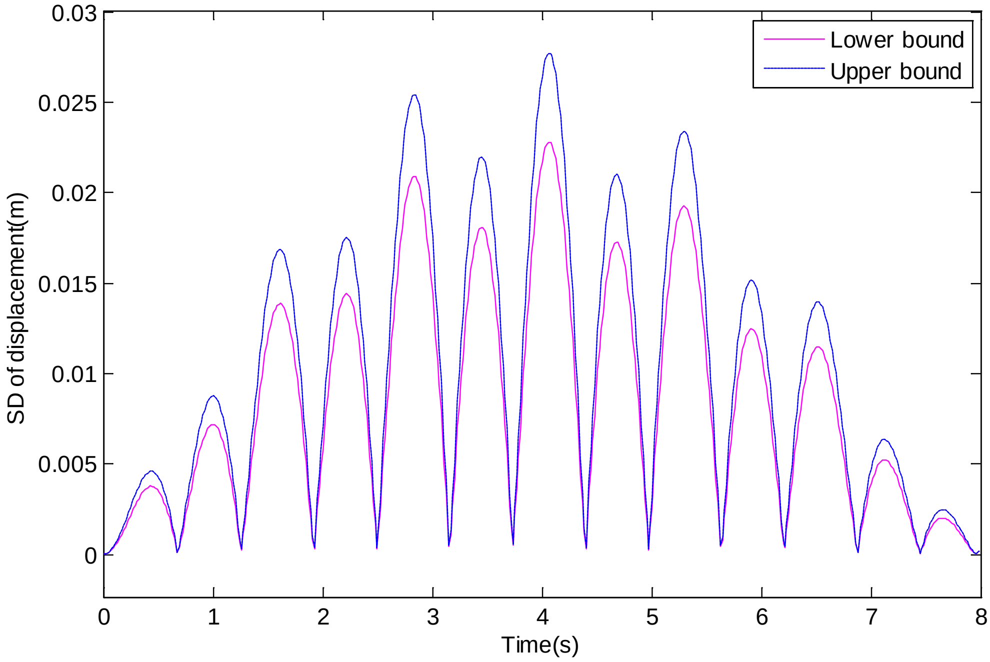

Figure 5.10 Standard deviation of bridge displacement at mid-span

(COV(E^R)=0.05, ICR(m_1^I, m_2^I, m_v^I)=0.2, $v = 5m/s$)

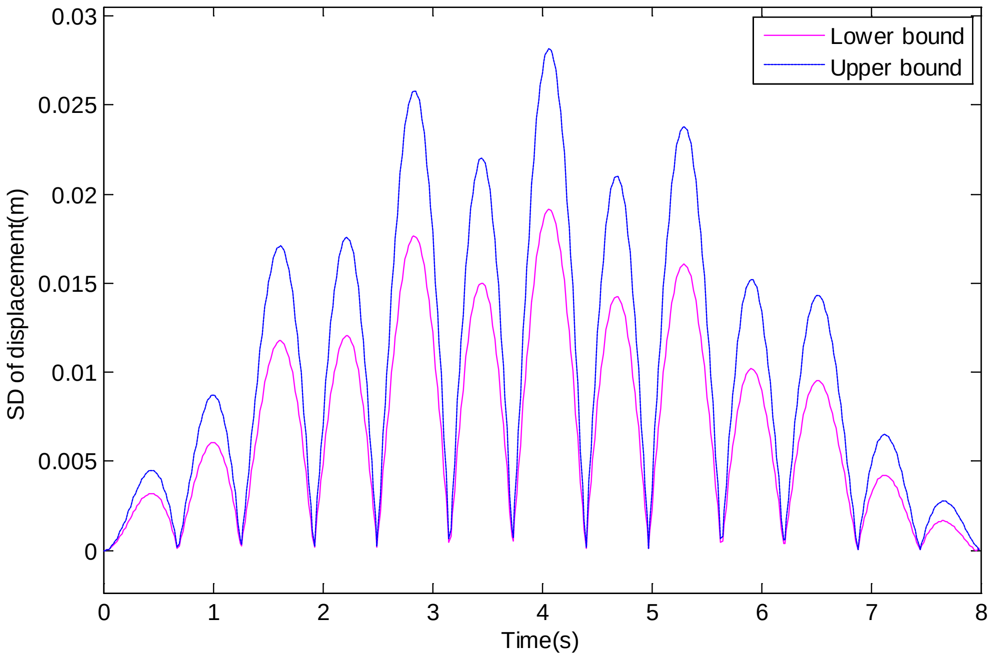

Figure 5.11 Standard deviation of bridge displacement at mid-span

(COV(I^R)=0.05, ICR(m_1^I, m_2^I, m_v^I)=0.2, $v = 5m/s$)

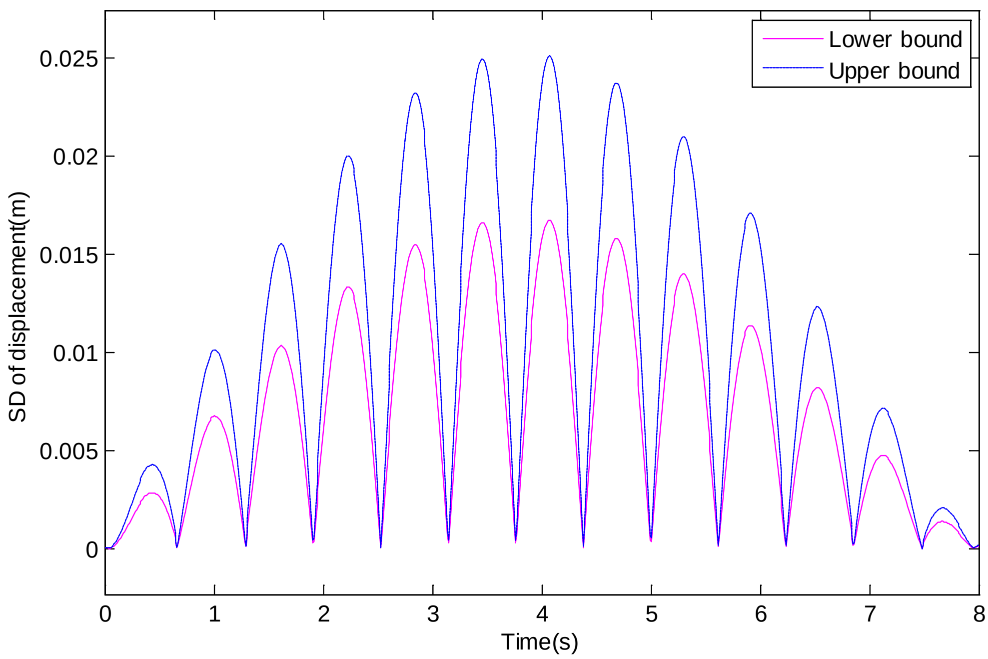

Figure 5.12 Standard deviation of bridge displacement at mid-span

(COV(ρ^R)=0.05, ICR(m_1^I, m_2^I, m_v^I)=0.2, $v = 5m/s$)

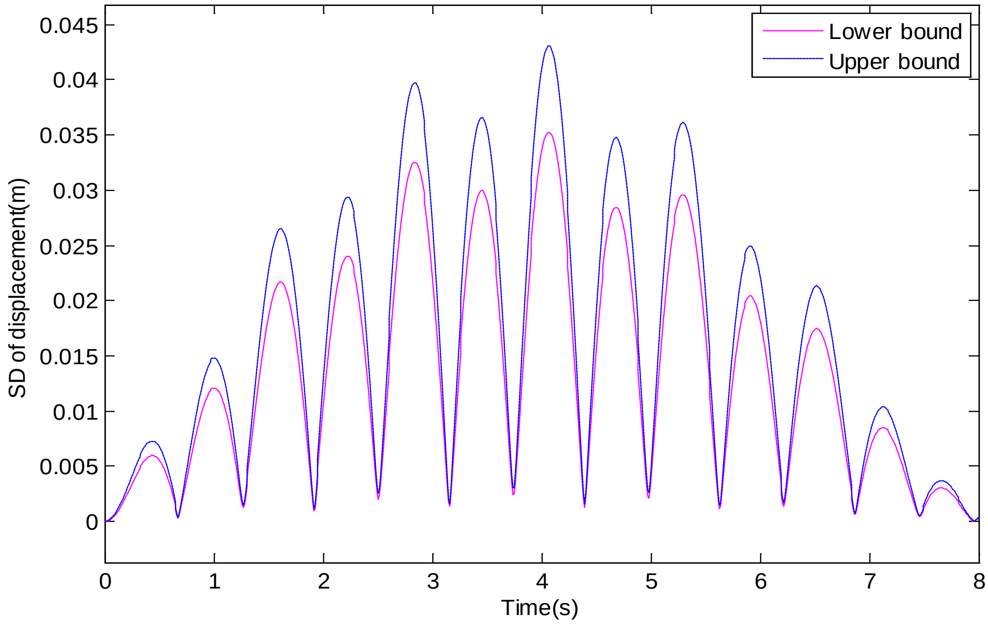

Figure 5.13 Standard deviation of bridge displacement at mid-span

(COV(ρ^R, E^R, I^R)=0.05, ICR(m_1^I, m_2^I, m_v^I)=0.1, $v = 5m/s$)

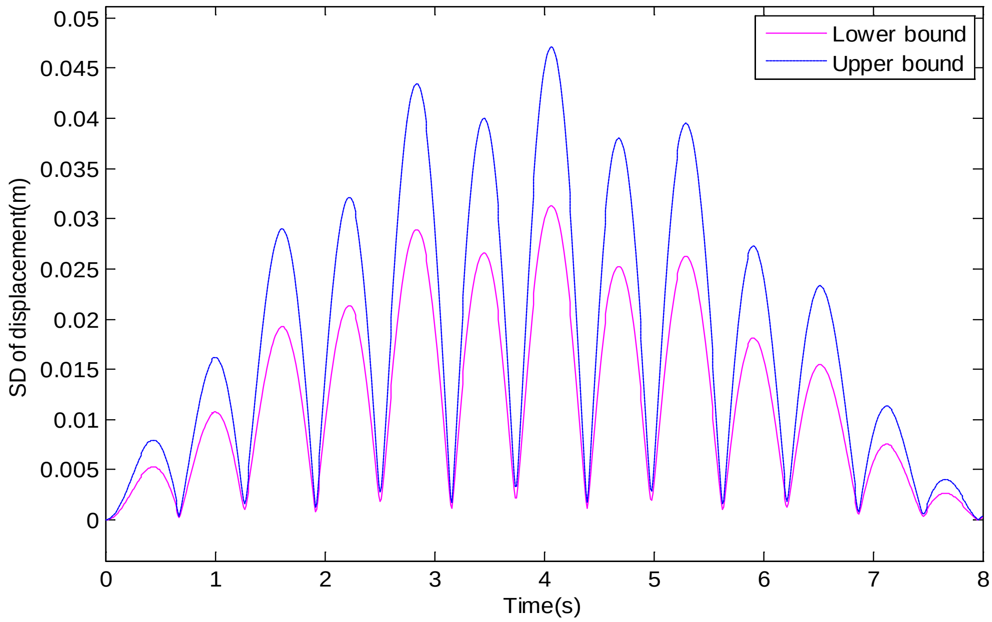

Figure 5.14 Standard deviation of bridge displacement at mid-span

(COV(ρ^R, E^R, I^R)=0.05, ICR(m_1^I, m_2^I, m_v^I)=0.2, $v = 5m/s$)

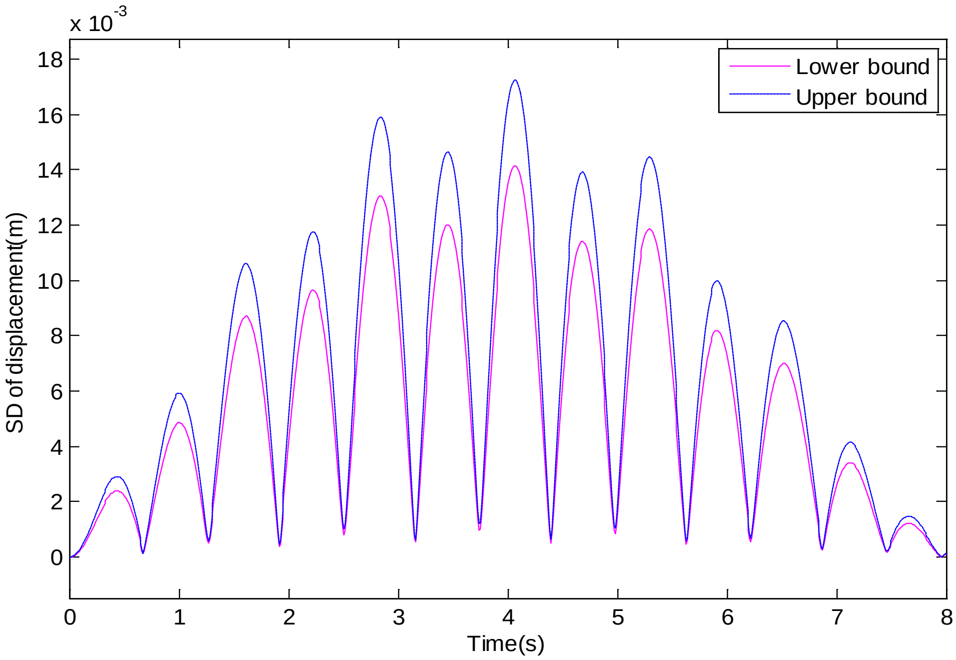

Figure 5.15 Standard deviation of bridge displacement at mid-span

(COV(ρ^R, E^R, I^R)=0.02, ICR(m_1^I, m_2^I, m_v^I)=0.1, $v = 5m/s$)

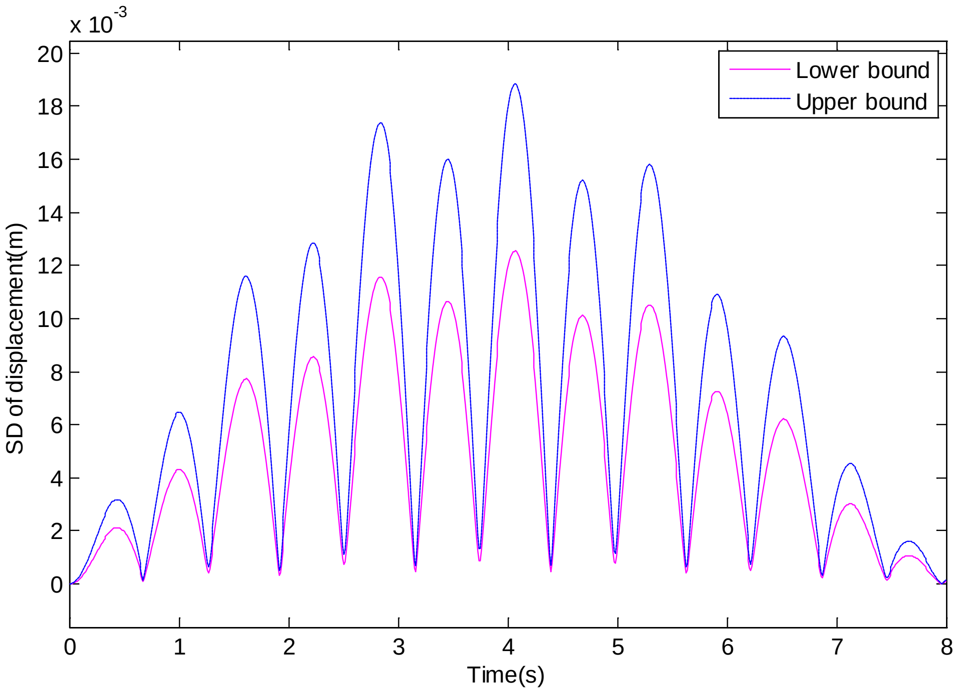

Figure 5.16 Standard deviation of bridge displacement at mid-span

(COV(ρ^R, E^R, I^R)=0.02, ICR(m_1^I, m_2^I, m_v^I)=0.2, $v = 5m/s$)

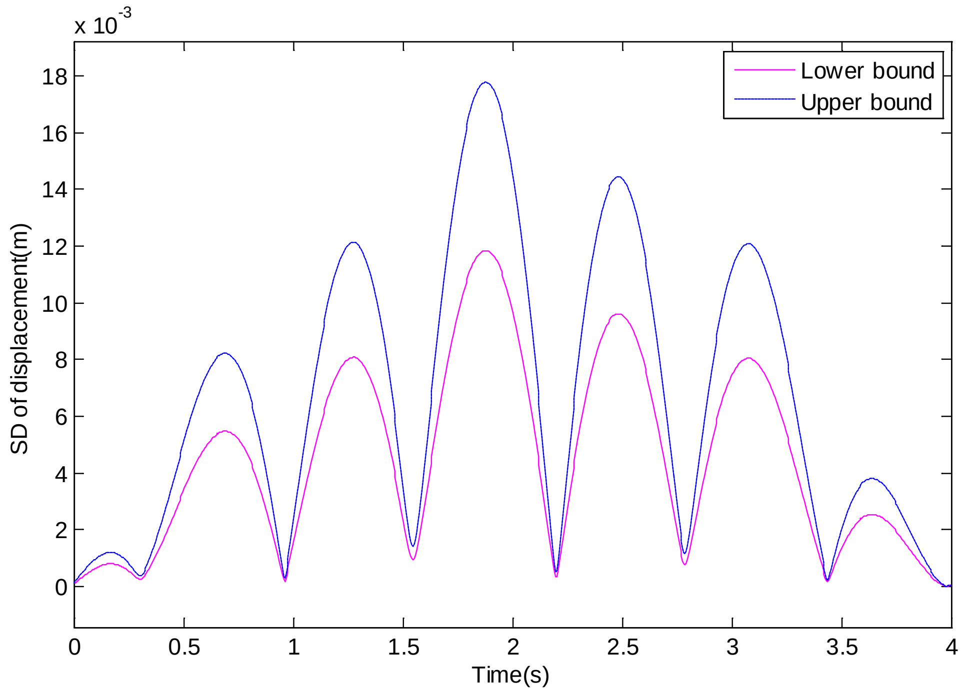

Figure 5.17 Standard deviation of bridge displacement at mid-span

(COV(ρ^R, E^R, I^R)=0.02, ICR(m_1^I, m_2^I, m_v^I)=0.2, $v = 10m/s$)

Table 5.3 Comparison of mean values of bridge displacement between RIPM and HSM (COV (E) =0.05, ICR(all)=0.2, v=5m/s)

Time	Upper bound			Lower bound		
	RIPM	HSM	Difference	RIPM	HSM	Difference
1	0.02673	0.02679	0.22%	0.01795	0.01791	0.22%
2	0.04439	0.04463	0.54%	0.02958	0.02946	0.42%
3	0.05327	0.05353	0.49%	0.035531	0.03549	0.12%
4	0.05757	0.05768	0.19%	0.037821	0.03768	0.37%
5	0.0546	0.05467	0.13%	0.036439	0.0361	0.94%
6	0.04428	0.04436	0.18%	0.029516	0.02929	0.77%
7	0.02489	0.02506	0.67%	0.016376	0.01625	0.78%

Table 5.4 Comparison of standard deviations of bridge displacement between RIMM and HSM (COV(E)=0.05, ICR(all)=0.2, v=10m/s)

Time	Lower bound			Upper bound		
	RIMM	HSM	Difference	RIMM	HSM	Difference
0.5	0.018461	0.018138	1.78%	0.012218	0.012329	0.90%
1	0.052795	0.052456	0.65%	0.035042	0.035626	1.64%
1.5	0.048893	0.048436	0.94%	0.032506	0.033259	2.26%
2	0.068011	0.064706	5.11%	0.045772	0.046589	1.75%
2.5	0.056501	0.054601	3.48%	0.037383	0.038879	3.85%
3	0.039919	0.039739	0.45%	0.026849	0.027017	0.62%
3.5	0.031141	0.030011	3.76%	0.020996	0.021511	2.39%

Table 5.5 Comparison of standard deviation of bridge displacement between RIMM and HSM (Cov(E)=0.02, ICR(all)=0.2, v=5m/s)

Time	Upper bound			Lower bound		
	RIMM	HSM	Difference	RIMM	HSM	Difference
1	0.007967	0.008028	0.76%	0.00291	0.00288	1.24%
2	0.00803	0.008081	0.63%	0.00986	0.00977	0.95%
3	0.015356	0.015436	0.52%	0.00519	0.00517	0.43%
4	0.02546	0.025946	1.87%	0.02022	0.01992	1.50%
5	0.007083	0.007112	0.41%	0.01365	0.01358	0.55%
6	0.012198	0.012432	1.88%	0.00449	0.00443	1.45%
7	0.004809	0.004891	1.67%	0.00658	0.00651	1.04%

Table 5.6 Comparison of standard deviation of bridge displacement between RIMM and HSM (Cov(I)=0.02, ICR(all)=0.2, v=5m/s)

Time	Upper bound			Lower bound		
	RIMM	HSM	Difference	RIMM	HSM	Difference
1	0.007965	0.008028	0.78%	0.00656	0.00651	0.74%
2	0.008043	0.008081	0.47%	0.00455	0.00443	2.71%
3	0.015357	0.015436	0.51%	0.01362	0.01358	0.28%
4	0.025446	0.025946	1.93%	0.02030	0.01992	1.93%
5	0.00708	0.007112	0.45%	0.00519	0.00517	0.52%
6	0.012195	0.012432	1.91%	0.00987	0.00977	1.02%
7	0.004809	0.004891	1.68%	0.00290	0.00288	0.78%

Table 5.7 Comparison of standard deviation of bridge displacement between RIMM and HSM (Cov(ρ)=0.05, ICR(all)=0.2, v=5m/s)

Time	Upper bound			Lower bound		
	RIMM	HSM	Difference	RIMM	HSM	Difference
1	0.009065	0.009087	0.24%	0.0077404	0.007706	0.44%
2	0.009028	0.009087	0.65%	0.0067994	0.006596	3.08%
3	0.014476	0.014535	0.40%	0.0114549	0.011345	0.96%
4	0.021905	0.022019	0.52%	0.0181409	0.018014	0.70%
5	0.000658	0.000666	1.15%	0.0005096	0.000508	0.27%
6	0.014426	0.014483	0.39%	0.0115539	0.011426	1.12%
7	0.005165	0.005202	0.70%	0.004125	0.004101	0.58%

Table 5.8 Comparison of standard deviation of bridge displacement between RIMM and HSM (Cov(all)=0.05, ICR(all)=0.2, v=5m/s)

Time	Upper bound			Lower bound		
	RIMM	HSM	Difference	RIMM	HSM	Difference
1	0.016003	0.016132	0.80%	0.0107009	0.010522	1.70%
2	0.015003	0.015187	1.21%	0.0080997	0.00803	0.87%
3	0.03061	0.030966	1.15%	0.0204054	0.020021	1.92%
4	0.044417	0.046014	3.47%	0.0297097	0.028797	3.17%
5	0.004698	0.004707	0.19%	0.002397	0.002352	1.91%
6	0.024307	0.024856	2.21%	0.0164035	0.01603	2.33%
7	0.0085	0.008585	0.99%	0.0058987	0.005814	1.46%

Table 5.9 Comparison of standard deviation of bridge displacement between RIMM and HSM (Cov(all)=0.02, ICR(all)=0.2, v=5m/s)

Time	Upper bound			Lower bound		
	RIMM	HSM	Difference	RIMM	HSM	Difference
1	0.006443	0.006515	1.10%	0.0042416	0.004203	0.92%
2	0.005603	0.005676	1.30%	0.003481	0.003402	2.33%
3	0.011647	0.011984	2.81%	0.0084848	0.008446	0.46%
4	0.017772	0.017998	1.26%	0.0118874	0.011719	1.44%
5	0.00196	0.001969	0.45%	0.0009991	0.000987	1.23%
6	0.009846	0.009978	1.33%	0.0064032	0.006326	1.22%
7	0.003401	0.003418	0.50%	0.0021601	0.002082	3.77%

Table 5.10 Comparison of standard deviation of bridge displacement between RIMM and HSM (Cov(all)=0.05, ICR(all)=0.1, v=5m/s)

Time	Upper bound			Lower bound		
	RIMM	HSM	Difference	RIMM	HSM	Difference
1	0.014727	0.014987	1.74%	0.0118905	0.011829	0.52%
2	0.012988	0.013063	0.57%	0.0097861	0.009479	3.24%
3	0.028085	0.028761	2.35%	0.0214058	0.020914	2.35%
4	0.041169	0.041653	1.16%	0.033849	0.033185	2.00%
5	0.003839	0.003898	1.53%	0.003656	0.003577	2.22%
6	0.022687	0.023527	3.57%	0.0182951	0.01803	1.47%
7	0.007773	0.007988	2.69%	0.0061264	0.006091	0.58%

Similarly as last chapter, a hybrid simulation method (HSM) is employed to verify the accuracy of the accuracy of the random interval perturbation method (RIPM) presented herein. These hybrid simulations are implemented in MATLAB platform. The results obtained by the HSM are given in Tables 5.3-5.10.

A comparison of the results generated by the RIPM and HSM and the differences of mean values and standard deviations of bridge displacement are listed in Tables 5.3-5.10. From Table 5.3, it is easily obtained that the mean values, calculated by RIPM and HSM, are very closed to each other, The maximum difference of mean value is only 0.91% while the coefficients of variation for all random parameters are 0.05, the interval change ratios of all interval variables are 0.2 and the vehicle velocity is 5m/s. Tables 5.4-5.10 show the standard deviations of bridge displacement while the parameters of the vehicle-bridge interaction system are considered as uncertain variables. From these tables, the maximum difference of the standard deviation is 5.11%, while the coefficients of variation for all random parameters are 0.05, the interval change ratios of all interval parameters are 0.2 and the velocity of vehicle is 10m/s. The difference can be accepted because the hybrid simulation times used in this study are not enough to provide convergent results which have been mentioned in previous chapter. Generally, the accuracy of these results is satisfactory in real engineering. The presented random interval perturbation method has much less computational work than the simulation method, especially for complex structure. It can be concluded that the proposed method for vehicle-bridge interaction system with uncertainties can maintain a satisfactory accuracy.

5.6 Conclusions

In this chapter, the finite element model has been employed to describe vehicle-bridge interaction systems. The nondeterministic dynamic response of bridge subjects to moving vehicle with uncertain system parameters is investigated by using the random interval perturbation method. The uncertainties of vehicle are modeled as interval variables and the parameters of bridge are considered as randomness. The expressions for calculating the bounds of expectation and variance of bridge response have been derived by using the random interval perturbation method. Using these formulations, the upper and lower bounds can be very easily obtained. The effects of random and interval parameters on bridge response are also studied.

The random interval perturbation method has good accuracy even the vehicle-bridge interaction system has different type of uncertain parameters simultaneously. The random interval perturbation method will be further developed to investigate the non-deterministic dynamic behaviors of a bridge under multiple moving vehicles based on finite element model, and this method will also be applied to other engineering structural system. In addition, optimization methods also can be used to obtain more accuracy result for some smart structure.

Chapter 6 Conclusion, Summary and Future Work

This chapter summarizes the aims of this thesis, concludes the reported research work and discusses the potential tasks.

6.1 Summary and Conclusions

This thesis deals with the non-deterministic dynamic response of a bridge subjected to a moving vehicle with uncertain system parameters. The research is expected to serve as a base for further studies in the field of vehicle-bridge structure engineering and its application has potential to be extended to other types of structural systems.

This thesis aims to provide predictive techniques for dynamic vibration analysis of vehicle-bridge interaction systems with uncertainties in the structural parameters. This has been achieved by developing a range of innovative and inter-disciplinary methods.

The first part of this thesis is an extensive literature review on dynamic analysis of vehicle-bridge interaction system with/without uncertainties and innovative methods developed to address uncertain problems in structural dynamics. In the second part of the thesis, dynamic behavior of vehicle-bridge interaction system with uncertain parameters is investigated by models represented by a moving-sprung-mass and a quarter-car moving on a simply supported beam. Different road surface conditions are considered. Random moment method is applied to analyze the dynamic response of bridge subjected to moving vehicle with uncertainties. The vehicle and bridge parameters are treated as random variables and the road roughness is considered as random process. The effect of individual parameters is investigated.

In Chapter 3, the moving vehicle is modeled as a half car. Vehicle and bridge parameters are considered as interval variables due to lack of sufficient data or large change ranges. Interval analysis method is employed to examine the variations of bridge responses induced by the moving vehicle with uncertain parameters. Young's modulus, density and moment of inertia of the bridge as well as the sprung mass and suspension masses of the vehicle are set to vary within the predefined small change ranges. The limitations of this method are that it only predicts the upper and lower bounds of the displacement response of bridge. No information could be obtained for the statistical distribution of the response within these bounds. In addition, LHNPSO, a novel particle swarm optimization method with low-discrepancy sequence initialized particles and high-order nonlinear time-varying inertia weight and constant acceleration coefficients, is developed to find the sharp bounds of bridge displacement. The results obtained from interval analysis method and LHNPSO have been verified by Monte-Carlo simulations. Three methods have a good agreement mutually.

After methods for dynamic response of vehicle-bridge interaction system with pure random or pure interval parameters are successfully developed, a mixture of different types of uncertainties are investigated ranging from randomness in the bridge material properties and interval uncertainties in the vehicle parameters of vehicle-bridge interaction system in Chapter 4. The random interval moment method is introduced into the dynamic analysis of vehicle-bridge interaction system when mixed random and interval parameters are under consideration. In this chapter, the verification of the proposed method is implemented using a hybrid simulation method. This hybrid simulation method (HSM) combines direct simulation for interval variables and Monte-Carlo simulations for random variables. In every hybrid simulation, the first step is to arbitrarily generate values within the given intervals for all interval variables, and the second step is using Monte-Carlo simulations to handle the random variables.

Finally, finite element model integrating with the vehicle-bridge interaction system is presented in Chapter 5. The random interval perturbation method is used to investigate the bridge nondeterministic dynamic response under moving vehicle with a mixture of uncertain system parameters. The uncertainties of vehicle parameters are described by interval variables and uncertain parameters of the bridge are modeled as random variables. Using the formulations developed by the random interval perturbation method, the upper and lower bounds of expectation and variance of bridge response can be very easily determined. The effects of individual random and interval parameters on bridge response are also investigated. Results generated by the hybrid simulation method successfully confirmed the accuracy and efficiency of the proposed method in this chapter.

In conclusion, this thesis systematically studied the non-deterministic dynamic properties of the vehicle-bridge interaction system with variety types of uncertainties. Probabilistic, non-probabilistic and hybrid probabilistic and non-probabilistic methods have been developed to analyze the dynamic response of a bridge under moving vehicles accounting for the uncertain parameters in the coupling system. In addition, LHNPSO has been presented to find the exact ranges of bridge response. All of the results obtained by the proposed methods have been verified by simulation methods.

6.2 Recommendations and Future Work

The research in this thesis demonstrated the effectiveness of the proposed method for the dynamic response of vehicle-bridge interaction system with uncertain properties. There are a range of areas where the work could be extended in this thesis. The recommendations and future work are discussed as follows:

1. It may be possible to establish more complicated vehicle-bridge interaction system models. The analytical model of vehicle should be further improved from a half-car model to more complicated 3D vehicle models. The bridge can be improved from simply supported beam to a more complex beam and plate. Future work can be conducted to construct a more accurate and reliable bridge-vehicle model. Consequently, the corresponding solution methods need to be developed.
2. Uncertainties of more parameters could be considered in the vehicle-bridge interaction system. It could include variations in material properties such as stiffness and damping of the vehicle, as well as other geometric parameters of the vehicle. Different types of uncertainties can be considered in each subsystem. In addition, the road surface conditions need to be deeply studied in the uncertain vehicle-bridge interaction dynamic models as they can significantly affect the system behavior.
3. Optimization methods can be further developed to obtain more accurate solutions for interval dynamic problems involving uncertain-but-bounded system parameters. Non-deterministic finite element methods could be incorporated into the vehicle-bridge interaction system with different types of

uncertainties.

4. Application of the methods presented in this thesis to other types of structures can be investigated. In the future, it may be possible to extend to train-bridge, train-rail-sleeper-foundation interaction systems and so on.

References

[1] S. H. Ju, H. T. Lin, A finite element model of vehicle-bridge interaction considering braking and acceleration , Journal of Sound and Vibration, 303(1-2) (2007) 46-57.

[2] L. Kwasniewski, H.Y. Li,, Finite element analysis of vehicle-bridge interaction, Finite Elements in Analysis and Design, 42(11) (2006) 950-959.

[3] Y. B. Yang, C. W. Lin, Vehicle-bridge interaction dynamics and potential applications, Journal of Sound and Vibration, 284(1-2) (2005) 205-226.

[4] Y. B. Yang, Y. S. Wu, A versatile element for analyzing vehicle-bridge interaction response, Engineering Structures, 23(5) (2001) 452-469.

[5] X.M. Shi, C. S. Cai, S. Chen, Vehicle induced dynamic behavior of short-span slab bridges considering effect of approach slab condition. Journal of Bridge Engineering, 13 (2008) 83-92.

[6] W. Gao, N. Kessissoglou, Dynamic response analysis of stochastic truss structures under non-stationary random excitation using the random factor method, Computer methods in applied mechanics and engineering, 196 (2007) 2765-2773.

[7] P. Marek, J. Brozzetti, M. Gustar, I. Elishakoff, Probabilistic Assessment of Structures using Monte Carlo Simulations, Applied Mechanics Reviews, 55 (2002) 31.

[8] Y. Xia, H. Hao, J.M. Brownjohn, P.Q. Xia, Damage identification of structures with uncertain frequency and mode shape data, Earthquake engineering & structural dynamics, 31 (2002) 1053-1066.

[9] J. Baroth, P. Bressolette, C. Chauvière, M. Fogli, An efficient SFE method using Lagrange polynomials: application to nonlinear mechanical problems with uncertain parameters, Computer methods in applied mechanics and engineering, 196 (2007) 4419-4429.

[10] W. Gao, C. Song, F. Tin-Loi, Probabilistic interval analysis for structures with uncertainty, Structural Safety, 32 (2010) 191-199.

[11] W. Gao, Random seismic response analysis of truss structures with uncertain parameters, Engineering structures, 29 (2007) 1487-1498.

[12] W. Gao, N. Zhang, J. Dai, A stochastic quarter-car model for dynamic analysis of vehicles with uncertain parameters, Vehicle System Dynamics, 46 (2008) 1159-1169.

[13] S.Q. Wu, S.S. Law, Dynamic analysis of bridge with non-Gaussian uncertainties under a moving vehicle. Probabilistic Engineering Mechanics, 26(2) (2011) 281-293.

[14] T. P. Chang, G. L. Lin, E. Chang, Vibration analysis of a beam with an internal hinge subjected to a random moving oscillator, International Journal of Solids and Structures, 43(21) (2006), pp. 6398-6412.

[15] L. Ding, H. Hao, X. Q. Zhu, Evaluation of dynamic vehicle axle loads on bridges with different surface conditions, Journal of Sound and Vibration, 323(3-5) (2009) 826-848.

[16] A.S. Ang, D. De Leon, Modeling and analysis of uncertainties for risk-informed decisions in infrastructures engineering, Structure and infrastructure engineering, 1 (2005) 19-31.

[17] F.O. Hoffman, J.S. Hammonds, Propagation of uncertainty in risk assessments: the need to distinguish between uncertainty due to lack of knowledge and

uncertainty due to variability, Risk Analysis, 14 (1994) 707-712.

[18] L. Manjarrez, D. de León, A.H. Ang, Structural Reliability of the Tampico Bridge under Wind Loading, Ciencia Ergo Sum, 15 (2008) 161-166.

[19] C. O'Connor, T.H.T. Chan, Dynamic wheel loads from bridge strains, Journal of Structural Engineering, 114 (1988) 1703-1723.

[20] M.F. Green, D. Cebon, D.J. Cole, Effects of vehicle suspension design on dynamics of highway bridges, Journal of Structural Engineering, 121 (1995) 272-282.

[21] M. Foda, Z. Abduljabbar, A dynamic green function formulation for the response of a beam structure to a moving mass, Journal of sound and vibration, 210 (1998) 295-306.

[22] M. Abu-Hilal, M. Mohsen, Vibration of beams with general boundary conditions due to a moving harmonic load, Journal of Sound and Vibration, 232 (2000) 703-717.

[23] M. Ichikawa, Y. Miyakawa, A. Matsuda, Vibration analysis of the continuous beam subjected to a moving mass, Journal of Sound and Vibration, 230 (2000) 493-506.

[24] G. Michaltsos, A. Kounadis, The effects of centripetal and Coriolis forces on the dynamic response of light bridges under moving loads, Journal of Vibration and Control, 7 (2001) 315-326.

[25] S.S. Law, X.Q. Zhu, Bridge dynamic responses due to road surface roughness and braking of vehicle, Journal of Sound and Vibration, 282(3–5) (2005), pp. 805–30.

[26] M. Mahmoud, M. Abou Zaid, Dynamic response of a beam with a crack subject to a moving mass, Journal of Sound and Vibration, 256 (2002) 591-603.

[27] A. Nikkhoo, F. Rofooei, M. Shadnam, Dynamic behavior and modal control of beams under moving mass, Journal of Sound and Vibration, 306 (2007) 712-724.

[28] P. Chatterjee, T. Datta, C. Surana, Vibration of continuous bridges under moving vehicles, Journal of Sound and Vibration, 169 (1994) 619-632p.

[29] H. Lee, The dynamic response of a Timoshenko beam subjected to a moving mass, Journal of sound and vibration, 198 (1996) 249-256.

[30] R.T. Wang, Vibration of multi-span Timoshenko beams to a moving force, Journal of sound and vibration, 207 (1997) 731-742.

[31] K. Henchi, M. Fafard, M. Talbot, G. Dhatt, An efficient algorithm for dynamic analysis of bridges under moving vehicles using a coupled modal and physical components approach, Journal of Sound and Vibration, 212 (1998) 663-683.

[32] R.T. Wang, T.H. Chou, Non-linear vibration of Timoshenko beam due to a moving force and the weight of beam, Journal of Sound and Vibration, 218 (1998) 117-131.

[33] E. Esmailzadeh, A. Ohadi, Vibration and stability analysis of non-uniform Timoshenko beams under axial and distributed tangential loads, Journal of sound and vibration, 236 (2000) 443-456.

[34] Y.H. Lin, M. Trethewey, Finite element analysis of elastic beams subjected to moving dynamic loads, Journal of Sound and Vibration, 136 (1990) 323-342.

[35] S. Marchesiello, A. Fasana, L. Garibaldi, B. Piombo, Dynamics of multi-span continuous straight bridges subject to multi-degrees of freedom moving vehicle excitation, Journal of Sound and Vibration, 224 (1999) 541-561.

[36] X.Q. Zhu, S.S. Law, Dynamic load on continuous multi-lane bridge deck from moving vehicles, Journal of Sound and Vibration, 251 (2002) 697-716.

[37] H.C. Kwon, M.C. Kim, I.W. Lee, Vibration control of bridges under moving

loads, Computers & structures, 66 (1998) 473-480.

[38] E. Savin, Dynamic amplification factor and response spectrum for the evaluation of vibrations of beams under successive moving loads, Journal of Sound and Vibration, 248 (2001) 267-288.

[39] Y.B. Yang, J. Yau, Y. Wu, Vehicle-bridge interaction dynamics, World Scientific, 2004.

[40] S. Sadiku, H. Leipholz, On the dynamics of elastic systems with moving concentrated masses, Ingenieur-Archiv, 57 (1987) 223-242.

[41] J.R. Rieker, Y.H. Lin, M.W. Trethewey, Discretization considerations in moving load finite element beam models, Finite elements in analysis and design, 21 (1996) 129-144.

[42] A.V. Pesterev, L.A. Bergman, Response of elastic continuum carrying moving linear oscillator, Journal of engineering mechanics, 123 (1997) 878-884.

[43] Y. Li, E. OBrien, A. González, The development of a dynamic amplification estimator for bridges with good road profiles, Journal of sound and vibration, 293 (2006) 125-137.

[44] E. Esmailzadeh, N. Jalili, Vehicle–passenger–structure interaction of uniform bridges traversed by moving vehicles, Journal of sound and vibration, 260 (2003) 611-635.

[45] G. Tsampardoukas, C.W. Stammers, E. Guglielmino, Hybrid balance control of a magnetorheological truck suspension, Journal of Sound and Vibration, 317 (2008) 514-536.

[46] L. Deng, C. Cai, Identification of parameters of vehicles moving on bridges, Engineering Structures, 31 (2009) 2474-2485.

[47] G. Tan, G. Brameld, D. Thambiratnam, Development of an analytical model for

treating bridge-vehicle interaction, Engineering Structures, 20 (1998) 54-61.

[48] D. Huang, T.L. Wang, M. Shahawy, Vibration of horizontally curved box girder bridges due to vehicles, Computers & structures, 68 (1998) 513-528.

[49] H. Xia, N. Zhang, G. De Roeck, Dynamic analysis of high speed railway bridge under articulated trains, Computers & structures, 81 (2003) 2467-2478.

[50] Q.L. Zhang, A. Vrouwenvelder, J. Wardenier, Numerical simulation of train–bridge interactive dynamics, Computers & Structures, 79 (2001) 1059-1075.

[51] C. Liu, T.L. Wang, D. Huang, Impact study for multi-girder bridge based on correlated road roughness, Structural Engineering and Mechanics(South Korea), 11 (2001) 259-272.

[52] M.K. Song, H.C. Noh, C.K. Choi, A new three-dimensional finite element analysis model of high-speed train–bridge interactions, Engineering Structures, 25 (2003) 1611-1626.

[53] S.H. Kim, Y.S. Lee, K.Y. Cho, Analysis of horizontal reactions due to moving vehicle loads in curved bridges with varied support conditions, Advances in Structural Engineering, 8 (2005) 529-545.

[54] D. Zheng, Y. Cheung, F. Au, Y. Cheng, Vibration of multi-span non-uniform beams under moving loads by using modified beam vibration functions, Journal of sound and Vibration, 212 (1998) 455-467.

[55] B. Kuran, H. Özgüven, A modal superposition method for non-linear structures, Journal of Sound and vibration, 189 (1996) 315-339.

[56] J. Yang, H.-S. Shen, Vibration characteristics and transient response of shear-deformable functionally graded plates in thermal environments, Journal of Sound and Vibration, 255 (2002) 579-602.

[57] J. Gu, Z.-D. Ma, G. M Hulbert, A new load-dependent Ritz vector method for

structural dynamics analyses: quasi-static Ritz vectors, Finite Elements in Analysis and Design, 36 (2000) 261-278.

[58] Q. Zhang, T. Hisada, Analysis of fluid–structure interaction problems with structural buckling and large domain changes by ALE finite element method, Computer methods in applied mechanics and engineering, 190 (2001) 6341-6357.

[59] H. Xia, N. Zhang, G. De Roeck, Dynamic analysis of high speed railway bridge under articulated trains, Computers & structures, 81 (2003) 2467-2478.

[60] J. Yau, Dynamic response analysis of suspended beams subjected to moving vehicles and multiple support excitations, Journal of Sound and Vibration, 325 (2009) 907-922.

[61] J.Q. Li, X.L. Leng, T. Fang, Evolutionary random response problem of a coupled vehicle-bridge system, Archive of Applied Mechanics, 72 (2002) 536-544.

[62] S.S. Law, T.H. Chan, X.Q. Zhu, Q.H. Zeng, Regularization in moving force identification, Journal of engineering mechanics, 127 (2001) 136-148.

[63] L. Fryba, Vibration of solids and structures under moving loads, Thomas Telford, 1999.

[64] J.S. Wu, M.L. Lee, T.S. Lai, The dynamic analysis of a flat plate under a moving load by the finite element method, International Journal for Numerical Methods in Engineering, 24 (1987) 743-762.

[65] J.L. Humar, A.H. Kashif, Dynamic response analysis of slab-type bridges, Journal of Structural Engineering, 121 (1995) 48-62.

[66] Y.B. Yang, J.D. Yau, Vehicle-bridge interaction element for dynamic analysis, Journal of Structural Engineering, 123 (1997) 1512-1518.

[67] K. Henchi, M. Fafard, G. Dhatt, M. Talbot, Dynamic behaviour of multi-span

beams under moving loads, Journal of Sound and Vibration, 199 (1997) 33-50.

[68] S. Law, X. Zhu, Bridge dynamic responses due to road surface roughness and braking of vehicle, Journal of Sound and Vibration, 282 (2005) 805-830.

[69] S.H. Ju, H.T. Lin, A finite element model of vehicle–bridge interaction considering braking and acceleration, Journal of sound and vibration, 303 (2007) 46-57.

[70] J.J. Wu, Dynamic analysis of an inclined beam due to moving loads, Journal of sound and vibration, 288 (2005) 107-131.

[71] T.C. Pan, J. Li, Dynamic vehicle element method for transient response of coupled vehicle-structure systems, Journal of Structural Engineering, 128 (2002) 214-223.

[72] S. Mohebpour, A. Fiouz, A. Ahmadzadeh, Dynamic investigation of laminated composite beams with shear and rotary inertia effect subjected to the moving oscillators using FEM, Composite Structures, 93 (2011) 1118-1126.

[73] J. Da Silva, Dynamical performance of highway bridge decks with irregular pavement surface, Computers & structures, 82 (2004) 871-881.

[74] M. Tanabe, Y. Yamada, W. Hajime, Modal method for interaction of train and bridge, Computers & Structures, 27 (1987) 119-127.

[75] M.R. Taheri, E.C. Ting, Dynamic response of plates to moving loads: finite element method, Computers & structures, 34 (1990) 509-521.

[76] X. Lei, N.-A. Noda, Analyses of dynamic response of vehicle and track coupling system with random irregularity of track vertical profile, Journal of Sound and Vibration, 258 (2002) 147-165.

[77] Ö. Çavdar, A. Bayraktar, S. Adanur, Stochastic finite element analysis of a cable-stayed bridge system with varying material properties, Probabilistic Engineering

Mechanics, 25 (2010) 279-289.

[78] J. Lu, H. Zhang, Y. Yang, Monte Carlo simulation of kinetics and chain-length distribution in radical polymerization, Macromolecular Theory and Simulations, 2 (1993) 747-760.

[79] S. Soyoz, M.Q. Feng, Long-Term Monitoring and Identification of Bridge Structural Parameters, Computer-Aided Civil and Infrastructure Engineering, 24 (2009) 82-92.

[80] G. Falsone, N. Impollonia, A new approach for the stochastic analysis of finite element modelled structures with uncertain parameters, Computer Methods in Applied Mechanics and Engineering, 191 (2002) 5067-5085.

[81] M. Kamiński, M. Kleiber, Perturbation based stochastic finite element method for homogenization of two-phase elastic composites, Computers & Structures, 78 (2000) 811-826.

[82] P. Kokotovic, H.K. Khali, J. O'reilly, Singular perturbation methods in control: analysis and design, Siam, 1987.

[83] H. Benaroya, M. Rehak, The Neumann series/Born approximation applied to parametrically excited stochastic systems, Probabilistic engineering mechanics, 2 (1987) 74-81.

[84] L. Frýba, S. Nakagiri, N. Yoshikawa, Stochastic finite elements for a beam on a random foundation with uncertain damping under a moving force, Journal of sound and vibration, 163 (1993) 31-45.

[85] T.L. Wang, D. Huang, M. Shahawy, K. Huang, Dynamic response of highway girder bridges, Computers & structures, 60 (1996) 1021-1027.

[86] S.S. Law, X.Q. Zhu, Dynamic behavior of damaged concrete bridge structures under moving vehicular loads, Engineering Structures, 26 (2004) 1279-1293.

[87] A. Der Kiureghian, J.B. Ke, The stochastic finite element method in structural reliability, Probabilistic Engineering Mechanics, 3 (1988) 83-91.

[88] I. Elishakoff, Essay on uncertainties in elastic and viscoelastic structures: from AM Freudenthal's criticisms to modern convex modeling, Computers & Structures, 56 (1995) 871-895.

[89] D. Moens, D. Vandepitte, Recent advances in non-probabilistic approaches for non-deterministic dynamic finite element analysis, Archives of Computational Methods in Engineering, 13 (2006) 389-464.

[90] B. Möller, M. Beer, Engineering computation under uncertainty–capabilities of non-traditional models, Computers & Structures, 86 (2008) 1024-1041.

[91] G. Falsone, N. Impollonia, A new approach for the stochastic analysis of finite element modelled structures with uncertain parameters, Computer Methods in Applied Mechanics and Engineering, 191 (2002) 5067-5085.

[92] G. Stefanou, M. Papadrakakis, Stochastic finite element analysis of shells with combined random material and geometric properties, Computer Methods in Applied Mechanics and Engineering, 193 (2004) 139-160.

[93] G. Stefanou, The stochastic finite element method: past, present and future, Computer Methods in Applied Mechanics and Engineering, 198 (2009) 1031-1051.

[94] R.E. Moore, Interval analysis, Prentice-Hall Englewood Cliffs, 1966.

[95] R.E. Moore, R. Moore, Methods and applications of interval analysis, SIAM, 1979.

[96] G. Alefeld, J. Herzberger, Introduction to interval computation, Access Online via Elsevier, 1984.

[97] W. Gao, Interval finite element analysis using interval factor method,

Computational Mechanics, 39 (2007) 709-717.

[98] W.F. Chen, L. Duan, Bridge engineering handbook, CRC press, 2010.

[99] Z. Qiu, X. Wang, Comparison of dynamic response of structures with uncertain-but-bounded parameters using non-probabilistic interval analysis method and probabilistic approach, International Journal of Solids and Structures, 40 (2003) 5423-5439.

[100] P. Suresh, A. Babar, V.V. Raj, Uncertainty in fault tree analysis: a fuzzy approach, Fuzzy Sets and Systems, 83 (1996) 135-141.

[101] S.S. Rao, L. Berke, Analysis of uncertain structural systems using interval analysis, AIAA journal, 35 (1997) 727-735.

[102] L. Chen, S. Rao, Fuzzy finite-element approach for the vibration analysis of imprecisely-defined systems, Finite Elements in Analysis and Design, 27 (1997) 69-83.

[103] D. Moens, D. Vandepitte, Fuzzy finite element method for frequency response function analysis of uncertain structures, AIAA journal, 40 (2002) 126-136.

[104] S.S. Rao, J.P. Sawyer, Fuzzy finite element approach for analysis of imprecisely defined systems, AIAA journal, 33 (1995) 2364-2370.

[105] S. Dey, N. Balasubramanian, Dynamic response of orthotropic curved bridge decks due to moving loads, Computers & structures, 18 (1984) 27-32.

[106] M. Rassem, A. Ghobarah, A. Heidebrecht, Site effects on the seismic response of a suspension bridge, Engineering structures, 18 (1996) 363-370.

[107] L. Kwasniewski, H. Li, J. Wekezer, J. Malachowski, Finite element analysis of vehicle–bridge interaction, Finite Elements in Analysis and Design, 42 (2006) 950-959.

[108] Y.B. Yang, K.C. Chang, Extraction of bridge frequencies from the dynamic

response of a passing vehicle enhanced by the EMD technique, Journal of sound and vibration, 322 (2009) 718-739.

[109] Y.B. Yang, K.C. Chang, Extracting the bridge frequencies indirectly from a passing vehicle: Parametric study, Engineering Structures, 31 (2009) 2448-2459.

[110] A. Gupta, K. Hughes, C. Sellars, Glass-lubricated hot extrusion of stainless steel, Metals Technology, 7 (1980) 323-331.

[111] E.S. Hwang, A.S. Nowak, Simulation of dynamic load for bridges, Journal of Structural Engineering, 117 (1991) 1413-1434.

[112] C.W. Kim, M. Kawatani, K.B. Kim, Three-dimensional dynamic analysis for bridge–vehicle interaction with roadway roughness, Computers & structures, 83 (2005) 1627-1645.

[113] R.Y. Rubinstein, D.P. Kroese, Simulation and the Monte Carlo method, Wiley. com, 2011.

[114] F. Lu, J. Lin, D. Kennedy, F. Williams, An algorithm to study non-stationary random vibrations of vehicle–bridge systems, Computers & Structures, 87 (2009) 177-185.

[115] R. Ghanem, P.D. Spanos, Stochastic finite elements: a spectral approach, DoverPublications. com, 2003.

[116] R. Gaignaire, S. Clenet, B. Sudret, O. Moreau, 3-D spectral stochastic finite element method in electromagnetism, Magnetics, IEEE Transactions on, 43 (2007) 1209-1212.

[117] International Standards Organisation. Mechanical vibration – road surface profiles-reporting of measured data. ISO 8608; 1995.

[118] H. Honda, Y. Kajikawa, T. Kobori, Spectra of road surface roughness on bridges, Journal of the structural Division, 108 (1982) 1956-1966.

[119] S. Türkay, H. Akçay, A study of random vibration characteristics of the quarter-car model, Journal of sound and vibration, 282 (2005) 111-124.

[120] J. Kennedy, R. Eberhart, Particle swarm optimization, in: Proceeding of the IEEE International Conference on Neural Networks, Piscataway, vol. IV, 1995, 1942–1948.

[121] Y.H. Shi, R.C. Eberhart, A modified particle swarm optimizer, in: Proceedings of the 1998 IEEE International Conference on Evolutionary Computation (CEC98), Anchorage, Alaska, USA, 4-9 May 1998, 69–73.

[122] P. C. Fourie, A. Groenwold, The particle swarm optimization algorithm in size and shape optimization, Structural and Multidisciplinary Optimization, 23 (2002), 259–67.

[123] F. Li, Z. Luo, G.Y. Sun, Reliability-based multi-objective design optimization under interval uncertainty, CMES: Computer Modeling in Engineering & Sciences, 74 (2011), 34-69.

[124] F. Li, Z. Luo, G.Y. Sun, N. Zhang, An uncertain multidisciplinary design optimization method using interval convex models, Engineering Optimization, 45(6) (2013),.697-718.

[125] C. Jiang, X. Han, G.P. Liu, A nonlinear interval number programming method for uncertain optimization problems, European Journal of Operational Research, 188 (2008), 1-13.

[126] P. Asokan, R. Saravanan, K. Vijayakumar, Machining parameters optimisation for turning cylindrical stock into a continuous finished profile using genetic algorithm (GA) and simulated annealing (SA), The International Journal of Advanced Manufacturing Technology, 21 (2003) 1-9.

[127] G. Venter, J. Sobieszczanski-Sobieski, Multidisciplinary optimization of a

transport aircraft wing using particle swarm optimization, Structural and Multidisciplinary Optimization, 26 (2004), 121–31

[128] L. Li, Z. Huang, F. Liu, Q. Wu, A heuristic particle swarm optimizer for optimization of pin connected structures. Computers and Structures, 87 (7–8) (2009), 435–443.

[129] V. Plevris, M. Papadrakakis, A hybrid particle swarm-gradient algorithm for global structural optimization, Computer-Aided Civil and Infrastructure Engineering, 26 (2011), 48-68.

[130] R. Perez, K. Behdinan, Particle swarm approach for structural design optimization, Computers & Structures, 85 (2007) 1579-1588.

[131] W. Gao, C. W. Yang, N. G. Liu, C. M. Song, Y. L. Pi, Low-discrepancy sequence initialized particle swarm optimization algorithm with high-order nonlinear time-varying inertia weight, Submitted to Applied Mathematics and Computation.

[132] Q. Wu, Product demand forecasts using wavelet kernel support vector machine and particle swarm optimization in manufacture system, Journal of Computational and Applied Mathematics, 233(10) (2010), 2481-2491.

[133] W. F. Abd-El-Wahed, A. A. Mousa, M. A. El-Shorbagy, Integrating particle swarm optimization with genetic algorithms for solving nonlinear optimization problems, Journal of Computational and Applied Mathematics, 235(5) (2011), 1446-1453.

[134] J. Guo, X.P. Du, Reliability sensitivity analysis with random and interval variables, International Journal for Numerical Methods in Engineering 78 (13) (2009) 1585-1617.

[135] C. Jiang, W.X. Li, X. Han, L.X. Liu, P.H. Le, Structural reliability analysis based on random distributions with interval parameters, Computers & Structures 89 (23-24) (2011) 2292-2302.

[136] C. Jiang, X. Han, W. X. Li, J. Liu, and Z. Zhang. A hybrid reliability approach based on probability and interval for uncertain structures. Journal of Mechanical Design 134 (2012) 031001.

[137] G. Muscolino, S. Benfratello, A. Sidoti, Dynamics analysis of distributed parameter system subjected to a moving oscillator with random mass, velocity and acceleration, Probabilistic Engineering Mechanics 17 (1) (2002) 63–72.

[138] N. Liu, W. Gao, C. Song, N. Zhang, Probabilistic Dynamic Analysis of Vehicle-Bridge Interaction System with Uncertain Parameters, Computer Modeling in Engineering & Sciences(CMES), 72 (2011) 79-102.

Appendix

Dynamic response of structure with uncertainties by Newmark-β method

The Newmark-β method is a method of numerical integration used to solve differential equations. It is used in finite element analysis to model dynamic systems, recalling the continuous-time equation of motion.

The relationships between the displacement, velocity and acceleration developed by Newmark (1959) are given by

$$X\left(t+\Delta t\right)=X\left(t\right)+\Delta t\dot{X}\left(t\right)+\Delta t^{2}\left[\left(\frac{1}{2}-\beta\right)\ddot{X}\left(t\right)+\beta\ddot{X}\left(t+\Delta t\right)\right] \tag{A.1}$$

$$\dot{X}\left(t+\Delta t\right)=\dot{X}\left(t\right)+\Delta t\left[\left(1-\gamma\right)\ddot{X}\left(t\right)+\gamma\ddot{X}\left(t+\Delta t\right)\right] \tag{A.2}$$

where parameters β and γ determine the stability and accuracy of the solutions, and usually selections are $\frac{1}{6}\leq\beta\leq\frac{1}{4}$ and $\gamma=\frac{1}{2}$.

The constants δ_i are defined as

$$\delta_0=\frac{1}{\beta\cdot\Delta t^2}\,,\delta_1=\frac{\gamma}{\beta\cdot\Delta t}\,,\delta_2=\frac{1}{\beta\cdot\Delta t}\,,\delta_3=\frac{1}{2\beta}-1\,,\delta_4=\frac{\gamma}{\beta}-1\,,$$

$$\delta_5=\frac{\Delta t}{2}\left(\frac{\gamma}{\beta}-2\right)\,,\delta_6=\Delta t\cdot(1-\gamma)\,,\delta_7=\Delta t\cdot\gamma \tag{A.3}$$

$$[K^*]X(t+\Delta t)=F^*(t+\Delta t) \tag{A.4}$$

where

$$\left[K^*\right] = [K] + \delta_0 [M] + \delta_1 [C] \tag{A.5}$$

$$F^*(t+\Delta t) = F(t+\Delta t) + [M]\left[\delta_0 X(t) + \delta_2 \dot{X}(t) + \delta_3 \ddot{X}(t)\right]$$
$$+[C]\left[\delta_1 X(t) + \delta_4 \dot{X}(t) + \delta_5 \ddot{X}(t)\right] \tag{A.5}$$

The velocity and acceleration are

$$\ddot{X}(t+\Delta t) = \delta_0\left(X(t+\Delta t) - X(t)\right) - \delta_2 \dot{X}(t) - \delta_3 \ddot{X}(t) \tag{A.6}$$

and

$$\dot{X}(t+\Delta t) = \dot{X}(t) + \delta_6 \ddot{X}(t) + \delta_7 \ddot{X}(t+\Delta t) \tag{A.7}$$

Differentiating Eq.(A.5) with respect to the random variable a_i^R (or interval variable b_i^R) gives

$$\left[K^*\right]\frac{\partial X(t+\Delta t)}{\partial a_i^R} = \frac{\partial F^*(t+\Delta t)}{\partial a_i^R} - \frac{\partial\left[K^*\right]}{\partial a_i^R} X(t+\Delta t) \tag{A.8}$$

where

$$\frac{\partial\left[K^*\right]}{\partial a_i^R} = \frac{\partial[K]}{\partial a_i^R} + \delta_0 \frac{\partial[M]}{\partial a_i^R} + \delta_1 \frac{\partial[C]}{\partial a_i^R} \tag{A.8}$$

$$\frac{\partial F^*(t+\Delta t)}{\partial a_i^R} = \frac{\partial[M]}{\partial a_i^R}\left[\delta_0 X(t) + \delta_2 \dot{X}(t) + \delta_3 \ddot{X}(t)\right]$$
$$+[M]\left[\delta_0 \frac{\partial X(t)}{\partial a_i^R} + \delta_2 \frac{\partial \dot{X}(t)}{\partial a_i^R} + \delta_3 \frac{\partial \ddot{X}(t)}{\partial a_i^R}\right] + \frac{\partial[C]}{\partial a_i^R}\left[\delta_1 X(t) + \delta_4 \dot{X}(t) + \delta_5 \ddot{X}(t)\right]$$

$$+[C]\left[\delta_1 \frac{\partial X(t)}{\partial a_i^R} + \delta_4 \frac{\partial \dot{X}(t)}{\partial a_i^R} + \delta_5 \frac{\partial \ddot{X}(t)}{\partial a_i^R}\right] \tag{A.9}$$

Similarly, differentiating Eq. (A.6) and (A.7) with respect to the random variable a_i^R yields

$$\frac{\partial \ddot{X}\left(t+\Delta t\right)}{\partial a_i^R}=\delta_0\left(\frac{\partial X\left(t+\Delta t\right)}{\partial a_i^R}-\frac{\partial X\left(t\right)}{\partial a_i^R}\right)-\delta_2\frac{\partial \dot{X}\left(t\right)}{\partial a_i^R}-\delta_3\frac{\partial \ddot{X}\left(t\right)}{\partial a_i^R} \tag{A.10}$$

and

$$\frac{\partial \dot{X}\left(t+\Delta t\right)}{\partial a_i^R}=\frac{\partial \dot{X}\left(t\right)}{\partial a_i^R}+\delta_6\frac{\partial \ddot{X}\left(t\right)}{\partial a_i^R}+\delta_7\frac{\partial \ddot{X}\left(t+\Delta t\right)}{\partial a_i^R} \tag{A.11}$$

Second time derivative of dynamic response (interval variable b_j^I) can be solved as

$$\left[K^*\right]\frac{\partial^2 X\left(t+\Delta t\right)}{\partial a_i^R b_j^I}=\frac{\partial^2 F^*\left(t+\Delta t\right)}{\partial a_i^R b_j^I}-\frac{\partial^2\left[K^*\right]}{\partial a_i^R b_j^I}X\left(t+\Delta t\right)$$

$$-\frac{\partial\left[K^*\right]}{\partial a_i^R}\frac{\partial X\left(t+\Delta t\right)}{\partial b_j^I}-\frac{\partial\left[K^*\right]}{\partial b_j^I}\frac{\partial X\left(t+\Delta t\right)}{\partial a_i^R} \tag{A.12}$$

where

$$\frac{\partial\left[K^*\right]}{\partial a_i^R}=\frac{\partial\left[K\right]}{\partial a_i^R}+\delta_0\frac{\partial\left[M\right]}{\partial a_i^R}+\delta_1\frac{\partial\left[C\right]}{\partial a_i^R} \tag{A.13}$$

$$\frac{\partial^2 F^*\left(t+\Delta t\right)}{\partial a_i^R\partial b_j^I}=$$

$$\frac{\partial^2\left[M\right]}{\partial a_i^R\partial b_j^I}\left[\delta_0 X\left(t\right)+\delta_2\dot{X}\left(t\right)+\delta_3\ddot{X}\left(t\right)\right]+\left[M\right]\left[\delta_0\frac{\partial^2 X\left(t\right)}{\partial a_i^R b_j^I}+\delta_2\frac{\partial^2\dot{X}\left(t\right)}{\partial a_i^R b_j^I}+\delta_3\frac{\partial^2\ddot{X}\left(t\right)}{\partial a_i^R b_j^I}\right]$$

$$+\frac{\partial\left[M\right]}{\partial b_j^I}\left[\delta_0\frac{\partial X\left(t\right)}{\partial a_i^R}+\delta_2\frac{\partial\dot{X}\left(t\right)}{\partial a_i^R}+\delta_3\frac{\partial\ddot{X}\left(t\right)}{\partial a_i^R}\right]+\frac{\partial\left[M\right]}{\partial a_i^R}\left[\delta_0\frac{\partial X\left(t\right)}{\partial b_j^I}+\delta_2\frac{\partial\dot{X}\left(t\right)}{\partial b_j^I}+\delta_3\frac{\partial\ddot{X}\left(t\right)}{\partial b_j^I}\right]$$

$$+\frac{\partial^2[C]}{\partial a_i^R \partial b_j^I}\left[\delta_1 X(t)+\delta_4 \dot{X}(t)+\delta_5 \ddot{X}(t)\right]+\frac{\partial[C]}{\partial b_j^I}\left[\delta_1 \frac{\partial X(t)}{\partial a_i^R}+\delta_4 \frac{\partial \dot{X}(t)}{\partial a_i^R}+\delta_5 \frac{\partial \ddot{X}(t)}{\partial a_i^R}\right]$$

$$+\frac{\partial[C]}{\partial a_i^R}\left[\delta_0 \frac{\partial X(t)}{\partial b_j^I}+\delta_2 \frac{\partial \dot{X}(t)}{\partial b_j^I}+\delta_3 \frac{\partial \ddot{X}(t)}{\partial b_j^I}\right]+[C]\left[\delta_0 \frac{\partial^2 X(t)}{\partial a_i^R b_j^I}+\delta_2 \frac{\partial^2 \dot{X}(t)}{\partial a_i^R b_j^I}+\delta_3 \frac{\partial^2 \ddot{X}(t)}{\partial a_i^R b_j^I}\right] \tag{A.14}$$

Similarly, differentiating Eqs.(A.10) and (A.11) with respect to the interval variable b_j^I, the acceleration and velocity can be expressed as

$$\frac{\partial^2 \ddot{X}(t+\Delta t)}{\partial a_i^R \partial b_j^I}=\delta_0\left(\frac{\partial^2 X(t+\Delta t)}{\partial a_i^R \partial b_j^I}-\frac{\partial^2 X(t)}{\partial a_i^R \partial b_j^I}\right)-\delta_2 \frac{\partial^2 \dot{X}(t)}{\partial a_i^R \partial b_j^I}-\delta_3 \frac{\partial^2 \ddot{X}(t)}{\partial a_i^R \partial b_j^I} \tag{A.15}$$

and

$$\frac{\partial^2 \dot{X}(t+\Delta t)}{\partial a_i^R \partial b_j^I}=\frac{\partial^2 \dot{X}(t)}{\partial a_i^R \partial b_j^I}+\delta_6 \frac{\partial^2 \ddot{X}(t)}{\partial a_i^R \partial b_j^I}+\delta_7 \frac{\partial^2 \ddot{X}(t+\Delta t)}{\partial a_i^R \partial b_j^I} \tag{A.16}$$